



2007

This is to certify that the  
dissertation entitled

SYNTHESIS AND CHARACTERIZATION OF POLYLACTIDE  
DERIVATIVES WITH HIGH GLASS TRANSITION  
TEMPERATURES

presented by

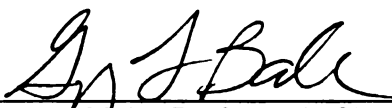
Feng Jing

has been accepted towards fulfillment  
of the requirements for the

Doctoral

degree in

Chemistry



Major Professor's Signature

July 28, 2006

Date

*MSU is an Affirmative Action/Equal Opportunity Institution*

LIBRARY  
Michigan State  
University

**PLACE IN RETURN BOX** to remove this checkout from your record.  
**TO AVOID FINES** return on or before date due.  
**MAY BE RECALLED** with earlier due date if requested.

| DATE DUE | DATE DUE | DATE DUE |
|----------|----------|----------|
|          |          |          |
|          |          |          |
|          |          |          |
|          |          |          |
|          |          |          |
|          |          |          |
|          |          |          |
|          |          |          |
|          |          |          |
|          |          |          |

**SYNTHESIS AND CHARACTERIZATION OF POLYLACTIDE DERIVATIVES WITH  
HIGH GLASS TRANSITION TEMPERATURES**

**By**

**Feng Jing**

**A DISSERTATION**

**Submitted to  
Michigan State University  
in partial fulfillment of the requirements  
for the degree of**

**DOCTOR OF PHILOSOPHY**

**Department of Chemistry**

**2006**



## ABSTRACT

### SYNTHESIS AND CHARACTERIZATION OF POLYLACTIDE DERIVATIVES WITH HIGH GLASS TRANSITION TEMPERATURES

By

Feng Jing

Poly lactide is one of the most widely used degradable polyesters with applications ranging from surgical sutures to packaging materials. Because of its low glass transition temperature, polylactide materials designed for use above 50 °C typically rely on crystallinity to provide dimensional stability and higher use temperatures. Glassy polylactides analogous to polystyrene are currently unavailable. The goal of this research is the synthesis of amorphous polylactide derivatives with high glass transition temperatures ( $T_g$ ).

We synthesized lactide monomers with bulky substituents such as cyclohexyl and isopropyl groups, which were polymerized using  $\text{Sn}(\text{2-ethylhexanoate})_2$  as the catalyst and 4-*tert*-butylbenzyl alcohol as the initiator. Ring-opening polymerization of dicyclohexylglycolide, diisopropylglycolide, and methylcyclohexylglycolide yielded high molecular weight polylactide derivatives with  $T_g$ s as high as 98 °C. The effect of chirality on the properties of poly(dicyclohexylglycolide) were examined by comparing poly(*rac*-dicyclohexylglycolide), poly(*meso*-dicyclohexylglycolide), and poly(*R,R*-dicyclohexylglycolide). Their stereosequence differences were confirmed by  $^1\text{H}$  and  $^{13}\text{C}$  NMR, but no crystallinity was observed from poly(*R,R*-

dicyclohexylglycolide), despite its stereoregularity. All poly(dicyclohexylglycolide)s are amorphous with  $T_g$ s ranging from 96 °C-104 °C.

Dicyclohexylglycolide-based random and block copolymers were synthesized and characterized. The  $T_g$  of random copolymers of dicyclohexylglycolide and dihexylglycolide ranged from -38 °C to 92 °C. To improve toughness and ductility by introducing phase separation, the ABA triblock copolymer poly(dicyclohexylglycolide)-*block*-poly(ethylene glycol)-*block*-poly(dicyclohexyl-glycolide) (PDCG-PEG-PDCG) with a low  $T_g$  PEG middle block were designed and synthesized. With a medium-sized PEG middle block (number average molecular weight: 2000), PDCG-PEG2000-PDCG copolymer showed clear sign of phase separation with two distinct glass transitions on DSC, and no PEG crystallization. Phase separation was further confirmed by Tapping-mode Atomic Force Microscopy.

We synthesized poly(1,4-benzodioxepin-3-methyl-2,5-dione) and poly(1,4-benzodioxepin-3-cyclohexyl-2,5-dione) via ring-opening polymerization catalyzed by 4-(dimethylamino)pyridine. The kinetics of solution and bulk polymerizations of 1,4-benzodioxepin-3-alkyl-2,5-diones are first-order in monomer. Incorporating salicylic acid repeating units into the polymer backbone provided amorphous poly(1,4-benzodioxepin-3-methyl-2,5-dione) and poly(1,4-benzodioxepin-3-cyclohexyl-2,5-dione) with glass transition temperatures of 92 °C and 120 °C, which marks them as degradable alternatives to polystyrene.

To my family

## **ACKNOWLEDGMENTS**

I would like to thank my advisor, Dr. Gregory Baker, for his guidance and assistance during my graduate study. I would like to thank Mitch Smith for his guidance, patience and suggestions. I would also like to thank my committee members, Ned Jackson and Michael Mackay for their guidance and assistance.

My thanks go to all Baker group members: Fadi, Bao, Leslie, Ping, Xuwei, Ying, DJ, Erin, Qin, and Jon and all my friends in Michigan State University. I would like to thank Long Le, Kermit Johnson, Dan Holmes, Riu Huang, Kathy Severin, Tiffany Dukette, and David Bohnsack for their help on the instruments.

Finally, I would like to thank my wife Xiaoping for her love and support. Life would be so boring without her staying here with me.

## TABLE OF CONTENTS

|   |      |
|---|------|
| LIST OF TABLES.....   | viii |
| LIST OF FIGURES.....  | ix   |
| LIST OF SCHEMES.....  | xv   |
| LIST OF ABBREVIATIONS.....  | xvii |
| Chapter 1    Introduction.....  | 1    |
| Substituted glycolides.....   | 5    |
| Alkyl-, alkenyl-, and aryl-substituted glycolides .....                 | 6    |
| Glycolides with other functionalities .....                             | 21   |
| <i>p</i> -Dioxanone and derivatives .....                               | 27   |
| <i>p</i> -Dioxanone.....  | 27   |
| 3-Methyl- <i>p</i> -dioxanone .....                                     | 29   |
| 6,13-Dimethyltetraoxcyclotetradecanedione .....                         | 30   |
| 6-Hydroxymethyl- <i>p</i> -dioxanone .....                              | 32   |
| Dioxepanedione and benzodioxepindione.....                              | 34   |
| Depsipeptides.....  | 36   |
| Alkyl-substituted morpholine-2,5-diones .....                           | 37   |
| Morpholine-2,5-diones with other functionalities .....                  | 39   |
| Chapter 2    Poly(dicyclohexylglycolide)s .....                         | 44   |
| Monomer synthesis .....   | 46   |
| Solution polymerization kinetics of substituted glycolides.....         | 50   |
| Bulk polymerization kinetics of <i>rac</i> -dicyclohexylglycolide ..... | 53   |
| Physical properties of substituted polyglycolides.....                  | 60   |

|   |     |
|---|-----|
| Stereochemical effects on poly(dicyclohexylglycolide)s .....  | 65  |
| Degradation of poly( <i>rac</i> -dicyclohexylglycolide).....  | 72  |
| Chapter 3 Dicyclohexylglycolide-based copolymers.....   | 76  |
| Random copolymers of dicyclohexylglycolide and dihexylglycolide. ....   | 77  |
| Poly(dicyclohexylglycolide)- <i>block</i> -poly(ethylene glycol)- <i>block</i> -poly(dicyclohexylglycolide) triblock copolymers. .... | 87  |
| Chapter 4 Poly(1,4-benzodioxepin-3-alkyl-2,5-dione)s.....   | 99  |
| Synthesis of 1,4-benzodioxepin-3-alkyl-2,5-diones .....   | 102 |
| Initiator studies on the ring-opening polymerization of 1,4-benzodioxepin-3-alkyl-2,5-diones .....                                    | 103 |
| Solution polymerization kinetics of 1,4-benzodioxepin-3-alkyl-2,5-diones .....  | 111 |
| Bulk polymerization kinetics of 1,4-benzodioxepin-3-alkyl-2,5-diones .....  | 114 |
| Physical properties of poly(1,4-benzodioxepin-3-alkyl-2,5-dione)s.....  | 120 |
| Chapter 5 Experimental Section.....   | 123 |
| Appendix .....  | 138 |
| References.....   | 187 |

## LIST OF TABLES

|  |     |
|--|-----|
| Table 1. Applications of polylactide as commodity polymers (NatureWorks LLC) <sup>43</sup>                           |     |
| Table 2. Properties of symmetrical dialkylglycolide polymers .....   | 8   |
| Table 3. Properties of nonsymmetrical dialkylglycolides polymers.....  | 11  |
| Table 4. Physical properties of poly(diphenyllactide) and its derivatives .....                                      | 18  |
| Table 5. Physical properties of polymandelide and its derivatives .....  | 19  |
| Table 6. Physical properties of poly(DIPAGYL-co- <i>rac</i> -lactide) and poly(DIPALYL-co- <i>rac</i> -lactide)..... | 25  |
| Table 7. Physical properties of poly( $\alpha,\alpha'$ -difluorolactide).....  | 26  |
| Table 8. Thermodynamic parameters of cyclic esters polymerized at 100 °C .....                                       | 29  |
| Table 9. Physical properties of poly(morpholine-2,5-dione)s .....  | 39  |
| Table 10. Solution polymerization rates of polyglycolides .....  | 51  |
| Table 11. Properties of substituted polyglycolides .....   | 60  |
| Table 12. Properties of poly(dicyclohexylglycolide)s .....   | 65  |
| Table 13. Butanolysis of poly( <i>rac</i> -dicyclohexylglycolide).....   | 73  |
| Table 14. Properties of poly(dicyclohexylglycolide-co-dihexylglycolide)s.....  | 78  |
| Table 15. Properties of poly(hexylcyclohexylglycolide) .....   | 81  |
| Table 16. Characterization of PDCG-PEG-PDCG copolymers .....   | 91  |
| Table 17. Thermal properties of PDCG-PEG-PDCG copolymers .....   | 92  |
| Table 18. Characterization of poly(1,4-benzodioxepin-3-methyl-2,5-dione).....  | 103 |
| Table 19. Solution polymerization rates of 1,4-benzodioxepin-3-alkyl-2,5-diones .....                                | 112 |
| Table 20. Properties of poly(1,4-benzodioxepin-3-alkyl-2,5-dione)s .....   | 120 |

## LIST OF FIGURES

|  |    |
|--|----|
| Figure 1. NatureWorks LLC process for the manufacture of polylactide .....   | 2  |
| Figure 2. Structures of $\alpha$ -hydroxy acid-containing cyclic esters .....  | 5  |
| Figure 3. Structures of lactide stereoisomers .....  | 6  |
| Figure 4. Structures of symmetrical dialkylglycolides .....  | 7  |
| Figure 5. Structures of nonsymmetrical alkyl-substituted glycolides .....  | 10 |
| Figure 6. Structures of other alkyl-substituted glycolides .....   | 12 |
| Figure 7. Structure of 2,2'-bis( $\epsilon$ -caprolatone-4-yl)propane .....  | 13 |
| Figure 8. Structures of diphenyllactide and derivatives .....  | 17 |
| Figure 9. Structures of mandelide and methyphenylglycolide .....   | 18 |
| Figure 10. Structures of poly(malic acid)s .....   | 21 |
| Figure 11. Structures of alkyl-substituted morpholine-2,5-diones .....   | 37 |
| Figure 12. Structures of high $T_g$ polylactides .....   | 44 |
| Figure 13. Structures of lactide derivatives with bulky side groups .....  | 45 |
| Figure 14. 500 MHz $^1\text{H}$ NMR spectra for <i>rac</i> -dicyclohexylglycolide and <i>meso</i> -dicyclohexylglycolide .....   | 49 |
| Figure 15. Solution polymerization kinetics of <i>rac</i> -lactide (▲), <i>rac</i> -methylcyclohexylglycolide (●), <i>rac</i> -diisopropylglycolide (■), and <i>rac</i> -dicyclohexylglycolide (◆). Polymerization conditions: 90 °C, [monomer]: [Sn(2-ethylhexanoate) <sub>2</sub> ]: [4- <i>tert</i> -butylbenzyl alcohol] = 100: 1: 1. .... | 52 |
| Figure 16. Polymerization (◆) and depolymerization (▲) data for the bulk polymerization of <i>rac</i> -dicyclohexylglycolide. Conditions: 200 °C, [monomer]: [Sn(2-ethylhexanoate) <sub>2</sub> ]: [4- <i>tert</i> -butylbenzyl alcohol] = 100: 1: 1. ....   | 56 |
| Figure 17. Bulk polymerization kinetics of <i>rac</i> -dicyclohexylglycolide. Polymerization conditions: 200 °C, [monomer]: [Sn(2-ethylhexanoate) <sub>2</sub> ]: [4- <i>tert</i> -butylbenzyl alcohol] = 100: 1: 1. ....  | 57 |



- Figure 18. The evolution of conversion with polymerization time for the bulk polymerization of *rac*-dicyclohexylglycolide. The data were fit using an equilibrium model (dashed line), and the equilibrium model but assuming some loss of active chain ends (solid line). Conditions: 200 °C, [monomer]: [Sn(2-ethylhexanoate)<sub>2</sub>]: [4-*tert*-butylbenzyl alcohol] = 100: 1: 1. ....58
- Figure 19. The evolution of molecular weight (♦) and polydispersity (▲) with conversion for the bulk polymerization of *rac*-dicyclohexylglycolide. Polymerization conditions: 200 °C, [monomer]: [Sn(2-ethylhexanoate)<sub>2</sub>]: [4-*tert*-butylbenzyl alcohol] = 100: 1: 1.....59
- Figure 20. Thermogravimetric analysis results for substituted polyglycolides. Samples were run in air at a heating rate of 10 °C/min. ....62
- Figure 21. DSC analyses of substituted polyglycolides. Heating rate: 10 °C/min under nitrogen. The data are from the second heating scan, taken after flash quenching from 120 °C. ....63
- Figure 22. Comparisons on the *T<sub>g</sub>*s of polyolefins and polyglycolides.....64
- Figure 23. DSC analyses of poly(dicyclohexylglycolide)s. Heating rate: 10 °C/min under nitrogen. The data are from the second heating scan, taken after flash quenching from 120 °C. ....68
- Figure 24. 500 MHz <sup>1</sup>H NMR spectra for poly(*rac*-dicyclohexylglycolide), poly(*meso*-dicyclohexylglycolide), and poly(*R,R*-dicyclohexylglycolide)...69
- Figure 25. 125 MHz <sup>13</sup>C NMR spectra for poly(*rac*-dicyclohexylglycolide), poly(*meso*-dicyclohexylglycolide), and poly(*R,R*-dicyclohexylglycolide)...70
- Figure 26. 125 MHz <sup>13</sup>C NMR spectra of the carbonyl regions of poly(*R,R*-dicyclohexylglycolide) synthesized by bulk polymerization (200 °C) and solution polymerization (90 °C).....71
- Figure 27. GPC traces of poly(*rac*-dicyclohexylglycolide) during butanolysis. The polymer was refluxed in *n*-butanol with catalytic amount of sulfuric acid..74
- Figure 28. Molecular weight changes of poly(*rac*-dicyclohexylglycolide) in butanolysis. The polymer was refluxed in *n*-butanol with catalytic amount of sulfuric acid. ....75
- Figure 29. 500 MHz <sup>1</sup>H NMR spectra of poly(dicyclohexylglycolide-co-dihexylglycolide)s .....83
- Figure 30. DSC analyses for poly(dicyclohexylglycolide-co-dihexylglycolide)s and poly(hexylcyclohexylglycolide). The ratios shown in the figure are the dicyclohexylglycolide: dihexylglycolide copolymer composition ratios;

|  |     |
|--|-----|
| poly(hexylcyclohexylglycolide) is shown as an alternating 50:50 copolymer. Heating rate: 10 °C/min under nitrogen. The data are second heating scans taken after flash quenching from 120 °C. ....                                 | 84  |
| Figure 31. Glass transition temperatures of poly(dicyclohexylglycolide-co-dihexylglycolide)s (♦) and poly(hexylcyclohexylglycolide) (▲) fit to the Fox equation.....   | 85  |
| Figure 32. DSC analysis of a 1:1 blend of poly(dicyclohexylglycolide) and poly(dihexylglycolide). Heating rate: 10 °C/min under nitrogen. The data are from the second heating scan, taken after flash quenching from 120 °C. .... | 86  |
| Figure 33. 500 MHz <sup>1</sup> H NMR spectra of poly(dicyclohexylglycolide)- <i>b</i> -poly(ethylene glycol)- <i>b</i> -poly(dicyclohexylglycolide)s .....  | 94  |
| Figure 34. GPC traces of PDCG-PEG-PDCG triblock copolymers .....   | 95  |
| Figure 35. DSC analyses of PDCG-PEG-PDCG triblock copolymers. Heating rate: 10 °C/min under nitrogen. The data are from second heating scans, taken after flash quenching from 120 °C. ....  | 96  |
| Figure 36. AFM height image (top) and phase image (bottom) of PDCG-PEG2000-PDCG triblock copolymer. ....   | 97  |
| Figure 37. AFM height image (top) and phase image (bottom) of poly(dicyclohexylglycolide) .....  | 98  |
| Figure 38. Structures of 1,4-benzodioxepin-3-alkyl-2,5-diones .....  | 101 |
| Figure 39. 500 MHz <sup>1</sup> H NMR spectra of 1,4-benzodioxepin-3-methyl-2,5-dione and its polymer .....  | 108 |
| Figure 40. 500 MHz <sup>1</sup> H NMR spectrum of 1,4-benzodioxepin-3-methyl-2,5-dione ring-opened product by Sn(2-ethylhexanoate) <sub>2</sub> and 4- <i>tert</i> -butylbenzyl alcohol .....                                      | 109 |
| Figure 41. 500 MHz <sup>1</sup> H NMR spectrum of 1,4-benzodioxepin-3-methyl-2,5-dione ring-opened product by DMAP and 1-phenylethanol .....   | 110 |
| Figure 42. Solution polymerization kinetics of 1,4-benzodioxepin-3-methyl-2,5-dione (♦) and 1,4-benzodioxepin-3-cyclohexyl-2,5-dione (▲). Polymerization conditions: 90 °C, [monomer]: [DMAP]: [1-phenylethanol] = 100: 2: 1. .... | 113 |

|   |     |
|---|-----|
| Figure 44. Bulk polymerization kinetics of 1,4-benzodioxepin-3-cyclohexyl-2,5-dione. Polymerization conditions: 160 °C, [monomer]: [DMAP]: [1-phenylethanol] = 100: 2: 1.....   | 117 |
| Figure 45. Evolution of the molecular weight (♦) and polydispersity (●) with conversion for the bulk polymerization of 1,4-benzodioxepin-3-methyl-2,5-dione. Polymerization conditions: 130 °C, [monomer]: [DMAP]: [1-phenylethanol] = 100: 2: 1.....     | 118 |
| Figure 46. Evolution of the molecular weight (♦) and polydispersity (●) with conversion for the bulk polymerization of 1,4-benzodioxepin-3-cyclohexyl-2,5-dione. Polymerization conditions: 160 °C, [monomer]: [DMAP]: [1-phenylethanol] = 100: 2: 1..... | 119 |
| Figure 47. Thermogravimetric analysis results for poly(1,4-benzodioxepin-3-alkyl-2,5-dione)s. Samples were run in air at a heating rate of 10 °C/min. ....  | 121 |
| Figure 48. DSC analyses of poly(1,4-benzodioxepin-3-alkyl-2,5-dione)s. Heating rate: 10 °C/min under nitrogen. The data are second heating scans, taken after flash quenching from 150 °C. ....   | 122 |
| Figure A- 1. <sup>1</sup> H NMR spectrum of 2-cyclohexyl-2-hydroxyacetic acid .....   | 139 |
| Figure A- 2. <sup>13</sup> C NMR spectrum of 2-cyclohexyl-2-hydroxyacetic acid .....  | 140 |
| Figure A- 3. FT-IR spectrum of 2-cyclohexyl-2-hydroxyacetic acid .....  | 141 |
| Figure A- 4. <sup>1</sup> H NMR spectrum of ( <i>R</i> )-(-)-2-cyclohexyl-2-hydroxyacetic acid ....   | 142 |
| Figure A- 5. <sup>13</sup> C NMR spectrum of ( <i>R</i> )-(-)-2-cyclohexyl-2-hydroxyacetic acid ...   | 143 |
| Figure A- 6. FT-IR spectrum of ( <i>R</i> )-(-)-2-cyclohexyl-2-hydroxyacetic acid .....   | 144 |
| Figure A- 7. <sup>1</sup> H NMR spectrum of <i>rac</i> -dicyclohexylglycolide .....   | 145 |
| Figure A- 8. <sup>13</sup> C NMR spectrum of <i>rac</i> -dicyclohexylglycolide .....  | 146 |
| Figure A- 9. FT-IR spectrum of <i>rac</i> -dicyclohexylglycolide .....  | 147 |
| Figure A- 10. <sup>1</sup> H NMR spectrum of <i>meso</i> -dicyclohexylglycolide.....  | 148 |
| Figure A- 11. <sup>13</sup> C NMR spectrum of <i>meso</i> -dicyclohexylglycolide .....  | 149 |
| Figure A- 12. FT-IR spectrum of <i>meso</i> -dicyclohexylglycolide .....  | 150 |
| Figure A- 13. <sup>1</sup> H NMR spectrum of <i>R,R</i> -dicyclohexylglycolide .....  | 151 |

|   |     |
|---|-----|
| Figure A- 14. $^{13}\text{C}$ NMR spectrum of <i>R,R</i> -dicyclohexylglycolide .....         | 152 |
| Figure A- 15. FT-IR spectrum of <i>R,R</i> -dicyclohexylglycolide .....                       | 153 |
| Figure A- 16. $^1\text{H}$ NMR spectrum of <i>rac</i> -diisopropylglycolide.....              | 154 |
| Figure A- 17. $^{13}\text{C}$ NMR spectrum of <i>rac</i> -diisopropylglycolide .....          | 155 |
| Figure A- 18. FT-IR spectrum of <i>rac</i> -diisopropylglycolide .....                        | 156 |
| Figure A- 19. $^1\text{H}$ NMR spectrum of <i>rac</i> -methylcyclohexylglycolide.....         | 157 |
| Figure A- 20. NOE NMR spectrum of <i>rac</i> -methylcyclohexylglycolide.....                  | 158 |
| Figure A- 21. $^{13}\text{C}$ NMR spectrum of <i>rac</i> -methylcyclohexylglycolide .....     | 159 |
| Figure A- 22. FT-IR spectrum of <i>rac</i> -methylcyclohexylglycolide.....                    | 160 |
| Figure A- 23. $^1\text{H}$ NMR spectrum of <i>rac</i> -hexylcyclohexylglycolide.....          | 161 |
| Figure A- 24. NOE NMR spectrum of <i>rac</i> -hexylcyclohexylglycolide.....                   | 162 |
| Figure A- 25. $^{13}\text{C}$ NMR spectrum of <i>rac</i> -hexylcyclohexylglycolide .....      | 163 |
| Figure A- 26. FT-IR spectrum of <i>rac</i> -hexylcyclohexylglycolide.....                     | 164 |
| Figure A- 27. $^1\text{H}$ NMR spectrum of 1,4-benzodioxepin-3-methyl-2,5-dione .....         | 165 |
| Figure A- 28. $^{13}\text{C}$ NMR spectrum of 1,4-benzodioxepin-3-methyl-2,5-dione .....      | 166 |
| Figure A- 29. FT-IR spectrum of 1,4-benzodioxepin-3-methyl-2,5-dione .....                    | 167 |
| Figure A- 30. $^1\text{H}$ NMR spectrum of 1,4-benzodioxepin-3-cyclohexyl-2,5-dione.....      | 168 |
| Figure A- 31. $^{13}\text{C}$ NMR spectrum of 1,4-benzodioxepin-3-cyclohexyl-2,5-dione .....  | 169 |
| Figure A- 32. FT-IR spectrum of 1,4-benzodioxepin-3-cyclohexyl-2,5-dione ....                 | 170 |
| Figure A- 33. $^1\text{H}$ NMR spectrum of poly( <i>rac</i> -dicyclohexylglycolide) .....     | 171 |
| Figure A- 34. $^{13}\text{C}$ NMR spectrum of poly( <i>rac</i> -dicyclohexylglycolide) .....  | 172 |
| Figure A- 35. $^1\text{H}$ NMR spectrum of poly( <i>meso</i> -dicyclohexylglycolide).....     | 173 |
| Figure A- 36. $^{13}\text{C}$ NMR spectrum of poly( <i>meso</i> -dicyclohexylglycolide) ..... | 174 |
| Figure A- 37. $^1\text{H}$ NMR spectrum of poly( <i>R,R</i> -dicyclohexylglycolide) .....     | 175 |

|  |     |
|--|-----|
| Figure A- 38. $^{13}\text{C}$ NMR spectrum of poly( <i>R,R</i> -dicyclohexylglycolide).....            | 176 |
| Figure A- 39. $^1\text{H}$ NMR spectrum of poly( <i>rac</i> -diisopropylglycolide).....                | 177 |
| Figure A- 40. $^{13}\text{C}$ NMR spectrum of poly( <i>rac</i> -diisopropylglycolide) .....            | 178 |
| Figure A- 41. $^1\text{H}$ NMR spectrum of poly( <i>rac</i> -methylcyclohexylglycolide).....           | 179 |
| Figure A- 42. $^{13}\text{C}$ NMR spectrum of poly( <i>rac</i> -methylcyclohexylglycolide) .....       | 180 |
| Figure A- 43. $^1\text{H}$ NMR spectrum of poly( <i>rac</i> -hexylcyclohexylglycolide).....            | 181 |
| Figure A- 44. $^{13}\text{C}$ NMR spectrum of poly( <i>rac</i> -hexylcyclohexylglycolide) .....        | 182 |
| Figure A- 45. $^1\text{H}$ NMR spectrum of poly(1,4-benzodioxepin-3-methyl-2,5-dione)<br>.....         | 183 |
| Figure A- 46. $^{13}\text{C}$ NMR spectrum of poly(1,4-benzodioxepin-3-methyl-2,5-dione)<br>.....      | 184 |
| Figure A- 47. $^1\text{H}$ NMR spectrum of poly(1,4-benzodioxepin-3-cyclohexyl-2,5-<br>dione) .....    | 185 |
| Figure A- 48. $^{13}\text{C}$ NMR spectrum of poly(1,4-benzodioxepin-3-cyclohexyl-2,5-<br>dione) ..... | 186 |

## LIST OF SCHEMES

|   |    |
|---|----|
| Scheme 1. Synthetic routes to symmetrical dialkylglycolides.....  | 7  |
| Scheme 2. Synthetic route to nonsymmetrical substituted glycolides .....  | 10 |
| Scheme 3. Anionic polymerization of tetramethylglycolide.....   | 13 |
| Scheme 4. Ring-opening of $\alpha,\alpha'$ -2,5-dioxabicyclo[2.2.2]octane-3,6-dione .....   | 14 |
| Scheme 5. Synthetic route to diallylglycolide .....   | 14 |
| Scheme 6. Polymer-bound olefin metathesis of poly(lactide-co-diallylglycolide)<br>with olefin substrates containing bioactive ligands ..... | 15 |
| Scheme 7. Polymer-bound hydroboration-oxidation and DCC coupling .....  | 15 |
| Scheme 8. Synthetic routes to dimethyleneglycolide and methylmethyleneglycolide .....   | 16 |
| Scheme 9. Equilibrium between <i>meso</i> -mandelide and <i>rac</i> -mandelide.....   | 19 |
| Scheme 10. Synthetic routes to benzyl-protected malides.....  | 22 |
| Scheme 11. Attaching Adriamycin to poly( $\alpha$ -malic acid) .....  | 22 |
| Scheme 12. Synthesis of benzyloxymethylglycolide and poly(glycolic acid- <i>alt</i> -glyceric acid) .....                                   | 23 |
| Scheme 13. Synthetic routes to DIPAGYL and DIPALYL .....  | 24 |
| Scheme 14. Deprotection of poly(DIPAGYL-co- <i>rac</i> -lactide).....   | 25 |
| Scheme 15. Synthesis and polymerization of $\alpha,\alpha'$ -difluorolactide .....  | 26 |
| Scheme 16. Synthetic route to <i>p</i> -dioxanone .....   | 28 |
| Scheme 17. Synthetic route to 3-methyl- <i>p</i> -dioxanone.....  | 30 |
| Scheme 18. Synthetic route to <i>S,S</i> -dimethyltetraoxacyclotetradecanedione .....   | 31 |
| Scheme 19. Synthetic route to 6-hydroxymethyl- <i>p</i> -dioxanone .....  | 32 |
| Scheme 20. Polymerization of 6-hydroxymethyl- <i>p</i> -dioxanone .....   | 33 |
| Scheme 21. Hyperbranched polymer made from AB <sub>2</sub> monomer.....   | 33 |

|   |     |
|---|-----|
| Scheme 22. Polymerization of 7-methyl-1,4-dioxepane-2,5-dione .....   | 34  |
| Scheme 23. Polymerization of 1,4-benzodioxepin-2,5(3H)-dione .....  | 35  |
| Scheme 24. Polymerization of morpholine-2,5-dione derivatives .....   | 36  |
| Scheme 25. Synthesis of poly(lactic acid- <i>alt</i> -L-lysine) .....   | 40  |
| Scheme 26. Synthesis of copolymers of L-lactide and morpholine-2,5-diones with<br>pendant protected hydroxyl groups ..... | 42  |
| Scheme 27. Synthesis of poly(glycolic acid- <i>alt</i> -aspartic acid) .....  | 42  |
| Scheme 28. Synthetic routes to $\alpha$ -hydroxy acids .....  | 46  |
| Scheme 29. Synthetic routes to lactide derivatives .....  | 46  |
| Scheme 30. Butanolysis of poly(dicyclohexylglycolide) .....   | 72  |
| Scheme 31. Copolymerization of dicyclohexylglycolide and dihexylglycolide .....   | 77  |
| Scheme 32. Synthetic route to hexylcyclohexylglycolide .....  | 80  |
| Scheme 33. Ring-opening polymerization of hexylcyclohexylglycolide .....  | 81  |
| Scheme 34. Phase separation and morphology changes of block copolymers ..   | 89  |
| Scheme 35. Synthesis of PDCG-PEG-PDCG triblock polymers .....   | 90  |
| Scheme 36. Synthesis and degradation of poly(1,4-benzodioxepin-2,5(3H)-dione)<br>.....                                    | 100 |
| Scheme 37. Synthetic route to 1,4-benzodioxepin-3-methyl-2,5-dione .....  | 102 |
| Scheme 38. Synthetic route to 1,4-benzodioxepin-3-cyclohexyl-2,5-dione .....  | 102 |
| Scheme 39. Pathways of ROP of 1,4-benzodioxepin-3-alkyl-2,5-diones .....  | 104 |
| Scheme 40. Mechanism of ROP of lactide initiated by DMAP and alcohol .....  | 105 |
| Scheme 41. Mechanism of ROP of 1,4-benzodioxepin-3-alkyl-2,5-dione initiated<br>by DMAP and alcohol .....                 | 106 |

## LIST OF ABBREVIATIONS

|                   |   |
|-------------------|---|
| $\alpha$          | angle of optical rotation   |
| AFM               | atomic force microscopy   |
| <i>alt</i>        | alternating   |
| $\delta$          | chemical shift  |
| d                 | doublet   |
| Da                | Dalton  |
| DCC               | N,N'-dicyclohexylcarbodiimide   |
| dd                | doublet of doublet  |
| DIPAGYL           | 3-(1,2-3,4-tetraoxobutyl-diisopropylidene)dioxane-2,5-dione           |
| DIPALYL           | 3-methyl-6-(1,2-3,4-tetraoxobutyl-diisopropylidene)-dioxane-2,5-dione |
| DMAP              | 4-dimethylaminopyridine   |
| DMSO              | dimethyl sulfoxide  |
| dq                | doublet of quartet  |
| DSC               | differential scanning calorimetry                                     |
| EI                | electron impact   |
| Et <sub>3</sub> N | triethyl amine  |
| GC                | gas chromatography  |
| GPC               | gel permeation chromatography   |
| HOct              | 2-ethylhexanoic acid  |
| Hz                | hertz   |
| IR                | infrared spectroscopy   |
| <i>J</i>          | coupling constant   |



|               |   |
|---------------|---|
| m             | multiplet   |
| M             | mole per liter  |
| $M_e$         | entanglement molecular weight   |
| MHz           | megahertz   |
| $M_n$         | number average molecular weight   |
| mp            | melting point   |
| MS            | mass spectroscopy   |
| $M_w$         | weight average molecular weight   |
| $m/z$         | The mass of an ion in atomic units divided by its charge number   |
| $\nu$         | wavenumber  |
| NFBS          | N-fluorobenzenesulfonimide  |
| NMR           | nuclear magnetic resonance spectroscopy   |
| NOE           | nuclear Overhauser effect   |
| $p$           | para  |
| PBT           | poly(butylene terephthalate)  |
| PDCG          | poly(dicyclohexylglycolide)   |
| PDCG-PEG-PDCG | poly(dicyclohexylglycolide)- <i>block</i> -poly(ethylene glycol)- <i>block</i> -poly(dicyclohexylglycolide) |
| PDI           | polydispersity index  |
| PEG           | poly(ethylene glycol)   |
| PEO           | poly(ethylene oxide)  |
| PET           | poly(ethylene terephthalate)  |
| PHB           | poly(3-hydroxybutyrate)   |
| PLA           | polylactide or poly(lactic acid)  |

|                      |                                      |
|----------------------|--------------------------------------|
| ppm                  | parts per million                    |
| psi                  | pound per square inch                |
| ROP                  | ring-opening polymerization          |
| s                    | singlet                              |
| sec                  | secondary                            |
| Sn(Oct) <sub>2</sub> | tin(II) 2-ethylhexanoate             |
| t                    | triplet                              |
| <i>tert</i>          | tertiary                             |
| $T_g$                | glass transition temperature         |
| TEM                  | transmission electron microscopy     |
| TGA                  | thermal gravimetric analysis         |
| THF                  | tetrahydrofuran                      |
| TM-AFM               | tapping-mode atomic force microscopy |
| TsOH                 | <i>p</i> -toluenesulfonic acid       |

## Chapter 1 Introduction

For the past 60 years, petroleum-based synthetic polymers have had a tremendous impact on our daily lives. Despite the numerous advantages of these materials, the resistance of synthetic polymer materials to degradation in the environment is becoming more and more problematic, especially when materials are used for a limited time before becoming waste. According to an Environmental Protection Agency study, the total amount of plastics in municipal solid waste has increased from less than 1 percent in 1960 to 11.1 percent, or 26.7 million tons, in 2003.

In response to the increasing plastic waste discarded in landfills, current research is aimed at the discovery of biodegradable substitutes for conventional commodity thermoplastics, especially those that can be obtained from renewable resources. Among the families of biodegradable polymers, aliphatic polyesters, especially polylactide and polyglycolide, have generated considerable interest because of their high mechanical strength, excellent shaping and molding properties, biocompatibility, and degradability.

Early studies on polylactides focused on applications that exploit their *in vivo* degradability such as materials for surgical implants and tissue repair. American Cyanamid Co. first developed polyglycolide resorbable sutures in 1967,<sup>1</sup> and glycolide-L-lactide copolymers became available a few years later.<sup>2</sup> Due to their high cost, polylactides were restricted to the biomedical area until Cargill Dow LLC (now NatureWorks LLC), a joint venture between Cargill

Incorporated and The Dow Chemical Company, developed a large-scale and low-cost process to make polylactide from renewable resources (**Figure 1**).<sup>3</sup>

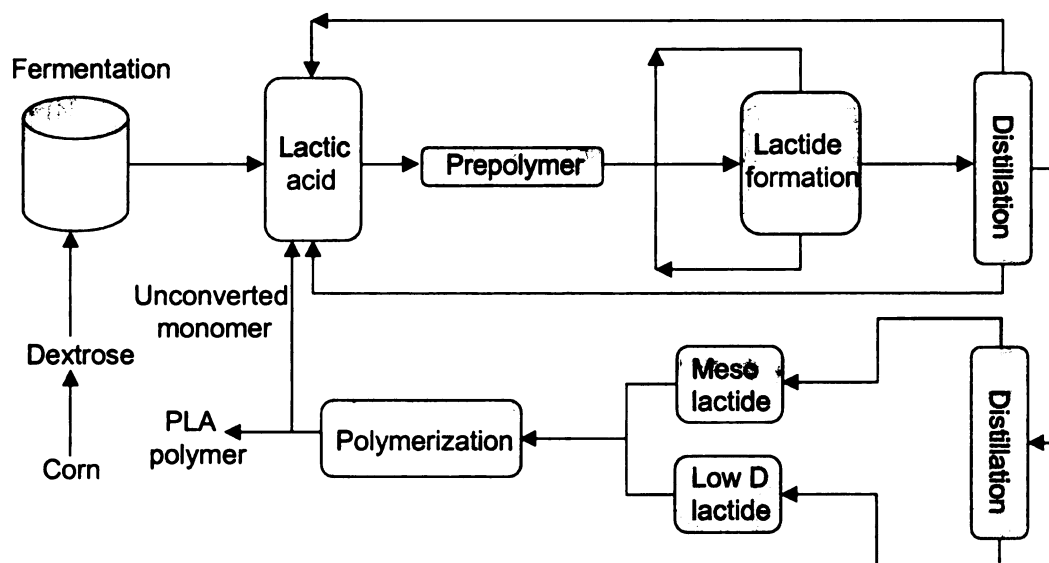


**Figure 1.** NatureWorks LLC process for the manufacture of polylactide

This solvent-free, continuous process for polylactide production starts with the fermentation of starch-rich renewable resources such as corn and maize to provide lactic acid. Condensation of lactic acid produces a low molecular weight polylactide prepolymer, which is then cracked to a mixture of lactide stereoisomers, primarily L-lactide. After purification by vacuum distillation, tin catalysts are used to polymerize lactide to high molecular weight polymer by ring-opening melt polymerization. Residual monomer is removed under vacuum and recycled.<sup>3</sup>

With reductions in manufacturing costs, polylactide is now attractive for applications in a broad array of products, such as food packaging, clothing, and hygiene products (**Table 1**).<sup>4</sup>

**Table 1.** Applications of polylactide as commodity polymers (NatureWorks LLC)<sup>4</sup>

| <b>Business segment</b>                       | <b>Commercially available applications</b>   |
|---|--|
| Rigid thermoforms<br>(NatureWorks™)           | <ul style="list-style-type: none"><li>▪ Clear fresh fruit and vegetable clamshells</li><li>▪ Deli meat trays</li><li>▪ Opaque dairy (yogurt) containers</li><li>▪ Bakery, fresh herb and candy containers</li><li>▪ Consumer displays &amp; electronics packaging</li><li>▪ Disposable articles and cold drink cups</li></ul>  |
| Biaxially-oriented<br>films<br>(NatureWorks™) | <ul style="list-style-type: none"><li>▪ Candy twist and flow wrap</li><li>▪ Envelop and display carton windows</li><li>▪ Lamination film</li><li>▪ Product (gift basket) overwrap</li><li>▪ Lidding stock</li><li>▪ Die cut labels</li><li>▪ Floral wrap</li><li>▪ Tapes</li><li>▪ Shrink sleeves</li><li>▪ Stand-up pouches</li><li>▪ Cake mix, cereal and bread bags</li></ul> |
| Bottles<br>(NatureWorks™)                     | <ul style="list-style-type: none"><li>▪ Short shelf-life milk</li><li>▪ Edible oils</li><li>▪ Bottled water</li></ul>  |
| Apparel (Ingeo™)                              | Casual, sports, active, and underwear and fashion  |
| Non-wovens<br>(Ingeo™)                        | Wipes, hygiene products, diapers, shoe liners,<br>automotive head and door liners and paper<br>reinforcement   |
| Furnishings<br>(Ingeo™)                       | Blankets and panel, upholstery and decorative<br>fabrics   |
| Industrial (Ingeo™)                           | Agricultural and geo textiles  |
| Carpet (Ingeo™)                               | Residential/institutional broadloom and carpet tiles   |
| Fiberfill (Ingeo™)                            | Pillows, comforters, mattresses, furniture   |

However, to be suitable for different applications and replace current nondegradable commodity polymers such as aromatic polyesters, polyolefins, and nylons, polylactides must exhibit a broader range of physical properties while retaining the degradability of the parent polymer. Blending and copolymerization are two of the most common and economical ways to improve polymer properties, but they only provide limited solutions to the need for a broader spectrum of degradable polymers. Currently, the high crystallinity of polylactide interferes with controllable degradation, and the relatively low glass transition temperature ( $T_g$ ) limits its use as a rigid, clear replacement for large-volume thermoplastics such as polystyrene. Moreover, polylactides have no functional groups in their structures other than the backbone ester groups and chain ends, which limits further chemical modifications. These limitations motivate the synthesis of tailored polylactides which possess new features, such as increased functionality, new tacticities, controllable hydrophilicity, increased  $T_g$  for amorphous polymers, tunable  $T_m$  for crystalline polymers, and better impact resistance.

Of fundamental importance is the development of a clear understanding of the factors affecting the chemistry of ring-opening polymerization of cyclic esters and the influence of monomer structures on polymer properties, such as ring substitutions, ring size, and other functionalities within the ring. Current research is focused on four different types of  $\alpha$ -hydroxy acid-containing cyclic esters: substituted glycolides ( $\alpha$ -hydroxy acid –  $\alpha$ -hydroxy acid), *p*-dioxanone and derivatives ( $\alpha$ -hydroxy acid – ethylene glycol/propylene glycol), dioxepanedione

and derivatives ( $\alpha$ -hydroxy acid –  $\beta$ -hydroxy acid), and depsipeptides ( $\alpha$ -hydroxy acid –  $\alpha$ -amino acid) (**Figure 2**).

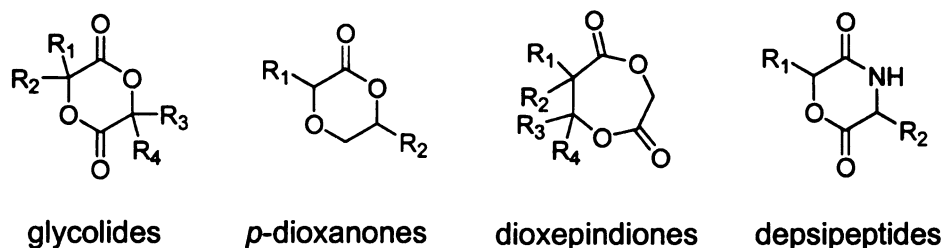


**Figure 2.** Structures of  $\alpha$ -hydroxy acid-containing cyclic esters

### Substituted glycolides

An often ignored but important fact is that polylactide degrades via simple chemical hydrolysis and not enzymatically,<sup>5</sup> despite the ability of certain enzymes such as proteinase K to cleave their main chain.<sup>6-11</sup> It is only at the last stages of the hydrolytic degradation process that oligomeric degradation byproducts become small enough to be processed by microorganisms. Because the structure of the polymer backbone is unchanged, polymers derived from modified lactide monomers will not sacrifice the degradability of the parent polymer.

As more  $\alpha$ -hydroxy acids can be directly made from fermentation of starch-rich renewable resources, such as 2-hydroxyisocaproic acid and  $\beta$ -phenyllactic acid by *Clostridium beijerinckii* strain HICA432,<sup>12</sup> the polymerization of substituted glycolides is attracting both academic and commercial interest.

## Alkyl-, alkenyl-, and aryl-substituted glycolides

### Symmetrical dialkylglycolides

Dimerizing DL-lactic acid forms D- (or *R,R*-)-lactide, L- (or *S,S*-) lactide, and *meso*-lactide (or *R,S*-lactide). An equal molar mixture of D-lactide and L-lactide is called racemic lactide (*rac*-lactide), and mixtures of *rac*-lactide and *meso*-lactide are sometimes called DL-lactide (**Figure 3**).

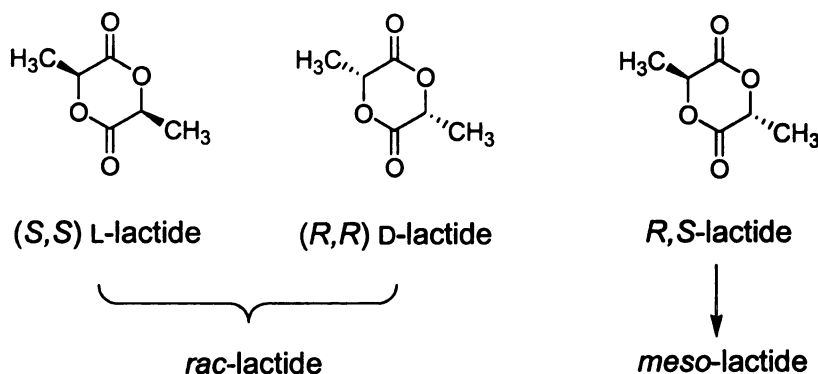


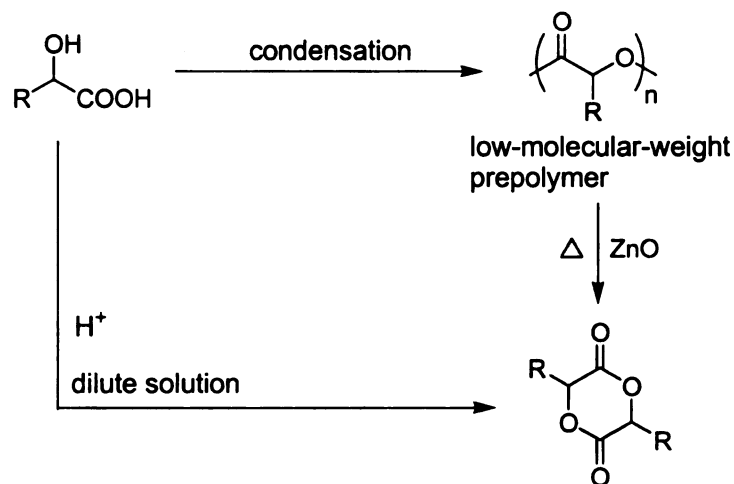
**Figure 3.** Structures of lactide stereoisomers

Like lactide, symmetrical dialkylglycolides exist as *R,R*-, *S,S*-, and *R,S*- stereoisomers, and can be synthesized by using zinc oxide to catalyze the thermal cracking of low molecular weight prepolymer, or dimerizing  $\alpha$ -hydroxy acids in dilute solution with azeotropic removal of water, to form the substituted glycolide directly (**Scheme 1**).

By changing the pendant methyl groups on lactide to ethyl, isopropyl, isobutyl, or hexyl groups, a series of polylactides with different side chains have been synthesized,<sup>13-16</sup> and their structures are shown in **Figure 4**. In this thesis,



lactide derivatives are described as substituted glycolides; for example, 3,6-diethyl-1,4-dioxane-2,5-dione corresponds to diethylglycolide.



**Scheme 1.** Synthetic routes to symmetrical dialkylglycolides

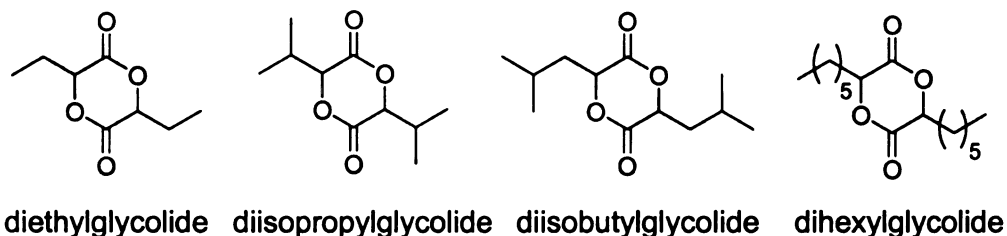


**Figure 4.** Structures of symmetrical dialkylglycolides

Homopolymers of diisopropylglycolide and diisobutylglycolide were first synthesized in 1971 by ring-opening polymerization of the corresponding DL- and L-glycolides.<sup>13</sup> Catalyzed by 0.5-1.5 wt% ZnO, polymerization of L-diisopropylglycolide at 180 °C for 80 hours provided a highly crystalline polymer with a  $T_m$  around 183-192 °C. Poly(L-diisobutylglycolide) prepared under similar polymerization conditions was amorphous. Thirty years later, the crystallinity of

poly(L-diisopropylglycolide) was re-examined.<sup>14</sup> This time the polymerization of optically pure L-diisopropylglycolide was catalyzed by Sn(2-ethylhexanoate)<sub>2</sub> with 4-*tert*-butylbenzyl alcohol as the initiator and run at 180 °C for only 1 hour (95% conversion) to minimize racemization. The resulting polymer had a melting point around ~230 °C, 50 °C higher than that of poly(L-lactide).

**Table 2.** Properties of symmetrical dialkylglycolide polymers

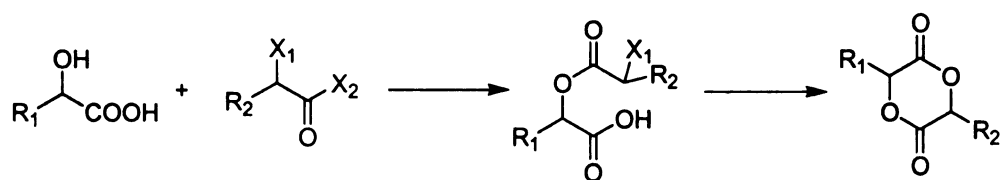
| Polymer                                  | $M_n$  | $M_w/M_n$ | $T_g$ (°C) |
|--|--------|-----------|------------|
| poly(diethylglycolide) <sup>14</sup>     | 45,600 | 1.78      | 15         |
| poly(diisopropylglycolide) <sup>14</sup> | N/A    | N/A       | 50         |
| poly(diisobutylglycolide) <sup>14</sup>  | 47,300 | 1.83      | 22         |
| poly(dihexylglycolide) <sup>14</sup>     | 43,200 | 1.91      | -37        |
| poly(dihexylglycolide) <sup>16</sup>     | 5,600  | 1.09      | -47        |

Polymerizations of optically inactive DL-lactides provide only amorphous polyesters.<sup>14,16</sup> One of most important physical properties of these materials is the  $T_g$ , since it defines the temperature range where the polymer is dimensionally stable. The  $T_g$  of a substituted polylactide depends on the flexibility of polymer chain and dipole-dipole interactions between polymer chains, although crystallinity and molecular weight also affect  $T_g$  to some extent. When the side chains are alkyl groups and only differ in the length of the alkyl chain, the secondary forces between polymer chains are only slightly affected, and steric hindrance and the size of side chains determine  $T_g$  (see the trend in **Table 2**).

Steric hindrance also affects the ring-opening polymerization rates of lactides, with increasing steric hindrance causing slower polymerization. However, Yin reported that the order of polymerization rates for substituted glycolides in toluene at 90 °C using  $\text{Al}(\text{OiPr})_3$  as the catalyst was diisobutylglycolide > lactide > diethylglycolide > dihexylglycolide.<sup>14</sup> Solution polymerizations using  $\text{Sn}(\text{2-ethylhexanoate})_2$  and 4-*tert*-butylbenzyl alcohol in toluene at 90 °C gave different results: lactide > diisobutylglycolide > diethylglycolide > dihexylglycolide.<sup>14</sup> In both solution polymerizations, the most sterically hindered monomer, diisobutylglycolide, did not have the slowest polymerization rate, although in bulk polymerizations at 130 °C diisobutylglycolide proved to be the slowest. Yin proposed that since both the  $\text{Al}(\text{OiPr})_3$  and  $\text{Sn}(\text{2-ethylhexanoate})_2/\text{ROH}$  initiator systems follow a coordination-insertion mechanism, the rate determining step might not be the nucleophilic attack of the metal alkoxide on the glycolide ring. However, other factors, such as monomer purity and differences in the racemic-meso isomer ratio, may be responsible for the changes in the order of polymerization rate.

### **Nonsymmetrical alkyl-substituted glycolides**

The synthetic route to nonsymmetrical glycolides is shown in **Scheme 2**, where  $\text{X}_1$  and  $\text{X}_2$  represent chloride or bromide. Simply heating the reactants or catalyzing the reaction with base in solution at low temperature (~0 °C) forms the linear dimer, which is then cyclized by using base in dilute solution to favor the intramolecular reaction.



**Scheme 2.** Synthetic route to nonsymmetrical substituted glycolides

The synthesis and polymerization of nonsymmetrical alkyl-substituted glycolides originated from the desire to synthesize chemically uniform lactide-glycolide copolymers.<sup>17</sup> When copolymerizing lactide and glycolide, the initial stages of the polymerization favors incorporation of glycolide due to its higher reactivity. On the other hand, polymerization of 3-methyl-1,4-dioxane-2,5-dione (methylglycolide, **Figure 5**) results in a polymer having lactic acid and glycolic acid repeating units homogeneously distributed along the chain.<sup>16-19</sup>

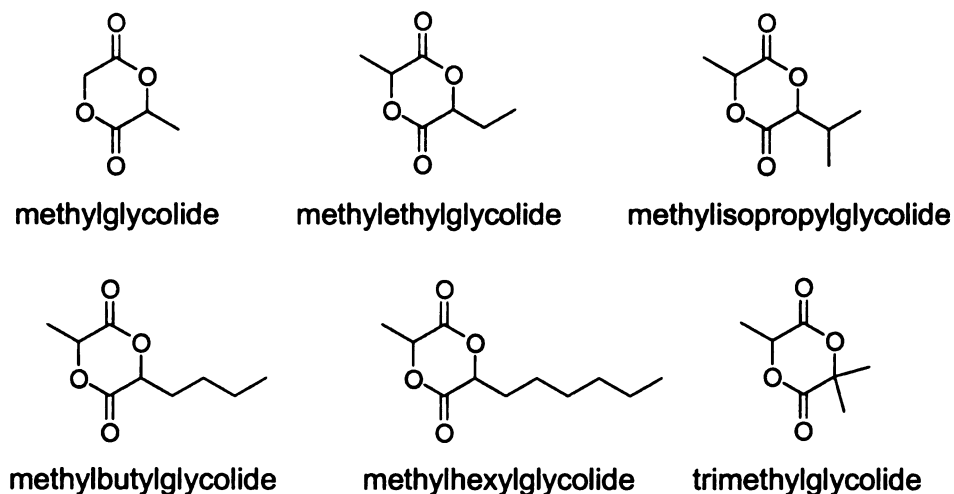


**Figure 5.** Structures of nonsymmetrical alkyl-substituted glycolides

The nonsymmetric nature of alkyl-substituted glycolides leads to preferential ring-opening at the less-hindered site. The experimentally

determined polymerization rates for methylbutylglycolide, methylhexylglycolide, and methylisopropylglycolide are similar, with methylbutylglycolide  $\geq$  methylhexylglycolide  $>$  methylisopropylglycolide.<sup>16</sup> Thus, the substituent opposite the methyl group has a minor influence on the ring-opening process. However, the trisubstituted glycolide trimethylglycolide is apparently so hindered that its polymerization rate is more than 50 times slower than the other glycolides shown in **Figure 5**. In order to reach high conversion, trimethylglycolide is polymerized either at high temperature for a long time, or with a much more active catalyst. Baker and coworkers initiated polymerization of trimethylglycolide with 4-*tert*-butylbenzyl alcohol and Sn(2-ethylhexanoate)<sub>2</sub> as the catalyst, obtaining 75% conversion after 24 hours at 180 °C.<sup>20</sup> Trimaille et al. used 4-(dimethylamino)pyridine (DMAP) and benzyl alcohol to polymerize trimethylglycolide at 100 °C, and they reported 75% conversion after 5 hours.<sup>16</sup>

**Table 3.** Properties of nonsymmetrical dialkylglycolides polymers

| Polymer                                      | $M_n$  | $M_w/M_n$ | $T_g$ (°C) |
|--|--------|-----------|------------|
| poly(methylglycolide) <sup>19</sup>          | N/A    | N/A       | 42         |
| poly(methylethylglycolide) <sup>16</sup>     | 31,200 | 1.81      | 22         |
| poly(methylisopropylglycolide) <sup>14</sup> | 2,000  | 1.18      | N/A        |
| poly(methylbutylglycolide) <sup>14</sup>     | 3,850  | 1.22      | N/A        |
| poly(methylhexylglycolide) <sup>14</sup>     | 4,450  | 1.13      | N/A        |
| poly(trimethylglycolide) <sup>16</sup>       | 4,200  | 1.25      | 50         |

Similar to the trends in **Table 2**, the  $T_g$ s of polymers derived from nonsymmetrical alkyl-substituted glycolides are determined by the bulkiness of their side groups. Their physical properties are listed in **Table 3**.<sup>14,16,19</sup>

### Other alkyl-substituted glycolides

The three lactide derivatives shown in **Figure 6** are particularly interesting. The first, tetramethylglycolide, is reported to be inert to ring-opening reactions.<sup>15,21-23</sup> Unsuccessful catalysts/initiators for ring-opening polymerization include Na/NaH, Sn(2-ethylhexanoate)<sub>2</sub>, and Ph<sub>3</sub>SnNMe<sub>2</sub>. This inertness, also seen to a lesser extent in trimethylglycolide, is caused by the steric hindrance from the four methyl groups, which shields the upper and lower faces of the six-membered ring and hinders nucleophilic attack at the carbonyl groups.

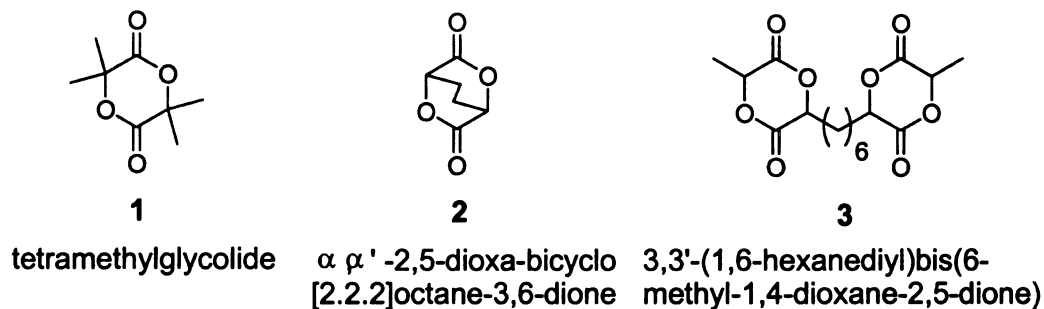
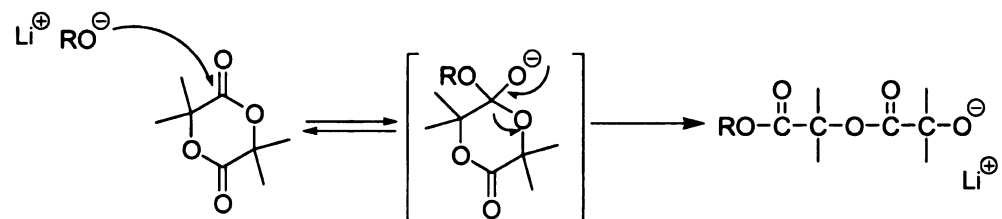


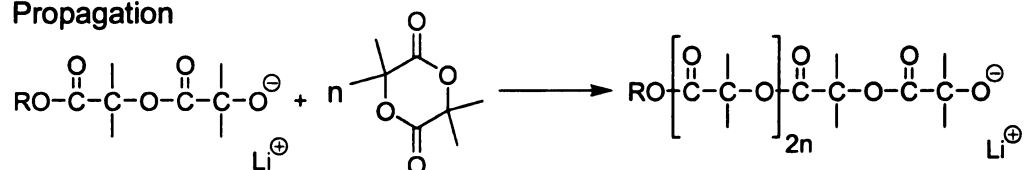
**Figure 6.** Structures of other alkyl-substituted glycolides

Tetramethylglycolide's inertness to ring-opening does not hold for certain anionic polymerization conditions. In 1971, poly(tetramethylglycolide) was successfully synthesized in > 90% yield with molecular weights up to 250,000 by using lithium *tert*-butylate as the initiator.<sup>24</sup> The polymerization followed the classical anionic polymerization mechanism, which is depicted in **Scheme 3**.

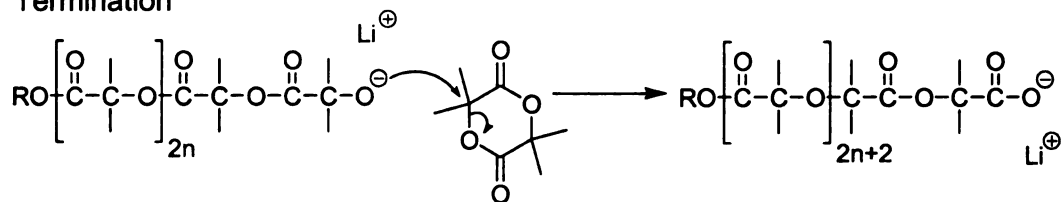
### Initiation



### Propagation



### Termination



**Scheme 3.** Anionic polymerization of tetramethylglycolide

The second monomer in **Figure 6**,  $\alpha,\alpha'$ -2,5-dioxabicyclo[2.2.2]octane-3,6-dione (**2**),<sup>25</sup> is a bicyclic lactone that resembles the well-studied 2,2'-bis( $\epsilon$ -caprolatone-4-yl)propane (**4** in **Figure 7**).<sup>26-29</sup> Because the monomers are tetrafunctional, both can be used to synthesize highly branched or completely crosslinked polyesters.

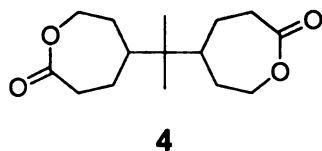
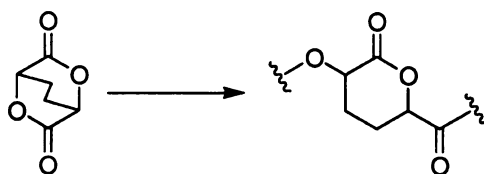


**Figure 7.** Structure of 2,2'-bis( $\epsilon$ -caprolatone-4-yl)propane

However, a significant difference is that the two esters in **4** are chemical equivalent, but the esters in **2** are not. Opening the first ring in **2** forms a less-strained and less reactive  $\delta$ -valerolactone (**Scheme 4**).<sup>23</sup>

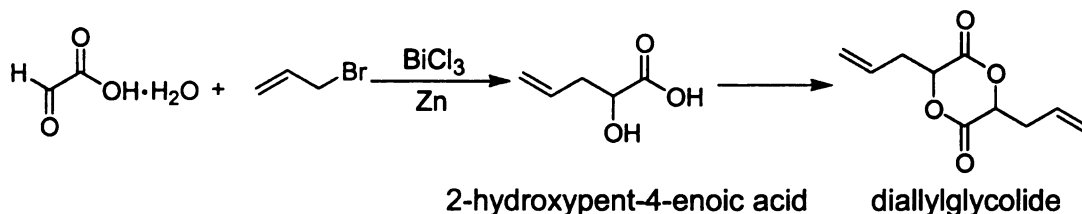


**Scheme 4.** Ring-opening of  $\alpha, \alpha'$ -2,5-dioxabicyclo[2.2.2]octane-3,6-dione

Obtaining equivalent reactivities requires linking two glycolide rings by a tether, as in 3,3'-(1,6-hexanediyl)bis(6-methyl-1,4-dioxane-2,5-dione) (monomer **3** in **Figure 6**).<sup>30</sup> In this case, opening one glycolide ring will not affect the reactivity of the remaining ring.

### Alkenyl-substituted glycolides

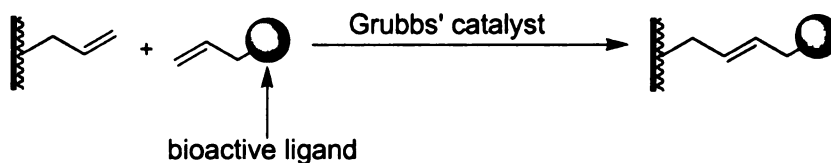
Incorporating double bonds into lactide to enable post-polymerization modification was the driving force for synthesizing alkenyl-substituted glycolides.<sup>31</sup> The synthesis of diallylglycolide is shown in **Scheme 5**.



**Scheme 5.** Synthetic route to diallylglycolide

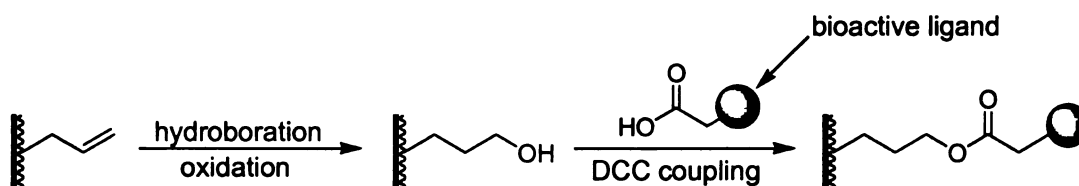


The DL-diallylglycolide homopolymer is amorphous with a  $T_g$  of -10 °C. Designed to act as a scaffold for various bioactive ligands, Grubbs' catalysts were used to perform olefin cross metathesis between poly(lactide-co-diallylglycolide) and small molecule olefin substrates (Scheme 6).<sup>31</sup>



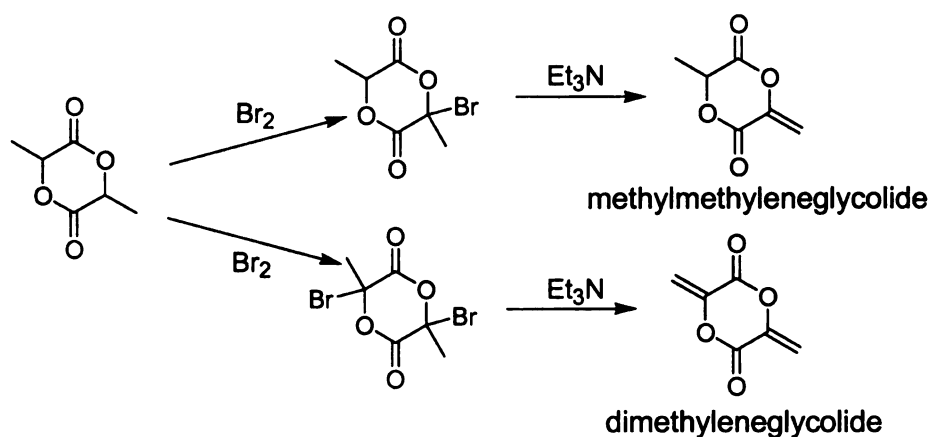
**Scheme 6.** Polymer-bond olefin metathesis of poly(lactide-co-diallylglycolide) with olefin substrates containing bioactive ligands

However, olefin cross metathesis has unwanted side reactions, such as ring-closing metathesis (formation of intramolecular polymer rings) and polymer-polymer cross metathesis (polymer branching and crosslinking). To overcome these problems and further expand the scope of applicable substrates, the double bonds of poly(lactide-co-diallylglycolide) were transformed by hydroboration-oxidation to hydroxyl groups, which were then coupled with various bioactive ligand-containing carboxylic acids (Scheme 7).<sup>31</sup>



**Scheme 7.** Polymer-bound hydroboration-oxidation and DCC coupling

Copolymerization of diallylglycolide places two reactive groups in close proximity and may favor intramolecular metathesis reactions. To achieve a more homogeneous distribution of allyl groups along the polymer backbone, Vogeley et al. synthesized methylallylglycolide<sup>32</sup> from 2-hydroxypent-4-enoic acid (the intermediate in **Scheme 5**), which provides more control over the placement of allyl groups in polylactide chains.



**Scheme 8.** Synthetic routes to dimethyleneglycolide and methylmethyleneglycolide

In addition to allyl-substituted glycolides, alkenyl-substituted glycolides have been reported by Scheibelhoffer et al., who synthesized dimethyleneglycolide and methylmethyleneglycolide (**Scheme 8**).<sup>33</sup> Although the original research was aimed at synthesizing polyolefins with hydrolyzable side chains, these monomers merit re-examination as precursors to functional polylactides. While there are various ways to chemically modify  $\epsilon$ -caprolactone,<sup>34-38</sup> direct modification of lactide ring is extremely limited because activating the methine also activates the carbonyl groups and leads to ring-

opened products. In addition, direct modification on lactide should provide a cheaper alternative to syntheses based on the expensive 2-hydroxypent-4-enoic acid, especially with the reported 84% crude yield of methyleneglycolide from lactide.<sup>33</sup>

### Aryl-substituted glycolides

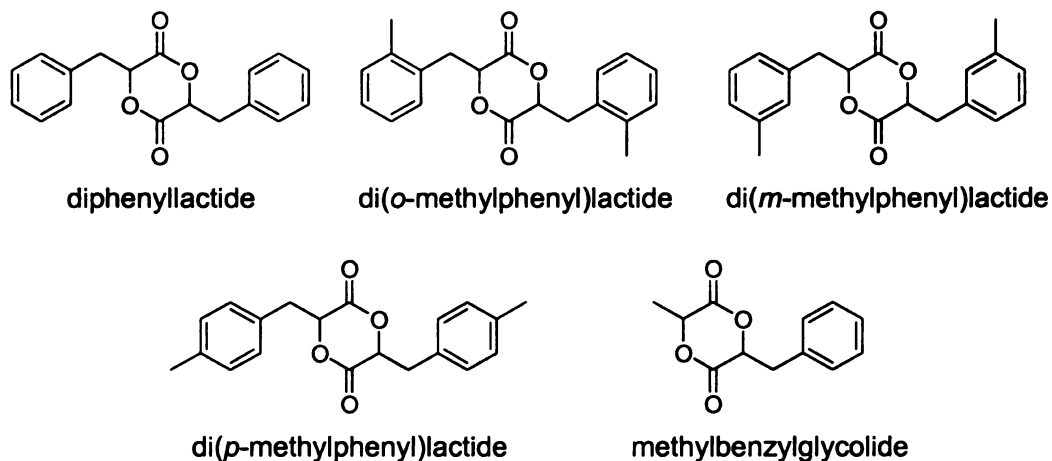


**Figure 8.** Structures of diphenyllactide and derivatives

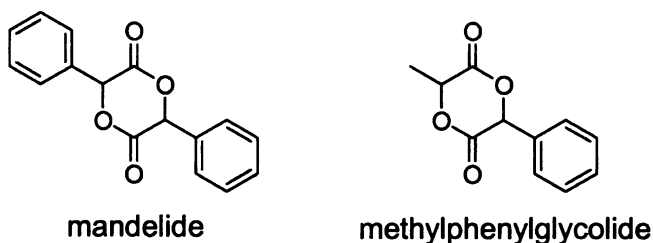
Degradable analogs of polystyrene having high glass transition temperatures are attractive research targets. Because of the structural resemblance of polystyrene and poly(phenyllactide) and the availability of phenyllactic acid via various biosynthetic pathways,<sup>12,39</sup> polymers based on diphenyllactide and its derivatives (**Figure 8**) were synthesized and studied.<sup>16,40,41</sup> However, the glass transition temperatures of high molecular weight poly(phenyllactide) and its derivatives are comparable to that of polylactide (**Table 4**). According to Simmons, these low  $T_g$ s are due to the added

flexibility induced by the methylene group between the main chain and the aromatic ring, making the polymer more similar to poly(allylbenzene) than polystyrene.<sup>41</sup>

**Table 4.** Physical properties of poly(diphenyllactide) and its derivatives

| Polymer  | $M_n$  | $M_w/M_n$ | $T_g$ (°C) |
|--|--------|-----------|------------|
| poly(diphenyllactide) <sup>41</sup>                    | 12,700 | 2.26      | 50         |
| poly(di( <i>o</i> -methylphenyl)lactide) <sup>41</sup> | N/A    | N/A       | 51         |
| poly(di( <i>m</i> -methylphenyl)lactide) <sup>41</sup> | N/A    | N/A       | 42         |
| poly(di( <i>p</i> -methylphenyl)lactide) <sup>41</sup> | N/A    | N/A       | 59         |
| poly(methylbenzylglycolide) <sup>16</sup>              | 3,100  | 1.14      | N/A        |

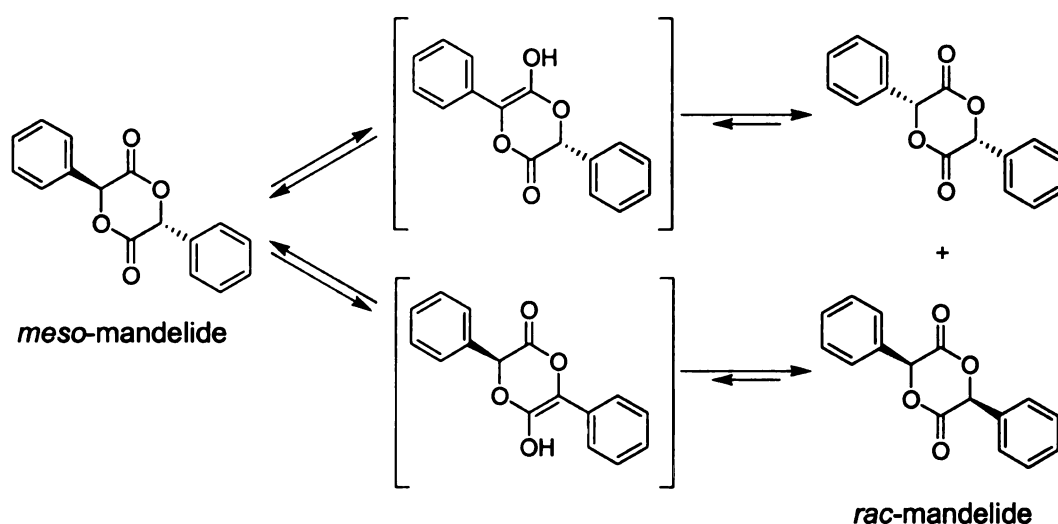
Obviously, removing the flexible methylene group will stiffen the polymer chain by greatly enhancing the steric hindrance from the benzene ring. Based on this hypothesis, mandelide and methylphenylglycolide were synthesized using the general methods described earlier for symmetrical and nonsymmetrical alkyl-substituted glycolides.<sup>14,41,42</sup> Their structures are shown in **Figure 9**.



**Figure 9.** Structures of mandelide and methylphenylglycolide

**Table 5.** Physical properties of polymandelide and its derivatives

| Polymer                                   | $M_n$  | $M_w/M_n$ | $T_g$ (°C) |
|---|--------|-----------|------------|
| polymandelide <sup>42</sup>               | 68,000 | 1.63      | 100        |
| poly(methylphenylglycolide) <sup>14</sup> | 31,200 | 1.81      | 85         |

**Scheme 9.** Equilibrium between *meso*-mandelide and *rac*-mandelide

As expected, the glass transition temperature of polymandelide was comparable to that of polystyrene (**Table 5**). However, the synthesis of mandelide poses problems. Two diastereomers form when mandelic acid is dimerized. Of these, *meso*-mandelide (*R,S*-mandelide) can be polymerized under bulk or solution polymerization conditions, while *rac*-mandelide is insoluble in common solvents and decomposes before melting. Furthermore, *meso*-mandelide is less stable than *rac*-mandelide, and readily isomerizes to *rac*-mandelide during purification (**Scheme 9**). In addition, the chemical lability of the

methine protons could foster thermal and photochemical degradation which leads to discoloration during melt processing.

## Glycolides with other functionalities

### Glycolides with pendant carboxyl groups

Poly(malic acid), a natural polymer found in grapes and apples, is a water-soluble, biodegradable, and bioabsorbable polyester.<sup>43</sup> Because malic acid has 2 carboxyl groups and 1 hydroxyl group, its polymer can exist in three different forms: poly( $\alpha$ -malic acid), poly( $\beta$ -malic acid), and poly( $\alpha,\beta$ -malic acid), a random copolymer of poly( $\alpha$ -malic acid) and poly( $\beta$ -malic acid) (**Figure 10**). Polycondensation of malic acid only leads to low molecular weight poly( $\alpha,\beta$ -malic acid).<sup>43</sup>

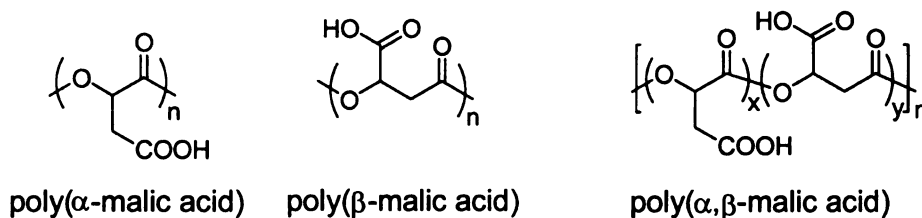
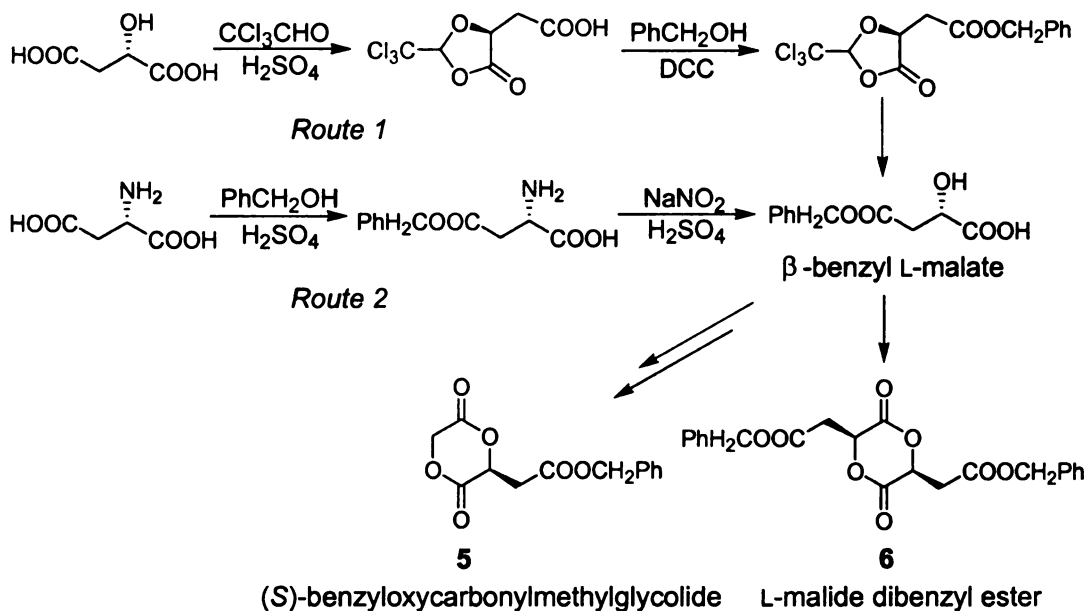


**Figure 10.** Structures of poly(malic acid)s

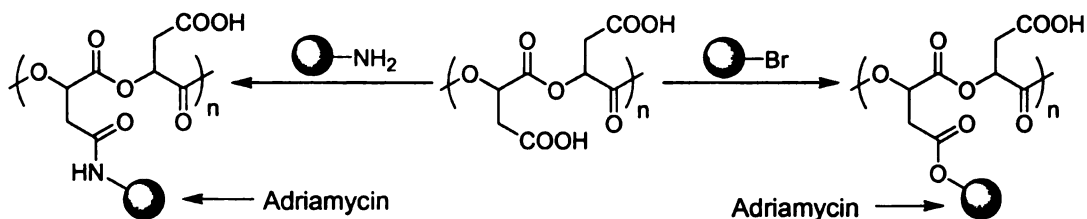
To synthesize high molecular weight poly( $\alpha$ -malic acid), one carboxyl group of malic acid was protected as a benzyl ester, and then the protected malides were polymerized.<sup>44,45</sup> The synthetic routes to the functionalized lactides are shown in **Scheme 10**. After polymerization, removal of the benzyl protecting groups by hydrogenolysis provided a polylactide derivative with a pendent carboxylic acid. Ring-opening polymerization of (*S*)-benzyloxycarbonyl methylglycolide (monomer **5** in **Scheme 10**) proceeded without racemization,

and provided poly(glycolic acid-*alt*-L-malic acid) as a white crystalline polymer with a  $T_m$  of 85-110 °C.<sup>45</sup>



**Scheme 10.** Synthetic routes to benzyl-protected malides

The pendant carboxyl groups of poly( $\alpha$ -malic acid) have been exploited as sites for tethering biological agents in biomedical applications. For example, Ohya et al. coupled the anticancer agent Adriamycin to poly( $\alpha$ -malic acid) and obtained a time-release version of the drug, which reduced the drug's side effects with retention of antitumor activity (**Scheme 11**).<sup>46</sup>

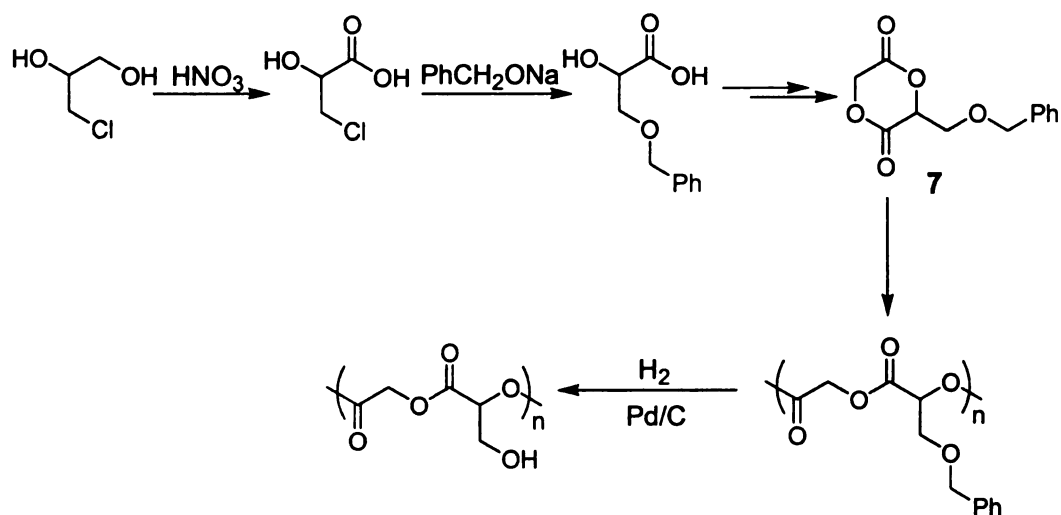


**Scheme 11.** Attaching Adriamycin to poly( $\alpha$ -malic acid)



## Glycolides with pendant hydroxyl groups

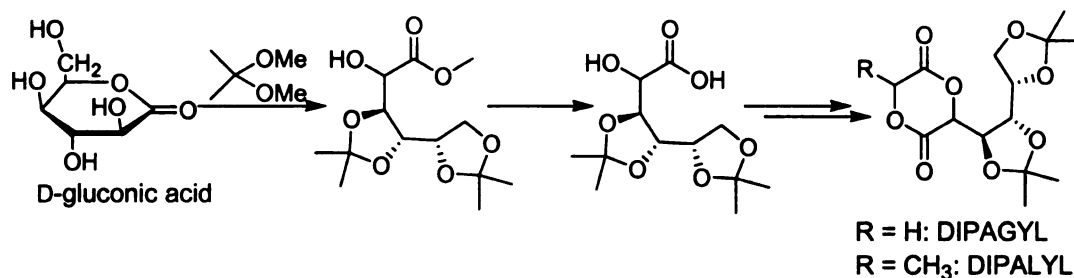
As described earlier, hydroxy-substituted polylactides were synthesized by post-polymerization hydroboration/oxidation of poly(lactide-co-diallylglycolide).<sup>31</sup> Direct polymerization of hydroxy-containing monomers is not possible since ring-opening polymerization of lactide can be initiated by alcohol or water, but protection/deprotection schemes can be applied to the synthesis of hydroxy substituted polylactides. Feng and coworkers synthesized 3-benzyloxymethyl-1,4-dioxane-2,5-dione (benzyloxymethylglycolide) (monomer **7** in **Scheme 12**) from 3-chloro-1,2-propanediol.<sup>47-49</sup>



**Scheme 12.** Synthesis of benzyloxymethylglycolide and poly(glycolic acid-*alt*-glyceric acid)

Ring-opening polymerization of benzyloxymethylglycolide catalyzed by Sn(2-ethylhexanoate)<sub>2</sub> formed an amorphous polyester ( $T_g = 33.7\text{ }^{\circ}\text{C}$ ). Hydrogenolysis to remove the benzyl protecting groups (**Scheme 12**) provided poly(glycolic acid-*alt*-glyceric acid) as a semi-crystalline polymer with a  $T_m$  of 120

°C and a  $T_g$  of 19.6 °C.<sup>46</sup> The polymer was highly hydrophilic, which was verified by contact angle and water uptake measurements.<sup>47</sup>



**Scheme 13.** Synthetic routes to DIPAGYL and DIPALYL

Vert and coworkers used D-gluconic acid, a naturally occurring  $\alpha$ -hydroxy acid involved in the glucose cycle of animals and microorganisms, to synthesize novel glycolides having pendant hydroxyl groups protected as acetals (**Scheme 13**).<sup>50,51</sup> The ring-opening polymerization of DIPAGYL (3-(1,2-3,4-tetraoxobutyl-diisopropylidene)dioxane-2,5-dione) catalyzed by Sn(2-ethylhexanoate)<sub>2</sub> yielded a brittle amorphous polyester, with a  $M_w$  of 20,000 Da and a  $T_g$  of ~95 °C.<sup>51</sup> The high  $T_g$  is presumably caused by the bulky isopropylidene rings appended to the polymer backbone. However, the polymerization of DIPALYL (3-methyl-6-(1,2-3,4-tetraoxobutyl-diisopropylidene)-dioxane-2,5-dione) only provided oligomers ( $M_w$  ~2,000 Da). To access higher molecular weights, *rac*-lactide was copolymerized with DIPAGYL and DIPALYL (**Table 6**).<sup>51</sup> The high polydispersity and low molecular weight of poly(DIPALYL-*co-rac*-lactide) suggests that DIPALYL monomer was impure.

**Table 6.** Physical properties of poly(DIPAGYL-*co-rac*-lactide) and poly(DIPALYL-*co-rac*-lactide)

| Polymer   | Lactide content (%) | $M_w$   | $M_w/M_n$ | $T_g$ (°C) |
|---|---------------------|---------|-----------|------------|
| poly(DIPAGYL- <i>co-rac</i> -lactide) <sup>51</sup> | 69                  | 115,000 | 2.1       | 73         |
| poly(DIPALYL- <i>co-rac</i> -lactide) <sup>51</sup> | 89                  | 36,000  | 3.3       | 58         |

The hydroxyl groups of poly(DIPAGYL) were deprotected using acetic acid/water/acetone and iodine in acetone/methanol (**Scheme 14**); the polyester chains degraded completely using other methods.<sup>50</sup> Because iodine or acetic acid selectively cleaves the isopropylidene groups protecting primary alcohols, the terminal hydroxyl groups were deprotected selectively. After deprotection, the polymer was fully soluble in hydrophilic solvents such as methanol and ethanol, and partially soluble in water.

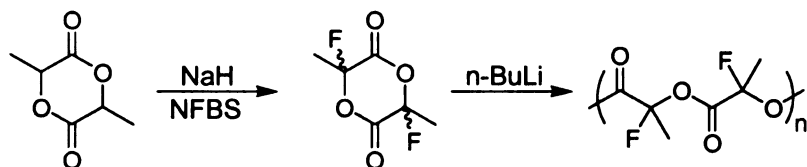


**Scheme 14.** Deprotection of poly(DIPAGYL-*co-rac*-lactide)

### Fluorinated lactide

Fluorination generally improves the thermal stability, lowers the surface energy, enhances barrier properties, and improves the hydrolytic stability of polymers. Commercially available DL-lactide was fluorinated using sodium hydride and N-fluorobenzenesulfonimide.<sup>52</sup> The fluorinated monomer,  $\alpha,\alpha'$ -

difluorolactide, was isolated in <10% yield, and was then polymerized by anionic polymerization (**Scheme 15**). As mentioned previously, direct chemical modifications of the lactide ring are rare.



**Scheme 15.** Synthesis and polymerization of  $\alpha,\alpha'$ -difluorolactide

The  $T_g$  of poly( $\alpha,\alpha'$ -difluorolactide) was  $\sim 15$   $^{\circ}\text{C}$  higher than polylactide, presumably due to the increased dipole-dipole interactions. Surprisingly, the polymer was semi-crystalline (**Table 7**). It is well known that poly(*rac*-lactide) is amorphous, and incorporation of more than 15% of *meso*-lactide in poly(L-lactide) will render the polymer completely amorphous.<sup>3</sup> Crystallization of the fluorinated DL-lactide polymer, if true, might be caused by the high dipole-dipole interaction between chains. Defects in the stereoregularity of the polymer chains may be responsible for the relatively low  $T_m$  (110  $^{\circ}\text{C}$ ).

**Table 7.** Physical properties of poly( $\alpha,\alpha'$ -difluorolactide)

| Polymer  | $M_n$  | $M_w/M_n$ | $T_g$ ( $^{\circ}\text{C}$ ) | $T_m$ ( $^{\circ}\text{C}$ ) |
|--|--------|-----------|------------------------------|------------------------------|
| poly( $\alpha,\alpha'$ -difluorolactide) <sup>52</sup> | 32,000 | 1.89      | 70                           | 110                          |

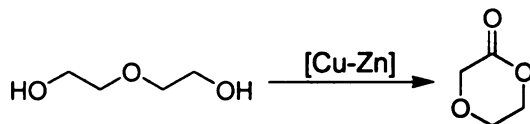
## ***p*-Dioxanone and derivatives**

### ***p*-Dioxanone**

Poly(*p*-dioxanone), or poly(1,4-dioxan-2-one), is a biocompatible and biodegradable poly(ester-*alt*-ether) thermoplastic material.<sup>53</sup> Poly(*p*-dioxanone) degrades completely in the body within 180 days.<sup>54</sup> Poly(*p*-dioxanone) can be used as films, molded products, laminates, foams, nonwoven materials, adhesives, and coatings.<sup>55</sup> While polylactide tends to be brittle and has a low elongation at break and moderate impact resistance, poly(*p*-dioxanone) has improved toughness and has a tensile strength close to 7000 psi and an ultimate elongation of ~ 500-600%.<sup>56</sup> Poly(*p*-dioxanone) has shown adequate properties as an osteosynthesis material and has been approved by the Food and Drug Administration as a suture material in gynecology.<sup>57</sup> Copolymers of *p*-dioxanone with glycolide, lactide, caprolactone, and trimethylenecarbonate have also been reported for the preparation of sutures with improved properties as well as for the preparation of drug delivery systems.<sup>53</sup>

The polymerization of *p*-dioxanone was first reported in the early 1960s,<sup>58-60</sup> with most of the available information on synthesis and properties of poly(*p*-dioxanone) restricted to the patent literature.<sup>53</sup> The recent development of a convenient one-step synthesis of *p*-dioxanone from an inexpensive substrate – diethylene glycol (**Scheme 16**),<sup>61</sup> positions poly(*p*-dioxanone) as a commodity thermoplastic. Active research is targeted at the synthesis of *p*-dioxanone from diethylene glycol by various dehydrogenation catalysts, including 4-acetylamino-

2,2,6,6-tetramethylpiperidine-1-oxoammonium tetrafluoroborate,<sup>62</sup> Pd(OAc)<sub>2</sub>/pyridine,<sup>63</sup> and Pd(II)-hydrotalcite/pyridine.<sup>64</sup>



**Scheme 16.** Synthetic route to *p*-dioxanone

Poly(*p*-dioxanone) is produced by ring-opening polymerization of *p*-dioxanone. Sn(2-ethylhexanoate)<sub>2</sub>,<sup>65-67</sup> aluminum triisopropoxide,<sup>55</sup> triethyl aluminum,<sup>65</sup> zinc L-lactate,<sup>68</sup> and even enzymes<sup>69</sup> have been used to catalyze/initiate the ring-opening polymerization. High molecular weight poly(*p*-dioxanone) is a semicrystalline polymer with a  $T_m$  of 110 °C and a  $T_g$  ranging from -15 °C to -8 °C.<sup>68</sup> In contrast to polylactides, poly(*p*-dioxanone) is insoluble in common solvents such as toluene, acetone, 1,4-dioxane and tetrahydrofuran. Dimethylsulfoxide and N,N-dimethylformamide are good solvents, but poly(*p*-dioxanone) is highly sensitive to hydrolytic degradation in these hygroscopic solvents.<sup>68</sup>

Compared to lactide and caprolactone, *p*-dioxanone has the least tendency to polymerize and the highest equilibrium monomer concentration because of its modest ring strain (**Table 8**).<sup>70</sup> Thermodynamically equilibrated systems contain a relatively high fraction of cyclic oligomers because these large rings have low strain.<sup>67</sup> Like most ring opening polymerizations, polymerization of *p*-dioxanone is accompanied by a decrease in entropy, and the equilibrium concentrations of monomer and cyclic oligomers increases with the reaction

temperature. The thermal instability of poly(*p*-dioxanone) has been rationalized as a manifestation of its relatively low ceiling temperature (265 °C).<sup>65</sup> Lowering the polymerization temperature leads to higher conversion, especially when the polymerization is carried out below the polymer's melting point.<sup>71</sup>

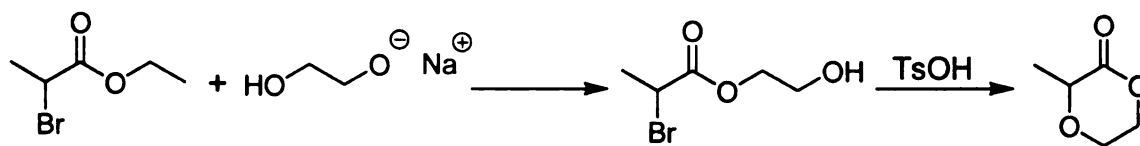
**Table 8.** Thermodynamic parameters of cyclic esters polymerized at 100 °C

| Monomer             | $\Delta H_p$ (KJ/mol) | $\Delta S_p^0$ (J/mol·K) | $[M]_{eq}$ (mol/L) |
|---------------------|-----------------------|--------------------------|--------------------|
| lactide             | -22.9                 | -41                      | 0.09               |
| caprolactone        | -13.9                 | -10.4                    | ~0                 |
| <i>p</i> -dioxanone | -13.8                 | -45                      | 2.5                |

In order to balance the equilibrium concentration and the polymerization rate, Müller et al. polymerized *p*-dioxanone using a decreasing reaction temperature profile.<sup>57</sup> By gradually reducing the polymerization temperature with conversion, the polymerization rate and monomer conversion were maximized.

### 3-Methyl-*p*-dioxanone

Poly(*p*-dioxanone) can be viewed as an alternating copolymer of glycolic acid and ethylene glycol, and the alternating copolymer of lactic acid and ethylene glycol can be realized by polymerizing 3-methyl-*p*-dioxanone (3-methyl-1,4-dioxan-2-one). Starting from ethyl 2-bromopropionate and the sodium salt of ethylene glycol, Hillmyer et al. successfully synthesized 3-methyl-*p*-dioxanone, but in low yield (**Scheme 17**).<sup>72</sup>



**Scheme 17.** Synthetic route to 3-methyl-*p*-dioxanone

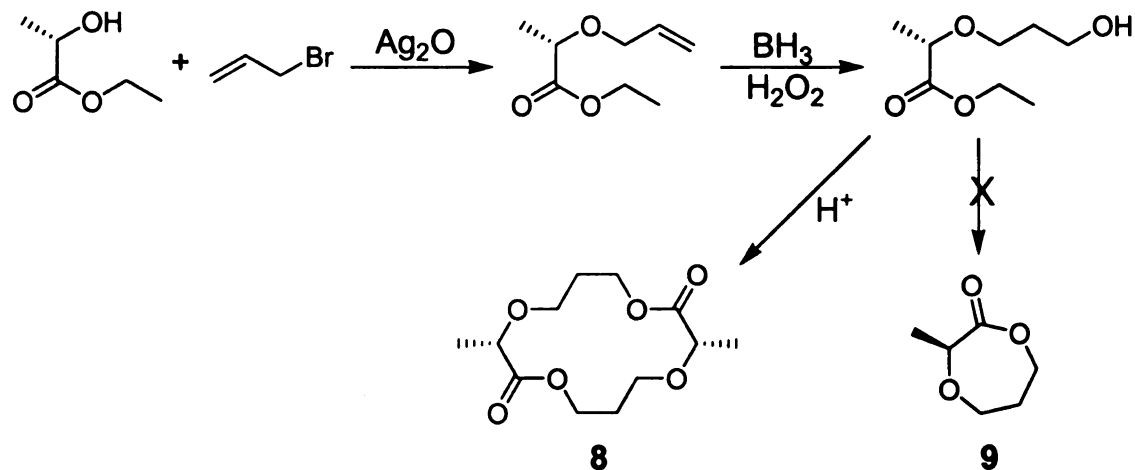
Using *n*-butanol and  $\text{Y}[\text{N}(\text{TMS})_2]_3$  to form a highly reactive yttrium alkoxide catalyst, they carried out solution polymerizations of 3-methyl-*p*-dioxanone at temperatures from -30 °C to 60 °C. The thermodynamic parameters calculated from the equilibrium monomer concentrations at different temperatures are  $\Delta H_p^0 = -12.1 \pm 5 \text{ kJ/mol}$  and  $\Delta S_p^0 = -42 \pm 2 \text{ J/mol}\cdot\text{K}$ . Both are very similar to those of *p*-dioxanone polymerization (**Table 8**). Because poly(3-methyl-*p*-dioxanone) was synthesized from racemic monomer, the polymer was amorphous with a  $T_g$  of ~ -26 °C to -19 °C, even lower than that of poly(*p*-dioxanone). The difference in the  $T_g$  of the the two polymers is probably due to the semi-crystalline nature of poly(*p*-dioxanone).

### 6,13-Dimethyltetraoxacyclotetradecanedione

Aiming to make a polymer miscible with polylactide but with a  $T_g$  lower than poly(3-methyl-*p*-dioxanone), Hillmyer et al. targeted the synthesis of the structurally similar poly(3-methyl-1,4-dioxepin-2-one), which would have alternating lactic acid and propylene glycol segments in the polymer backbone.<sup>73</sup> However, cyclization of ethyl 2-(*S*)-allyloxypropanoate yielded the dimer of 3-methyl-1,4-dioxepin-2-one, ((6*S*,13*S*)-6,13-dimethyl-1,4,8,11-tetraoxacyclotetradecane-2,9-dione, monomer **8** in **Scheme 18**), instead of the desired monomer,



despite prior reports of the successful synthesis of 3-methyl-1,4-dioxepin-2-one and derivatives (monomer **9** in **Scheme 18**).<sup>23,74,75</sup>



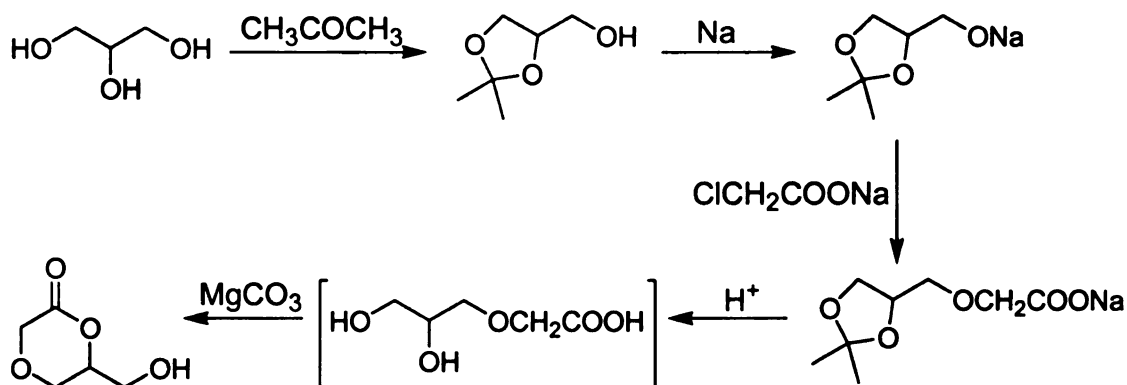
**Scheme 18.** Synthetic route to *S,S*-dimethyltetraoxacyclotetradecanedione 3-methyl-1,4-dioxepin-2-one

Nonetheless, polymerization of the 14-membered cyclic ester was successful and yielded high molecular weight poly(lactic acid-*alt*-propylene glycol). Based on simulation results, the driving force for the polymerization was the gain of entropy, not release of ring strain (enthalpy).

As expected, the extra methylene group in poly(dimethyltetraoxacyclotetradecanedione) compared to 3-methyl-*p*-dioxanone reduced the  $T_g$  to -32 °C (atactic) and -30 °C (isotactic), but surprisingly, DSC measurements showed that poly(*S,S*-dimethyltetraoxacyclotetradecanedione) was completely amorphous. Blends of poly(*S,S*-dimethyltetraoxacyclotetradecanedione) and atactic polylactide exhibited a single glass transition temperature over the entire composition range, which confirmed the complete miscibility of these two polymers.

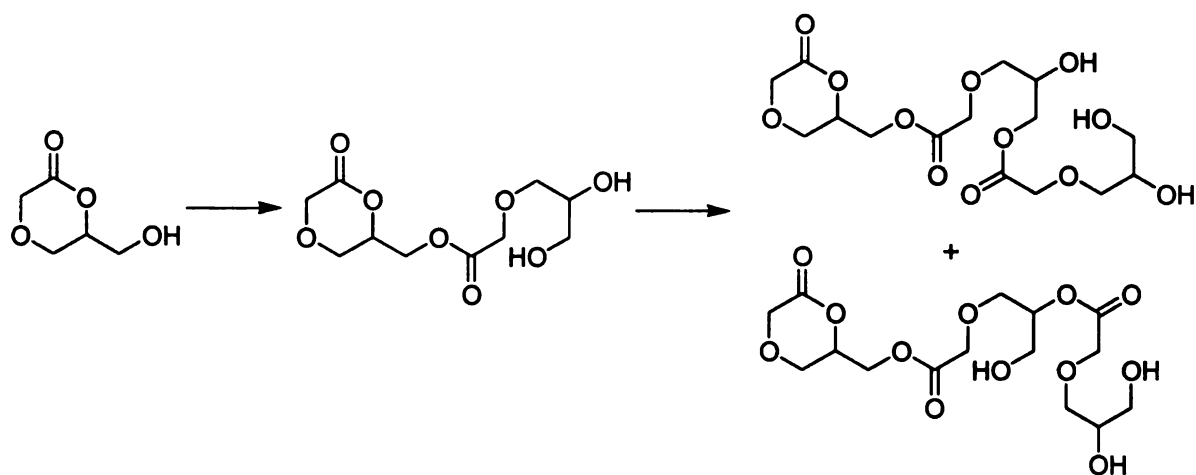
## 6-Hydroxymethyl-*p*-dioxanone

Recently, Zhuo et al. described 6-hydroxymethyl-*p*-dioxanone (6-hydroxymethyl-1,4-dioxane-2-one), an AB<sub>2</sub> monomer for the synthesis of hyperbranched aliphatic polyesters with unique mechanical and rheological properties (**Scheme 19**).<sup>76</sup>

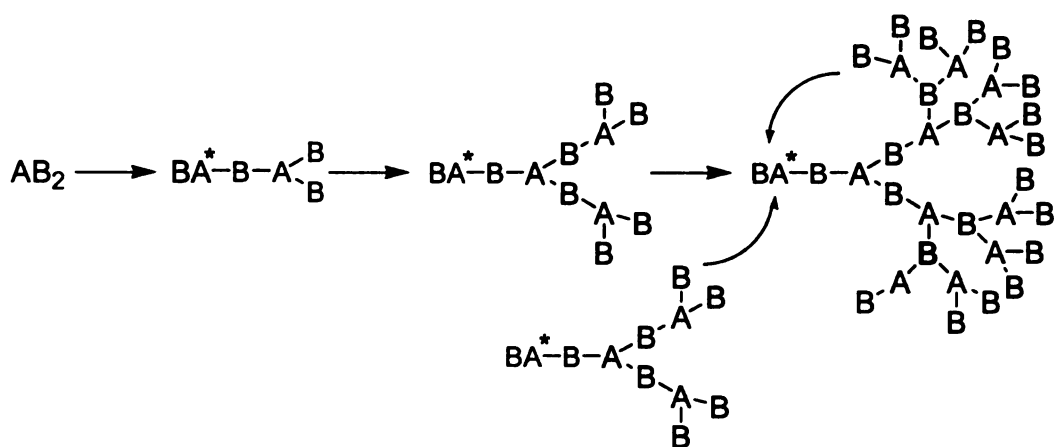


**Scheme 19.** Synthetic route to 6-hydroxymethyl-*p*-dioxanone

The first two steps of the 6-hydroxymethyl-*p*-dioxanone polymerization are shown in **Scheme 20**. Each ring opening step generates a dihydroxy intermediate which directly leads to the hyperbranched structure of the polymer (**Scheme 21**).<sup>77</sup> The focal point of the hyperbranched polymer is the *p*-dioxanone ring, shown as BA\* in the simplified representation of **Scheme 21**. Since the ring can be attacked by intra-molecular or inter-molecular ring-opening reactions, the polydispersity can be relatively high.



**Scheme 20.** Polymerization of 6-hydroxymethyl-*p*-dioxanone

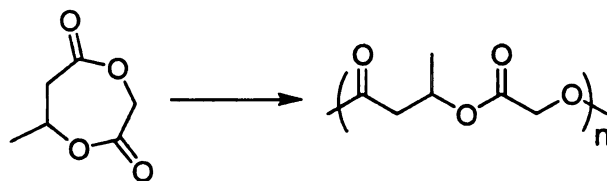


**Scheme 21.** Hyperbranched polymer made from  $AB_2$  monomer

Polymerization of 6-hydroxymethyl-*p*-dioxanone using  $\text{Sn}(\text{2-ethylhexanoate})_2$  as the catalyst provided a highly branched high molecular weight polyester ( $M_n$  and PDI  $\sim 22,000\text{-}26,000$  and  $2.0\text{-}2.2$  respectively).<sup>76</sup> The degree of branching was 0.40, which is quite close to similar  $AB_2$  systems ( $\sim 0.5$ ).<sup>77</sup>

## Dioxepanedione and benzodioxepindione

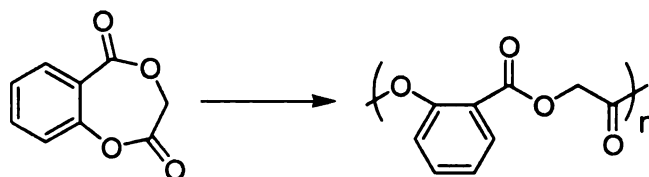
Poly(3-hydroxybutyrate), or PHB, is a widely used biocompatible and biodegradable polymer synthesized by a bacterial fermentation process. To access PHBs with new properties, the cyclic ester of 3-hydroxybutyric acid and glycolic acid was synthesized using the method previously described for nonsymmetrical alkyl-substituted glycolides (**Scheme 22**).<sup>78,79</sup> Polymerization of 7-methyl-1,4-dioxepane-2,5-dione was reported by Kimura in 1992.<sup>78</sup> Although few details were disclosed, the 7-methyl-1,4-dioxepane-2,5-dione homopolymer was described as a biodegradable polymer with excellent flexibility and elongation.



**Scheme 22.** Polymerization of 7-methyl-1,4-dioxepane-2,5-dione

Ten years later, Kimura and coworkers reported the synthesis of (*R*)-7-methyl-1,4-dioxepane-2,5-dione.<sup>79</sup> However, cationic, anionic, and organometallic catalysts all failed to polymerize the monomer, but copolymerization of (*R*)-7-methyl-1,4-dioxepane-2,5-dione with  $\beta$ -butyrolactone proved successful. Copolymers with glycolic acid contents ranging from 7% to 14% showed melting transitions at 97-122 °C and 114-142 °C, significantly lower than the  $T_m$  of (*R*)-PHB (170 °C). The copolymer  $T_g$  was  $\sim 0$  °C, similar to that of (*R*)-PHB.

The structure of 1,4-benzodioxepin-2,5(3H)-dione mimics that of 7-methyl-1,4-dioxepane-2,5-dione. The monomer was first reported in 1959,<sup>80</sup> and the polymer, poly(salicylic acid-*alt*-glycolic acid), was patented in 1992 (**Scheme 23**).<sup>81</sup>



**Scheme 23.** Polymerization of 1,4-benzodioxepin-2,5(3H)-dione

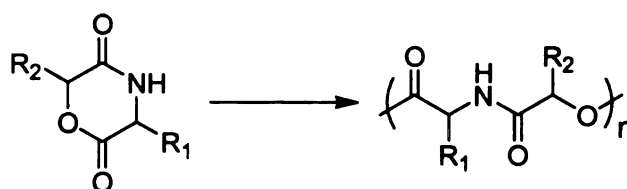
1,4-Benzodioxepin-2,5(3H)-dione was successfully polymerized by several methods: anionic ring-opening polymerization ( $\text{NaOPh} \cdot 3\text{H}_2\text{O}/15\text{-crown-5 ether}$ ), coordination-insertion ring-opening polymerization ( $\text{Sn(2-ethyl hexanoate)}_2$ ), and thermal ring-opening polymerization.<sup>81</sup> The polymers had relatively low molecular weights with  $M_n$ s ranging from 8,400 to 8,700 and polydispersities of  $\sim 1.5$ . The reported  $T_g$ s and  $T_m$ s, 57-73 °C and 165-168 °C respectively, are similar to poly(L-lactide), but probably are influenced by the low molecular weights.

Degradation of poly(1,4-benzodioxepin-2,5(3H)-dione) was examined *in vitro* and *in vivo*. Only 2% polymer remained after 17 days of degradation in pH 7.25 phosphate buffer at 50 °C and the polymer completely degraded within 26 weeks during *in vivo* tests in Long-Evans rats (in the ventral abdominal subcutis).<sup>81</sup>

## Depsipeptides

Polydepsipeptides are alternating copolymers of  $\alpha$ -amino acids and  $\alpha$ -hydroxy acids. They are nontoxic and degradable *in vitro* and *in vivo*.<sup>82</sup> Due to the presence of strong intermolecular hydrogen bonding between amide groups, polydepsipeptides have good mechanical properties, while the labile ester groups support a high degradation rate. Furthermore, the incorporation of natural amino acids in polydepsipeptides may enhance their susceptibility to enzymatic degradation.

Feijen carried out pioneering work on the synthesis of high molecular weight polydepsipeptides via ring-opening polymerization.<sup>83-85</sup> Ring-opening polymerization of morpholine-2,5-dione derivatives provides an efficient route to a broad range of polydepsipeptides since various morpholine-2,5-diones can be prepared by condensing different  $\alpha$ -amino acids and  $\alpha$ -hydroxy acids (**Scheme 24**).



**Scheme 24.** Polymerization of morpholine-2,5-dione derivatives

Morpholine-2,5-dione derivatives are usually synthesized by methods analogous to those used to prepare nonsymmetrical substituted glycolides (**Scheme 2**), with the main difference being the use of an  $\alpha$ -amino acid as the starting material. Chiral morpholine-2,5-dione derivatives can also be

synthesized, although a small extent of epimerization has been reported.<sup>86</sup> Other reaction schemes have been proposed to limit racemization and other side reactions.<sup>87</sup>

### Alkyl-substituted morpholine-2,5-diones

The alkyl-substituted morpholine-2,5-diones reported to date (without listing stereoisomers separately) are shown in **Figure 11**.<sup>82-85,88-97</sup>

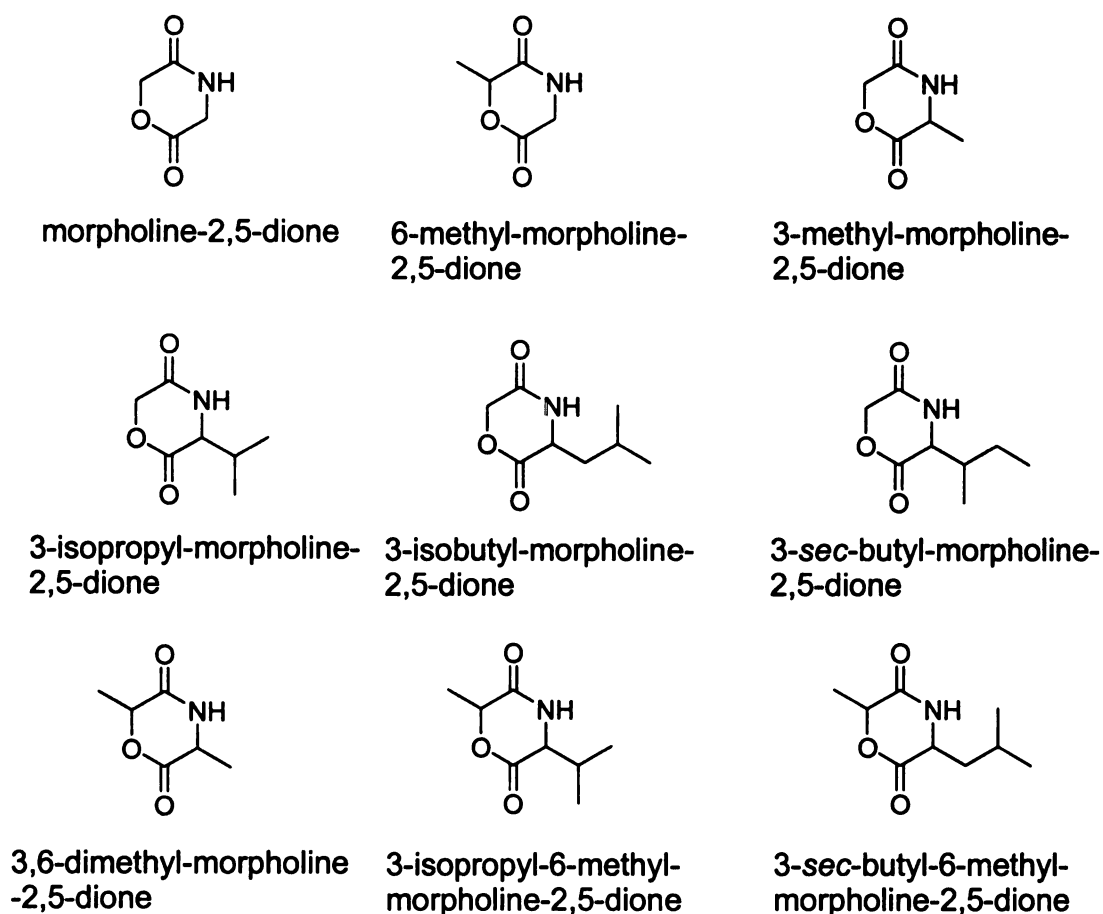


**Figure 11.** Structures of alkyl-substituted morpholine-2,5-diones

Morpholine-2,5-diones can be treated as a 6-membered lactam or a 6-membered lactone. Because lactams are more difficult to polymerize than

lactones,<sup>23</sup> the ring-opening polymerization of morpholine-2,5-dione takes place exclusively at the ester. The catalysts/initiators used for the polymerization of lactides can also be applied to morpholine-2,5-diones. While the most commonly used catalyst is Sn(2-ethylhexanoate)<sub>2</sub>, enzymatic polymerization catalyzed by porcine pancreatic lipase type II has been extensively studied by Höcker and coworkers.<sup>82,93-97</sup>

Because of the strong intermolecular hydrogen bonding between amide groups, poly(morpholine-2,5-dione)s have higher  $T_g$ s and  $T_m$ s than structurally analogous polylactides (**Table 9**). For example, the  $T_g$  of poly(6-methyl-morpholine-2,5-dione) is 117 °C, and poly((3S)-3-methyl-morpholine-2,5-dione) has a  $T_g$  of 117 °C and a  $T_m$  of 221 °C. Introducing bulky groups such as isopropyl in poly((3S)-3-isopropyl-morpholine-2,5-dione) decreases  $T_g$ . In this case the bulky isopropyl group interferes with hydrogen bonding, and the contribution to  $T_g$  from the stiffer chain is counter-balanced by weaker chain-chain interactions.

One problem associated with the polymerization of morpholine-2,5-diones is their relatively low-molecular weights, especially for 3,6-disubstituted derivatives. The explanation proposed is that free or weakly associated amide functional groups in morpholine-2,5-dione derivatives may interact with Sn(2-ethylhexanoate)<sub>2</sub> and interfere in the polymerization process.<sup>98</sup> Monomer polymorphs with differing extents of hydrogen bonding can be obtained by using different recrystallization solvents. These materials have different melting points and may affect polymerization.



**Table 9.** Physical properties of poly(morpholine-2,5-dione)s

| <b>Poly(morpholine-2,5-dione)s<br/>with different substituents</b> | <b><math>M_n</math></b> | <b><math>M_w</math></b> | <b><math>M_w/M_n</math></b> | <b><math>T_g</math> (°C)</b> | <b><math>T_m</math> (°C)</b> |
|--|-------------------------|-------------------------|-----------------------------|------------------------------|------------------------------|
| No substituent <sup>88</sup>                                       |                         |                         |                             | 67                           | 199                          |
| 6-methyl <sup>85</sup>   |                         | 23,000                  |                             | 117                          |                              |
| (3S)-3-methyl <sup>85</sup>  |                         | 45,000                  |                             | 103                          | 221                          |
| (3S)-3-isopropyl <sup>85</sup>                                     |                         | 74,000                  |                             | 99                           |                              |
| (3S)-3-isopropyl <sup>90</sup>                                     | 40,500                  | 64,700                  | 1.60                        | 56                           | 185                          |
| (3S)-3-isopropyl <sup>96</sup>                                     | 17,500                  | 18,500                  | 1.06                        | 74                           |                              |
| (3S)-3-isopropyl-6-methyl <sup>85</sup>                            |                         | 25,000                  |                             | 93                           |                              |
| (3S)-3,6-dimethyl <sup>85</sup>                                    |                         | 9,000                   |                             | 94                           |                              |
| (3S)-3,6-dimethyl <sup>91</sup>                                    | 24,000                  |                         | 1.16                        | 76                           |                              |
| (3S,6S)-3,6-dimethyl <sup>91</sup>                                 | 23,000                  |                         | 1.28                        | 76                           |                              |
| (3S,6R)-3,6-dimethyl <sup>91</sup>                                 | 28,000                  |                         | 1.41                        | 88                           |                              |

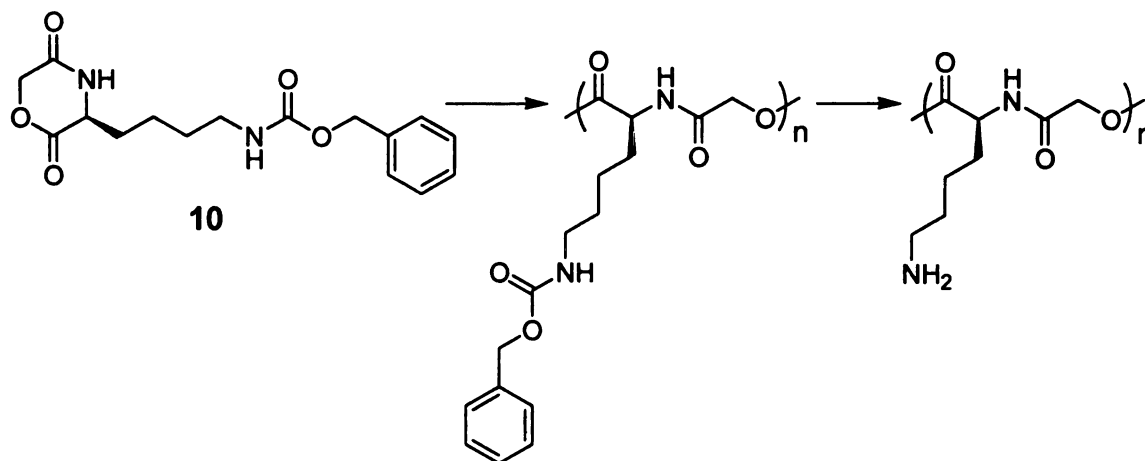
**Morpholine-2,5-diones with other functionalities**

As with polylactide, the use of alkyl-substituted morpholine-2,5-dione polymers for biomedical applications is limited due to the lack of functional groups to which bioactive ligands can be covalently attached. However the use of functional  $\alpha$ -amino acids (lysine, serine, aspartic acid, glutamic acid, cysteine,

etc.) enabled the preparation of polydepsipeptides with pendant amino,<sup>86,99-103</sup> hydroxyl,<sup>104-108</sup> and carboxylic acid functional groups.<sup>98,100-103,109-114</sup>

### Morpholine-2,5-diones with pendant amino group

Attempts to prepare poly(L-lactic acid-*alt*-L-lysine) by the polymerization of 3-(N<sup>ε</sup>-benzoxycarbonyl-L-lysine)-6-methyl-morpholine-2,5-dione were not successful.<sup>100</sup> With removal of the methyl group at the 6-position, 3-(N<sup>ε</sup>-benzoxycarbonyl-L-lysine)-morpholine-2,5-dione (monomer **10** in **Scheme 25**) was successfully polymerized ( $M_n$  up to 4,270) and subsequent deprotection using hydrogen bromide/acetic acid or trifluoromethanesulfonic acid provided the free amino groups (**Scheme 25**).<sup>101</sup> Deprotection by hydrogenation with palladium was less successful.



**Scheme 25.** Synthesis of poly(lactic acid-*alt*-L-lysine)

Langer et al. copolymerized 3-(N<sup>ε</sup>-benzoxycarbonyl-L-lysine)-6-methyl-morpholine-2,5-dione with L-lactide,<sup>86,99</sup> incorporating up to 10 mol% of the morpholine-2,5-dione derivative into the copolymer. However, increasing the

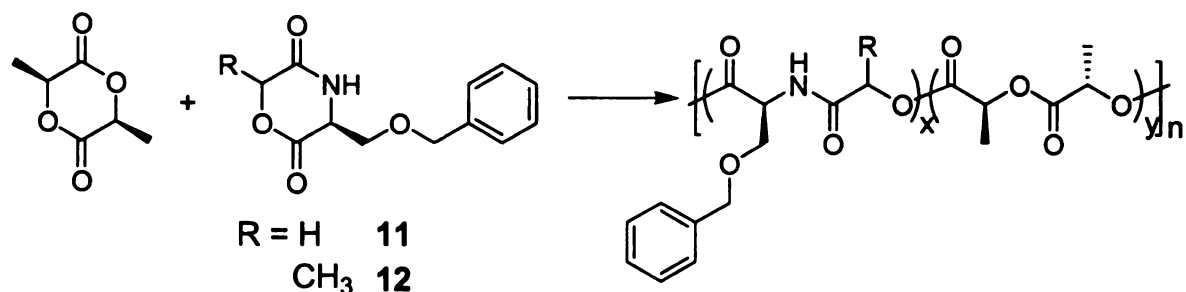
lysine content in the copolymer disrupted crystallinity and lowered the molecular weight. After removal of the benzyloxycarbonyl group using palladium chloride ( $M_w$  decreased from 64,000 to 40,000 Da), 1,1'-carbonyldiimidazole was used to couple the free amino group to a cell adhesion promoting peptide.

### **Morpholine-2,5-diones with pendant hydroxyl group**

Studies of polydepsipeptides with pendant hydroxyl groups focus on the polymerization of 3-(O-benzyl-L-serinyl)-morpholine-2,5-dione (**11**) and 3-(O-benzyl-L-serinyl)-6-methyl-morpholine-2,5-dione (**12**).<sup>104-108</sup> Polylactides having a low density of pendant hydroxyl groups were synthesized by copolymerizing L-lactide with either **11** or **12** (**Scheme 26**). The hydroxyl groups were deprotected using Pd/C-H<sub>2</sub>,<sup>107</sup> PdCl<sub>2</sub>/Et<sub>3</sub>SiH/Et<sub>3</sub>N,<sup>105</sup> and trifluoromethanesulfonic acid.<sup>108</sup>

Morita et al. coupled acryloyl chloride to the pendant hydroxyl groups of polydepsipeptides.<sup>104,106,107</sup> Photopolymerization of the acrylates provided crosslinked hydrogels that may be useful for encapsulating cell/drugs for injectable delivery. Another crosslinking scheme was that of Jin et al., who coupled poly(L-lactide-co-L-serine) with diisocyanate-terminated poly(ethylene glycol).<sup>105</sup>

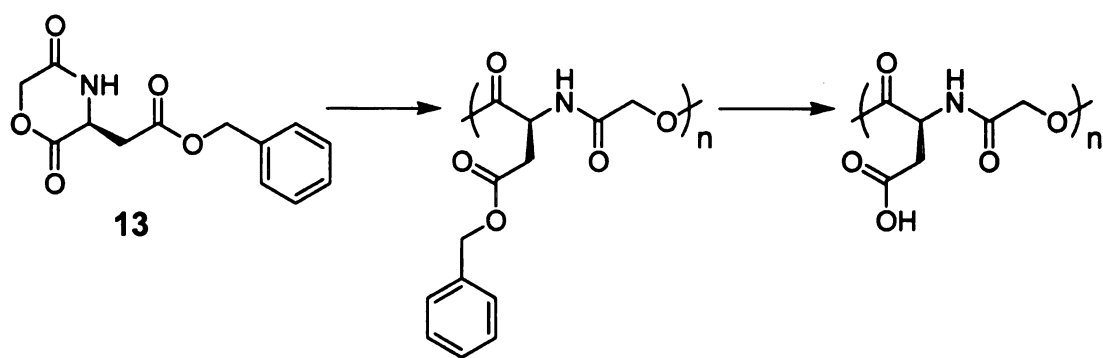
Copolymers with pendant hydroxyl groups were used by Ouchi et al. as macroinitiators for graft polymerization of lactide.<sup>108</sup> The resulting polylactide combs had lower  $T_g$ s,  $T_m$ s, and crystallinity than linear polylactides, and the degradation rate could be adjusted by controlling the molecular weight of polymer backbone and/or side chains, and the number of graft chains.



**Scheme 26.** Synthesis of copolymers of L-lactide and morpholine-2,5-diones with pendant protected hydroxyl groups

### Morpholine-2,5-diones with pendant carboxyl group

Feijen et al. attempted to prepare poly(lactic acid-*alt*-aspartic acid) by homopolymerization of 3-(benzyloxycarbonyl)methyl-6-methyl-morpholine-2,5-dione, but the polymerization failed due to excessive steric hindrance.<sup>100</sup> However, polymerization of the less hindered 3-(benzyloxycarbonyl)methyl-morpholine-2,5-dione (**13**) provided a successful route to poly(glycolic acid-*alt*-aspartic acid) (**Scheme 27**).<sup>101,103,109,111,113</sup>



**Scheme 27.** Synthesis of poly(glycolic acid-*alt*-aspartic acid)

The main chains of water-soluble poly(glycolic acid-*alt*-aspartic acid) slowly degraded by random cleavage in non-enzymatic systems, but the *in vitro* degradation was accelerated by the presence of enzymes.<sup>101,109</sup>

In addition to aspartic acid, glutamic acid is an attractive substrate for the synthesis of depsipeptides with pendant carboxyl groups. The ring-opening polymerization of 3-(benzyloxycarbonyl)ethyl-morpholine-2,5-dione provided the hydrophilic alternating copolymer of glycolic acid and glutamic acid.<sup>112,114</sup>

## Chapter 2 Poly(dicyclohexylglycolide)s

The limiting use temperature of thermoplastics is defined by the glass transition temperature ( $T_g$ ). Above  $T_g$ , polymer chain segments are mobile, and the material changes from a glassy to rubbery state, which compromises its physical properties. The glass transition temperatures of polylactides are  $< 60\text{ }^{\circ}\text{C}$ , which limits its use as a rigid, clear replacement for large-volume thermoplastics such as polystyrene ( $T_g \sim 100\text{ }^{\circ}\text{C}$ ).

It is well known that increasing the rigidity of polymer chains leads to higher  $T_g$ s with improved dimensional stability at high temperatures. Taking a cue from polyolefins, the rigidity of the polylactide chain can be increased by simply replacing the methyl groups with bulky groups. The substituted polylactides with highest  $T_g$ s are poly(3-(1,2-3,4-tetraoxobutyl-diisopropylidene)dioxane-2,5-dione) ( $T_g = 95\text{ }^{\circ}\text{C}$ ) and polymandelide ( $T_g = 100\text{ }^{\circ}\text{C}$ ) (**Figure 12**).

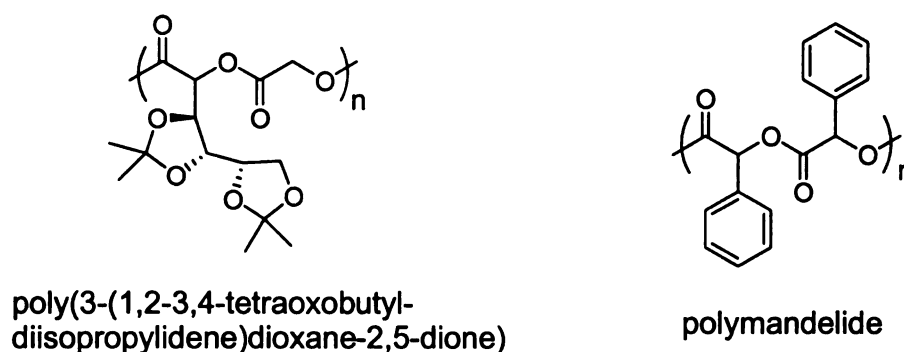


**Figure 12.** Structures of high  $T_g$  polylactides

However, poly(3-(1,2-3,4-tetraoxobutylidene)diisopropylidene)dioxane-2,5-dione) is difficult to polymerize. Furthermore, the expense associated with protecting the hydroxyl groups makes this polymer unsuitable as a commodity material.

As shown in **Scheme 9**, the synthesis of mandelide poses problems. First, *rac*-mandelide is insoluble in common solvents and decomposes before melting. Second, the polymerizable *meso*-mandelide is less stable than *rac*-mandelide, and readily transforms to *rac*-mandelide during purification. While the solvent-free, continuous process developed for polylactide should be applicable to large-scale polymandelide production, monomer synthesis and its instability impede its practical use.

Based on the assumption that the decomposition of *rac*-mandelide before melting is due to its labile  $\alpha$ -proton, replacing the aromatic ring of mandelide with an aliphatic bulky group is a reasonable strategy for stabilizing the monomers by reducing the activity of the methine protons. The approach applied here is to manipulate the rigidity of the polymer chains and their  $T_g$ s by increasing the steric demands of the alkyl group  $\alpha$  to the carbonyl on the glycolide ring, from methyl to isopropyl and cyclohexyl groups (**Figure 13**).

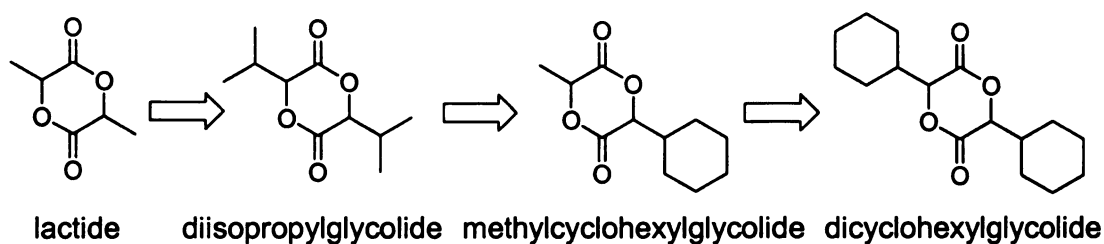
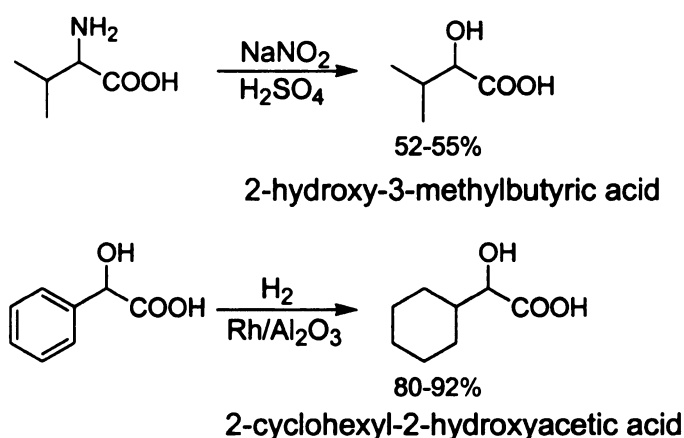


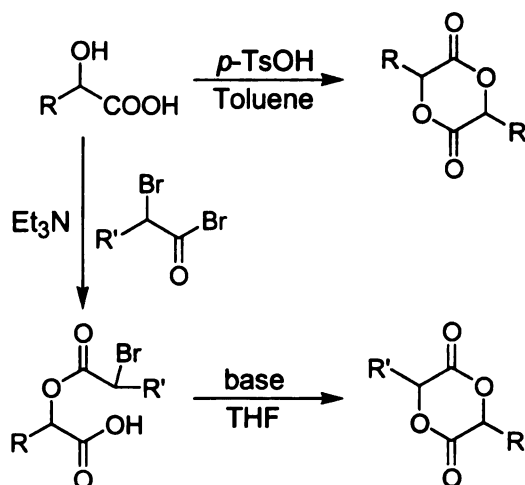
**Figure 13.** Structures of lactide derivatives with bulky side groups

## Monomer synthesis

Dicyclohexylglycolide, methylcyclohexylglycolide, and diisopropylglycolide were synthesized from 2-cyclohexyl-2-hydroxyacetic acid and 2-hydroxy-3-methylbutyric acid respectively. Diazotization of DL-valine provided 2-hydroxy-3-methylbutyric acid, <sup>115</sup> while hydrogenation of mandelic acid using a rhodium on alumina catalyst yielded 2-cyclohexyl-2-hydroxyacetic acid (**Scheme 28**). <sup>116,117</sup>



**Scheme 28.** Synthetic routes to  $\alpha$ -hydroxy acids



**Scheme 29.** Synthetic routes to lactide derivatives



The conversion of  $\alpha$ -hydroxy acids to symmetrical and nonsymmetrical lactide derivatives followed previously reported synthetic protocols (**Scheme 29**, see also **Scheme 1** and **Scheme 2** in **Chapter 1**).<sup>15</sup> The first was acid-catalyzed dimerization of the  $\alpha$ -hydroxy acids in toluene with the water removed by azeotropic distillation. Run in dilute solution to favor formation of the symmetrical dimers over linear oligomers, a mixture of the *R,S* (meso) and *R,R/S,S* (racemic) diastereomers was obtained in 20-40% yield. To prepare the nonsymmetrical methylcyclohexylglycolide, 2-cyclohexyl-2-hydroxyacetic acid was condensed with 2-bromopropionyl bromide. This route favors the formation of *R,R/S,S* products, with the *R,S/S,R* diastereomers as minor components.

*rac*-Dicyclohexylglycolide and *meso*-dicyclohexylglycolide melt without decomposition, which suggests that both isomers or their mixtures can be used in bulk polymerization. *rac*-Dicyclohexylglycolide has a melting point of 183-185 °C and *meso*-dicyclohexylglycolide melts at 80.5-81.5 °C. Unlike *rac*-mandelide, *rac*-dicyclohexylglycolide is soluble in common organic solvents, such as THF, dichloromethane, ethyl acetate, and acetone.

To compare the effects of different substituents on polymer properties and polymerization kinetics, lactide, diisopropylglycolide, methylcyclohexylglycolide, and dicyclohexylglycolide were polymerized. There are conflicting reports on the polymerization rates of *rac*-lactide and *meso*-lactide,<sup>14</sup> and studies using mixtures of racemic and meso isomers may complicate any interpretation of the polymerization kinetics. For this reason, all polymers were prepared from racemic glycolides that had been purified by recrystallization and/or column

chromatography to completely remove meso (or *R,S/S,R*) isomers. Representative  $^1\text{H}$  NMR spectra of *rac*-dicyclohexylglycolide and *meso*-dicyclohexylglycolide are shown in **Figure 14**. In the  $^{13}\text{C}$  NMR spectrum of dicyclohexylglycolide, the signals from the 6 carbons on the cyclohexyl group can be completely resolved by adding the NMR shift reagent europium(III) tris(3-(trifluoromethylhydroxymethylene)-*d*-camphorate)). The syn relationship between the methyl group and cyclohexyl group in *R,R/S,S*-methylcyclohexylglycolide was confirmed by NOE NMR spectroscopy (Appendix **Figure A- 20**).

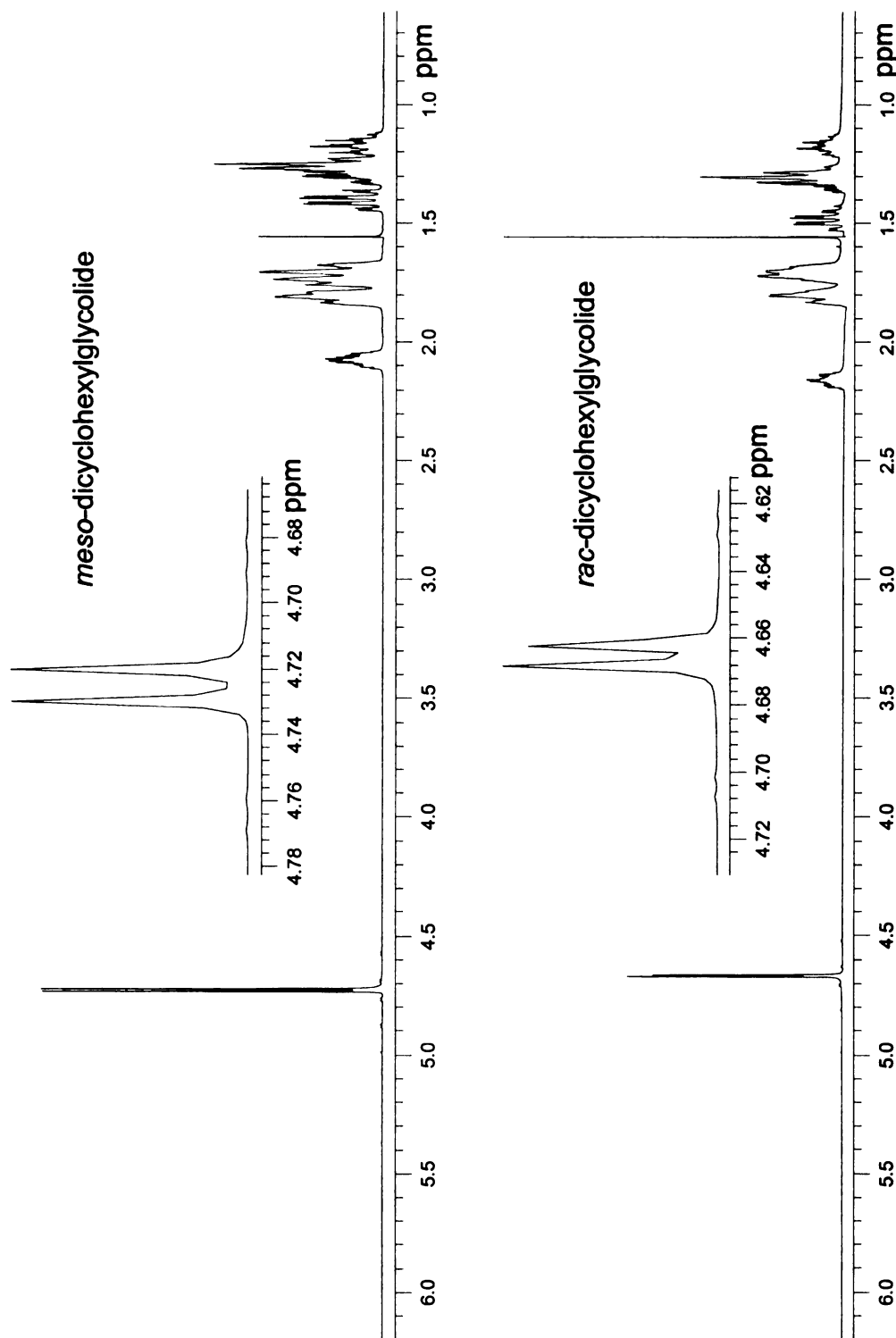


**Figure 14.** 500 MHz  $^1\text{H}$  NMR spectra for *rac*-dicyclohexylglycolide and *meso*-dicyclohexylglycolide

## Solution polymerization kinetics of substituted glycolides

Solution polymerizations of racemic glycolides using Sn(2-ethylhexanoate)<sub>2</sub> as the catalyst and 4-*tert*-butylbenzyl alcohol as the initiator were carried out in toluene to evaluate the effect of the size of glycolide ring substituents on the polymerization rate.

Ring-opening polymerizations of lactide derivatives typically follow pseudo first-order kinetics under low conversion when initiated by alcohols and catalyzed by Sn(2-ethylhexanoate)<sub>2</sub>.<sup>15,118,119</sup> For polymerizations at 90 °C with relatively low monomer concentrations (~0.2 M) and initiator and catalyst loadings (1 mol%), conversion is easily controlled, depolymerization is negligible, and the polymerization can be treated as an irreversible reaction<sup>118</sup> as expressed in equation 1,

$$R = -\frac{d[M]}{dt} = k_p[M][I] \quad (1)$$

where  $[M]$  and  $[I]$  are the concentration of monomer and initiator respectively, and  $k_p$  is the apparent rate constant for propagation. For a living polymerization,  $[I]$  is a constant, and plots of  $-\ln([M]_t/[M]_0)$  versus time  $t$  should be linear with slope  $k_p[I]$ , where  $[M]_t$  is the concentration of the monomer at time  $t$  and  $[M]_0$  is the initial monomer concentration.

The data shown in **Figure 15** are consistent with pseudo first-order kinetics. As expected, the polymerization rates (**Table 10**) depend on the size of the glycolide ring substituents, with the polymerization of *rac*-dicyclohexyl glycolide being the slowest, 1/70<sup>th</sup> of the polymerization rate of *rac*-lactide. The

isopropyl group should be a reasonable mimic for the cyclohexyl group, but the polymerization rate of *rac*-diisopropylglycolide is 4× faster than that of *rac*-dicyclohexylglycolide. The results for *rac*-methylcyclohexylglycolide are particularly interesting. The polymerization rate is ~10× that of *rac*-dicyclohexylglycolide, implying preferential ring opening at the carbonyl adjacent to the methyl group and an alternating sequence of methyl and cyclohexyl groups along the polymer backbone.

**Table 10.** Solution polymerization rates of polyglycolides

| Monomer                               | $k_p \text{ (L} \cdot \text{s}^{-1} \cdot \text{mol}^{-1}) \times 10^6$ |
|---------------------------------------|---|
| <i>rac</i> -lactide                   | 98.7  |
| <i>rac</i> -methylcyclohexylglycolide | 13.8  |
| <i>rac</i> -diisopropylglycolide      | 5.28  |
| <i>rac</i> -dicyclohexylglycolide     | 1.39  |

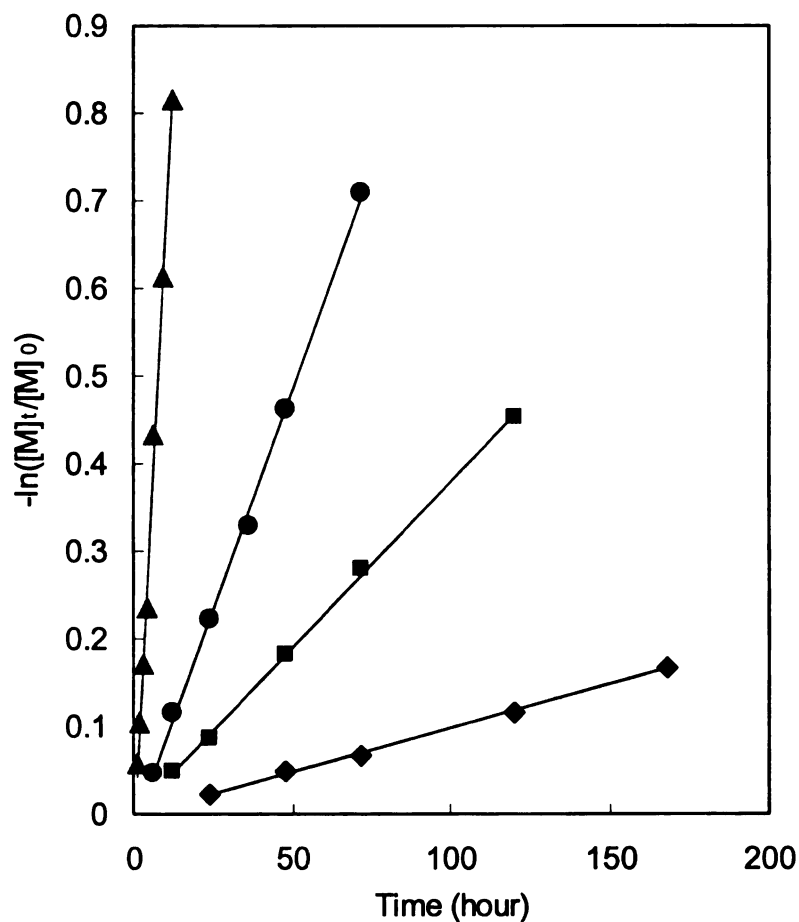


**Figure 15.** Solution polymerization kinetics of *rac*-lactide (▲), *rac*-methylcyclohexylglycolide (●), *rac*-diisopropylglycolide (■), and *rac*-dicyclohexylglycolide (◆). Polymerization conditions: 90 °C, [monomer]: [Sn(2-ethylhexanoate)<sub>2</sub>]: [4-*tert*-butylbenzyl alcohol] = 100: 1: 1.

## Bulk polymerization kinetics of *rac*-dicyclohexylglycolide

The kinetic behavior of bulk polymerizations of *rac*-dicyclohexylglycolide was examined because solvent-free polymerizations were used to generate most materials used for characterization. The kinetic data were taken at 200 °C since the monomer melts at >180 °C. Bulk polymerizations of *rac*-dicyclohexylglycolide were carried out by loading the monomer with 1 mol% each of Sn(2-ethylhexanoate)<sub>2</sub> and 4-*tert*-butylbenzyl alcohol into glass tubes, which were then sealed under vacuum. The tubes were immersed in a 200 °C oil bath and removed at desired times. High temperature runs introduce two complications: high polymerization rates make collecting data at low conversions very difficult; and the polymerization-depolymerization equilibrium must be taken into account in the kinetic analysis because the polymerizations run to high conversions.<sup>15,118</sup> The pseudo first-order kinetic equation revised to account for equilibrium monomer concentration  $[M]_{eq}$  is shown in equation 2:

$$-\ln\left(\frac{[M]_t - [M]_{eq}}{[M]_0 - [M]_{eq}}\right) = k_p[I]t \quad (2)$$

The equilibrium monomer concentration was determined from the limiting conversion reached during polymerizations at 200 °C, as well as depolymerization experiments carried out at the same temperature by adding Sn(2-ethylhexanoate)<sub>2</sub> to poly(*rac*-dicyclohexylglycolide) that had been purified by dissolving in dichloromethane, washing with HCl, and precipitated into methanol to remove all traces of monomer. Both experiments (**Figure 16**) gave ~2% residual monomer, which corresponds to  $[M]_{eq} \sim 0.07M$ .

The data for the bulk polymerization of *rac*-dicyclohexylglycolide are plotted in **Figure 17**, assuming 2% residual monomer. The points correspond to the average from three independent runs, except for the points at  $t = 3, 7$ , and 40 min, where only two samples were taken. However, the data are decidedly curved, even after the equilibrium monomer concentration was taken into account. A possible reason is that polymerization at 200 °C is sufficiently severe to cause a loss in active chain ends. The data can be linearized by assuming that the population of growing chain ends decays as

$$[I] = [I]_0 e^{-k_d t} \quad (3)$$

where  $k_d$  is the rate constant for the decomposition process, and  $[I]_0$  is the initial initiator concentration. The revised rate law is:

$$R = -\frac{d[M]}{dt} = k_p [I] ([M] - [M]_{eq}) = k_p [I]_0 ([M] - [M]_{eq}) e^{-k_d t} \quad (4)$$

and integration of equation 4 leads to:

$$Conversion = 1 - \frac{[M]_t}{[M]_0} = \left(1 - \frac{[M]_{eq}}{[M]_0}\right) \left(1 - e^{-\frac{k_p}{k_d} [I]_0 (e^{-k_d t} - 1)}\right) \quad (5)$$

Equation 5 was used to fit the data. As shown in **Figure 18**, using equation 5 improves the fit to data. A possible cause for losing active chains is the *in situ* generated carboxylic acid via *cis*-elimination.<sup>120-123</sup> This degradation model suggests that ~20% of the initiator remained after polymerization for 10 minutes.

**Figure 19** shows the evolution of the number-average molecular weight ( $M_n$ ) and polydispersity (PDI) with conversion. As the monomer conversion increases during bulk polymerization,  $M_n$  increases, reaches a maximum at high



conversion, and then drops. The PDI is nearly constant until 80% conversion, and then increases sharply. This behavior is typical of the ring-opening polymerization of lactides.<sup>15</sup> At low conversion,  $M_n$  increases linearly with conversion with an almost constant PDI because of the “living” nature of the ring-opening polymerization. When nearly all of the monomer is consumed, transesterification becomes competitive with propagation. While intermolecular transesterification only increases PDI, the formation of cyclic esters via intramolecular transesterification reduces  $M_n$  and increases PDI. Obviously, the kinetic data suggest degradation as an additional mechanism that can lower  $M_n$  and increase PDI.<sup>124</sup>

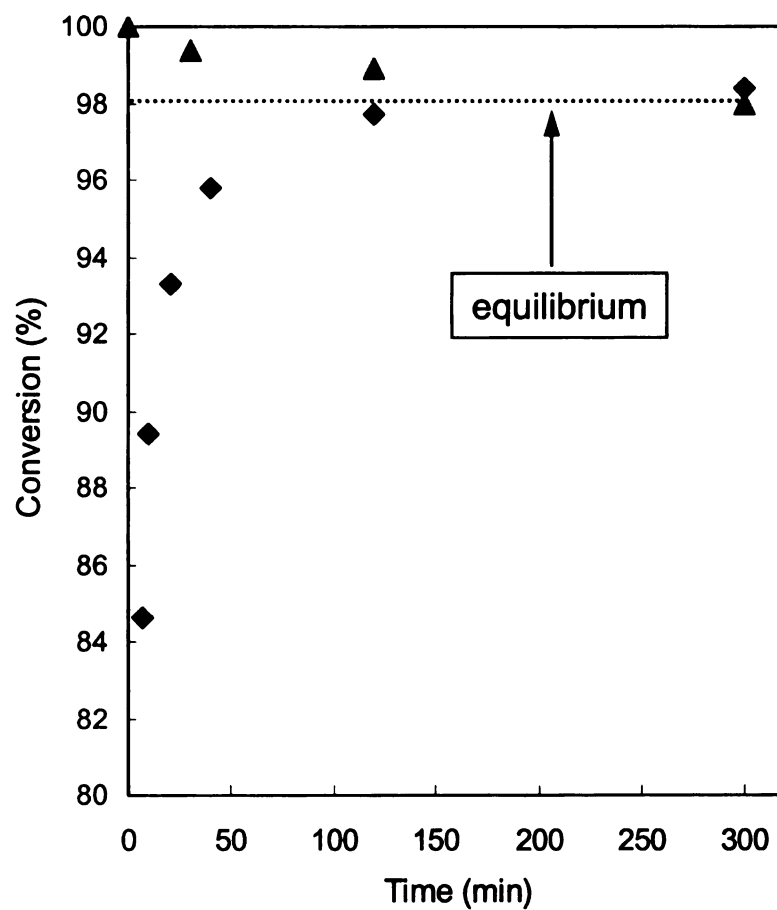


**Figure 16.** Polymerization (◆) and depolymerization (▲) data for the bulk polymerization of *rac*-dicyclohexylglycolide. Conditions: 200 °C, [monomer]: [Sn(2-ethylhexanoate)<sub>2</sub>]: [4-*tert*-butylbenzyl alcohol] = 100: 1: 1.

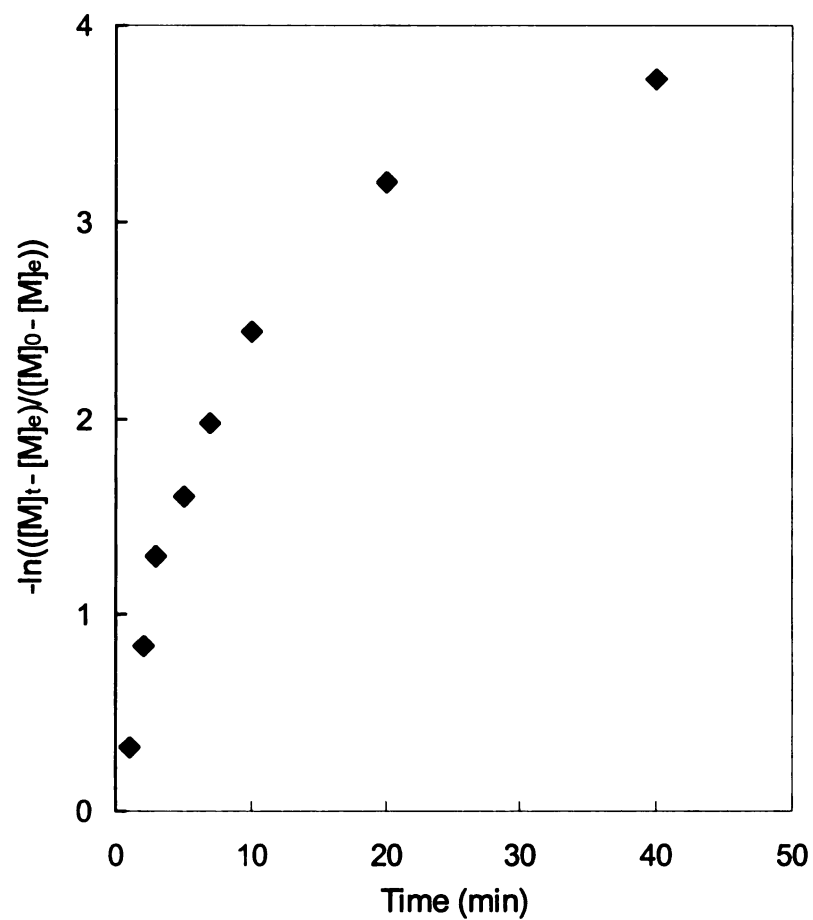


**Figure 17.** Bulk polymerization kinetics of *rac*-dicyclohexylglycolide. Polymerization conditions: 200 °C, [monomer]: [Sn(2-ethylhexanoate)<sub>2</sub>]: [4-*tert*-butylbenzyl alcohol] = 100: 1: 1.

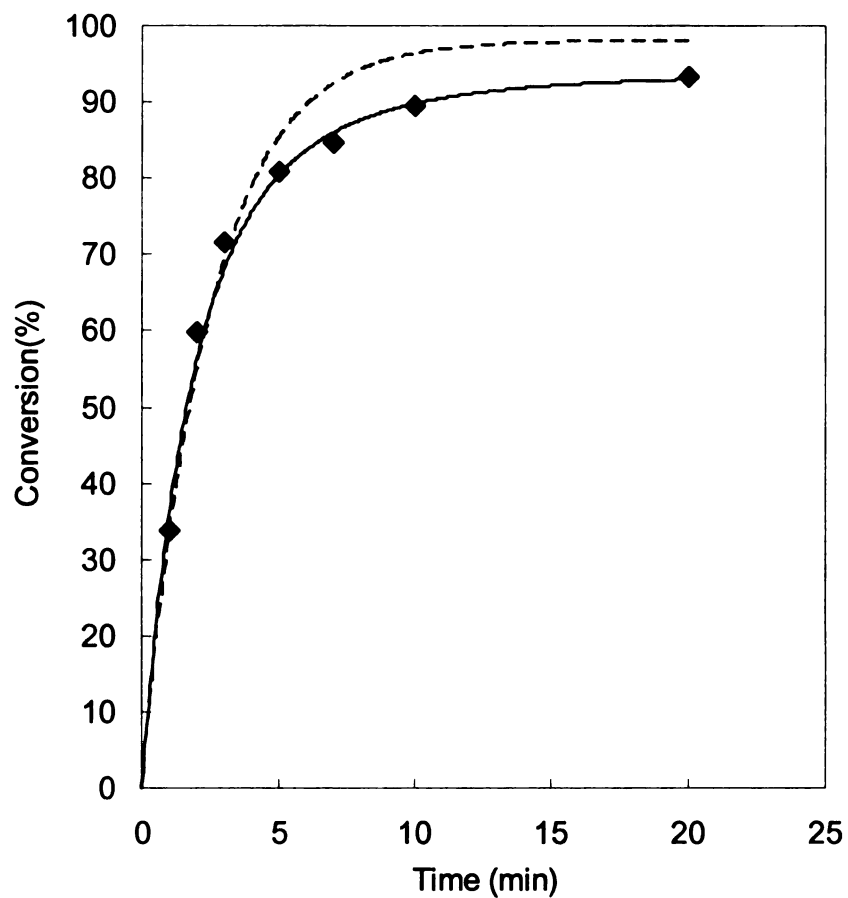


**Figure 18.** The evolution of conversion with polymerization time for the bulk polymerization of *rac*-dicyclohexylglycolide. The data were fit using an equilibrium model (dashed line), and the equilibrium model but assuming some loss of active chain ends (solid line). Conditions: 200 °C, [monomer]: [Sn(2-ethylhexanoate)<sub>2</sub>]: [4-*tert*-butylbenzyl alcohol] = 100: 1: 1.

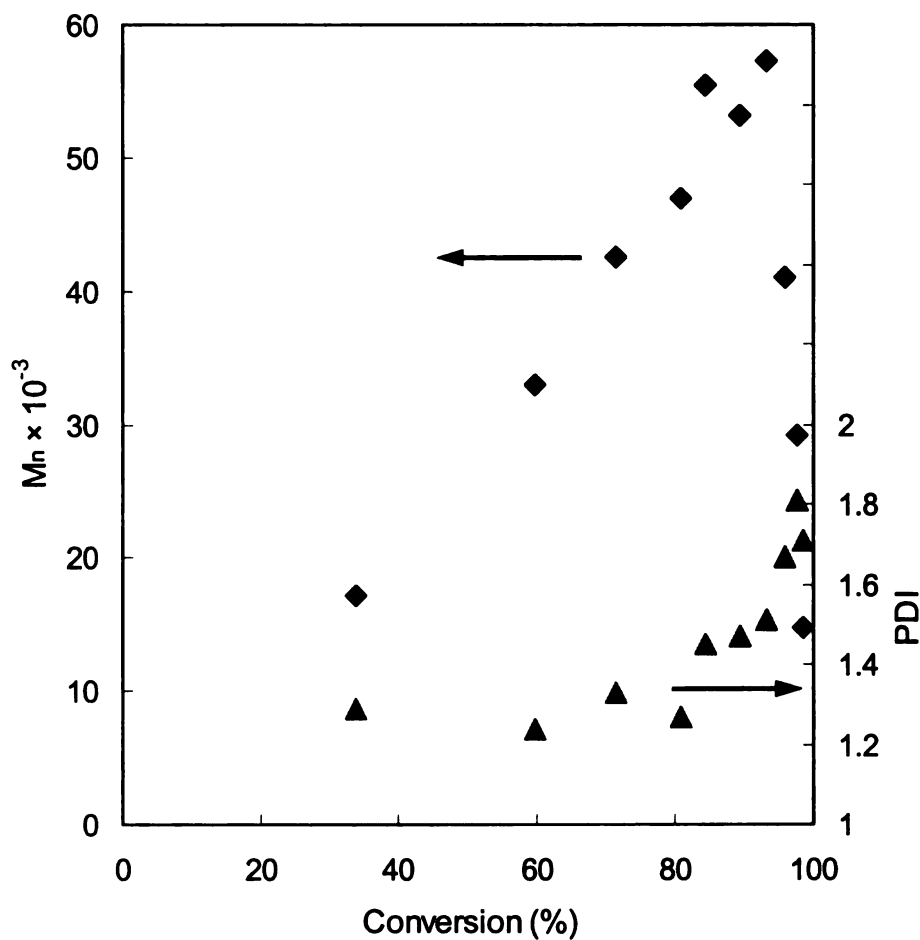


**Figure 19.** The evolution of molecular weight (♦) and polydispersity (▲) with conversion for the bulk polymerization of *rac*-dicyclohexylglycolide. Polymerization conditions: 200 °C, [monomer]: [Sn(2-ethylhexanoate)<sub>2</sub>]: [4-*tert*-butylbenzyl alcohol] = 100: 1: 1.

## Physical properties of substituted polyglycolides

Polymer properties were measured using materials prepared by bulk polymerizations with a monomer to initiator ratio of 300. The crude polymers were purified by repeated precipitation into cold methanol to remove monomers, washed with dilute HCl to remove catalyst residues,<sup>124</sup> and then dried to constant weight. The polymer molecular weights ranged from  $M_n = 40,000$  to 100,000 Da with polydispersities <1.5 (Table 11). The polymer decomposition temperatures measured using thermogravimetric analysis (TGA) define the limiting use temperatures of the polymers. As shown in Figure 20, the TGA traces for the polymers are similar with onsets for weight loss near 300 °C followed by nearly complete weight loss at 600 °C. TGA runs in air and nitrogen show only slight differences in their decomposition curves.

**Table 11.** Properties of substituted polyglycolides

| Polymer   | $M_n$  | $M_w/M_n$ | $T_g$ (°C) |
|---|--------|-----------|------------|
| poly( <i>rac</i> -lactide) <sup>a</sup>                   | 82,900 | 1.39      | 55         |
| poly( <i>rac</i> -diisopropylglycolide) <sup>b</sup>      | 89,300 | 1.18      | 41         |
| poly( <i>rac</i> -methylcyclohexylglycolide) <sup>a</sup> | 40,500 | 1.27      | 73         |
| poly( <i>rac</i> -dicyclohexylglycolide) <sup>c</sup>     | 99,300 | 1.38      | 98         |

a. bulk polymerized at 130 °C; b. bulk polymerized at 150 °C; c. bulk polymerized at 200 °C.

Glass transition temperatures measured by DSC are shown in Table 11 and Figure 21. In agreement with the notion that cyclohexyl substituents would

increase the rotation barriers of polyglycolide polymers and increase  $T_g$ , poly(*rac*-dicyclohexylglycolide) has the highest  $T_g$  (98 °C), 43 °C higher than that of poly(*rac*-lactide). The effects of the cyclohexyl ring on  $T_g$  were significant even for the nonsymmetrical poly(*rac*-methylcyclohexylglycolide) ( $T_g$  = 73 °C).

Somewhat surprising was a  $T_g$  of 41 °C for poly(*rac*-diisopropylglycolide), 14 °C lower than that of poly(*rac*-lactide) of comparable molecular weight. The kinetic data shown in **Figure 15** for the polymerization of these monomers suggest that the steric effects of the isopropyl group are close to that of cyclohexyl group and would predict a  $T_g$  higher than was measured. These data point to the importance of polar groups in polymer chains, such as the intermolecular dipole-dipole interactions and weak C—H...O hydrogen bonds in polylactides.<sup>125</sup> When van der Waals interactions dominate chain-chain interactions,  $T_g$  tracks the increase in rotation barriers. For example, polypropylene, poly(3-methyl-1-butene), and poly(cyclohexyl ethylene) have  $T_g$ s of -40, 50, and 148 °C respectively.<sup>126,127</sup> When dipole-dipole interactions become important as the case of polylactides, bulky side chains will not only increase rotation barriers (increase  $T_g$ ), but also interrupt dipole-dipole interactions (decrease  $T_g$ ) by shielding ester groups from each other. Apparently for poly(*rac*-diisopropylglycolide), the increase in the rotational barrier caused by the isopropyl groups cannot compensate for the decrease of dipole-dipole interactions, which leads to a lower  $T_g$  than poly(*rac*-lactide) (**Figure 22**).

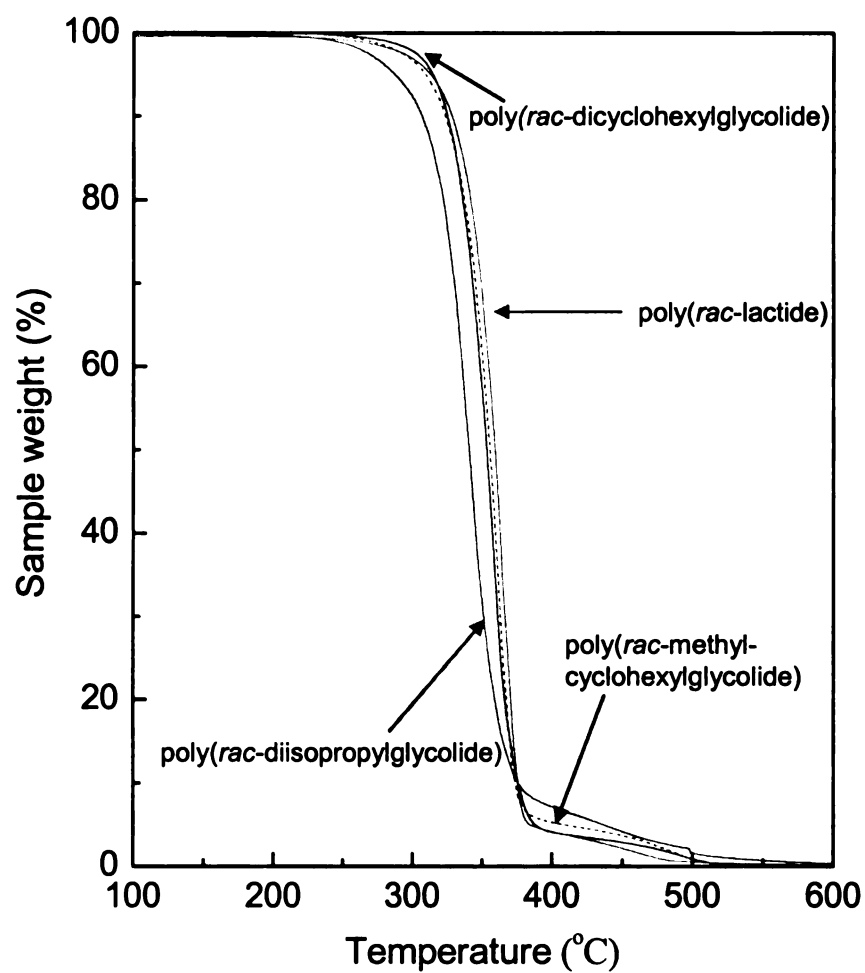


**Figure 20.** Thermogravimetric analysis results for substituted polyglycolides. Samples were run in air at a heating rate of 10 °C/min.



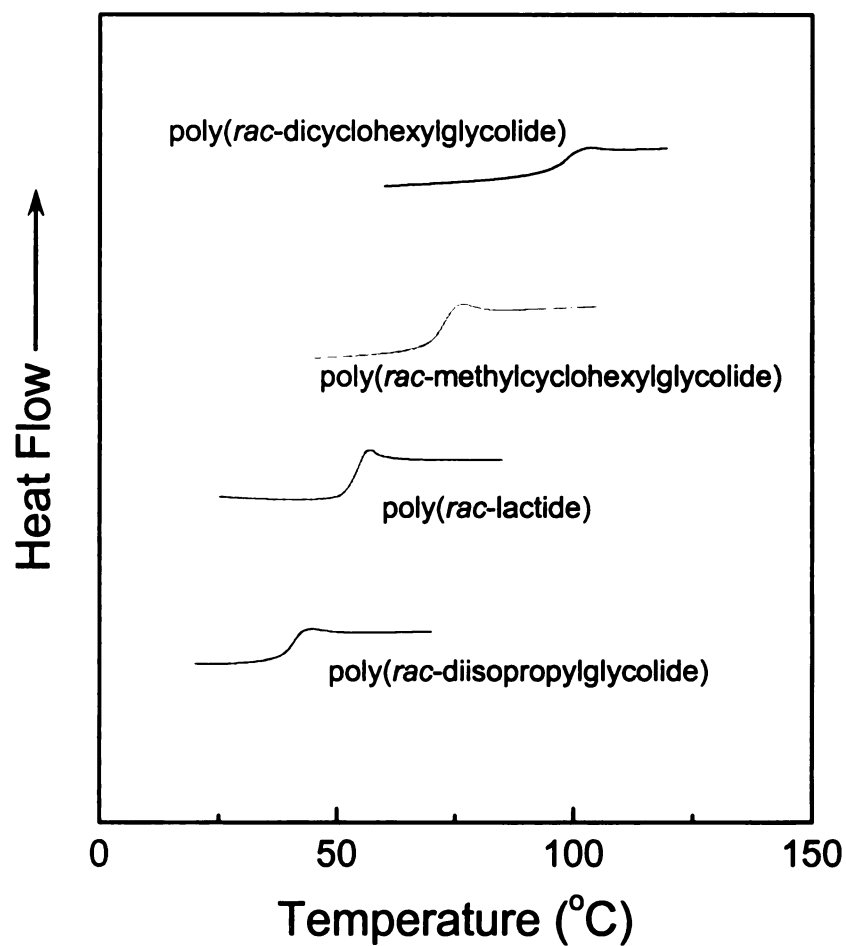


**Figure 21.** DSC analyses of substituted polyglycolides. Heating rate: 10 °C/min under nitrogen. The data are from the second heating scan, taken after flash quenching from 120 °C.

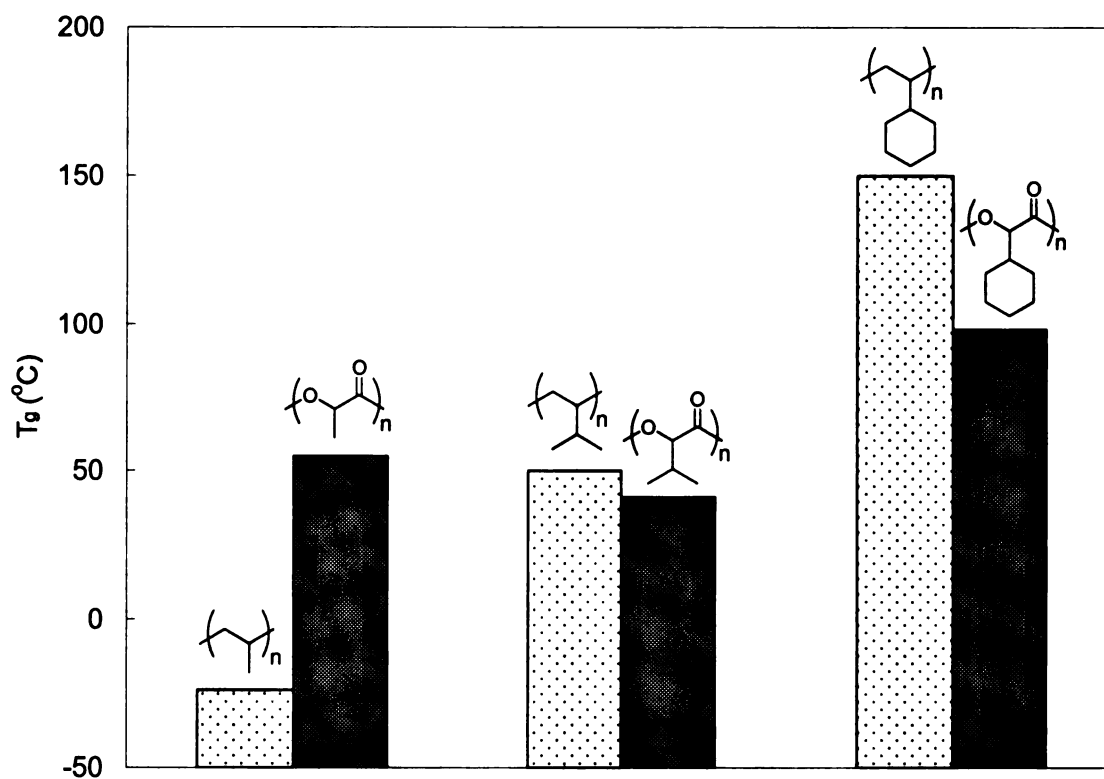


**Figure 22.** Comparisons on the  $T_g$ s of polyolefins and polyglycolides.

## Stereochemical effects on poly(dicyclohexylglycolide)s

Polymer stereoregularity that leads to crystallinity is a major factor in determining the physical properties and applications for polylactides.<sup>128-132</sup> In order to understand the consequences of stereoregularity in poly(dicyclohexylglycolide)s, *meso*- and *R,R*-dicyclohexylglycolides were isolated and polymerized. Access to *R,R*-dicyclohexylglycolide is straightforward since (*R*)-(-)-mandelic acid can be hydrogenated directly to (*R*)-2-cyclohexyl-2-hydroxyacetic acid with retention of configuration. The low melting *meso*-dicyclohexylglycolide was polymerized at 130 °C, while the higher melting *R,R*-dicyclohexylglycolide required heating to 200 °C, the same conditions used for the polymerization of *rac*-dicyclohexylglycolide. The glass transition temperatures and molecular weights are listed in **Table 12**.

**Table 12.** Properties of poly(dicyclohexylglycolide)s

| Polymer  | $M_n$   | $M_w/M_n$ | $T_g$ (°C) |
|--|---------|-----------|------------|
| poly( <i>rac</i> -dicyclohexylglycolide) <sup>a</sup>  | 99,300  | 1.38      | 98         |
| poly( <i>meso</i> -dicyclohexylglycolide) <sup>b</sup> | 89,700  | 1.22      | 96         |
| poly( <i>R,R</i> -dicyclohexylglycolide) <sup>a</sup>  | 102,500 | 1.42      | 104        |

a. bulk polymerized at 200 °C; b. bulk polymerized at 130 °C.

DSC traces of the polymers are shown in **Figure 23**. The *meso* and racemic polymers have  $T_g$ s of ~98 °C, but the  $T_g$  of poly(*R,R*-dicyclohexylglycolide) is noticeably higher, 104 °C. The specific rotation of the

*R,R* polymer is  $[\alpha]_D^{20} = +23.0^\circ$  ( $c = 1.0$ ,  $\text{CHCl}_3$ ), however, DSC scans and polarized optical microscopy studies of poly(*R,R*-dicyclohexylglycolide) samples detected no signs of crystallinity.

The degree of crystallinity in poly(L-lactide) is largely controlled by the presence of meso and D-lactide impurities,<sup>7</sup> which can be detected by  $^1\text{H}$  and  $^{13}\text{C}$  NMR. The  $^1\text{H}$  NMR and  $^{13}\text{C}$  NMR spectra of the *rac*-, *meso*- and *R,R*-poly(dicyclohexylglycolide)s are shown in **Figure 24** and **Figure 25**. An examination of the methine region in the  $^1\text{H}$  NMR spectrum suggests a high degree of stereoregularity. However, small signals at 5.16 and 5.05 ppm indicate possible contamination from meso dyads. The  $^{13}\text{C}$  NMR spectrum of poly(*R,R*-dicyclohexylglycolide) is consistent with the  $^1\text{H}$  NMR data. The carbonyl region of the spectrum is dominated by a singlet at 168.68 ppm, confirming the overall isotactic nature of the polymer, but it too shows minor resonances that imply a population of meso dyads. Integration of the carbonyl region places the isotactic content at 86%. Since the *R,R* monomer used in these polymerizations was >99% pure, epimerization likely occurred during polymerization. To confirm this notion, solution polymerization of the same monomer was carried out at 90 °C to minimize epimerization. Integration of the carbonyl region in the  $^{13}\text{C}$  NMR spectrum confirmed increased stereoregularity, with the isotactic resonance corresponding to 98% of the total carbonyl intensity (**Figure 26**). This polymer sample showed no signs of crystallization when examined by DSC and polarized optical microscopy. It appears that the bulky cyclohexyl groups hinder the main

chains packing and thus prevent the polymer from crystallizing under normal conditions, which is similar to the slow crystallization of isotactic polystyrene.<sup>133</sup>

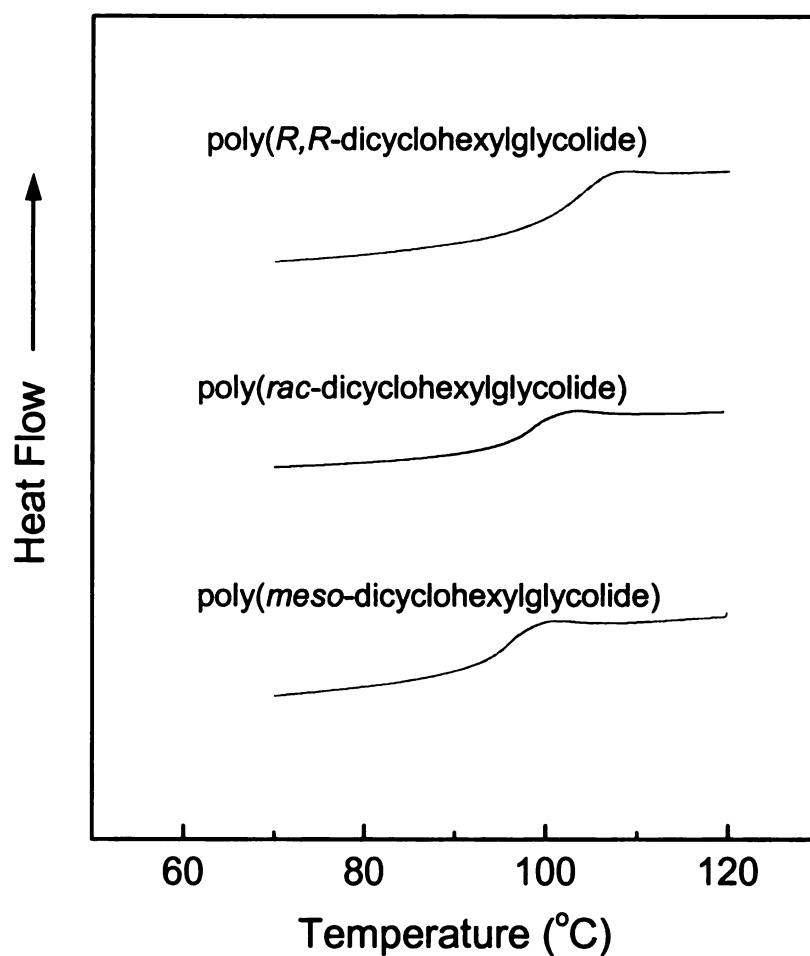


**Figure 23.** DSC analyses of poly(dicyclohexylglycolide)s. Heating rate: 10 °C/min under nitrogen. The data are from the second heating scan, taken after flash quenching from 120 °C.

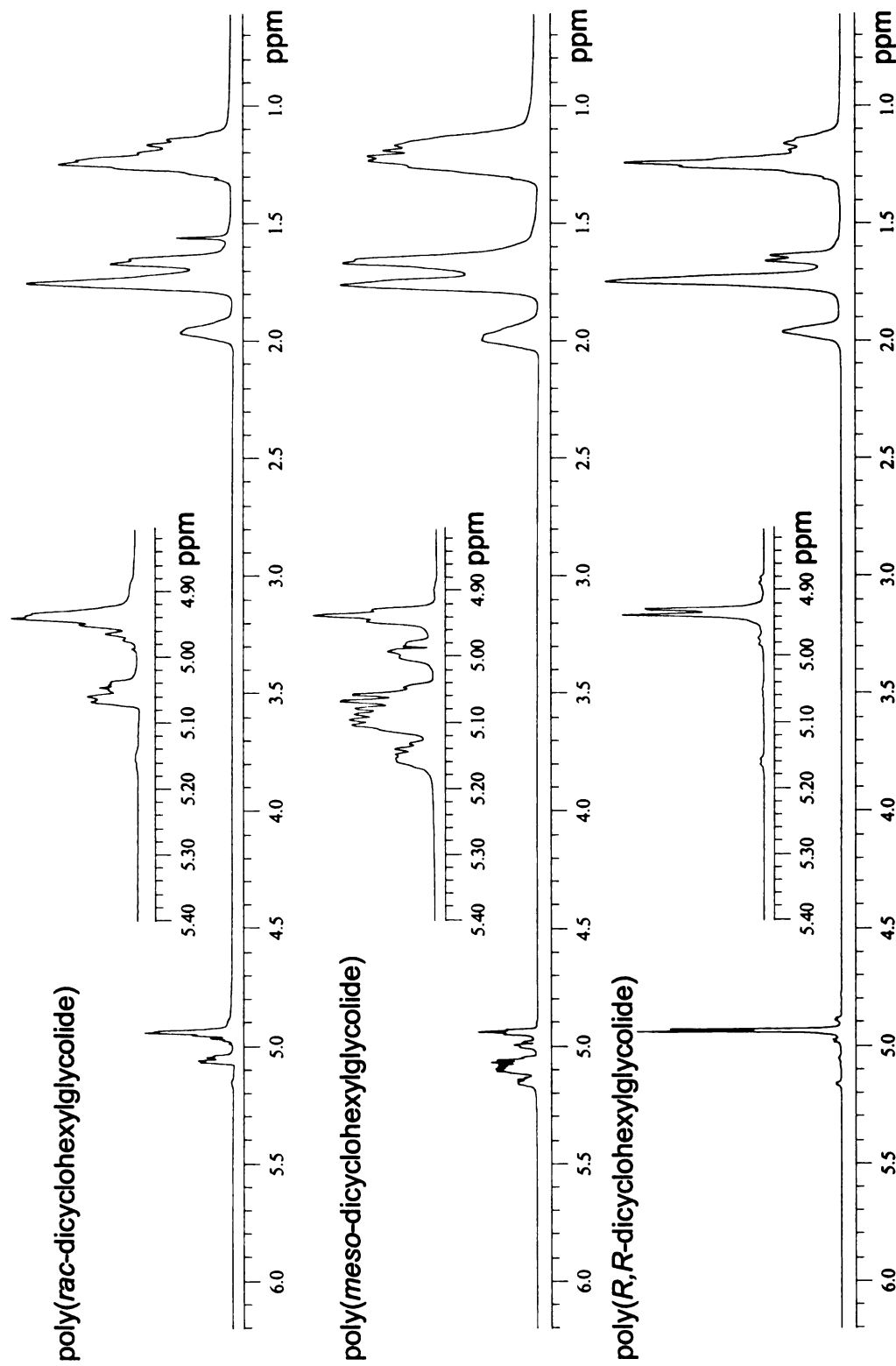


**Figure 24.** 500 MHz  $^1\text{H}$  NMR spectra for *poly(rac-dicyclohexylglycolide)*, *poly(meso-dicyclohexylglycolide)*, and *poly(R,R-dicyclohexylglycolide)*.

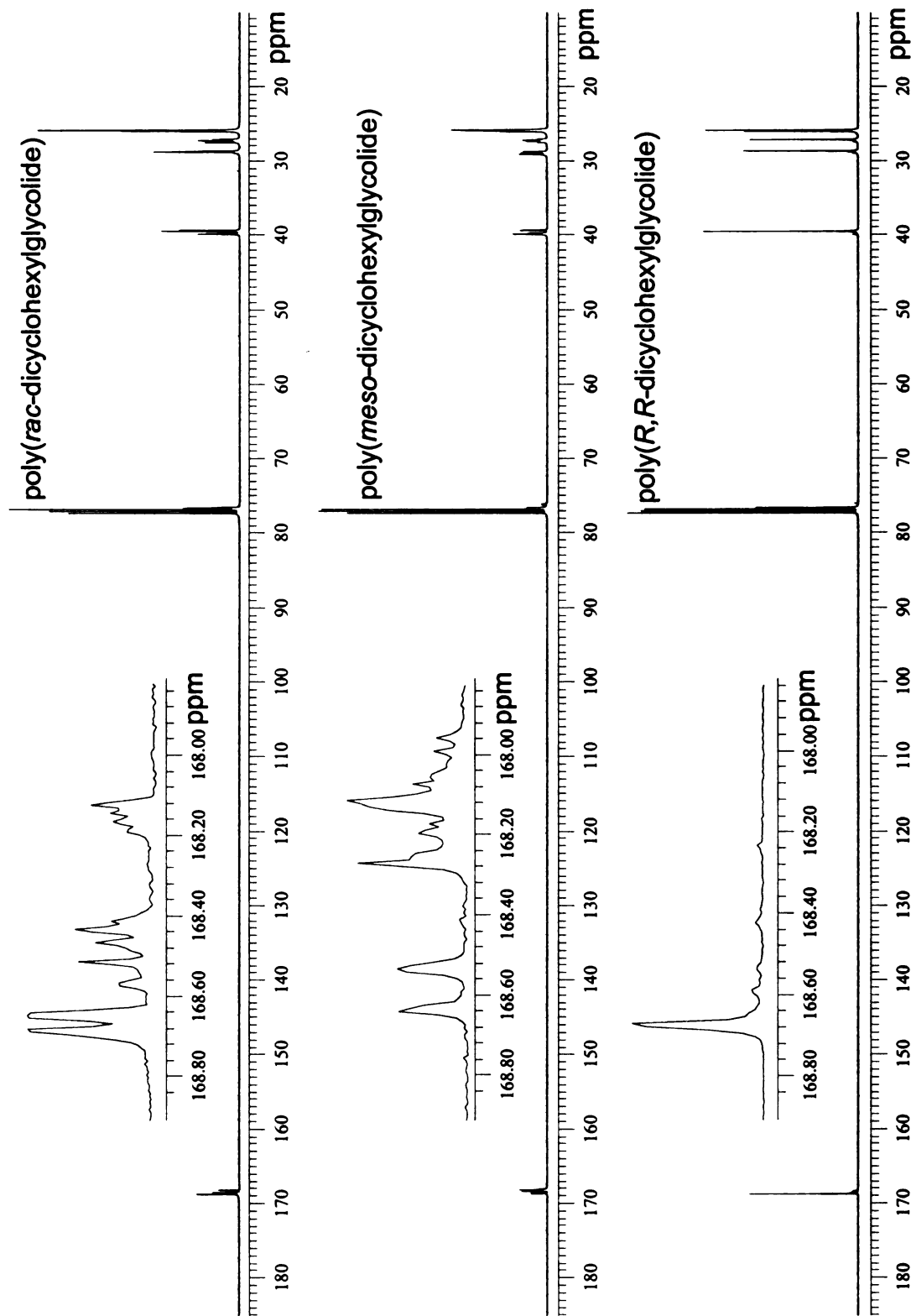


**Figure 25.** 125 MHz  $^{13}\text{C}$  NMR spectra for poly(*rac*-dicyclohexylglycolide), poly(*meso*-dicyclohexylglycolide), and poly(*R,R*-dicyclohexylglycolide)



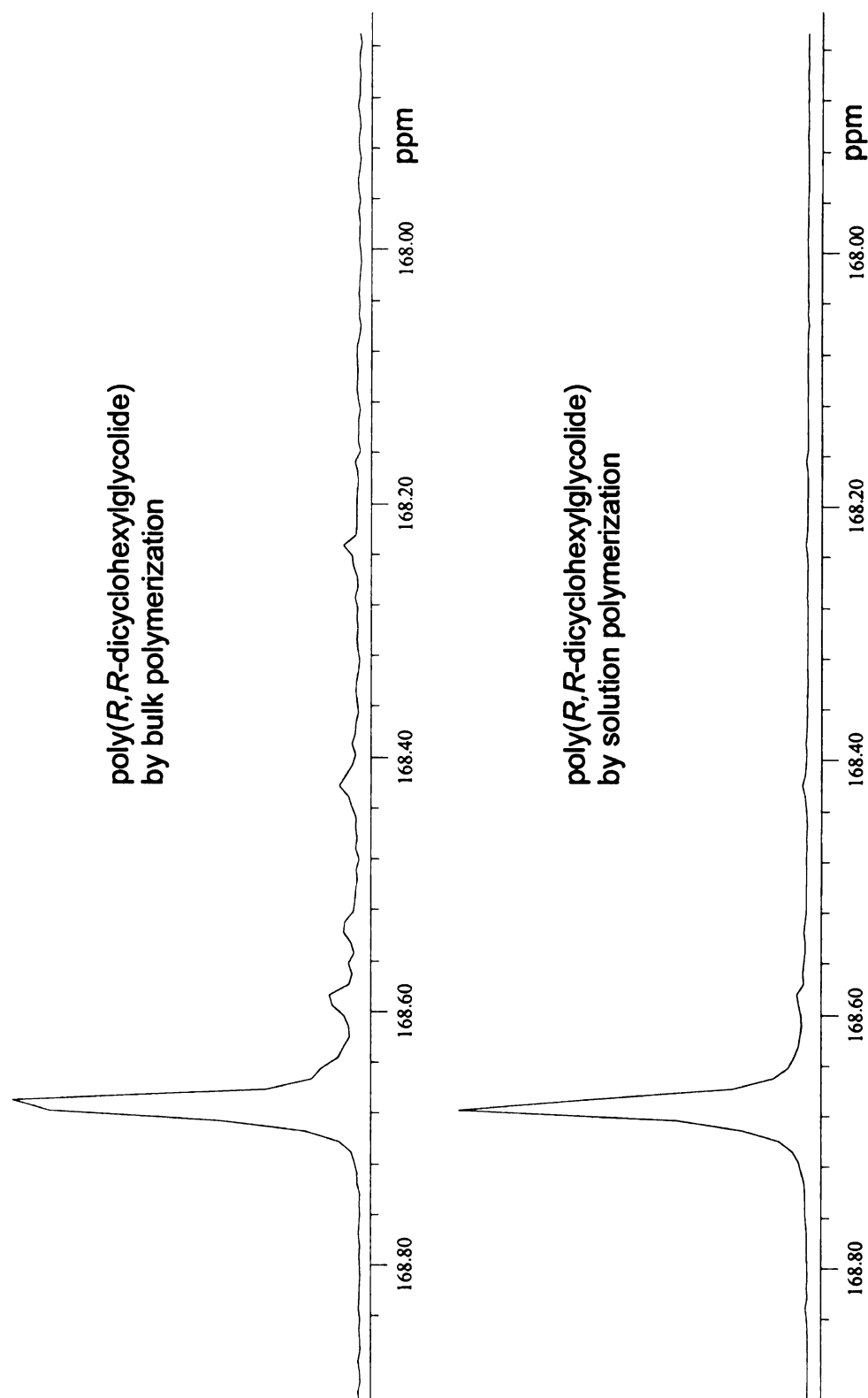
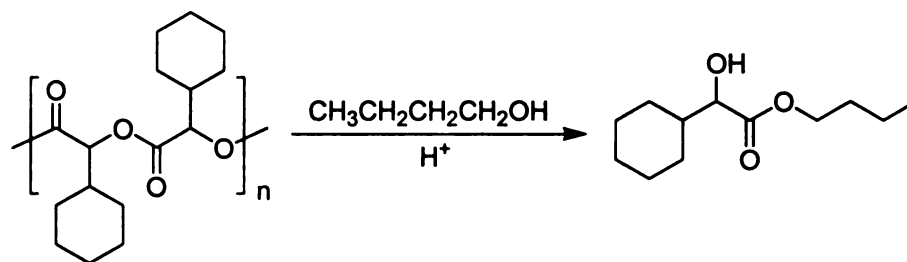


**Figure 26.** 125 MHz  $^{13}\text{C}$  NMR spectra of the carbonyl regions of poly(*R,R*-dicyclohexylglycolide) synthesized by bulk polymerization (200 °C) and solution polymerization (90 °C).

### Degradation of poly(*rac*-dicyclohexylglycolide).

The degradability of poly(*rac*-dicyclohexylglycolide) was first evaluated by hydrolysis in phosphate buffer solution (0.01M  $\text{KH}_2\text{PO}_4/\text{K}_2\text{HPO}_4$  solution) at 55 °C and  $\text{pH} = 7.4$ . These specific conditions allow direct comparison to degradation experiments run on other polylactide derivatives.<sup>14,42</sup> However, after 400 days under these conditions, poly(*rac*-dicyclohexylglycolide) samples show no signs of degradation. Because poly(dicyclohexylglycolide) has a high  $T_g$ , and also is highly hydrophobic, it is not surprising that poly(*rac*-dicyclohexylglycolide) has a very slow degradation rate at this temperature (>40 °C lower than its  $T_g$ ).



**Scheme 30.** Butanolysis of poly(dicyclohexylglycolide)

In order to degrade poly(dicyclohexylglycolide) faster and demonstrate that it is recyclable, the polymer was refluxed in *n*-butanol with a catalytic amount of sulfuric acid (**Scheme 30**). Butyl 2-cyclohexyl-2-hydroxyacetate was thus prepared via transesterification. Data for the evolution of molecular weight with reaction time are shown in **Figure 27** and **Table 13**.

**Table 13.** Butanolysis of poly(*rac*-dicyclohexylglycolide)

| Time (hour) | Remaining polymer (mol%) | $M_n$  | $M_w/M_n$ |
|-------------|--------------------------|--------|-----------|
| 0           | 100                      | 82,700 | 1.37      |
| 3           | 100                      | 15,100 | 1.77      |
| 6           | 100                      | 9,700  | 1.58      |
| 12          | 30.6                     | 6,200  | 1.29      |
| 24          | 14.5                     | 4,500  | 1.13      |
| 48          | 5.7                      | 3,500  | 1.03      |

While hydrolytic degradation of polylactide follows a random chain scission model,<sup>14,134</sup> the behavior during butanolysis of poly(*rac*-dicyclohexylglycolide) is unknown. In the random chain scission model,<sup>134</sup> the average number of bond cleavages per polymer molecule ( $N$ ) is:

$$N = M_n(0) / M_n(t) - 1 = k_d P_n(0)t \quad (6)$$

where  $M_n(0)$  and  $M_n(t)$  are the number-average molecular weights of polyesters at time 0 and time  $t$ ,  $k_d$  is the rate constant of hydrolytic degradation, and  $P_n(0)$  is the number-average degree of polymerization at time 0.

As shown in **Figure 28**, butanolysis of poly(*rac*-dicyclohexylglycolide) is not linear. Deviation from random chain scission model might be caused by incorrect determination of  $M_n$ . Initially, the molecular weight rapidly declined (**Figure 28**), and a significant population of oligomers formed. Since some oligomers were below the molecular weight cutoff in the GPC analysis,  $M_n$  was overestimated, causing the curvature.

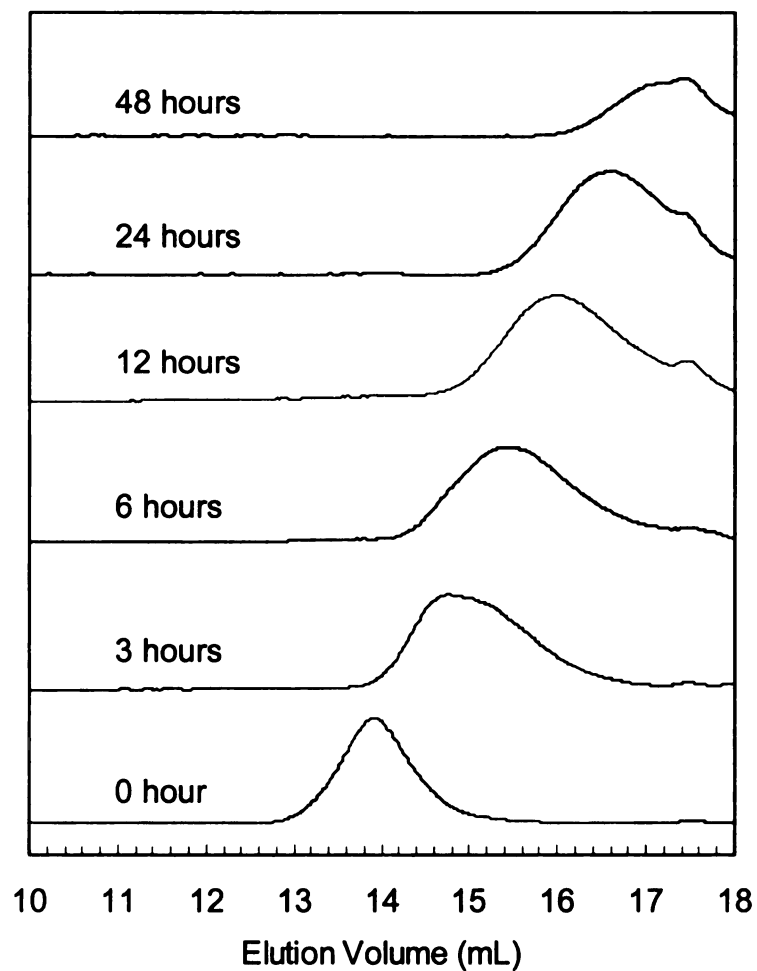


**Figure 27.** GPC traces of poly(*rac*-dicyclohexylglycolide) during butanolysis. The polymer was refluxed in *n*-butanol with catalytic amount of sulfuric acid.

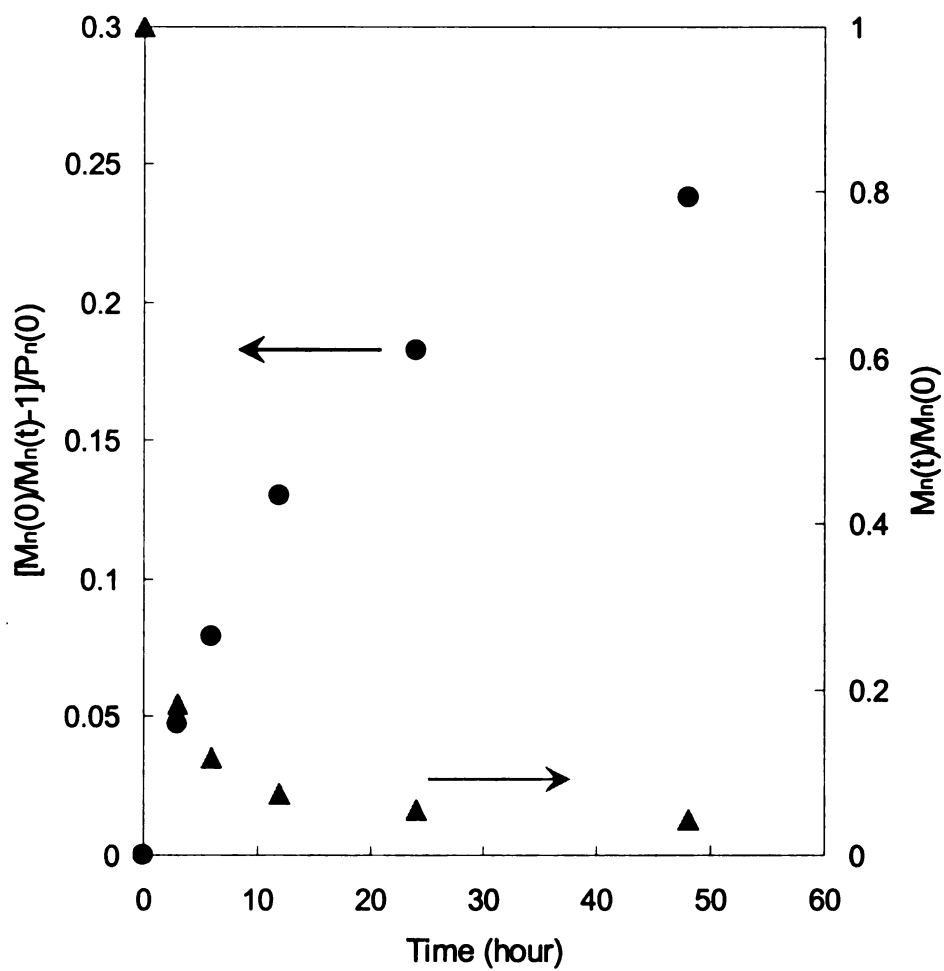


**Figure 28.** Molecular weight changes of poly(*rac*-dicyclohexylglycolide) in butanolysis. The polymer was refluxed in *n*-butanol with catalytic amount of sulfuric acid.

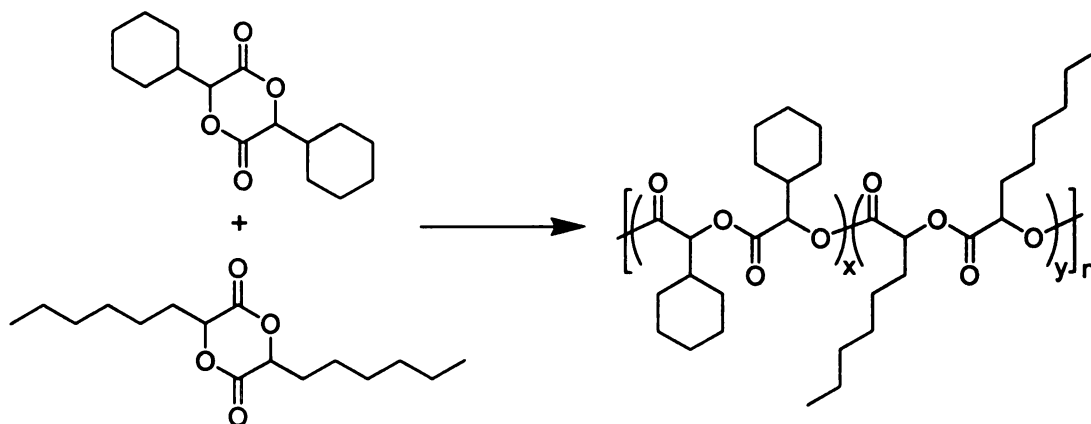
### Chapter 3 Dicyclohexylglycolide-based copolymers

Copolymerization is one of the most common and efficient ways to achieve desired polymer properties by utilizing available monomers. Various lactide-based copolymers with tailored polymer structures have been synthesized, such as random copolymers,<sup>135-138</sup> block copolymers,<sup>139-142</sup> graft copolymers,<sup>143-146</sup> star-shaped copolymers,<sup>147-149</sup> hyperbranched copolymers,<sup>150-152</sup> dendritic copolymers,<sup>153-155</sup> and comb-like copolymers.<sup>108,156-158</sup>

Lactide-based copolymers are commonly synthesized by copolymerizing lactide with other cyclic monomers such as glycolide,<sup>159</sup> lactones,<sup>160</sup> and cyclic carbonates.<sup>161</sup> Changing the sequence of monomer addition allows different polymer architectures to be realized. Lactide-based block copolymers are readily synthesized by using macroinitiators, e.g. polystyrene or poly(isoprene) with hydroxyl end groups, to initiate lactide polymerization.<sup>162,163</sup> *In situ* generated macroinitiators combine the advantages of ring-opening polymerization with other polymerization methods (cationic, anionic, and radical polymerizations). Alternating lactic acid-based polymers can be synthesized from nonsymmetrical cyclic monomers, such as nonsymmetrical lactides, *p*-dioxanones, dioxepanediones, benzodioxepindiones, and depsipeptides, as discussed in detail in **Chapter 1**. A less common route to lactide-based copolymers is to link polylactide with other polymers via coupling reactions. For example, a PEO-PLA-PEO triblock copolymer was prepared by DCC coupling of the hydroxy end groups of polylactide with carboxylic acid terminated poly(ethylene oxide).<sup>164</sup>

## Random copolymers of dicyclohexylglycolide and dihexylglycolide.

While the degradation rates of polylactide derivatives depend on the molecular weight, crystallinity, and hydrophobicity, the glass transition temperature also plays a critical role.<sup>14</sup> For example, poly(dihexylglycolide) has a much faster degradation rate than poly(dicyclohexylglycolide) due to its much lower glass transition temperature ( $T_g \sim -40\text{ }^\circ\text{C}$ ), although these two polymers have similar polymer structures and chemical compositions. To fine tune the properties of poly(dicyclohexylglycolide) and access novel polylactides with controllable  $T_g$ s ranging from  $-40\text{ }^\circ\text{C}$  to  $100\text{ }^\circ\text{C}$ , we synthesized random copolymers of dicyclohexylglycolide and dihexylglycolide and studied their physical properties.



**Scheme 31.** Copolymerization of dicyclohexylglycolide and dihexylglycolide

Random copolymers of dicyclohexylglycolide and dihexylglycolide were prepared by bulk polymerization at  $130\text{ }^\circ\text{C}$  for 2 hours using  $\text{Sn}(\text{2-ethylhexanoate})_2$  as the catalyst and 4-*tert*-butylbenzyl alcohol as the initiator

(Scheme 31). Because poly(*rac*-dicyclohexylglycolide) and poly(*meso*-dicyclohexylglycolide) have similar  $T_g$ s, there are advantages in using a mixture of *rac*-dicyclohexylglycolide and *meso*-dicyclohexylglycolide as the monomer pool. Such an approach not only simplifies monomer purification, but also enables lower polymerization temperatures that minimize side reactions due to the lower melting point of the mixture. For the same reasons, mixtures of *rac*-dihexylglycolide and *meso*-dihexylglycolide were used in copolymerizations. The monomer feed ratios and corresponding polymer composition ratios are listed in Table 14, and the NMR spectra of the copolymers are shown in Figure 29.

**Table 14.** Properties of poly(dicyclohexylglycolide-co-dihexylglycolide)s

| Feed ratio<br>(cyclohexyl: hexyl) | Composition ratio<br>(cyclohexyl: hexyl) | $M_n$  | $M_w/M_n$ | $T_g$ (°C) |
|-----------------------------------|--|--------|-----------|------------|
| 0:100                             | 0:100                                    | 45,900 | 1.22      | -38        |
| 15:85                             | 12:88                                    | 62,300 | 1.43      | -28        |
| 30:70                             | 26:74                                    | 65,100 | 1.44      | -19        |
| 50:50                             | 47:53                                    | 60,000 | 1.42      | -1         |
| 70:30                             | 61:39                                    | 43,000 | 1.33      | 21         |
| 85:15                             | 78:22                                    | 37,200 | 1.25      | 50         |
| 100:0                             | 100:0                                    | 30,300 | 1.23      | 92         |



As shown in **Table 14**, the composition of cyclohexylglycolide in the copolymer, determined by  $^1\text{H}$  NMR, is less than the corresponding feed ratio, a consequence of the lower reactivity of dicyclohexylglycolide compared to the less-hindered dihexylglycolide.

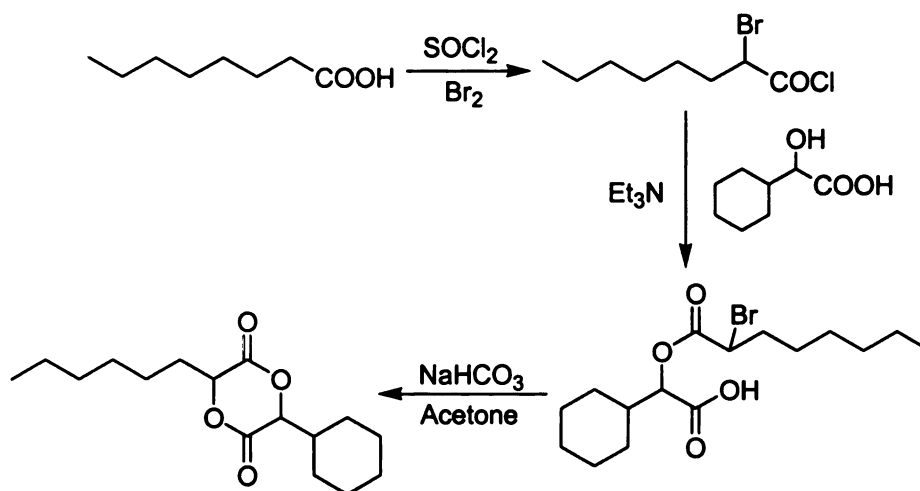
Differential scanning calorimetry data for the copolymers and their corresponding homopolymers are shown in **Figure 30**, and the polymer  $T_g$ s are listed in **Table 14**. As expected, higher dicyclohexylglycolide compositions lead to higher copolymer  $T_g$ s. By gradually changing the dicyclohexylglycolide: dihexylglycolide feed ratios, we can fine tune the glass transition from 92 °C to -38 °C.

Given that each copolymer shows a single  $T_g$ , the Fox equation (equation 7) may be applicable to this copolymer system if the random copolymers are homogenous.<sup>165</sup> The Fox equation is:

$$\frac{1}{T_g} = \frac{W_1}{T_{g1}} + \frac{W_2}{T_{g2}} \quad (7)$$

where  $T_g$ ,  $T_{g1}$ , and  $T_{g2}$  are the glass transition temperatures of the random copolymer, poly(dicyclohexylglycolide), and poly(dihexylglycolide) respectively, and  $W_1$  and  $W_2$  are the weight fractions of the dicyclohexylglycolide and dihexylglycolide repeating units in the copolymer. As shown in **Figure 31**, the Fox equation is a reasonable fit to the experimental data. Polymers having comparable dicyclohexylglycolide and dihexylglycolide compositions have broad transitions and the deviation seen for these points may be due to the difficulty of defining  $T_g$  for some DSC measurements.

The broad glass transitions also might indicate partial phase separation in these materials. Because dihexylglycolide is more reactive than dicyclohexylglycolide in ring-opening polymerization, the “random” copolymer of dicyclohexylglycolide and dihexylglycolide is perhaps better described as a gradient copolymer, dihexylglycolide rich at one end and dicyclohexylglycolide rich at the other. When the dicyclohexylglycolide and dihexylglycolide compositions are comparable, the two ends of the polymer are sufficiently different that they show slightly different  $T_g$ s, thus broadening the glass transition. The extreme case, a blend of the two homopolymers, both having  $M_n$  higher than 30,000, was examined using DSC. The results showed distinct glass transitions from each homopolymer (**Figure 32**).

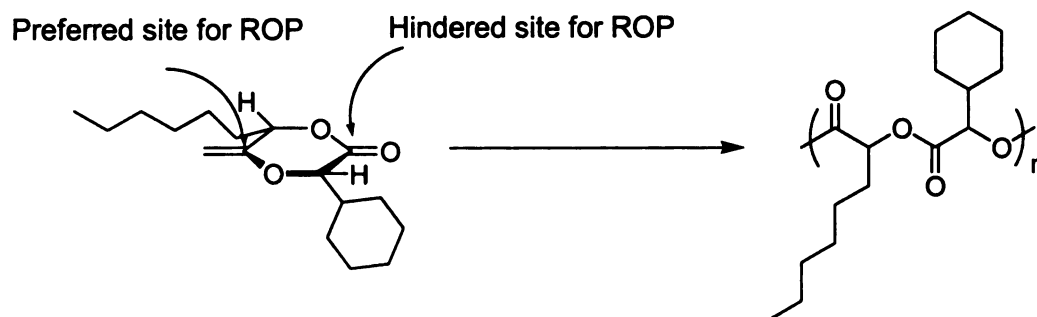


**Scheme 32.** Synthetic route to hexylcyclohexylglycolide

For comparison, we synthesized an AB monomer from cyclohexylglycolic acid (2-cyclohexyl-2-hydroxyacetic acid) and hexylglycolic acid (2-hydroxyoctanoic acid) (**Scheme 32**). As seen in the synthesis of

methylcyclohexylglycolide, formation of the *R,R/S,S* isomers is favored over the *R,S/S,R* isomers in the cyclization step, and the same was seen in the synthesis of hexylcyclohexylglycolide. Trace amounts of the *R,S/S,R* isomers were then removed by recrystallization, and the syn relationship between cyclohexyl and hexyl groups was confirmed by NOE NMR spectroscopy (**Figure A- 24**).

Ring-opening of hexylcyclohexylglycolide is preferred at the less hindered carbonyl, adjacent to the hexyl group, which favors an alternating copolymer of cyclohexylglycolic acid and hexylglycolic acid (**Scheme 33**). Verification of alternating structure by  $^{13}\text{C}$  NMR spectroscopy (**Figure A- 44**) is difficult since the monomer is a mixture of *R,R/S,S* isomers.



**Scheme 33.** Ring-opening polymerization of hexylcyclohexylglycolide

**Table 15.** Properties of poly(hexylcyclohexylglycolide)

| Polymer                        | $M_n$  | $M_w/M_n$ | $T_g$ (°C) |
|--------------------------------|--------|-----------|------------|
| poly(hexylcyclohexylglycolide) | 82,700 | 1.23      | 13         |

As shown in **Figure 30** and **Table 15**, the glass transition of this polymer is well-defined and sharper than that of poly(dicyclohexylglycolide-co-dihexylglycolide) having a similar chemical composition. Poly(hexylcyclohexylglycolide) also fits Fox equation better than random copolymers of comparable compositions (**Figure 31**), because the Fox equation assumes homogenous polymer systems and the random copolymers are “blocky”.

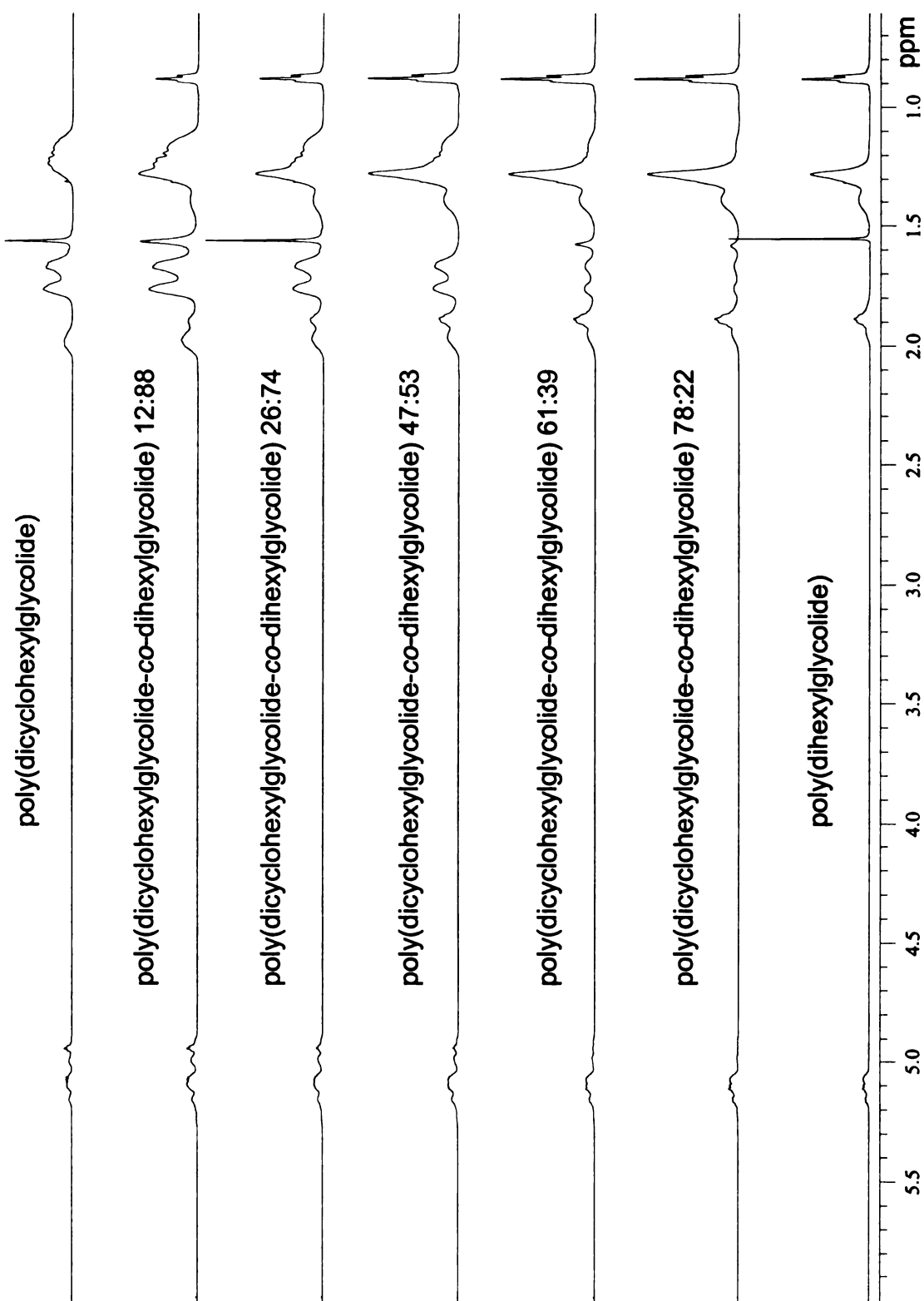


**Figure 29.** 500 MHz  $^1\text{H}$  NMR spectra of poly(dicyclohexylglycolide-co-dihexylglycolide)s

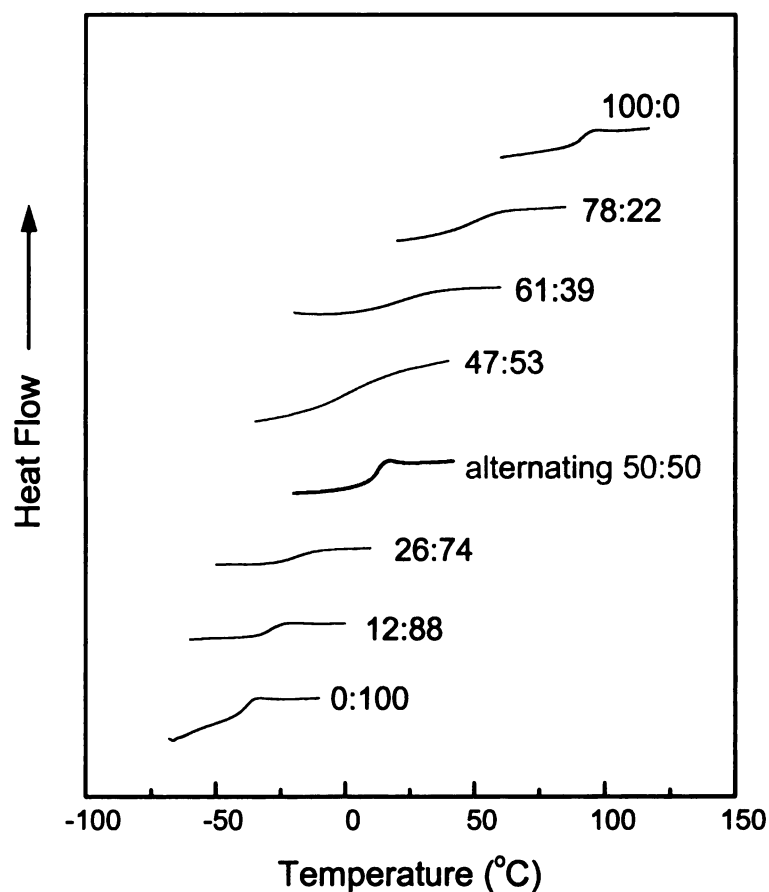


**Figure 30.** DSC analyses for poly(dicyclohexylglycolide-co-dihexylglycolide)s and poly(hexylcyclohexylglycolide). The ratios shown in the figure are the dicyclohexylglycolide: dihexylglycolide copolymer composition ratios; poly(hexylcyclohexylglycolide) is shown as an alternating 50:50 copolymer. Heating rate: 10 °C/min under nitrogen. The data are second heating scans taken after flash quenching from 120 °C.

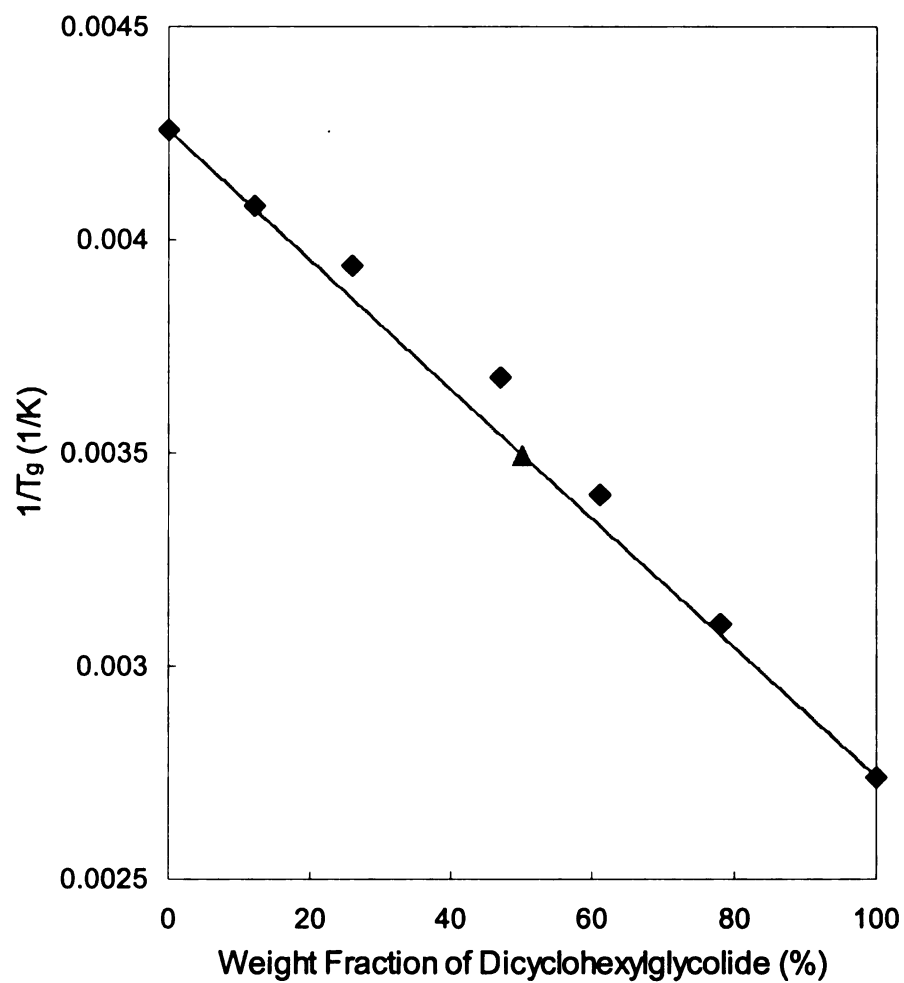


**Figure 31.** Glass transition temperatures of poly(dicyclohexylglycolide-co-hexylglycolide)s (♦) and poly(hexylcyclohexylglycolide) (▲) fit to the Fox equation.

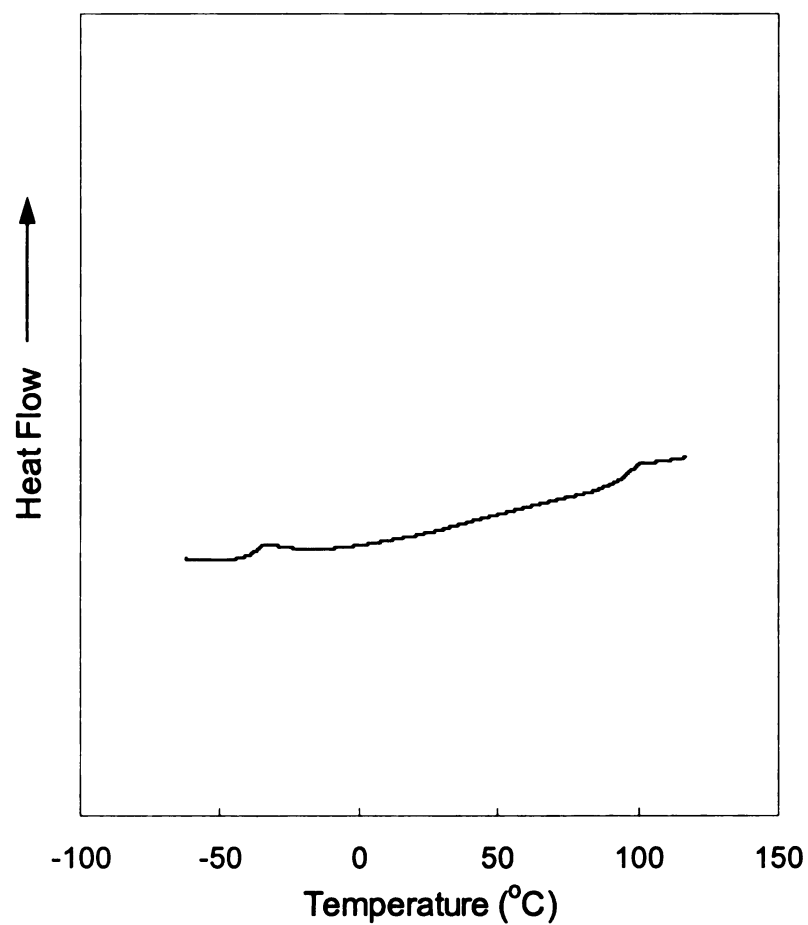


**Figure 32.** DSC analysis of a 1:1 blend of poly(dicyclohexylglycolide) and poly(dihexylglycolide). Heating rate: 10 °C/min under nitrogen. The data are from the second heating scan, taken after flash quenching from 120 °C.



**Poly(dicyclohexylglycolide)-*block*-poly(ethylene glycol)-*block*-poly(dicyclohexylglycolide) triblock copolymers.**

Like polystyrene, polylactide has a high modulus and high strength but is lacking in toughness.<sup>3</sup> The brittleness is due to the fact that the entangled strand density of amorphous polylactide is quite low (the entanglement molecular weight  $M_e \sim 10,000$ - $100,000$  Da), which favors crazing as the deformation mechanism in tensile and impact testing.<sup>166</sup> By replacing the methyl groups of polylactide with cyclohexyl groups, we successfully synthesized poly(dicyclohexylglycolide) which is rigidified by the bulky cyclohexyl side chains and features a high  $T_g$ . However, it is known that introducing bulky groups into polymer chains may cause brittleness and compromise the impact resistance by dramatically increasing the entanglement molecular weight. For example, poly(vinylcyclohexane) has a much higher entanglement molecular weight ( $M_e = 49,000$ ) than that of polyethylene ( $M_e = 1,200$ ).<sup>167</sup>

Based on the above, the homopolymer of dicyclohexylglycolide should be even more brittle than polylactide, but as yet there is no experimental verification. Brittleness is undesired and will limit the range of applications for poly(dicyclohexylglycolide). A widely used strategy for toughening amorphous polymers is to lower the  $T_g$  to below the use temperature.<sup>72</sup> However, in the case of poly(dicyclohexylglycolide), which was designed as a high use-temperature degradable polymer, this approach will counteract our efforts to increase  $T_g$ .

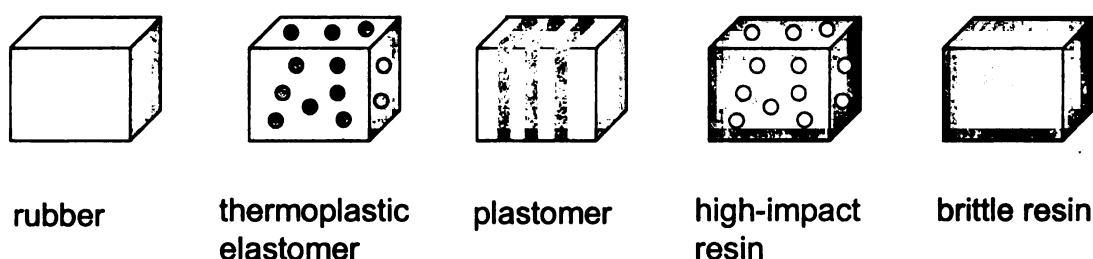
The common methods used to toughen brittle polymers without greatly sacrificing  $T_g$  are orientation, blending, and copolymerization.<sup>3</sup> Chain orientation

works well in situations where crystallites form during processing, because they can act as physical crosslinks by increasing the interconnectivity of polymer chains and decreasing the chance that a growing crack in a specimen will propagate. But since poly(dicyclohexylglycolide) is not crystalline, even for the highly isotactic polymer described in **Chapter 2**, orientation is obviously not applicable in this case.

Polymers also can be toughened by blending with low-molecular-weight plasticizers or high-molecular-weight low- $T_g$  polymers. When low-molecular-weight plasticizers are used, leaching of these small molecules is a potential problem, especially in applications such as food packaging. Blending with high-molecular-weight polymers to form discrete rubbery phase particles in a rigid polymer matrix can overcome this problem, but multi-component polymer systems generally exhibit unfavorable thermodynamics of mixing, leading to poor interfacial adhesion and inferior mechanical properties.<sup>168-171</sup>

These limitations can be overcome by synthesizing the corresponding block copolymers. The presence of the block copolymers at the interface between two polymer phases reduces the interfacial tension and inhibits coalescence, which allows the minor phase to remain dispersed as small particles. Furthermore, the block copolymer can also increase interfacial adhesion through entanglement with their respective blocks. The interfacial entanglements help stress to be transferred from the brittle matrix across the interface to the rubber particles.<sup>170</sup> High-impact polystyrene is an example of a polymer toughened by this approach. By controlling the volume fraction and

copolymer architecture, the morphology of ABA triblock copolymers can be controlled. Incorporating a low rubber content in a hard resin matrix (polybutadiene, shown as gray dispersed spheres in **Scheme 34**) improves the impact strength.<sup>172</sup>

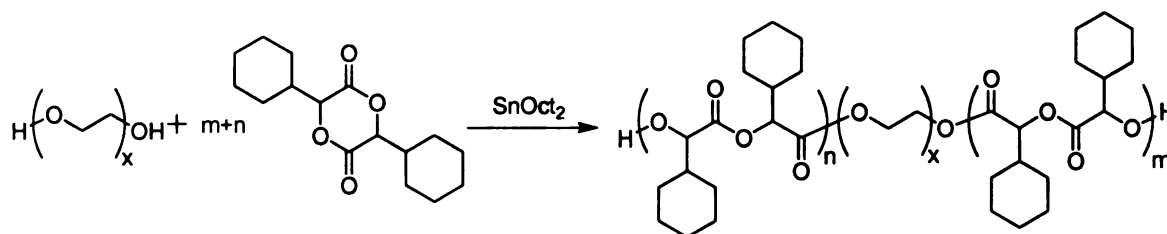


**Scheme 34.** Phase separation and morphology changes of block copolymers

Based on the same strategy, poly(dicyclohexylglycolide) can be toughened by synthesizing ABA triblock copolymers, where A represents poly(dicyclohexylglycolide) and B is an immiscible low- $T_g$  polymer, such as polyethylene, polycaprolactone, poly(trimethylene carbonate), polybutadiene, polyisoprene, or poly(ethylene glycol). While incorporating polyolefins can compromise the (bio)degradability to some extent, copolymerizing with polycaprolactone or other low- $T_g$  polyesters can be challenging because the high temperatures used for ring-opening polymerization causes side reactions such as transesterification. In contrast, poly(ethylene glycol) (PEG) is stable under the ring-opening polymerization conditions, and it has outstanding physiological properties, including biocompatibility, hydrophilicity, flexibility, and lack of toxicity.

Synthesizing lactide- and PEG-based ABA triblock copolymers is straightforward and has been studied for years: the terminal hydroxyl groups of poly(ethylene glycol) can be used with  $\text{Sn(2-ethylhexanoate)}_2$  to initiate ring-

opening polymerization.<sup>173-178</sup> The same synthetic approach was used to synthesize poly(dicyclohexylglycolide)-*block*-poly(ethylene glycol)-*block*-poly(dicyclohexylglycolide) (PDCG-PEG-PDCG) (**Scheme 35**). This preliminary study is targeted at PDCG-PEG-PDCG triblock copolymers that phase separate like the high-impact resin shown in **Scheme 34**.



**Scheme 35.** Synthesis of PDCG-PEG-PDCG triblock polymers

PDCG-PEG-PDCG triblock copolymers were synthesized using three different poly(ethylene glycol)s: PEG600, PEG2000, and PEG8000 (the numbers represents the number-average molecular weights). Before polymerization, all PEG samples were dried overnight under full vacuum (< 10 mTorr) at 130 °C to completely remove moisture. As a control, dicyclohexylglycolide homopolymer was synthesized under the same conditions using 1,4-cyclohexane dimethanol as the initiator. Characterization of these polymers by <sup>1</sup>H NMR spectroscopy is shown in **Figure 33**, and the molecular weights of the copolymers measured by GPC and their GPC traces are shown in **Figure 34**. These copolymers all show monomodal GPC traces, indicating that other impurities such as moisture play a trivial role in initiating the ring-opening polymerization and that the contamination

from homopolymer is negligible. A summary of the characterization data by DSC and  $^1\text{H}$  NMR is listed in **Table 16**.

**Table 16.** Characterization of PDCG-PEG-PDCG copolymers

| Polymer           | $M_n$  | $M_w/M_n$ | PDCG ratio in copolymer (wt%) |
|-------------------|--------|-----------|-------------------------------|
| PDCG              | 59,000 | 1.42      | 100                           |
| PDCG-PEG600-PDCG  | 44,800 | 1.41      | 99.3                          |
| PDCG-PEG2000-PDCG | 34,900 | 1.34      | 96.4                          |
| PDCG-PEG8000-PDCG | 32,700 | 1.21      | 86.7                          |

A potential problem when using PEG as the soft domain is that PEG can crystallize. This might complicate the morphology and lead to unexpected mechanical properties. In 1996, Vert et al. showed that PEG crystallization can be avoided in PLA-PEG-PLA triblock copolymers when the PEG chain length is shorter than the PLA block.<sup>175</sup> To realize a high-impact poly(dicyclohexylglycolide) with soft PEG domains dispersed in the hard PDCG matrix, the PEG chain should be long enough to induce phase separation, but too short to crystallize.

As shown in **Figure 35** for PDCG-PEG600-PDCG, the PEG block is too short for a  $T_g$  to be observed. However,  $T_g$ s are visible in the DSC data for the longer blocks in PDCG-PEG2000-PDCG and PDCG-PEG8000-PDCG, but the PEG block in PDCG-PEG8000-PDCG crystallizes, as evidenced by its melting transition in the DSC trace. Based on these results, only PDCG-PEG2000-PDCG

is amorphous and exhibits the desired phase separation among these three triblock copolymers.

**Table 17.** Thermal properties of PDCG-PEG-PDCG copolymers

| Polymer           | $T_{g1}$ (°C) | $T_{g2}$ (°C) | $T_m$ (°C) |
|-------------------|---------------|---------------|------------|
| PDCG              |               | 98            |            |
| PDCG-PEG600-PDCG  |               | 94            |            |
| PDCG-PEG2000-PDCG | -30           | 86            |            |
| PDCG-PEG8000-PDCG | -30           | 88            | 33         |

$T_{g1}$ :  $T_g$  of PEG block;  $T_{g2}$ :  $T_g$  of PDCG block,  $T_m$ :  $T_m$  of PEG block.

Another effect caused by PEG crystallization in PDCG-PEG8000-PDCG is that the  $T_g$  of the PDCG block is higher than in PDCG-PEG2000-PDCG. This is opposite to the general trend that the  $T_g$  of the PDCG block decreases when the PEG fraction increases (**Table 17**).

Based on DSC results, PDCG-PEG2000-PDCG is assumed to have soft PEG domains dispersed in a hard PDCG matrix. In order to characterize the morphology, samples were examined using Transmission Electron Microscopy (TEM). However, a suitable staining agent that differentiates the polyester phase from polyether phase was not found.<sup>164</sup>

The nanometer spatial resolution of Tapping Mode Atomic Force Microscopy (TM-AFM), together with its potential to distinguish different materials without staining, has made TM-AFM an attractive alternative to TEM.<sup>179</sup> In the TM-AFM measurement, the cantilever on which the tip is mounted is oscillated at

an amplitude  $A_0$  with a frequency near its resonance, typically, a few hundred kHz (~300 KHz in this experiment). During the scan (the scan rate is 0.85 Hz) the vertical displacement of the cantilever is displayed as the height image, and the phase shift, which is measured as the difference between the free end of the cantilever and the driving piezo element, is shown as the phase image. The height image yields topographic information about the sample, while phase image can be used to discriminate between different types of materials on the surface.

A thin uniform film of PDCG-PEG2000-PDCG was spin coated from a THF polymer solution (4 mg/mL) onto a UV-ozone cleaned silicon wafer. The average roughness of the film was 0.55 nm. The AFM phase image shows black domains dispersed on the surface. Black in an AFM phase image could be interpreted as either a lower surface height or a softer material, but since the height image shows a flat surface, black in this case must correspond to the soft PEG domains (**Figure 36**).

To confirm this conclusion, a thin film of PDCG homopolymer was spin coated using the same procedure. The average film roughness was 0.36 nm based on the AFM height image in **Figure 37**). The AFM phase image in **Figure 37** shows that the surface is free of heterogeneous domains, supporting the notion that the PDCG-PEG2000-PDCG triblock copolymer is phase separated.

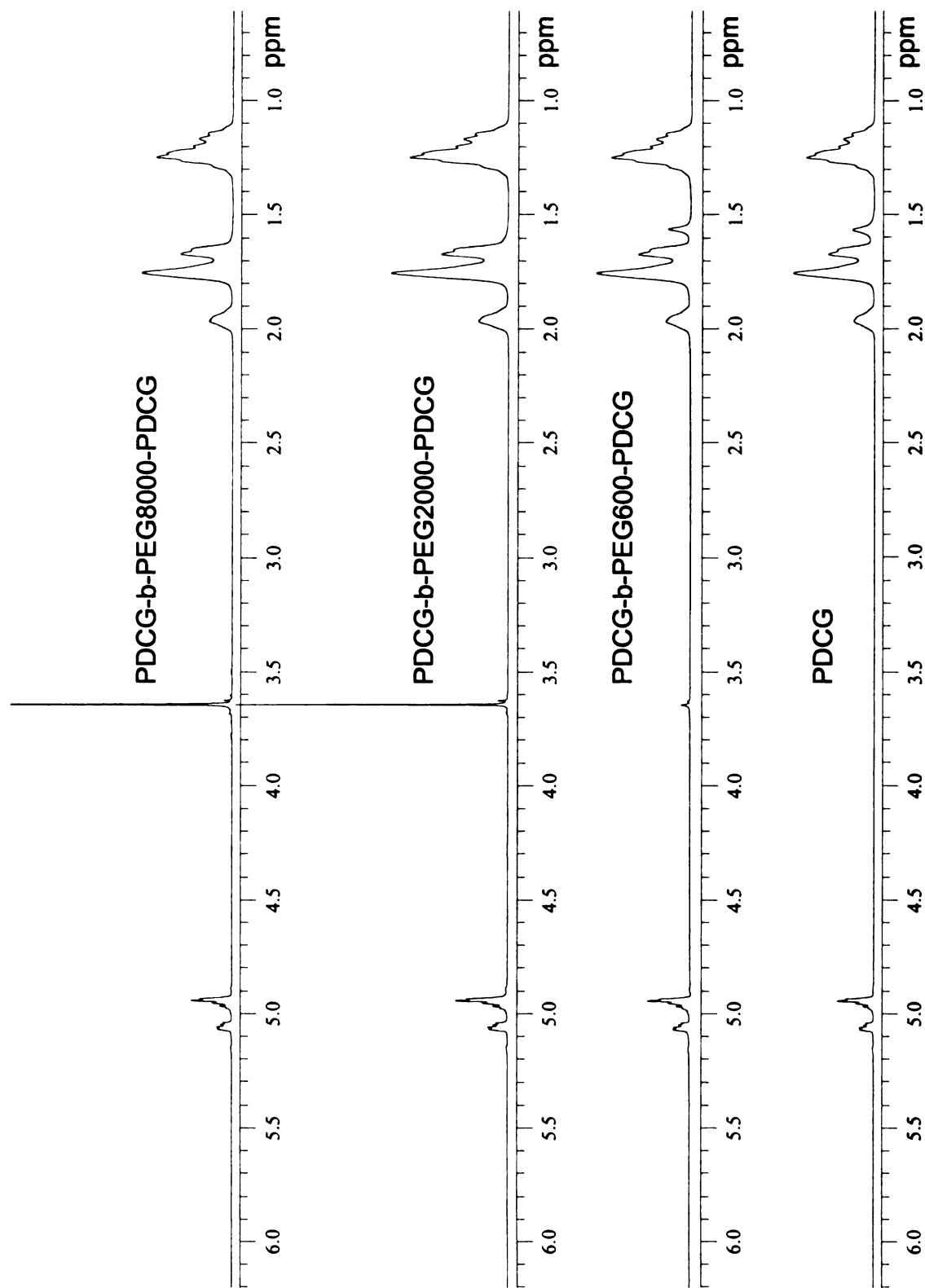


**Figure 33.** 500 MHz  $^1\text{H}$  NMR spectra of poly(dicyclohexylglycolide)-*b*-poly(ethylene glycol)-*b*-poly(dicyclohexylglycolide)s



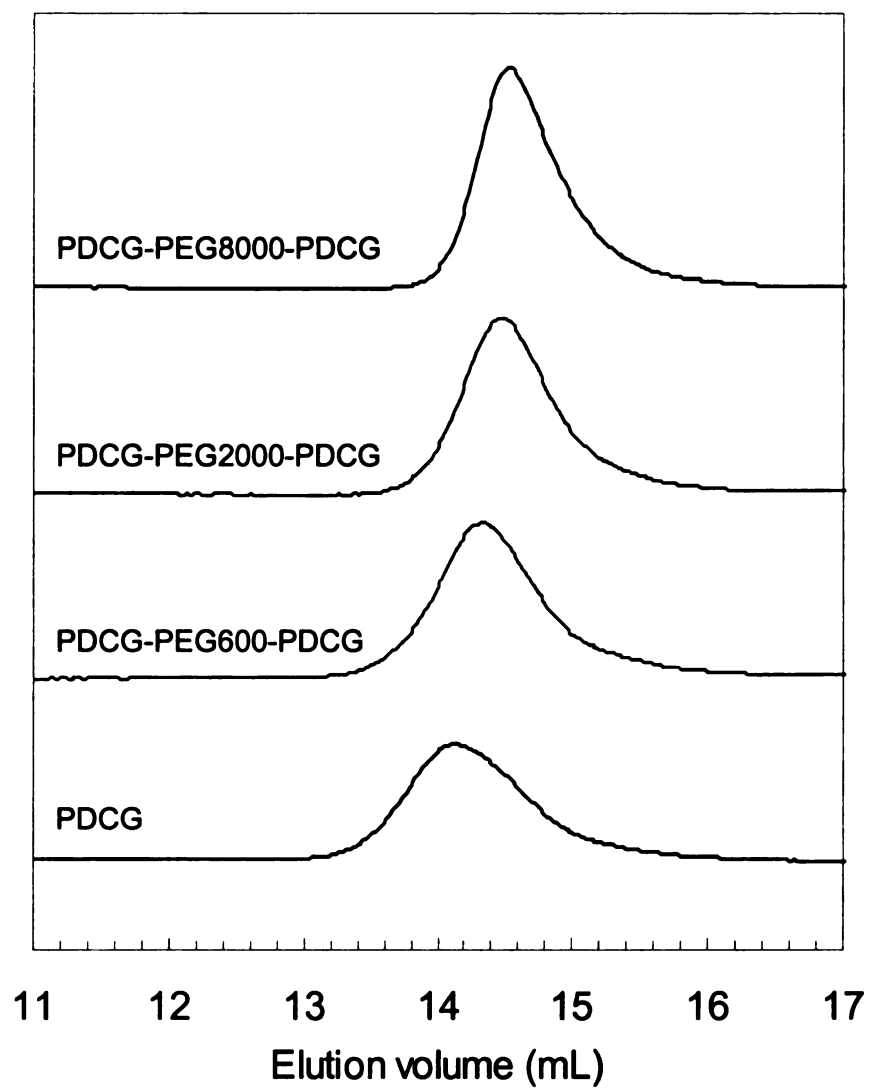


**Figure 34.** GPC traces of PDCG-PEG-PDCG triblock copolymers

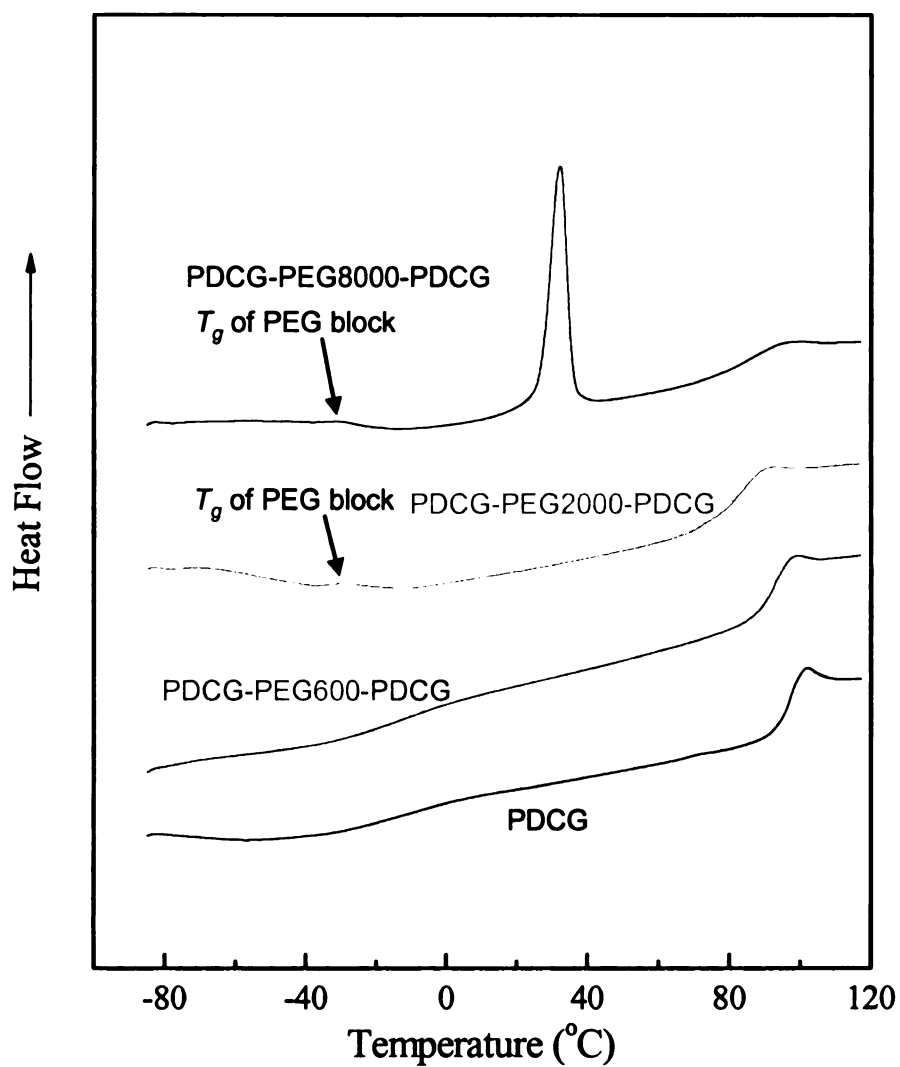


**Figure 35.** DSC analyses of PDCG-PEG-PDCG triblock copolymers. Heating rate: 10 °C/min under nitrogen. The data are from second heating scans, taken after flash quenching from 120 °C.

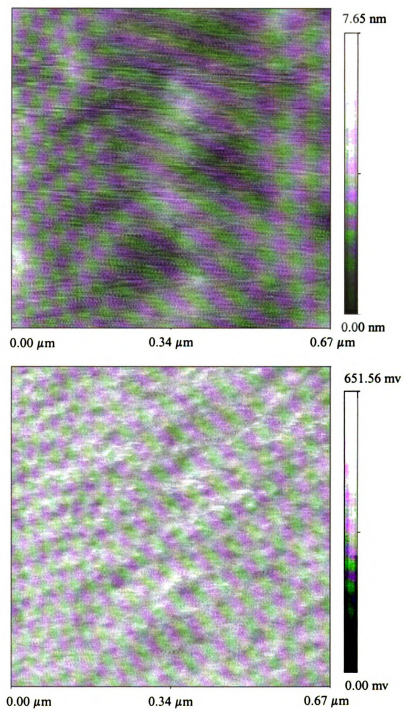


**Figure 36.** AFM height image (top) and phase image (bottom) of PDCG-PEG2000-PDCG triblock copolymer.

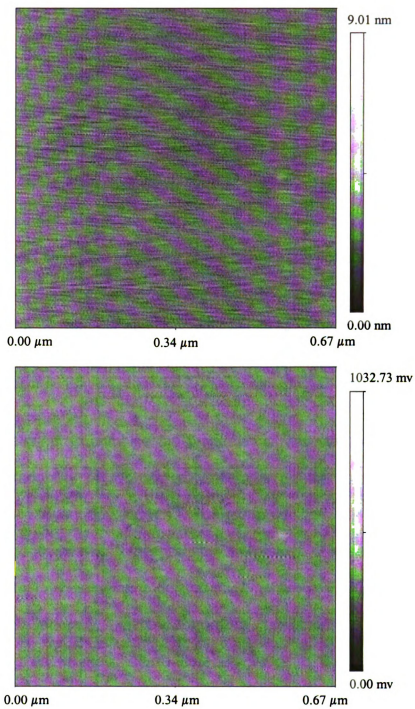


**Figure 37.** AFM height image (top) and phase image (bottom) of poly(dicyclohexylglycolide)

## Chapter 4 Poly(1,4-benzodioxepin-3-alkyl-2,5-dione)s

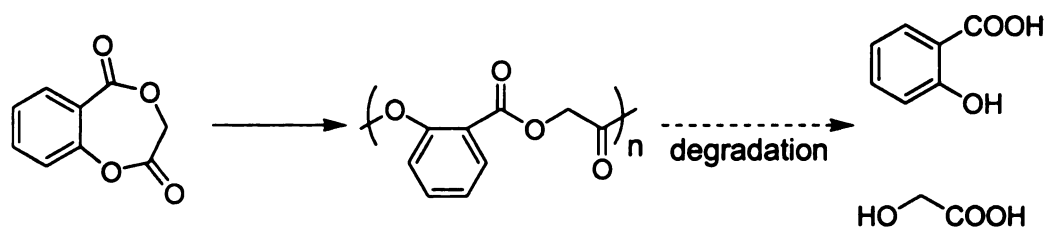
In the discovery and development of biodegradable plastics, aliphatic polyesters, such as polylactide<sup>180</sup> and poly(3-hydroxybutyrate),<sup>181</sup> have played a key role.<sup>182</sup> However, the modern polyester industry is still dominated by aromatic polyesters, e.g. poly(ethylene terephthalate (PET) and poly(butylene terephthalate) (PBT), because of their excellent thermal and mechanical properties, high chemical resistance and extremely low gas permeability.<sup>183</sup> Nonetheless, the high stability and biological inertness of these aromatic polyesters are becoming a major drawback, especially in the area of disposable materials, such as the widely used non-degradable PET-based beverage bottles. According to the EPA, only 5.2% of plastics in municipal solid waste was recovered in the United States in 2003.<sup>184</sup>

In an attempt to combine the properties of aromatic polyesters with the potential degradability of aliphatic polyesters, a number of aliphatic-aromatic polyesters have been developed.<sup>185</sup> For example, both BASF and Eastman Chemical currently market biodegradable polyesters of terephthalic acid and adipic acid with 1,4-butanediol under the trade names of Ecoflex and Eastar Bio respectively. Generally, aliphatic-aromatic polyesters are made by copolymerizing an aromatic diacid (terephthalic acid) and an aliphatic diacid (adipic acid, sebacic acid, or fumaric acid) with an aliphatic diol (ethylene glycol, PEG-diol, or 1,4-cyclohexane dimethanol) via a polycondensation reaction.<sup>185</sup>

However, incorporating flexible aliphatic ester chains into rigid aromatic polyesters to introduce degradability greatly reduces  $T_g$  and  $T_m$ . For example,

Ecoflex has a much lower  $T_g$  (-30 °C) and  $T_m$  (110-115 °C) than PET ( $T_g$  = 78 °C,  $T_m$  = 260 °C).<sup>182,186</sup> As a result, the use temperatures of aliphatic-aromatic polyesters are severely compromised, and their low  $T_g$  and high crystallinity will inevitably limit their potential as rigid, clear replacements for large-volume thermoplastics such as polystyrene. Furthermore, the use of polycondensation to synthesize aliphatic-aromatic polyesters often results in low molecular weight, high polydispersity, and poor control over the regioselectivity of the polymer structure.

Although the ring-opening polymerization of cyclic oligomers to form PET has been realized,<sup>187-189</sup> syntheses of aliphatic-aromatic polyesters by ring-opening polymerization are rare. An interesting approach to aliphatic-aromatic polyesters with better thermal stability is the ring-opening polymerization of 1,4-benzodioxepin-2,5(3H)-dione patented in 1992 by Ethicon Inc (**Scheme 36**, see also **Chapter 1**).<sup>81</sup> *In vitro* and *in vivo* degradation experiments showed that this polymer is completely biodegradable.



**Scheme 36.** Synthesis and degradation of poly(1,4-benzodioxepin-2,5(3H)-dione)

A potentially useful feature of poly(1,4-benzodioxepin-2,5(3H)-dione) is that its degradation product is the therapeutically active salicylic acid, and it shows similar features to the well-studied salicylate-based poly(anhydride

esters).<sup>190-194</sup> In both cases, the drug is released upon the hydrolysis of the polymer backbone, and the degradation profiles, as well as physical properties such as  $T_g$ , can be manipulated by incorporating different linkers.

Compared to amorphous and low- $T_g$  salicylate-based poly(anhydride-esters) ( $T_g \sim 13-57\text{ }^\circ\text{C}$ ),<sup>190</sup> poly(1,4-benzodioxepin-2,5(3H)-dione) is semi-crystalline and its  $T_g$  and  $T_m$  range from 57-73  $^\circ\text{C}$  and 165-168  $^\circ\text{C}$  respectively,<sup>81</sup> both of which are similar to those of poly(L-lactide).<sup>195</sup> Based on our studies aimed at increasing the  $T_g$  of polylactide, the thermal and mechanical properties of poly(1,4-benzodioxepin-2,5(3H)-dione) can be enhanced by introducing bulky side chains to the glycolic acid repeating units. By varying the substituent R (**Figure 38**) and/or stereochemistry, the crystallinity and the rigidity of polymer chains can be manipulated. In this study, we added methyl and cyclohexyl groups to the monomer and obtained racemic 1,4-benzodioxepin-3-alkyl-2,5-diones. In this way, the polymer rigidity is enhanced and crystallinity is eliminated by the random distribution of chiral centers, thus providing amorphous, high  $T_g$  polyesters with improved thermal and mechanical properties.

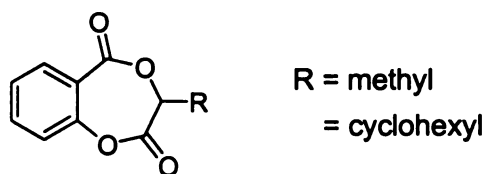
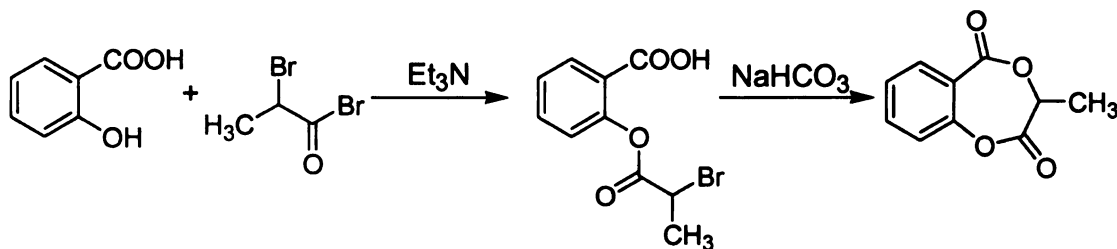


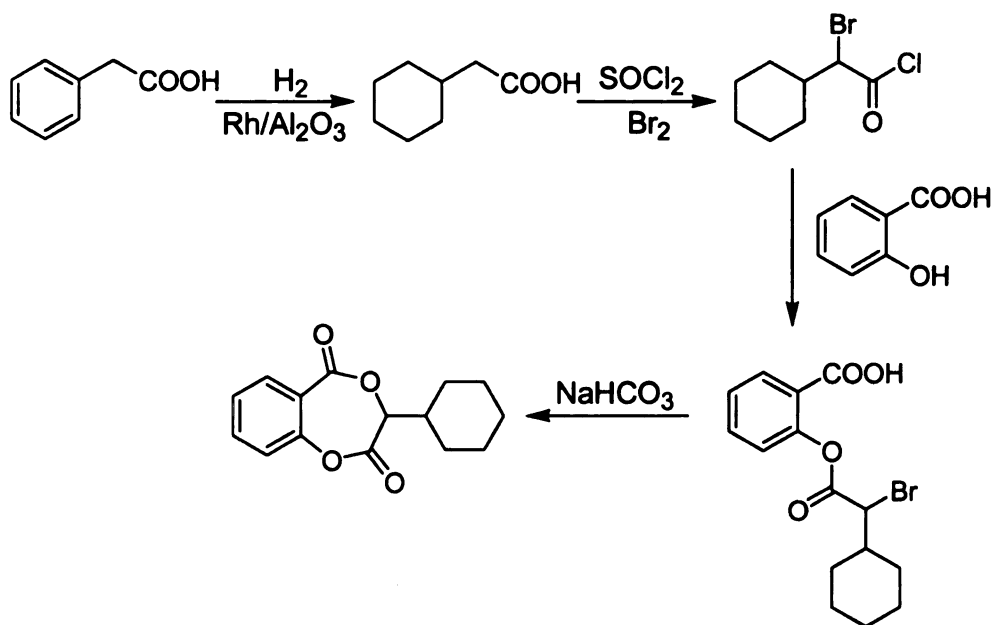
**Figure 38.** Structures of 1,4-benzodioxepin-3-alkyl-2,5-diones

## Synthesis of 1,4-benzodioxepin-3-alkyl-2,5-diones

1,4-Benzodioxepin-3-methyl-2,5-dione and 1,4-benzodioxepin-3-cyclohexyl-2,5-dione, shown in **Scheme 37** and **Scheme 38** respectively were synthesized using the reported synthetic protocol.<sup>80,81</sup>



**Scheme 37.** Synthetic route to 1,4-benzodioxepin-3-methyl-2,5-dione



**Scheme 38.** Synthetic route to 1,4-benzodioxepin-3-cyclohexyl-2,5-dione

The synthesis is based on the esterification of salicylic acid with the desired  $\alpha$ -bromo acid bromide or chloride, followed by the intramolecular



cyclization of the linear intermediate, promoted by NaHCO<sub>3</sub> in acetone. Various commercially available  $\alpha$ -bromo acid halides can be coupled with salicylic acid (**Scheme 37**); alternatively, they can be easily synthesized via  $\alpha$ -bromination of the corresponding carboxylic acids (**Scheme 38**). These methods enable different side chains to be attached to the 7-membered lactone ring, which in turn will provide polymers with tailored physical properties.

#### Initiator studies on the ring-opening polymerization of 1,4-benzodioxepin-3-alkyl-2,5-diones

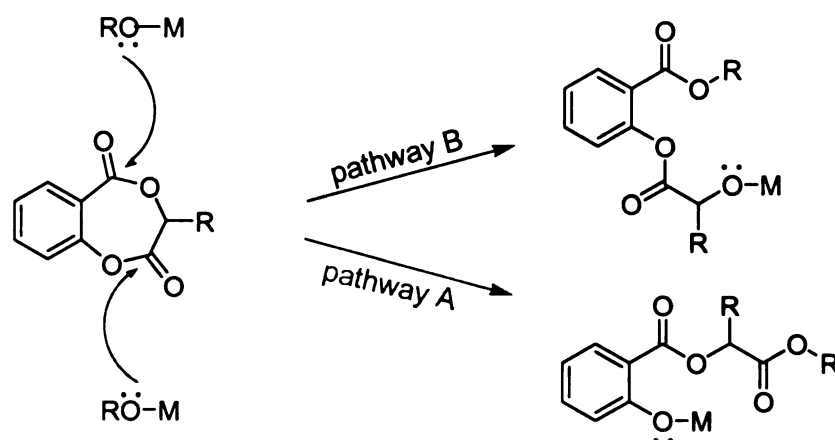
The ring-opening polymerization of 1,4-benzodioxepin-3-methyl-2,5-dione was catalyzed by Sn(2-ethylhexanoate)<sub>2</sub> using 4-*tert*-butylbenzyl alcohol as the initiator. The <sup>1</sup>H NMR spectra of the monomer and the polymer are shown in **Figure 39**, and the characterization data for the polymer are listed in **Table 18**.

**Table 18.** Characterization of poly(1,4-benzodioxepin-3-methyl-2,5-dione)

| $M_n$  | $M_w/M_n$ | $T_g$ (°C) |
|--------|-----------|------------|
| 22,700 | 1.86      | 92         |

Bulk polymerization posed problems as less than 5% polymer formed after polymerizing 1,4-benzodioxepin-3-methyl-2,5-dione at 160 °C for 1 hour with a 1 mol% loading ratio of catalyst and initiator. The nonsymmetric structure of the monomer suggests that preferential ring opening can be effected by choosing catalysts with suitable steric demands. **Scheme 39** identifies the two possible

sites for nucleophilic attack. In pathway A, the adjacent substituent R may have a large effect on the ring opening, so the use of a less hindered initiator/catalyst system should increase the polymerization rate. Nucleophilic attack at the other carbonyl is less congested and overcoming the stability of the aromatic carbonyl will be the determining factor for pathway B.

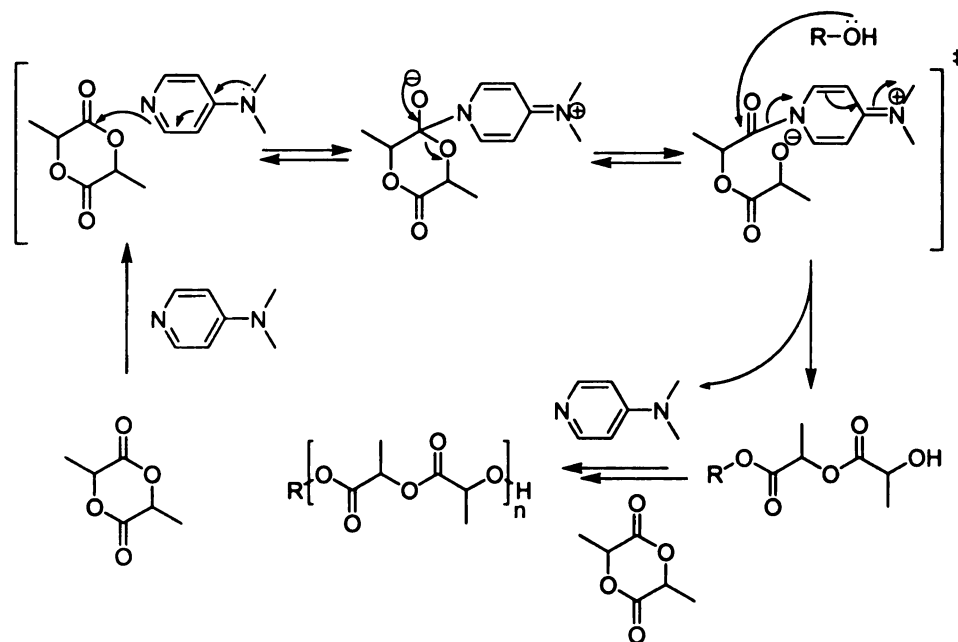


**Scheme 39.** Pathways of ROP of 1,4-benzodioxepin-3-alkyl-2,5-diones

The difference in polymerization rates for 1,4-benzodioxepin-3-methyl-2,5-dione and 1,4-benzodioxepin-3-cyclohexyl-2,5-dione supports pathway A since the polymerization rate was sensitive to the size of the side chains. To quantitate the preference for pathway A, 1,4-benzodioxepin-3-methyl-2,5-dione was reacted with one equivalent of 4-*tert*-butylbenzyl alcohol and  $\text{Sn}(\text{2-ethylhexanoate})_2$ , and the final product (**Scheme 39**) was then analyzed by  $^1\text{H}$  NMR spectroscopy. As shown in **Figure 40**, products formed via pathway B were not observed and the ring-opening reaction proceeded almost exclusively by pathway A.

Catalysts used for the ring-opening polymerizations of lactide and glycolide have been extensively studied, and the mostly common catalysts use

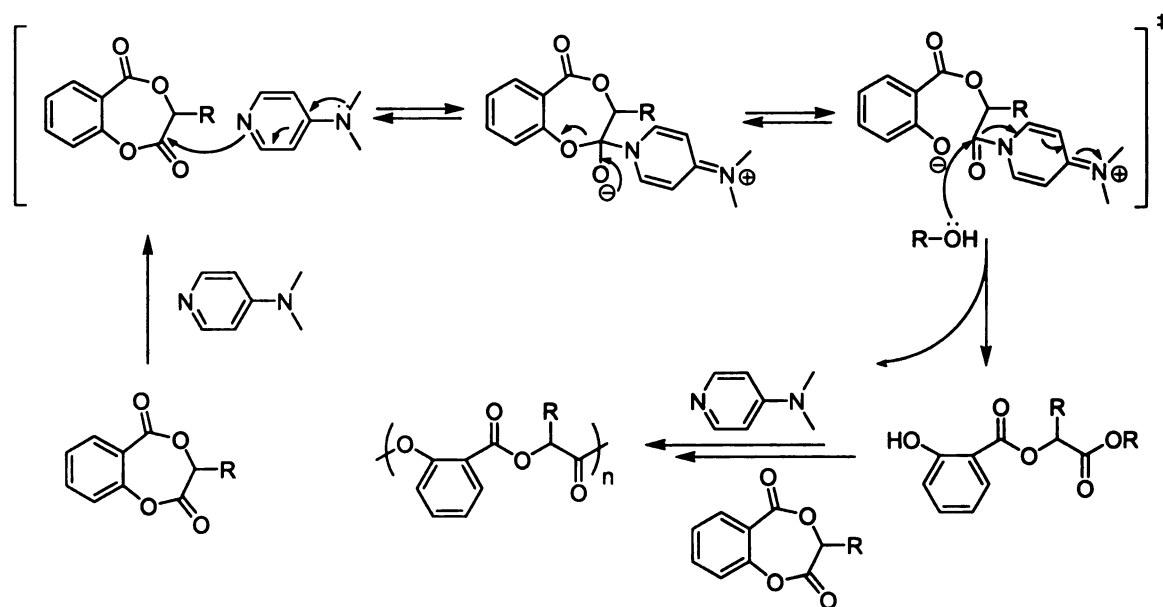
metals such as aluminum, tin, zinc, and yttrium. All operate through a coordination-insertion mechanism,<sup>180</sup> and require the coordination of monomer to the metal catalyst to activate the ester carbonyl. Subsequent nucleophilic attack by the initiator breaks the ester bond. The reaction intermediate is crowded by the presence of monomer, metal catalyst, and initiator.<sup>119</sup> To reduce the steric hindrance in the intermediate, other polymerization methods were considered, such as cationic polymerization, anionic polymerization, and nucleophilic polymerization.<sup>180</sup> Anionic polymerization normally causes extensive transesterification and racemization,<sup>180</sup> and cationic polymerization of 1,4-benzodioxepin-3-methyl-2,5-dione using HCl-Et<sub>2</sub>O as the catalyst has been tried but has seen little success.



**Scheme 40.** Mechanism of ROP of lactide initiated by DMAP and alcohol

As shown by Hedrick et al. for the ring-opening polymerization of lactide, 4-(dimethylamino)pyridine (DMAP) can be an effective catalyst when used with

an alcohol initiator.<sup>196,197</sup> The mechanism<sup>197</sup> of the nucleophilic polymerization by DMAP/alcohol (**Scheme 40**) seems applicable to the polymerization of 1,4-benzodioxepin-3-cyclohexyl-2,5-dione, because DMAP breaks the ester bond before the addition of alcohol initiator, which greatly relieves the steric congestion of the intermediate. A preliminary study on the bulk polymerization of 1,4-benzodioxepin-3-cyclohexyl-2,5-dione showed that the polymerization was complete within minutes at 160 °C.

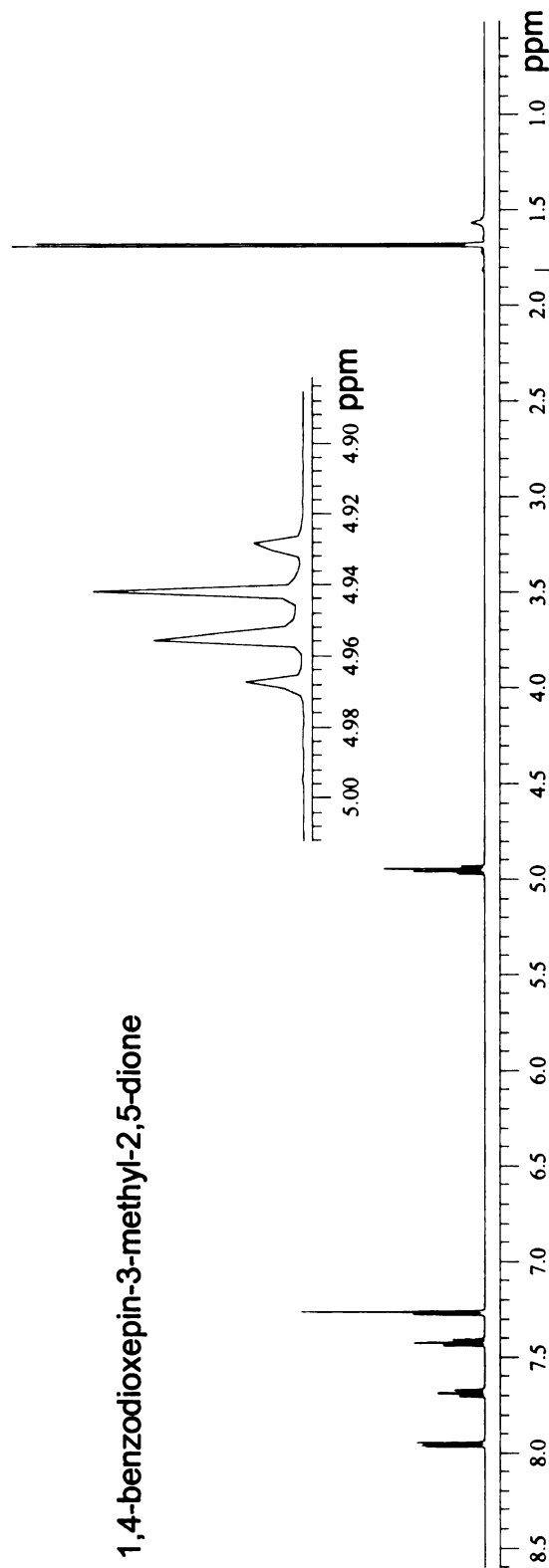


**Scheme 41.** Mechanism of ROP of 1,4-benzodioxepin-3-alkyl-2,5-dione initiated by DMAP and alcohol

A regioselectivity study of the ring-opening polymerization of 1,4-benzodioxepin-3-methyl-2,5-dione was performed using DMAP as the catalyst and 1-phenylethanol as the initiator. As shown in **Figure 41**, the site for ring-opening is the same site favored when  $\text{Sn}(\text{2-ethylhexanoate})_2$  is used as the

catalyst. A plausible mechanism of the ring-opening polymerization of 1,4-benzodioxepin-3-alkyl-2,5-dione catalyzed by DMAP and alcohol is shown in **Scheme 41**.

1,4-benzodioxepin-3-methyl-2,5-dione



poly(1,4-benzodioxepin-3-methyl-2,5-dione)

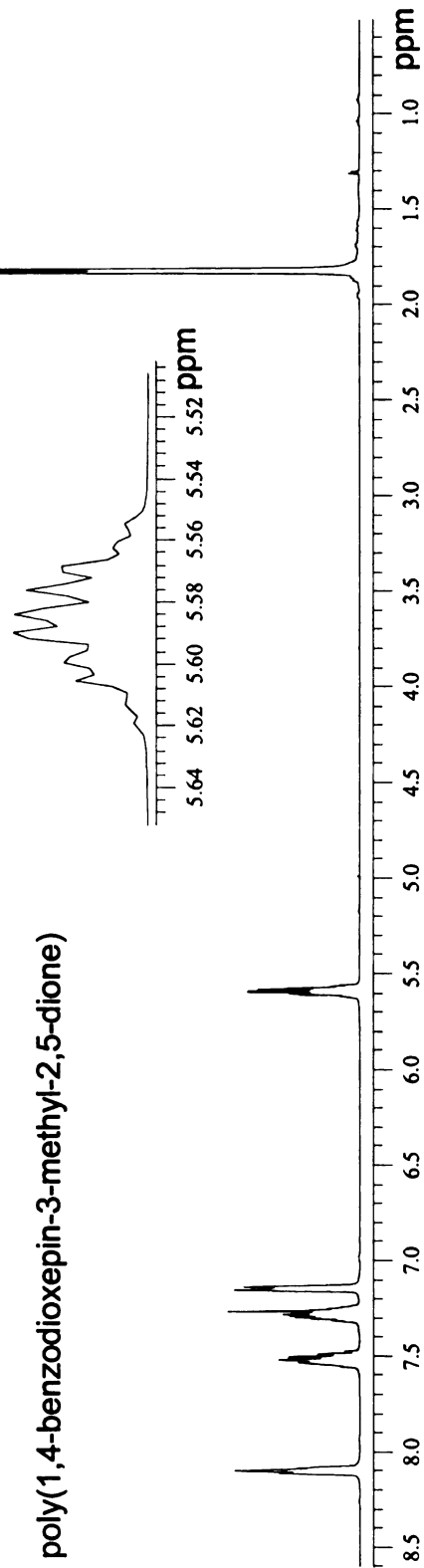
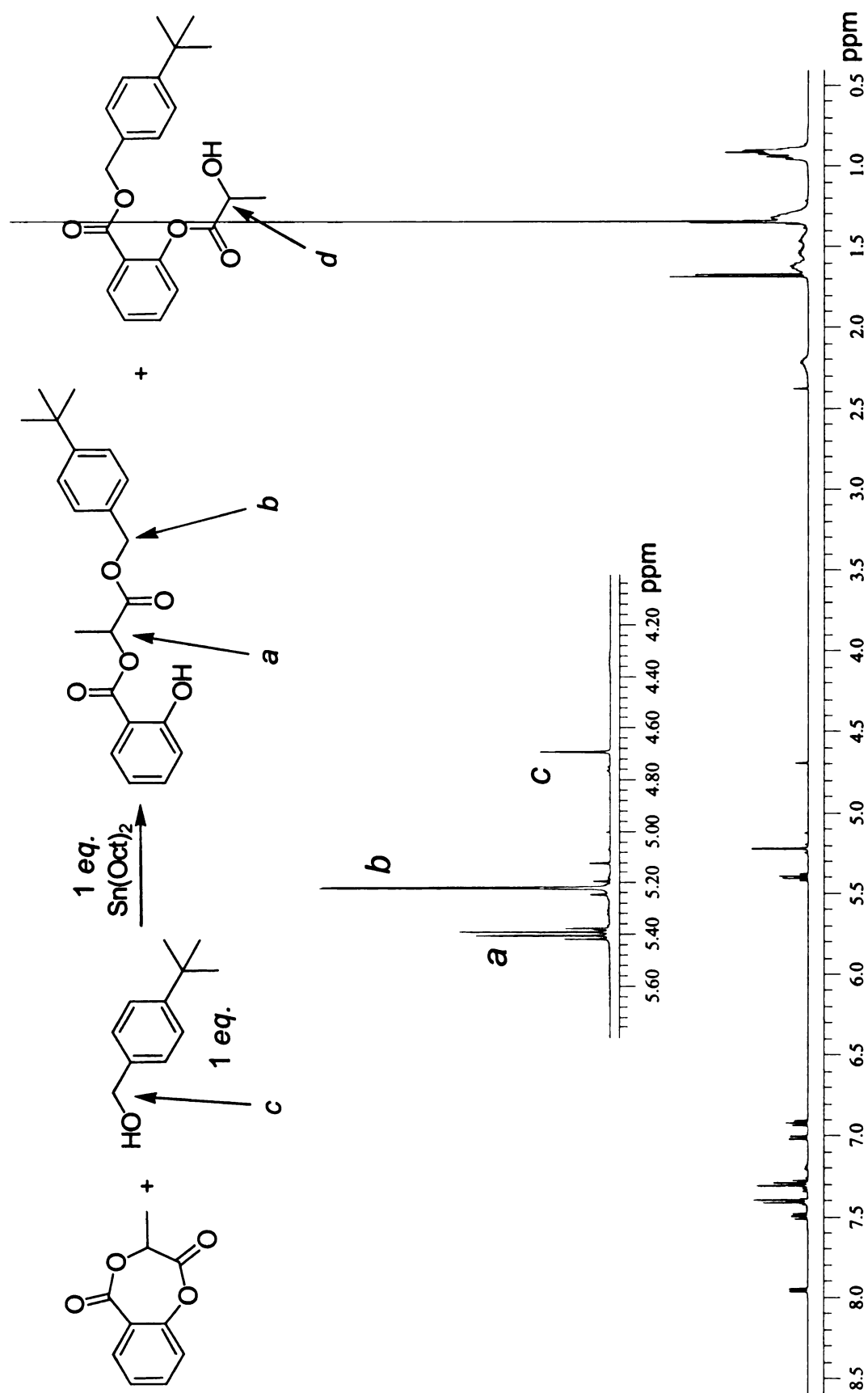
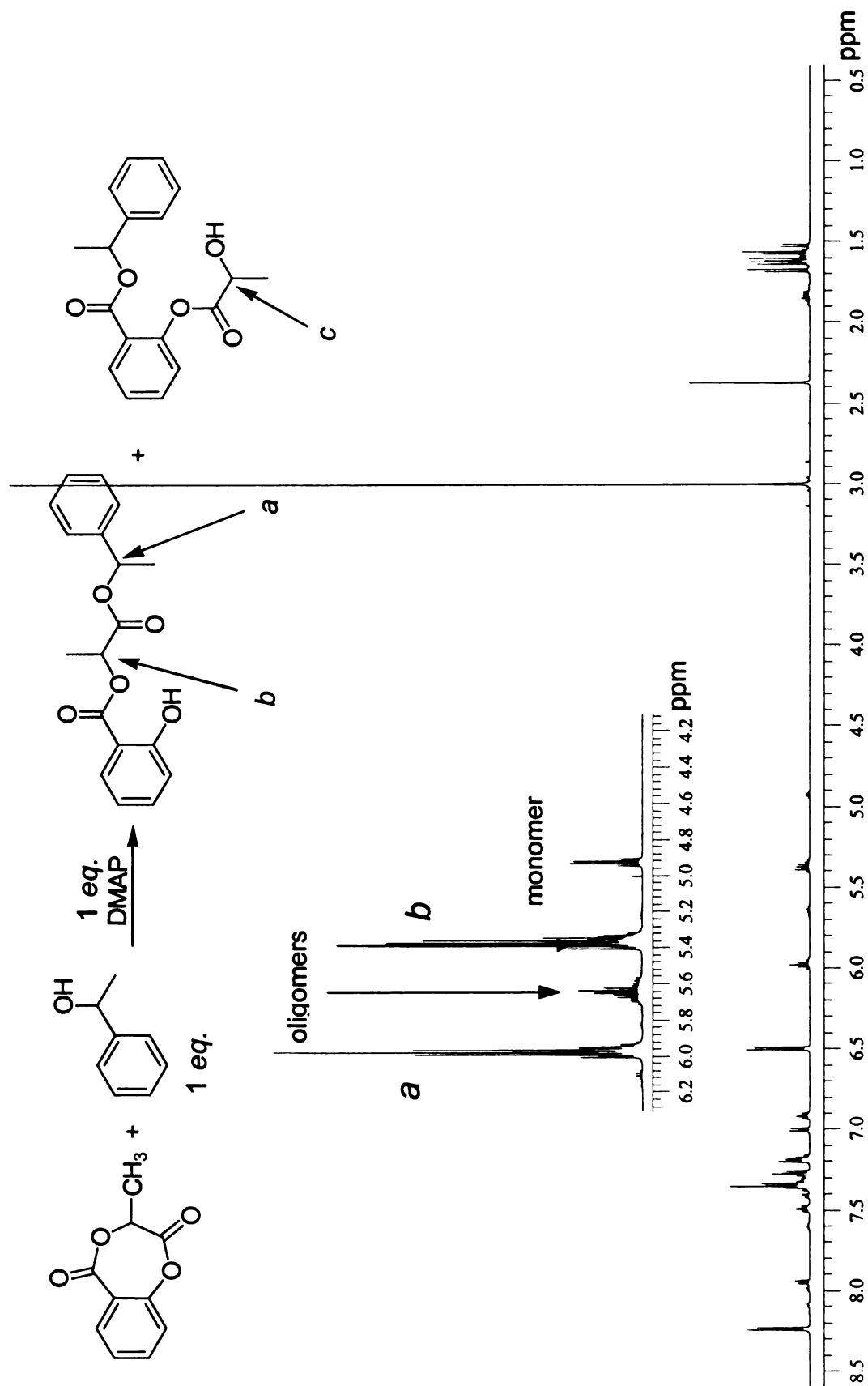


Figure 39. 500 MHz <sup>1</sup>H NMR spectra of 1,4-benzodioxepin-3-methyl-2,5-dione and its polymer



**Figure 40.** 500 MHz  $^1\text{H}$  NMR spectrum of 1,4-benzodioxepin-3-methyl-2,5-dione ring-opened product by  $\text{Sn}(\text{2-ethylhexanoate})_2$  and 4-*tert*-butylbenzyl alcohol



**Figure 41.** 500 MHz  $^1\text{H}$  NMR spectrum of 1,4-benzodioxepin-3-methyl-2,5-dione ring-opened product by DMAP and 1-phenylethanol



## Solution polymerization kinetics of 1,4-benzodioxepin-3-alkyl-2,5-diones

Solution polymerizations of 1,4-benzodioxepin-3-methyl-2,5-dione and 1,4-benzodioxepin-3-cyclohexyl-2,5-dione using DMAP as the catalyst and 1-phenylethanol as the initiator were carried out in toluene to evaluate the effect of the size of alkyl substituents on the polymerization rate.

While the ring-opening polymerization of lactide catalyzed by DMAP and alcohol was proven to be a living polymerization,<sup>197</sup> no kinetic data have been reported. As shown in **Scheme 41**, if the formation of the monomer-DMAP complex is at equilibrium, the rate-limiting step will be the addition of alcohol to the monomer-DMAP intermediate. The ring-opening polymerization can then be treated as a first-order reaction where the concentrations of catalyst and initiator are approximately constant. To test this assumption, solution polymerizations were run at low concentration to low conversions.

For polymerizations at 90 °C with relatively low monomer concentrations (~0.2 M) and initiator and catalyst loadings (≤2 mol%), the conversion is easily controlled, depolymerization is negligible, and the polymerization can be treated as an irreversible reaction<sup>118</sup> as expressed in equation 8,

$$R = -\frac{d[M]}{dt} = k_p[M][I] \quad (8)$$

where  $[M]$  and  $[I]$  are the concentration of monomer and initiator respectively, and  $k_p$  is the apparent rate constant for propagation. For a living polymerization,  $[I]$  is a constant, and plots of  $-\ln([M]_t/[M]_0)$  versus time  $t$  should be linear with slope

$k_p[\eta]$ , where  $[M]_t$  is the concentration of the monomer at time  $t$  and  $[M]_0$  is the initial monomer concentration.

The data shown in **Figure 42** are consistent with first-order kinetics. As expected, the polymerization rates (**Table 19**) depend on the size of the alkyl substituents, with  $k_p$  of 1,4-benzodioxepin-3-cyclohexyl-2,5-dione being 1/15<sup>th</sup> of 1,4-benzodioxepin-3-methyl-2,5-dione.

**Table 19.** Solution polymerization rates of 1,4-benzodioxepin-3-alkyl-2,5-diones

| Monomer                                  | $k_p \text{ (L}\cdot\text{s}^{-1}\cdot\text{mol}^{-1}) \times 10^6$ |
|--|---|
| 1,4-benzodioxepin-3-methyl-2,5-dione     | 118   |
| 1,4-benzodioxepin-3-cyclohexyl-2,5-dione | 7.78  |

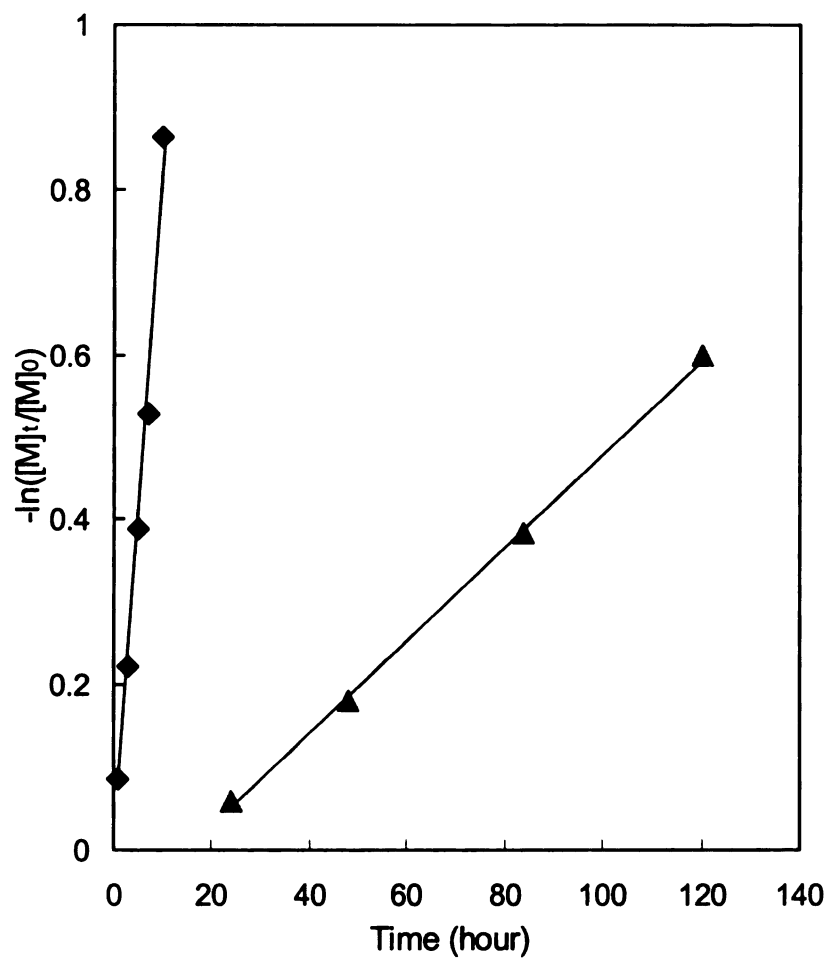


**Figure 42.** Solution polymerization kinetics of 1,4-benzodioxpein-3-methyl-2,5-dione (♦) and 1,4-benzodioxpein-3-cyclohexyl-2,5-dione (▲). Polymerization conditions: 90 °C, [monomer]: [DMAP]: [1-phenylethanol] = 100: 2: 1.

### **Bulk polymerization kinetics of 1,4-benzodioxepin-3-alkyl-2,5-diones**

The kinetic behavior of bulk polymerizations of 1,4-benzodioxepin-3-methyl-2,5-dione and 1,4-benzodioxepin-3-cyclohexyl-2,5-dione were examined at 130 °C and 160 °C respectively. The monomer, 2 mol% DMAP, and 1 mol% 1-phenylethanol were loaded into glass tubes and the tubes were then sealed under vacuum. The tubes were immersed in oil bath at predetermined temperature and removed at desired times.

As noted earlier for the bulk polymerization of dicyclohexylglycolide, high temperature runs may introduce complications, such as high polymerization rates that make collecting data at low conversions difficult, and the polymerization-depolymerization equilibrium must be taken into account.<sup>118</sup> However, the bulk polymerization kinetics of 1,4-benzodioxepin-3-methyl-2,5-dione and 1,4-benzodioxepin-3-cyclohexyl-2,5-dione followed pseudo first-order kinetics, even to relatively high conversions (**Figure 43** and **Figure 44**).

The evolution of the number-average molecular weight ( $M_n$ ) and polydispersity (PDI) with conversion in the polymerization of 1,4-benzodioxepin-3-methyl-2,5-dione and 1,4-benzodioxepin-3-cyclohexyl-2,5-dione are shown in **Figure 45** and **Figure 46** respectively. As the monomer conversion increases during bulk polymerization,  $M_n$  increases, reaches a maximum at high conversion, and then drops. This behavior is consistent with the mechanism for ring-opening polymerization of lactides.<sup>15</sup> At low conversion,  $M_n$  increases linearly with conversion because of the “living” nature of the ring-opening polymerization. When the monomer is nearly consumed, transesterification becomes competitive

with propagation. While intermolecular transesterification only affects the PDI, the formation of cyclic esters via intramolecular transesterification causes a reduction in  $M_n$ . Polydispersities are fairly high for these living polymerizations, probably because of extensive intermolecular and intramolecular transesterifications.

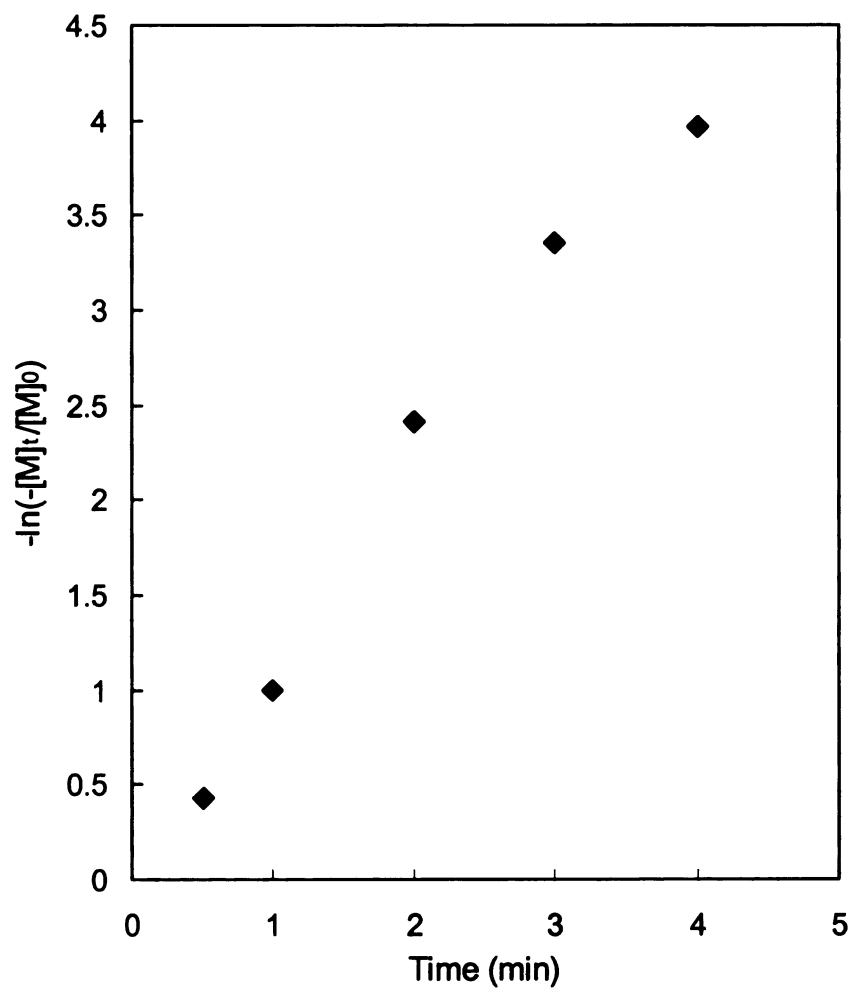


**Figure 43.** Bulk polymerization kinetics of 1,4-benzodioxpein-3-methyl-2,5-dione. Polymerization conditions: 130 °C, [monomer]: [DMAP]: [1-phenylethanol] = 100: 2: 1.

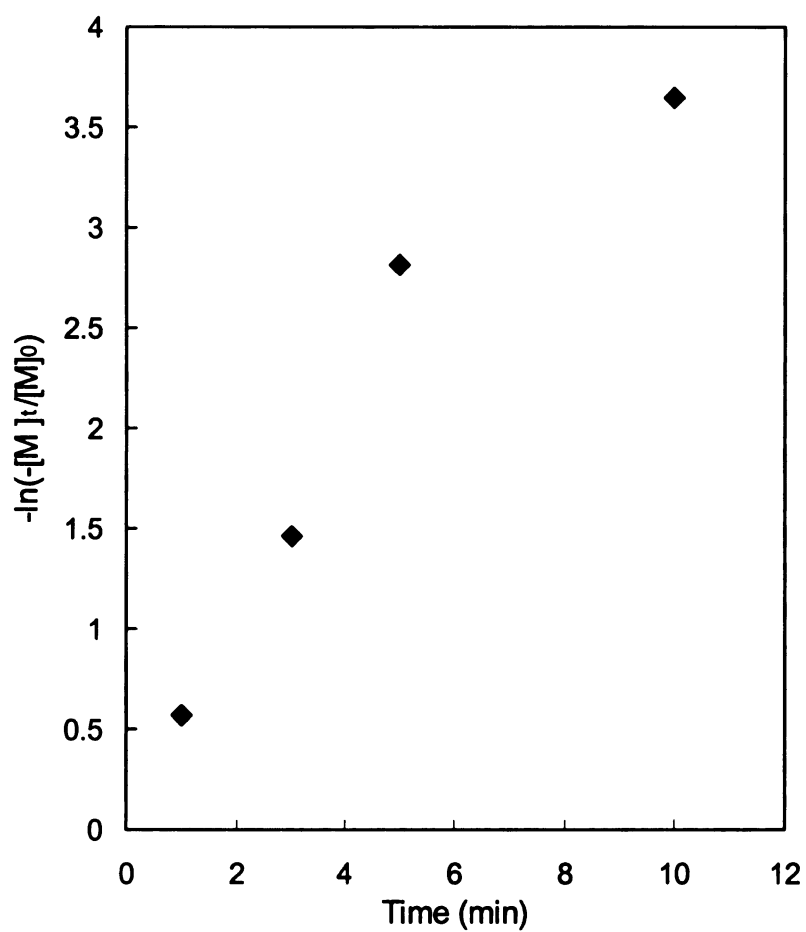


**Figure 44.** Bulk polymerization kinetics of 1,4-benzodioxpein-3-cyclohexyl-2,5-dione. Polymerization conditions: 160 °C, [monomer]: [DMAP]: [1-phenylethanol] = 100: 2: 1.

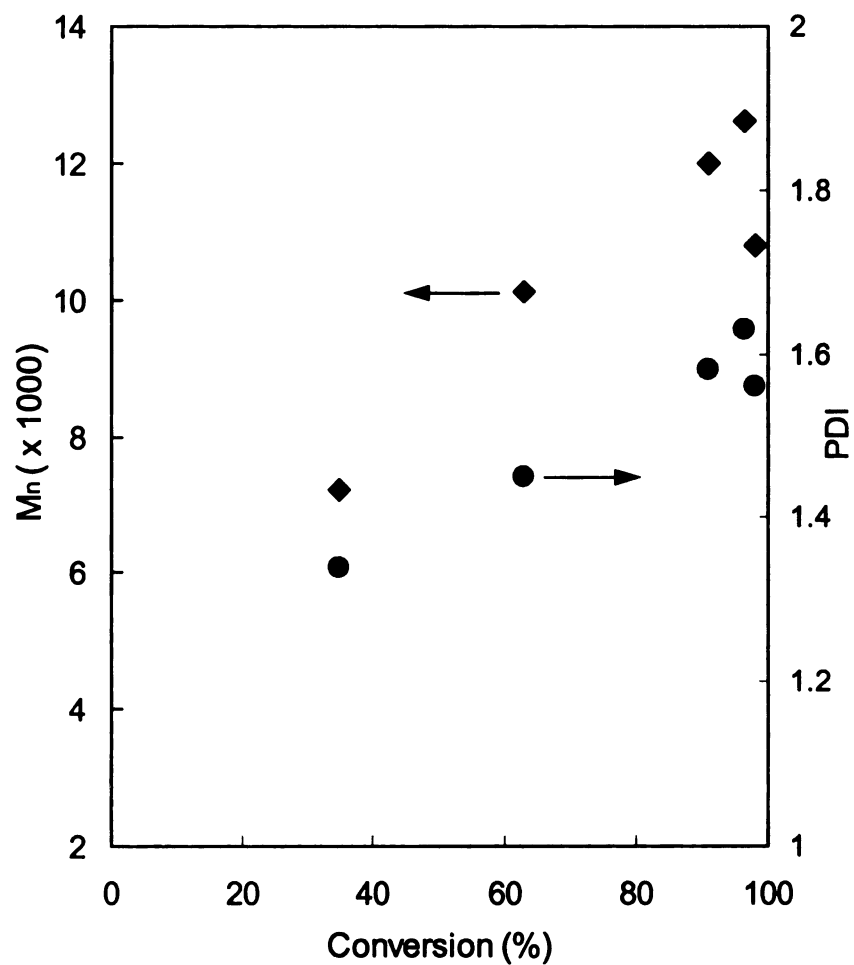


**Figure 45.** Evolution of the molecular weight (♦) and polydispersity (●) with conversion for the bulk polymerization of 1,4-benzodioxpein-3-methyl-2,5-dione. Polymerization conditions: 130 °C, [monomer]: [DMAP]: [1-phenylethanol] = 100: 2: 1.



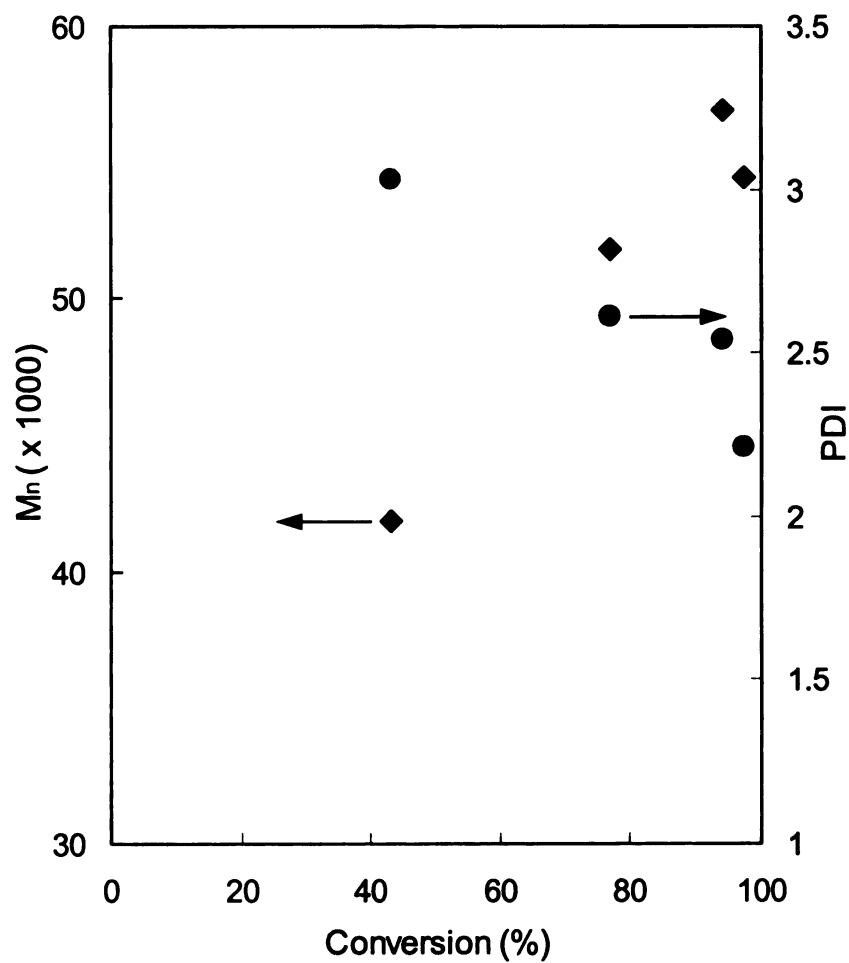


**Figure 46.** Evolution of the molecular weight (♦) and polydispersity (●) with conversion for the bulk polymerization of 1,4-benzodioxpein-3-cyclohexyl-2,5-dione. Polymerization conditions: 160 °C, [monomer]: [DMAP]: [1-phenylethanol] = 100: 2: 1.

### Physical properties of poly(1,4-benzodioxepin-3-alkyl-2,5-dione)s.

The decomposition temperatures of polymers measured using thermogravimetric analysis (TGA) define the limiting use temperatures of the polymers. As shown in **Figure 47**, the TGA trace for poly(1,4-benzodioxepin-3-cyclohexyl-2,5-dione) is similar to those of polylactides with onsets for weight loss near 300 °C followed by nearly complete weight loss. However, the onset temperature for weight loss for poly(1,4-benzodioxepin-3-methyl-2,5-dione) is much lower, ~230 °C. This may be due to its low molecular weight.

**Table 20.** Properties of poly(1,4-benzodioxepin-3-alkyl-2,5-dione)s

| Polymer   | $M_n$  | $M_w/M_n$ | $T_g$ (°C) |
|---|--------|-----------|------------|
| poly(1,4-benzodioxepin-3-methyl-2,5-dione) <sup>a</sup>     | 10,500 | 1.50      | 92         |
| poly(1,4-benzodioxepin-3-cyclohexyl-2,5-dione) <sup>b</sup> | 61,900 | 1.96      | 120        |

a. bulk polymerized at 130 °C; b. bulk polymerized at 160 °C.

The glass transition temperatures measured by DSC are shown in **Table 20** and **Figure 48**. In agreement with the argument that incorporating aromatic rings into polymer backbone would increase the rotation barriers of polymers and hence  $T_g$ , poly(1,4-benzodioxepin-3-methyl-2,5-dione) has a  $T_g$  of 92 °C, comparable to that of poly(dicyclohexylglycolide). By increasing the steric demands of the side chains, poly(1,4-benzodioxepin-3-cyclohexyl-2,5-dione) shows an exceptionally high  $T_g$  of 120 °C. Because only racemic monomers were used, both polymers are amorphous (no melting transition), showing them as promising replacements for polystyrene.

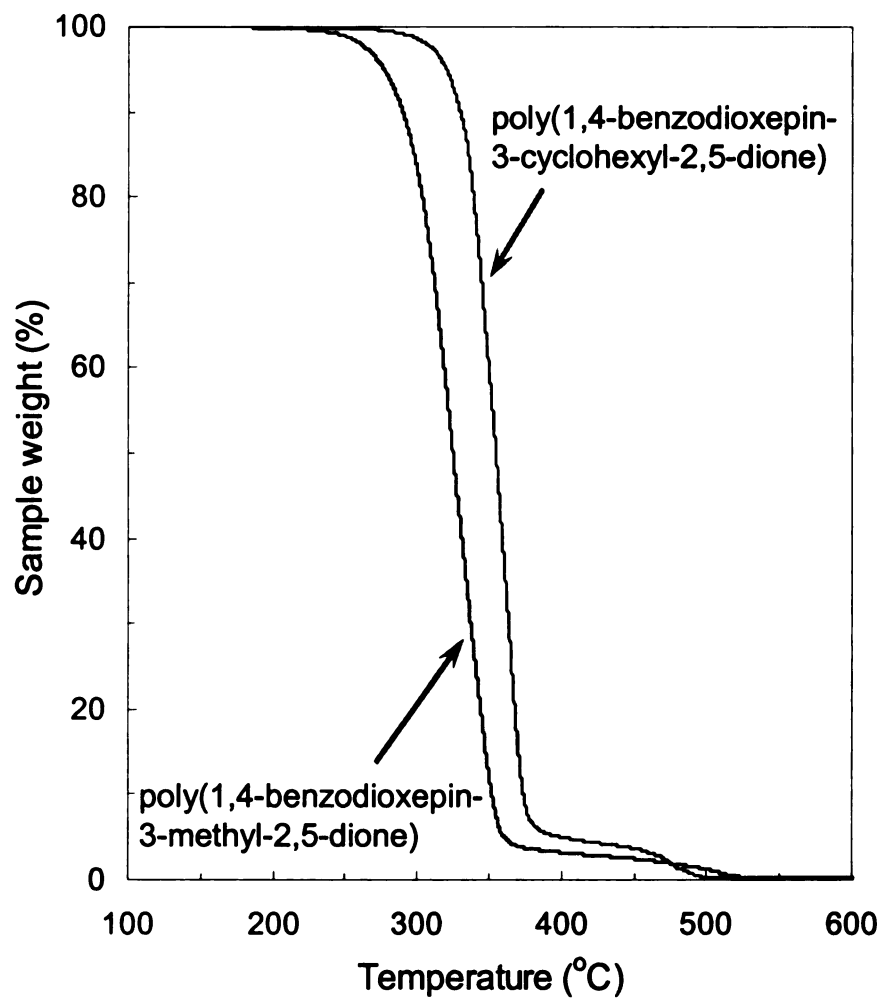


**Figure 47.** Thermogravimetric analysis results for poly(1,4-benzodioxepin-3-alkyl-2,5-dione)s. Samples were run in air at a heating rate of 10 °C/min.

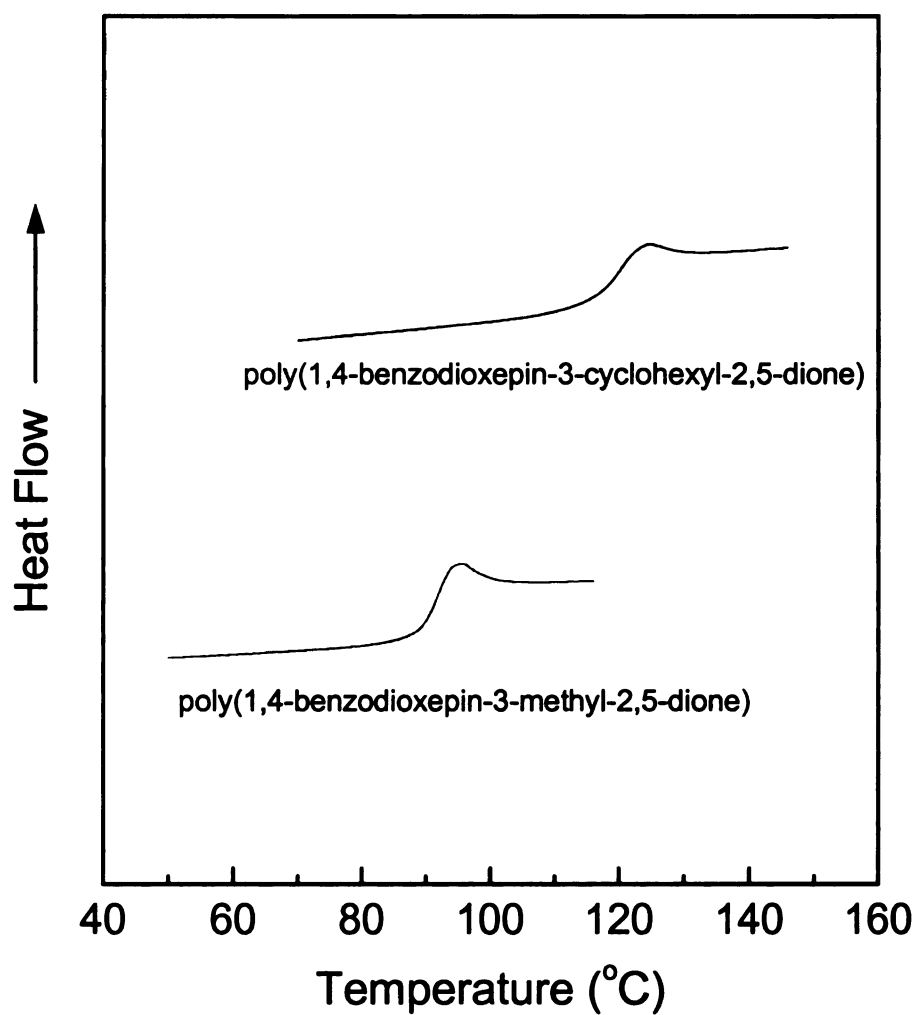
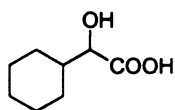


**Figure 48.** DSC analyses of poly(1,4-benzodioxepin-3-alkyl-2,5-dione)s. Heating rate: 10 °C/min under nitrogen. The data are second heating scans, taken after flash quenching from 150 °C.

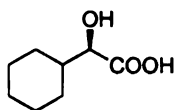
## Chapter 5 Experimental Section

Unless otherwise specified, ACS reagent grade starting materials and solvents were used as received from commercial suppliers without further purification.  $^1\text{H}$  NMR analyses were carried out at room temperature on a Varian UnityPlus-500 spectrometer at 500 MHz with the chemical shifts referenced to signals from residual protons in the solvent.  $^{13}\text{C}$  NMR spectra were obtained on a Varian UnityPlus-500 at 125 MHz with the chemical shifts referenced to signals from residual protons in the solvent. IR spectra were taken with Mattson Galaxy 3000 FT-IR. Elemental analyses were determined using a Perkin-Elmer 2400 CHNS/O Analyzer. Mass spectral analyses were carried out on a VG Masslab Trio-1. Melting points were taken on a Electrothermal capillary melting point apparatus and are uncorrected. Optical rotations were obtained on a Perkin-Elmer 141 polarimeter at 589 nm (sodium D line) using a 1.0 dm cell.

**General procedure for the reduction of mandelic acid.** To a solution of 200 mL methanol were added 38.0 g (0.25 mol) mandelic acid, 2.5 mL acetic acid, and 7.5 g rhodium on alumina (5%, Engelhard 5864). The mixture was sealed in an autoclave, purged with nitrogen, and then filled with hydrogen gas. Hydrogenation was carried out at room temperature for 8 hours under 1400 psi. The reaction mixture was then removed from the autoclave and filtered. After evaporating methanol, the crude product was recrystallized from toluene.



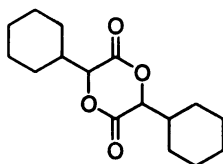
**2-Cyclohexyl-2-hydroxyacetic acid.** Colorless crystals were collected by filtration and dried under vacuum to give 31.8 g (80.5%) of racemic 2-cyclohexyl-2-hydroxyacetic acid.  $^1\text{H}$  NMR ( $\text{DMSO}-d_6$ ):  $\delta$  (ppm) 3.71 (d,  $J = 4.4$  Hz, 1H), 1.81-1.41 (m, 6H), 1.29-0.94 (m, 5H).  $^{13}\text{C}$  NMR ( $\text{DMSO}-d_6$ ):  $\delta$  (ppm) 175.27, 74.19, 41.15, 28.86, 26.74, 25.84, 25.76, 25.57. IR (KBr):  $\nu$  ( $\text{cm}^{-1}$ ) 3440, 2933, 2856, 1718, 1450, 1280, 1255, 1230, 1103. Anal. Calcd. for  $\text{C}_8\text{H}_{14}\text{O}_3$ : C, 60.74; H, 8.92. Found: C, 61.12; H, 9.28. mp 135-136 °C [Lit.<sup>198</sup> mp 136-137 °C].



**(*R*)-(-)-2-Cyclohexyl-2-hydroxyacetic acid.** Colorless crystals were collected by filtration and dried under vacuum to give 19.8 g (*R*)-(-)-2-cyclohexyl-2-hydroxyacetic acid (92.0% yield from 20.7 g (*R*)-(-)-mandelic acid).  $^1\text{H}$  NMR ( $\text{DMSO}-d_6$ ):  $\delta$  (ppm) 3.71 (d,  $J = 4.4$  Hz, 1H), 1.77-1.43 (m, 6H), 1.27-0.94 (m, 5H).  $^{13}\text{C}$  NMR ( $\text{DMSO}-d_6$ ):  $\delta$  (ppm) 175.27, 74.19, 41.15, 28.86, 26.74, 25.84, 25.76, 25.57. IR (KBr):  $\nu$  ( $\text{cm}^{-1}$ ) 3442, 2935, 2854, 1716, 1452, 1280, 1261, 1232, 1112, 1099. Anal. Calcd. for  $\text{C}_8\text{H}_{14}\text{O}_3$ : C, 60.74; H, 8.92. Found: C, 60.89; H, 8.90. mp 124-126 °C [Lit.<sup>199</sup> mp 130-131 °C].  $[\alpha]_D^{20} = -12.0^\circ$  ( $c = 1.0$ ,  $\text{CH}_3\text{OH}$ ), [lit.<sup>200</sup>  $[\alpha]_D^{20} = -22.8^\circ$  ( $c = 1.01$ , acetic acid)].

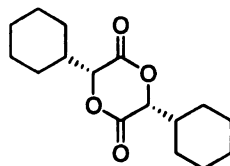
**General procedure for the synthesis of symmetrical substituted glycolides.** A mixture of 0.16 mol of the appropriate  $\alpha$ -hydroxy acid and 1.0 g of *p*-toluenesulfonic acid in 1600 mL toluene was refluxed for 6 days, with the water removed azeotropically via a Dean-Stark trap. Toluene was removed by rotary evaporation and the resulting solid was dissolved in ethyl acetate. The solution

was washed with saturated  $\text{NaHCO}_3$  and dried over  $\text{MgSO}_4$ . After removing ethyl acetate, the crude product was recrystallized from cyclohexane, hexane, or toluene.



**3,6-Dicyclohexyl-1,4-dioxane-2,5-dione.** *rac*-Dicyclohexylglycolide was recrystallized from toluene, and then cyclohexane. The white crystals were collected by filtration and dried under vacuum to give 4.8 g (21%) of *rac*-dicyclohexylglycolide.  $^1\text{H}$  NMR ( $\text{CDCl}_3$ ):  $\delta$  (ppm) 4.66 (d,  $J = 3.4$  Hz, 2H), 2.23-2.09 (m, 2H), 1.89-1.64 (m, 10H), 1.54-1.41 (dq,  $J = 3.7$  Hz,  $J = 12.8$  Hz, 2H), 1.39-1.24 (m, 6H), 1.24-1.08 (m, 2H).  $^{13}\text{C}$  NMR ( $\text{CDCl}_3$ ):  $\delta$  (ppm) 166.24, 79.33, 38.82, 28.94, 26.11, 25.75, 25.73 (peaks at 25.75 and 25.73 ppm were resolved to three separate peaks by adding the NMR shift reagent europium(III) tris(3-(trifluoromethylhydroxymethylene)-*d*-camphorate)). IR (KBr):  $\nu$  ( $\text{cm}^{-1}$ ) 2930, 2852, 1758, 1451, 1370, 1303, 1261, 1185, 1111. Anal. Calcd. for  $\text{C}_{16}\text{H}_{24}\text{O}_4$ : C, 68.54; H, 8.63. Found: C, 68.73; H, 8.51. MS (EI)  $m/z$  198.1 (100), 123.0 (24), 94.9 (72), 54.9 (41). mp 183-185  $^\circ\text{C}$ . The toluene mother liquor from the initial recrystallization of *rac*-dicyclohexylglycolide was evaporated to dryness and the residue was crystallized from hexane to provide crude *meso*-dicyclohexylglycolide. Contamination from residual *rac*-dicyclohexylglycolide was eliminated by column chromatography on silica gel (ether/hexanes 1/3) to give 0.86 g (3.8%) of *meso*-dicyclohexylglycolide.  $^1\text{H}$  NMR ( $\text{CDCl}_3$ ):  $\delta$  (ppm) 4.72 (d,  $J = 4.9$  Hz, 2H), 2.14-2.01 (m, 2H), 1.87-1.64 (m, 10H), 1.47-1.35 (dq,  $J = 3.5$  Hz,  $J$

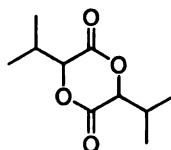
= 12.5 Hz, 2H), 1.34-1.09 (m, 8H).  $^{13}\text{C}$  NMR ( $\text{CDCl}_3$ ):  $\delta$  (ppm) 165.22, 80.59, 80.56, 41.02, 28.57, 26.82, 25.77, 25.54, 25.52. IR (KBr):  $\nu$  ( $\text{cm}^{-1}$ ) 2929, 2852, 1752, 1450, 1379, 1308, 1274, 1110. Anal. Calcd. for  $\text{C}_{16}\text{H}_{24}\text{O}_4$ : C, 68.54; H, 8.63. Found: C, 68.93; H, 8.51. MS (EI)  $m/z$  198.1 (100), 123.0 (27), 94.9 (77), 54.9 (54). mp 80.5-81.5  $^{\circ}\text{C}$ .



**(3*R*,6*R*)-(+)-3,6-Dicyclohexyl-1,4-dioxane-2,5-dione.**

*R,R*-

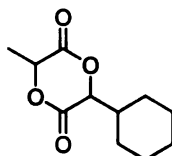
Dicyclohexylglycolide was recrystallized from cyclohexane. The colorless crystals were collected by filtration and dried under vacuum to give 4.5 g *R,R*-dicyclohexylglycolide (40% yield from 0.08 mol (*R*)-(-)-2-cyclohexyl-2-hydroxyacetic acid).  $^1\text{H}$  NMR ( $\text{CDCl}_3$ ):  $\delta$  (ppm) 4.66 (d,  $J$  = 2.9 Hz, 2H), 2.21-2.09 (m, 2H), 1.88-1.63 (m, 10H), 1.54-1.41 (dq,  $J$  = 3.5 Hz,  $J$  = 12.8 Hz, 2H), 1.39-1.24 (m, 6H), 1.22-1.09 (m, 2H).  $^{13}\text{C}$  NMR ( $\text{CDCl}_3$ ):  $\delta$  (ppm) 166.27, 79.27, 38.76, 28.90, 26.07, 25.71, 25.70. IR (KBr):  $\nu$  ( $\text{cm}^{-1}$ ) 2932, 2853, 1760, 1452, 1371, 1302, 1256, 1253, 1185, 1113. Anal. Calcd. for  $\text{C}_{16}\text{H}_{24}\text{O}_4$ : C, 68.54; H, 8.63. Found: C, 68.78; H, 8.67. MS (EI)  $m/z$  198.1 (100), 123.0 (25), 94.9 (75), 54.9 (44). mp 194-196  $^{\circ}\text{C}$ .  $[\alpha]_D^{20}$  = +190.0 $^{\circ}$  ( $c$  = 1.0,  $\text{CHCl}_3$ ).



**3,6-Diisopropyl-1,4-dioxane-2,5-dione.** *rac*-Diisopropylglycolide was recrystallized from toluene, and contamination from residual *meso*-

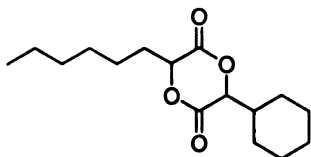


diisopropylglycolide was eliminated by column chromatography on silica gel (ether/hexane 1/2) to give 1.5 g of *rac*-diisopropylglycolide (16% yield from 10.7 g 2-hydroxy-3-methylbutyric acid).  $^1\text{H}$  NMR ( $\text{CDCl}_3$ ):  $\delta$  (ppm) 4.70 (d,  $J$  = 3.1 Hz, 2H), 2.55-2.47 (m, 2H), 1.19-1.14 (d,  $J$  = 6.9 Hz, 6H), 1.09-1.04 (d,  $J$  = 6.9 Hz, 6H).  $^{13}\text{C}$  NMR ( $\text{CDCl}_3$ ):  $\delta$  (ppm) 166.33, 79.59, 29.42, 18.59, 15.85. IR (KBr):  $\nu$  ( $\text{cm}^{-1}$ ) 2975, 2940, 2881, 1753, 1473, 1367, 1311, 1257, 1134, 1043. Anal. Calcd. for  $\text{C}_{10}\text{H}_{16}\text{O}_4$ : C, 59.98; H, 8.05. Found: C, 60.45; H, 7.83. MS (EI)  $m/z$  158.0 (73), 84.0 (38), 82.8 (39), 68.9 (100), 56.0 (59), 40.9 (40). mp 137.0-137.5 °C.



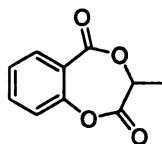
**3-Cyclohexyl-6-methyl-1,4-dioxane-2,5-dione.** To a 500 mL 3-neck flask were added 12.66 g (0.08 mol) of 2-cyclohexyl-2-hydroxyacetic acid, 20.7 g (0.096 mol) of 2-bromopropionyl bromide, and 200 mL THF. The flask was purged with nitrogen and then cooled in a salt-ice bath. A mixture of 14.5 mL  $\text{Et}_3\text{N}$  and 50 mL THF was added dropwise under mechanical stirring and the solution was cooled and stirred overnight. The solution was filtered to remove a white solid, and the filtrate was evaporated to dryness. The solid was dissolved in ethyl acetate. The solution was washed with 2 M HCl (3×100 mL), saturated NaCl, dried over  $\text{MgSO}_4$ , and then concentrated to give a solution of the crude linear acid ester. The viscous liquid was mixed with 1600 mL acetone and 27 g  $\text{NaHCO}_3$ , and refluxed for 2 days. The solids were removed by filtration and the acetone was evaporated to dryness. The crude product was dissolved in ethyl acetate, dried over  $\text{MgSO}_4$ , and the ethyl acetate was removed by rotary

evaporation. The crude product was recrystallized from cyclohexane, and the colorless crystals were collected by filtration and dried under vacuum to give 10.0 g (59%) of *rac*-methylcyclohexylglycolide.  $^1\text{H}$  NMR ( $\text{CDCl}_3$ ):  $\delta$  (ppm) 4.97 (q,  $J$  = 6.8 Hz, 1H), 4.71 (d,  $J$  = 2.9 Hz, 1H), 2.21-2.11 (m, 1H), 1.87-1.68 (m, 8H), 1.54-1.42 (dq,  $J$  = 3.8 Hz,  $J$  = 12.7 Hz, 1H), 1.39-1.24 (m, 3H), 1.23-1.11 (m, 1H).  $^{13}\text{C}$  NMR ( $\text{CDCl}_3$ ):  $\delta$  (ppm) 167.50, 166.02, 79.64, 72.12, 38.68, 28.93, 26.09, 25.74, 15.99. IR (KBr):  $\nu$  ( $\text{cm}^{-1}$ ) 2999, 2939, 2853, 1763, 1761, 1451, 1379, 1341, 1296, 1245, 1184, 1098. Anal. Calcd. for  $\text{C}_{11}\text{H}_{16}\text{O}_4$ : C, 62.25; H, 7.60. Found: C, 62.34; H, 7.67. MS (EI)  $m/z$  129.9 (100), 83.0 (10), 56.0 (13), 55.0 (26). mp 80.5-82.0  $^\circ\text{C}$ . The *cis* relationship of the methyl and cyclohexyl groups on the glycolide ring was verified by 1D Gradient-Selected Transient Nuclear Overhauser Effect Experiment (NOESY1D).



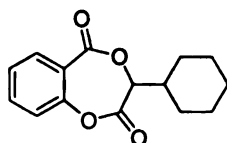
**3-Cyclohexyl-6-hexyl-1,4-dioxane-2,5-dione.** To a 500 mL 3-neck flask were added 12.66 g (0.08 mol) of 2-cyclohexyl-2-hydroxyacetic acid, 23.2 g (0.096 mol) of 2-bromooctanoyl chloride, and 200 mL THF. The flask was purged with nitrogen and then cooled in a salt-ice bath. A mixture of 14.5 mL  $\text{Et}_3\text{N}$  and 50 mL THF was added dropwise under mechanical stirring and the solution was cooled and stirred overnight. The solution was filtered to remove a white solid, and the filtrate was evaporated to dryness. The solid was dissolved in ethyl acetate. The solution was washed with 2 M HCl (3 $\times$ 100 mL), saturated NaCl, dried over  $\text{MgSO}_4$ , and then concentrated to give a solution of the crude linear

acid ester. The viscous liquid was mixed with 1600 mL acetone and 27 g  $\text{NaHCO}_3$ , and refluxed for 60 hours. The solids were removed by filtration and the acetone was evaporated to dryness. The crude product was dissolved in ethyl acetate, dried over  $\text{MgSO}_4$ , and the ethyl acetate was removed by rotary evaporation. The crude product was recrystallized from cyclohexane, and the colorless crystals were collected by filtration and dried under vacuum to give 5.6 g (25%) of *rac*-hexylcyclohexylglycolide.  $^1\text{H}$  NMR ( $\text{CDCl}_3$ ):  $\delta$  (ppm) 4.83 (dd,  $J = 4.3$  Hz,  $J = 7.8$  Hz, 1H), 4.69 (d,  $J = 3.2$  Hz, 1H), 2.20-2.04 (m, 2H), 1.99-1.89 (m, 1H), 1.86-1.65 (m, 5H), 1.62-1.41 (m, 3H), 1.40-1.24 (m, 9H), 1.23-1.11 (m, 1H), 0.91-0.84 (t,  $J = 7.0$  Hz, 3H).  $^{13}\text{C}$  NMR ( $\text{CDCl}_3$ ):  $\delta$  (ppm) 167.04, 166.17, 79.44, 75.48, 38.72, 31.44, 30.22, 28.94, 26.09, 25.76, 25.74, 25.72, 24.33, 22.48, 14.01. IR (KBr):  $\nu$  ( $\text{cm}^{-1}$ ) 2954, 2925, 2853, 1764, 1762, 1449, 1306, 1249, 1296, 1090. Anal. Calcd. for  $\text{C}_{16}\text{H}_{26}\text{O}_4$ : C, 68.06; H, 9.28. Found: C, 68.13; H, 9.37. MS (EI)  $m/z$  200.3 (35), 142.2 (33), 125.3 (20.8), 95.2 (38), 67.2 (35), 55.5 (100). mp 94.5-95.5  $^\circ\text{C}$ . The *cis* relationship of the hexyl and cyclohexyl groups on the glycolide ring was verified by 1D Gradient-Selected Transient Nuclear Overhauser Effect Experiment (NOESY1D).



**1,4-Benzodioxepin-3-methyl-2,5-dione.** To a 500 mL 3-neck flask were added 27.6 g (0.2 mol) of salicylic acid, 24.3 mL (0.23 mol) of 2-bromopropionyl bromide, and 300 mL THF. The flask was purged with nitrogen and then cooled in a salt-ice bath. A mixture of 34.8 mL  $\text{Et}_3\text{N}$  and 50 mL THF was added dropwise

under mechanical stirring and the solution was cooled and stirred overnight. The solution was filtered to remove a white solid, and the filtrate was evaporated to dryness. The solid was dissolved in ethyl acetate. The solution was washed with 2 M HCl (3×100 mL), saturated NaCl, dried over MgSO<sub>4</sub>, and then concentrated to give a pale pink crystal of the crude linear acid ester. The crystal was mixed with 1600 mL acetone and 67 g NaHCO<sub>3</sub>, and refluxed for 2 hours. The solids were removed by filtration and the acetone was evaporated to dryness. The crude product was dissolved in dichloromethane, dried over MgSO<sub>4</sub>, and the dichloromethane was removed by rotary evaporation. The crude product was recrystallized from toluene once and benzene twice, and the white crystals were collected by filtration and dried under vacuum to give 9.66 g (25%) of 1,4-benzodioxepin-3-methyl-2,5-dione. <sup>1</sup>H NMR (CDCl<sub>3</sub>): δ (ppm) 7.95 (d, *J* = 7.5 Hz, 1H), 7.68 (t, *J* = 7.8 Hz, 1H), 7.42 (t, *J* = 7.6 Hz, 1H), 7.26 (d, *J* = 8.3 Hz, 1H), 4.94 (q, *J* = 6.4 Hz, 1H), 1.68 (d, *J* = 6.5 Hz, 3H). <sup>13</sup>C NMR (CDCl<sub>3</sub>): δ (ppm) 165.81, 165.61, 149.66, 135.53, 132.56, 126.69, 120.79, 120.25, 69.64, 15.63. IR (KBr): ν (cm<sup>-1</sup>) 3085, 2998, 2944, 1788, 1718, 1604, 1454, 1302, 1247, 1213, 1176, 1138, 1073. Anal. Calcd. for C<sub>10</sub>H<sub>8</sub>O<sub>4</sub>: C, 62.50; H, 4.20. Found: C, 62.37; H, 7.16. MS (EI) *m/z* 192.1 (3.7), 164.0 (10), 121.1 (10), 120.0 (100), 92.0 (45), 64.1 (12), 62.9 (19). mp 118-119 °C.



**1,4-Benzodioxepin-3-cyclohexyl-2,5-dione.** To a solution of 200 mL methanol were added 27.2 g phenylacetic acid, 2.5 mL acetic acid, and 7.5 g

rhodium on alumina (5%, Engelhard 5864). The mixture was sealed in an autoclave, purged with nitrogen, and then filled with hydrogen gas. Hydrogenation was carried out at room temperature for 8 hours under 1400 psi. The reaction mixture was then removed from the autoclave and filtered. The filtrate was concentrated to give 28.0 g (98%) crude 2-cyclohexylacetic acid. The crude acid was used directly without further purification. To a 500 mL 3-neck flask were added 85.7 g (0.6 mol) of 2-cyclohexylacetic acid, 86 mL thionyl chloride (1.2 mol), and a magnetic stir bar. The solution was stirred first at room temperature for 1 hour, and then at 85 °C for 1 hour. 38 mL bromine (0.75 mol) was added dropwise over 30 minutes, and the solution was stirred overnight at 85 °C. The solution was vacuum distilled to give 2-cyclohexyl-2-bromoacetyl chloride as a bright pale yellow liquid. To a 500 mL 3-neck flask were added 27.6 g (0.2 mol) of salicylic acid, 55.1 g (0.23 mol) of 2-cyclohexyl-2-bromoacetyl chloride, and 300 mL THF. The flask was purged with nitrogen and then cooled in a salt-ice bath. A mixture of 34.8 mL Et<sub>3</sub>N and 50 mL THF was added dropwise under mechanical stirring and the solution was cooled and stirred overnight. The solution was filtered to remove a white solid, and the filtrate was evaporated to dryness. The solid was dissolved in ethyl acetate. The solution was washed with 2 M HCl (3×100 mL), saturated NaCl, dried over MgSO<sub>4</sub>, and then concentrated to give a pale yellow crystal of the crude linear acid ester. 17.1 g of the acid ester intermediate was mixed with 400 mL THF and 10.5 mL (0.075 mol) Et<sub>3</sub>N, and refluxed overnight. The solids were removed by filtration and the THF was evaporated to dryness. The crude product was dissolved in ethyl acetate,

washed with 2 M HCl (3×100 mL), saturated NaCl, dried over MgSO<sub>4</sub>, and the ethyl acetate was removed by rotary evaporation. The crude product was recrystallized from toluene twice, and the needle-like colorless crystals were collected by filtration and dried under vacuum to give 5.85 g (45%) of 1,4-benzodioxepin-3-cyclohexyl-2,5-dione. <sup>1</sup>H NMR (CDCl<sub>3</sub>): δ (ppm) 7.94 (d, *J* = 7.8 Hz, 1H), 7.68 (t, *J* = 7.9 Hz, 1H), 7.41 (t, *J* = 7.6 Hz, 1H), 7.25 (d, *J* = 8.3 Hz, 1H), 4.40 (d, *J* = 7.6 Hz, 1H), 2.24-2.08 (m, 2H), 1.88-1.65 (m, 4H), 1.42-1.25 (m, 2H), 1.24-0.99 (m, 3H). <sup>13</sup>C NMR (CDCl<sub>3</sub>): δ (ppm) 166.03, 164.11, 149.82, 135.48, 132.56, 126.55, 120.72, 120.11, 76.53, 37.70, 28.90, 27.28, 26.07, 25.51, 25.33. IR (KBr): ν (cm<sup>-1</sup>) 3074, 2954, 2933, 2851, 1783, 1729, 1606, 1453, 1297, 1247, 1212, 1133. Anal. Calcd. for C<sub>15</sub>H<sub>16</sub>O<sub>4</sub>: C, 69.22; H, 6.20. Found: C, 69.28; H, 6.17. MS (EI) *m/z* 260.1 (0.3), 232.1 (2.9), 149.0 (10), 120.0 (100), 92.0 (33). mp 156-157 °C.

**Solution polymerization of substituted glycolides.** A Schlenk flask containing 2.0 mmol of substituted glycolide and a magnetic stir bar was fitted with a septum and then evacuated and refilled with argon three times. Predetermined amounts of anhydrous toluene, and toluene solutions of Sn(2-ethylhexanoate)<sub>2</sub> and 4-*tert*-butylbenzyl alcohol were then added via syringe through the septum to yield a 0.2 M monomer concentration. The Schlenk flask was then suspended in a 90 °C oil bath to initiate polymerization. For kinetic studies, a syringe was used to remove aliquots of the reaction solution at specific intervals and were analyzed by NMR to determine the monomer conversion.

**Bulk polymerization of substituted glycolides.** Solvent-free polymerizations were carried out in sealed ampoules prepared from  $\frac{3}{8}$  in. diameter glass tubing. After charging with the substituted glycolide and a stir bar, the ampoule was connected to a vacuum line through a vacuum adapter. After evacuating the ampoule for 2 hours, it was filled with argon, and a syringe was used to add a predetermined amount of the  $\text{Sn}(\text{2-ethylhexanoate})_2$  and 4-*tert*-butylbenzyl alcohol solutions to the ampoule through the adapter. The solvent was removed *in vacuo*, and the ampoule was flame-sealed and immersed in oil bath. At the end of the polymerization, the ampoule was cooled, opened, and the polymer was dissolved in  $\text{CH}_2\text{Cl}_2$ . A portion of the solution was evacuated to dryness and analyzed by NMR for conversion. The rest of polymer solution was precipitated three times into cold methanol, dissolved  $\text{CH}_2\text{Cl}_2$ , and washed with 2M HCl. Re-precipitation into cold methanol gave polymer free of residual monomer and catalysts.

**Bulk copolymerization of dicyclohexylglycolide and dihexylglycolide.** Solvent-free copolymerizations were carried out in sealed ampoules prepared from  $\frac{3}{8}$  in. diameter glass tubing. After charging with the predetermined amounts of dicyclohexylglycolide and dihexylglycolide, and a stir bar, the ampoule was connected to a vacuum line through a vacuum adapter. After evacuating the ampoule for 2 hours, it was filled with argon, and a syringe was used to add a predetermined amount of the  $\text{Sn}(\text{2-ethylhexanoate})_2$  and 4-*tert*-butylbenzyl alcohol solutions to the ampoule through the adapter. The solvent was removed *in vacuo*, and the ampoule was flame-sealed and immersed in oil bath. At the

end of the polymerization, the ampoule was cooled, opened, and the polymer was dissolved in  $\text{CH}_2\text{Cl}_2$ . A portion of the solution was evacuated to dryness and analyzed by NMR for conversion. The rest of polymer solution was precipitated three times into cold methanol.

**Bulk polymerization of dicyclohexylglycolide via poly(ethylene glycol).** Solvent-free polymerizations were carried out in sealed ampoules prepared from  $\frac{3}{8}$  in. diameter glass tubing. After charging with the predetermined amounts of poly(ethylene glycol), the ampoule was dried overnight at 130 °C under full vacuum (5-10 mTorr) to completely remove moisture. *rac*-Dicyclohexylglycolide (560 mg) was then added into the flask under argon. After evacuating the flask for 2 hours, the flask was back-filled with argon, the desired amount of  $\text{Sn}(\text{2-ethylhexanoate})_2$  as a solution in dry toluene was added via syringe through a septum. The solvent was removed *in vacuo*, and the ampoule was flame-sealed and immersed in a 200 °C oil bath for 20 minutes. At the end of the polymerization, the ampoule was cooled, opened, and the polymer was dissolved in  $\text{CH}_2\text{Cl}_2$ . A portion of the solution was evacuated to dryness and analyzed by NMR for conversion. The rest of polymer solution was precipitated two times into cold methanol. For comparison, *rac*-dicyclohexylglycolide homopolymer was synthesized using the same procedure with 1,4-cyclohexanedimethanol as the initiator.

**Solution polymerization of 1,4-benzodioxepin-3-alkyl-2,5-diones.** A Schlenk flask containing 2.0 mmol of 1,4-benzodioxepin-3-alkyl-2,5-dione and a magnetic stir bar was fitted with a septum and then evacuated and refilled with



argon three times. Predetermined amounts of anhydrous toluene, and toluene solutions of 4-(dimethylamino)pyridine and 1-phenylethanol were then added via syringe through the septum to yield a 0.2 M monomer concentration. The Schlenk flask was then suspended in a 90 °C oil bath to initiate polymerization. For kinetic studies, aliquots of the reaction solution were removed by using a syringe at specific intervals and were analyzed by NMR to determine the monomer conversion.

**Bulk polymerization of 1,4-benzodioxepin-3-alkyl-2,5-diones.** Solvent-free polymerizations were carried out in sealed ampoules prepared from  $\frac{3}{8}$  in. diameter glass tubing. After charging with the 1,4-benzodioxepin-3-alkyl-2,5-dione and a stir bar, the ampoule was connected to a vacuum line through a vacuum adapter. After evacuating the ampoule for 2 hours, it was filled with argon, and a syringe was used to add a predetermined amount of the 4-(dimethylamino)pyridine and 1-phenylethanol solutions to the ampoule through the adapter. The solvent was removed *in vacuo*, and the ampoule was flame-sealed and immersed in oil bath. At the end of the polymerization, the ampoule was cooled, opened, and the polymer was dissolved in  $\text{CH}_2\text{Cl}_2$ . A portion of the solution was evacuated to dryness and analyzed by NMR for conversion. The rest of polymer solution was precipitated three times into cold methanol.

**Polymer characterization.** The molecular weights of polymers were determined by Gel Permeation Chromatography (GPC) using a PLgel 20 m Mixed A column and a Waters 2410 differential refractometer detector at 35 °C. THF was used as the eluting solvent at a flow rate of 1 mL/min, and

monodisperse polystyrene standards were used to calibrate the molecular weights. Differential Scanning Calorimetry (DSC) analyses of the polymers were obtained using a TA DSC Q100. Samples were run under a nitrogen atmosphere at a heating rate of 10 °C/min, with the temperature calibrated with an indium standard. Thermogravimetric analyses (TGA) were run both in air and under nitrogen at a heating rate of 10 °C/min using a Perkin-Elmer TGA 7. Atomic Force Microscopy (AFM) analyses of the polymer thin film were run at room temperature in non-contact mode (tapping mode) using Pacific Nanotechnology Nano-R AFM. Polymer thin films were prepared by spin-coating the polymer solution (4 mg/mL in THF) on the silicon wafer and vacuum dried at room temperature. The measurement was done with the lightest set point possible at a scanning rate of 0.85Hz and oscillation frequency around 300 KHz.

**Hydrolytic degradation of poly(dicyclohexylglycolide).** The phosphate buffer solution with a pH of 7.4 was prepared by adding dilute NaOH solution into commercially available phosphate buffer solution (pH = 7.0) at 55 °C. Around 50 mg of the polymer powder was placed inside each test tube and 15 mL of freshly prepared phosphate buffer solution was added. Test tube was then capped with a septum and sealed under slight vacuum with a syringe. Multiple samples were prepared and placed into a water/ethylene glycol bath thermal stated at  $55 \pm 0.2$  °C. At desired time, the test tubes were removed from the bath. The solutions were then filtered through pre-weighed fritted glass funnels, and the collected polymers were rinsed repeatedly with a large amount of distilled water. The polymer and the funnel were dried together under vacuum for 2 days.

**Alcoholic degradation of poly(dicyclohexylglycolide).** To a 100 mL flask were added 200 mg of the polymer power, 50 mL butanol, and several drops of sulfuric acid. The solution was refluxed. At desired time, around 1 mL of solution was taken out of the flask. The solution was evacuated to dryness. A portion of the solid was analyzed by NMR for conversion, and the rest was dissolved in THF and analyzed by GPC for molecular weight and polydispersity.

## **Appendix**

|                   |                                   |                         |                |
|-------------------|-----------------------------------|-------------------------|----------------|
| <i>Sample</i>     | 2-cyclohexyl-2-hydroxyacetic acid |                         |                |
| <i>Instrument</i> | Varian UnityPlus500               | <i>Frequency (MHz)</i>  | 500            |
| <i>Solvent</i>    | DMSO- <i>d</i> <sub>6</sub>       | <i>Temperature (°C)</i> | 25             |
|                   |                                   |                         | <sup>1</sup> H |

**Table of Integrals**

| No. | Chemical Shift (ppm) | Value |
|-----|----------------------|-------|
| 1   | 3.75 – 3.68          | 1     |
| 2   | 1.81 – 1.41          | 6.77  |
| 3   | 1.29 – 0.94          | 5.67  |

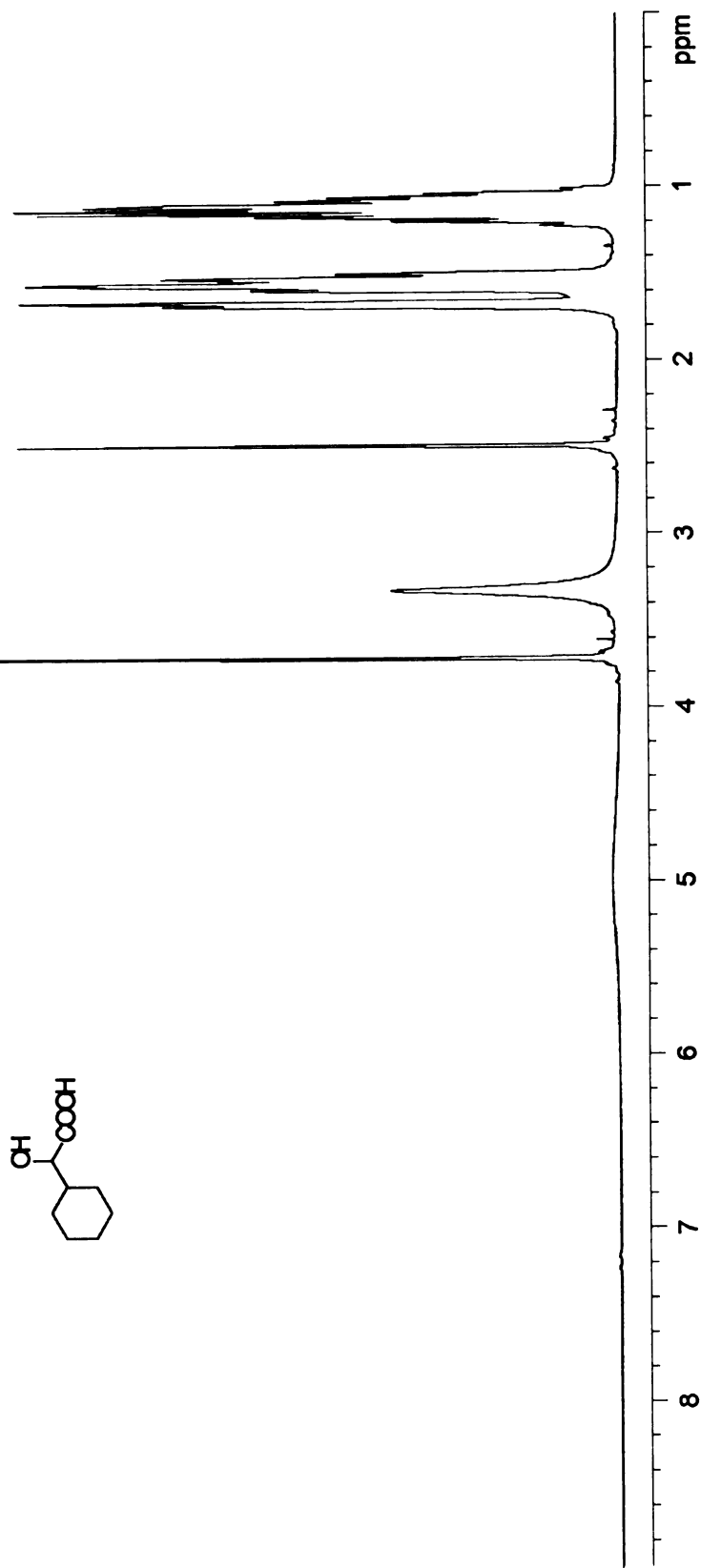


**Figure A-1. <sup>1</sup>H NMR spectrum of 2-cyclohexyl-2-hydroxyacetic acid**

|                   |                                   |                         |                 |
|-------------------|-----------------------------------|-------------------------|-----------------|
| <b>Sample</b>     | 2-cyclohexyl-2-hydroxyacetic acid |                         |                 |
| <b>Instrument</b> | Varian UnityPlus500               | <b>Frequency (MHz)</b>  | 125             |
| <b>Solvent</b>    | DMSO- <i>d</i> <sub>6</sub>       | <b>Temperature (°C)</b> | 25              |
|                   |                                   | <b>Nucleus</b>          | <sup>13</sup> C |

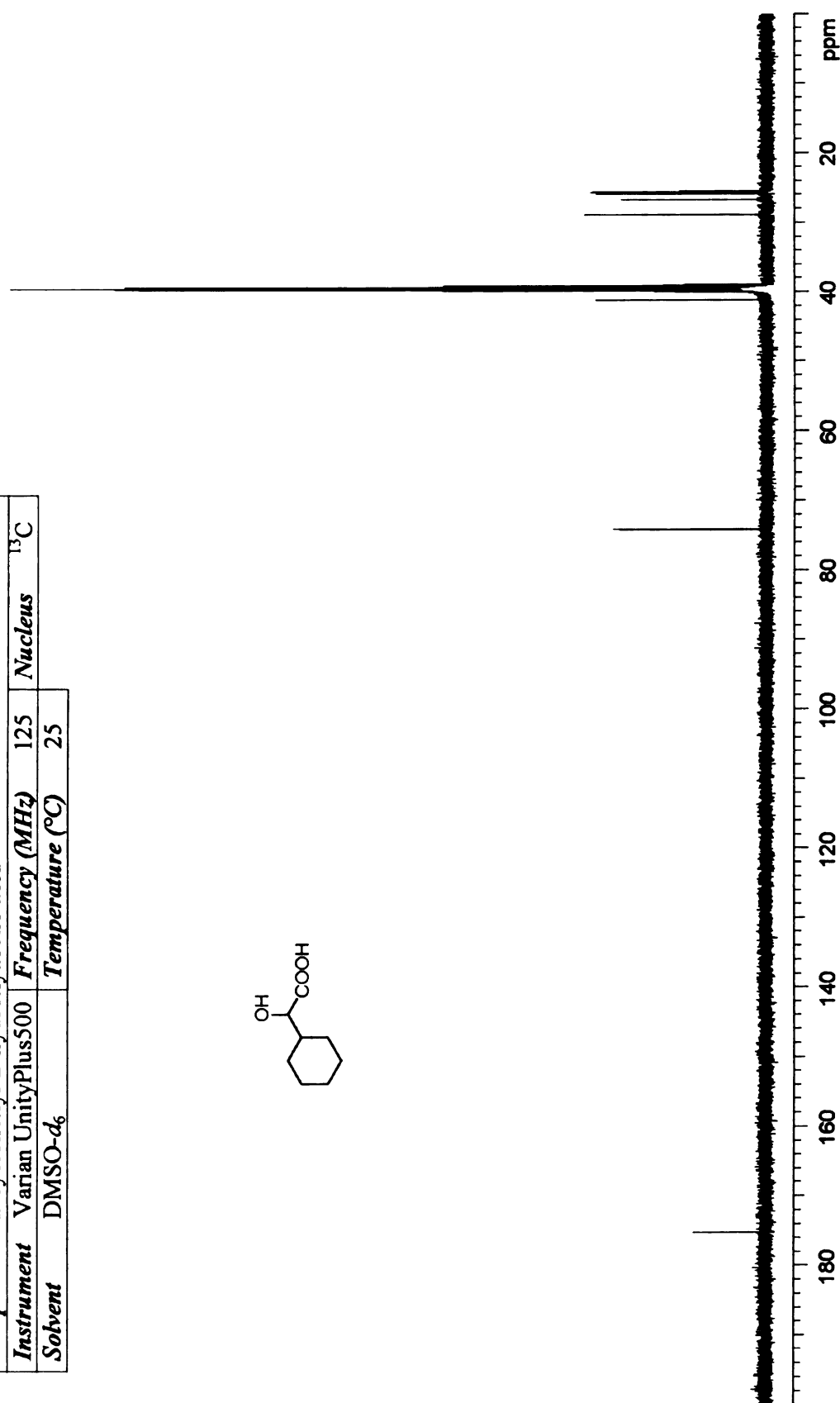
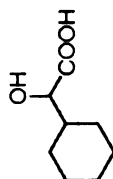


**Figure A-2.** <sup>13</sup>C NMR spectrum of 2-cyclohexyl-2-hydroxyacetic acid

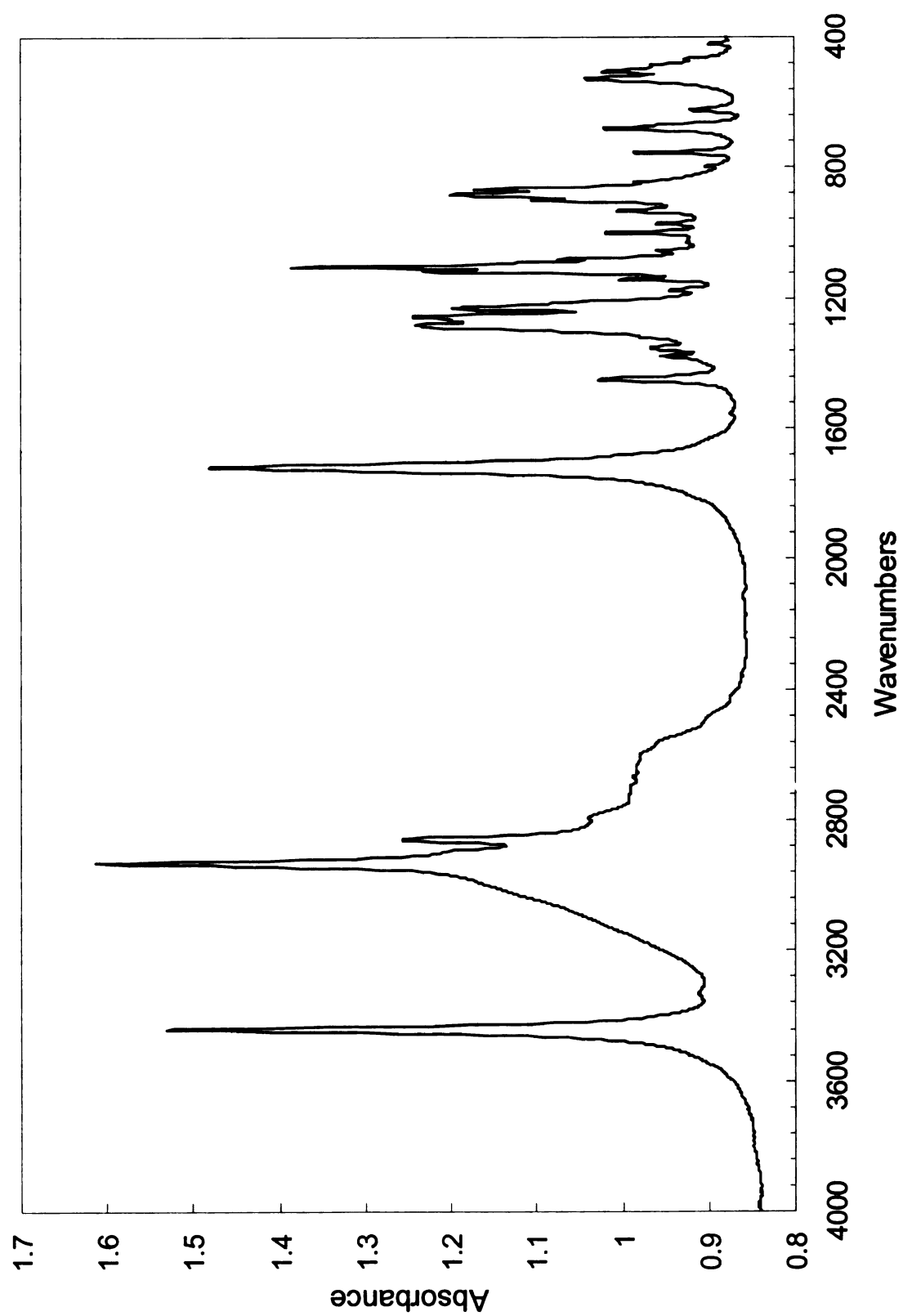


**Figure A- 3.** FT-IR spectrum of 2-cyclohexyl-2-hydroxyacetic acid

|                   |   |                         |     |                |
|-------------------|---|-------------------------|-----|----------------|
| <b>Sample</b>     | (R)-(-)-2-cyclohexyl-2-hydroxyacetic acid |                         |     |                |
| <b>Instrument</b> | Varian UnityPlus500                       | <b>Frequency (MHz)</b>  | 500 | <sup>1</sup> H |
| <b>Solvent</b>    | DMSO- <i>d</i> <sub>6</sub>               | <b>Temperature (°C)</b> | 25  |                |

Table of Integrals

| No. | Chemical Shift (ppm) | Value |
|-----|----------------------|-------|
| 1   | 3.75 – 3.67          | 1     |
| 2   | 1.77 – 1.43          | 6.49  |
| 3   | 1.27 – 0.94          | 5.46  |

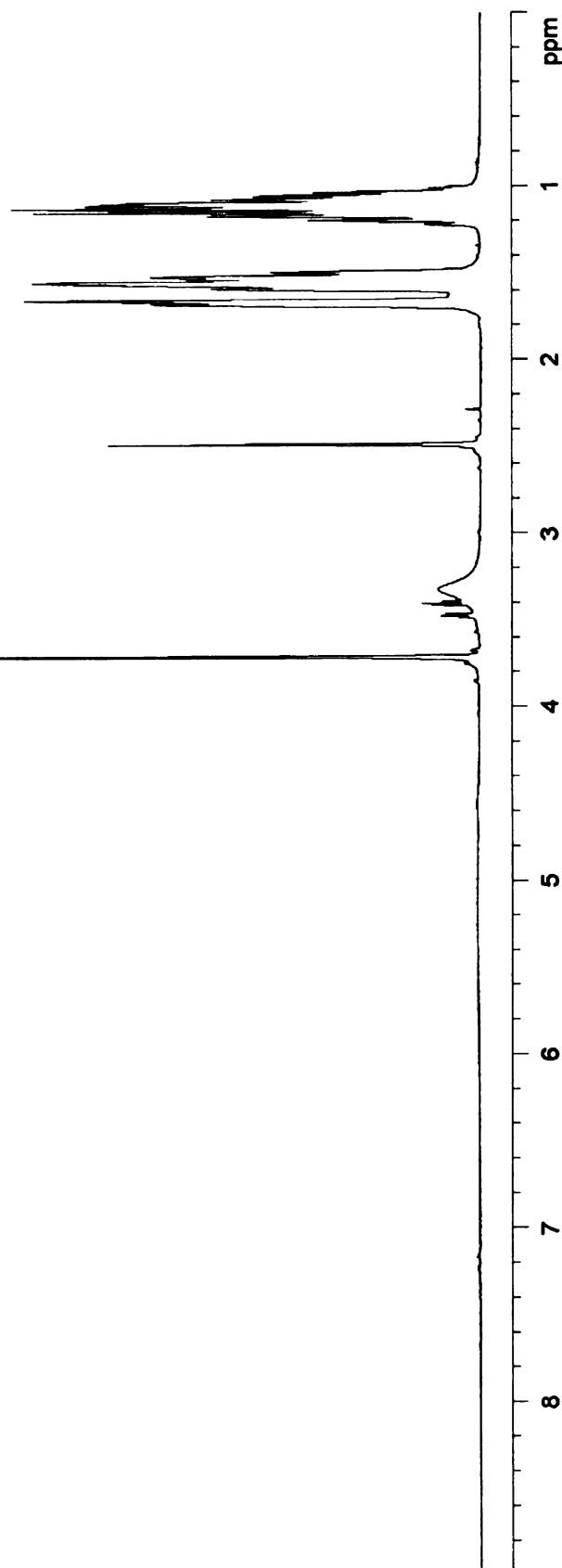
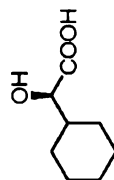
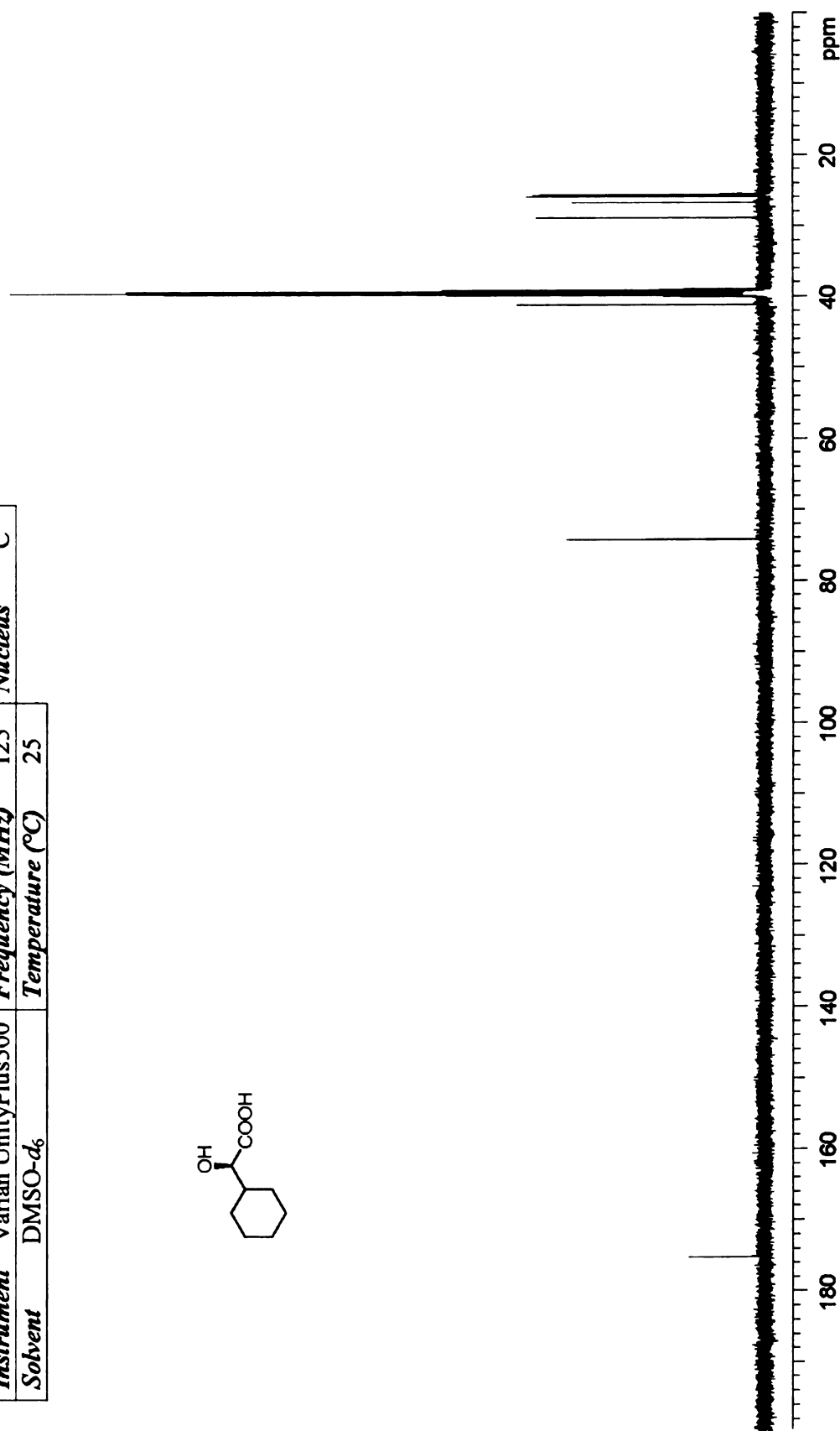
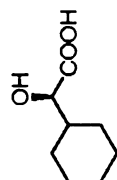


Figure A- 4. <sup>1</sup>H NMR spectrum of (R)-(-)-2-cyclohexyl-2-hydroxyacetic acid



|                   |   |                         |                 |
|-------------------|---|-------------------------|-----------------|
| <b>Sample</b>     | <i>(R)</i> -2-cyclohexyl-2-hydroxyacetic acid |                         |                 |
| <b>Instrument</b> | Varian UnityPlus500                           | <b>Frequency (MHz)</b>  | 125             |
| <b>Solvent</b>    | DMSO- <i>d</i> <sub>6</sub>                   | <b>Temperature (°C)</b> | 25              |
|                   |   | <b>Nucleus</b>          | <sup>13</sup> C |



**Figure A- 5.** <sup>13</sup>C NMR spectrum of *(R)*-(-)-2-cyclohexyl-2-hydroxyacetic acid

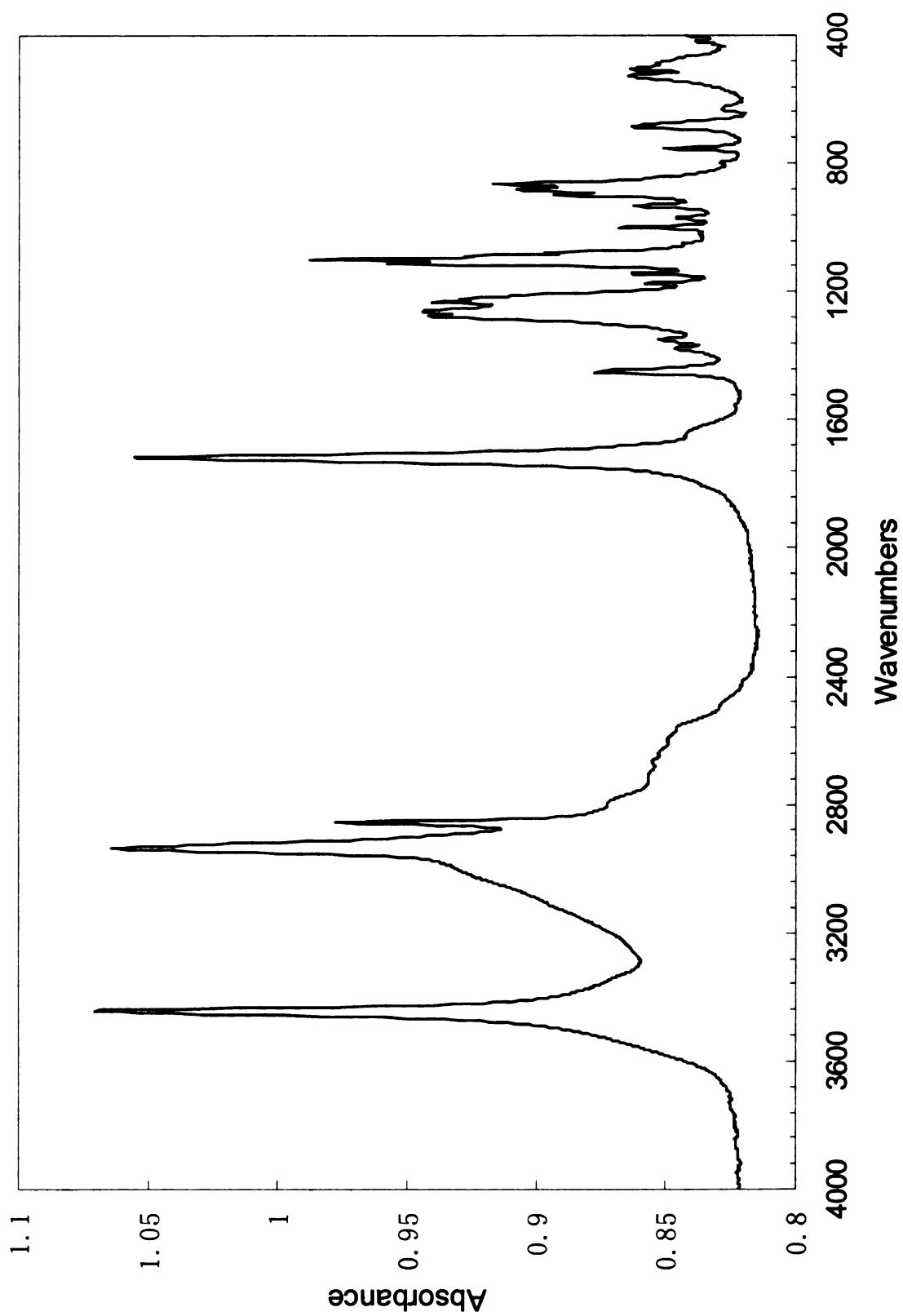


**Figure A- 6.** FT-IR spectrum of (R)-(-)-2-cyclohexyl-2-hydroxyacetic acid

|                   |  |                         |     |                               |
|-------------------|--|-------------------------|-----|-------------------------------|
| <b>Sample</b>     | <i>rac</i> -3,6-dicyclohexyl-1,4-dioxane-2,5-dione |                         |     |                               |
| <b>Instrument</b> | Varian UnityPlus500                                | <b>Frequency (MHz)</b>  | 500 | <b>Nucleus</b> <sup>1</sup> H |
| <b>Solvent</b>    | CDCl <sub>3</sub>                                  | <b>Temperature (°C)</b> | 25  |                               |

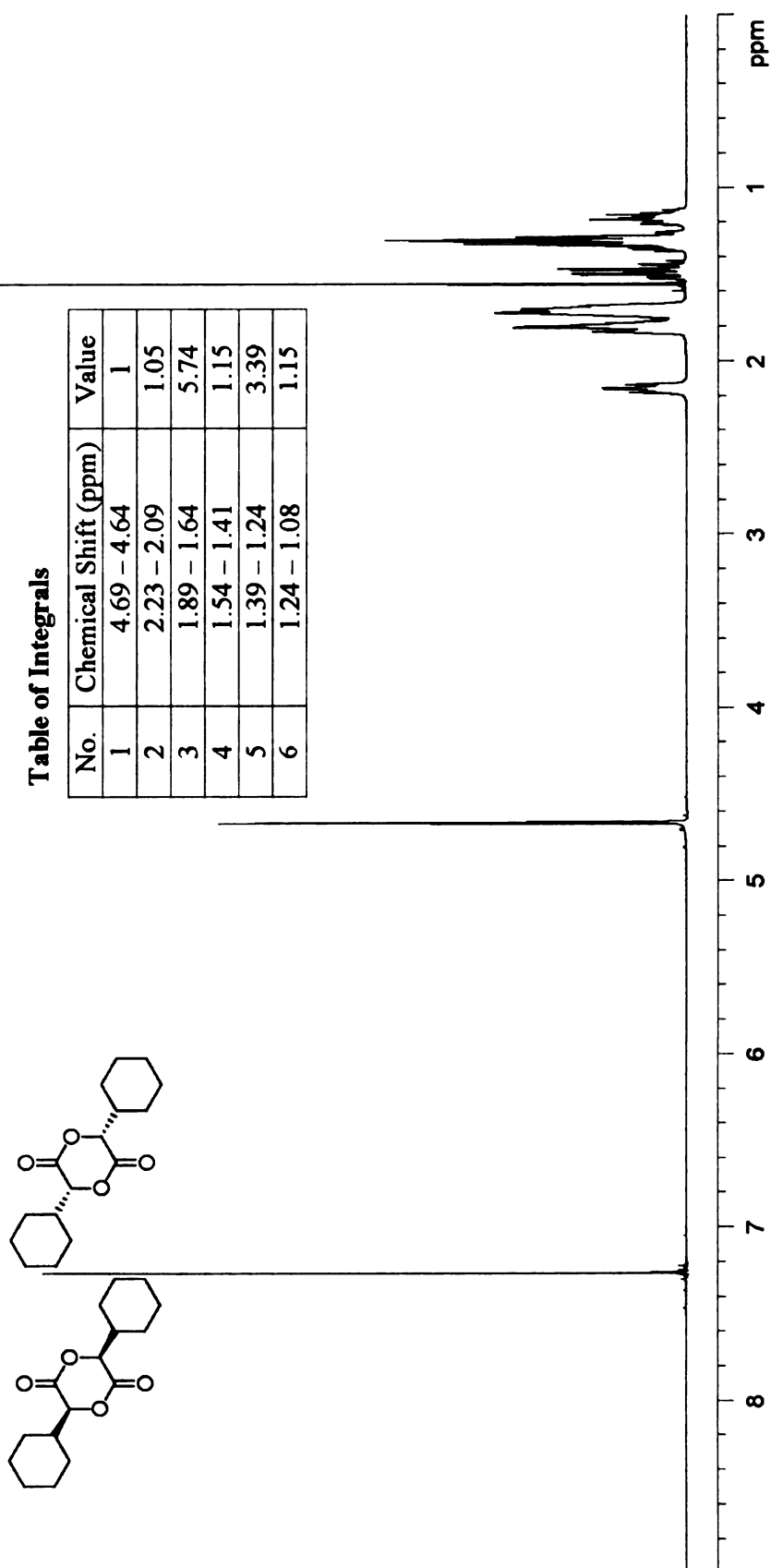


**Figure A-7.** <sup>1</sup>H NMR spectrum of *rac*-dicyclohexylglycolide

|                   |  |                         |                 |
|-------------------|--|-------------------------|-----------------|
| <b>Sample</b>     | <i>rac</i> -3,6-dicyclohexyl-1,4-dioxane-2,5-dione |                         |                 |
| <b>Instrument</b> | Varian UnityPlus500                                | <b>Frequency (MHz)</b>  | 125             |
| <b>Solvent</b>    | CDCl <sub>3</sub>                                  | <b>Temperature (°C)</b> | 25              |
|                   |  | <b>Nucleus</b>          | <sup>13</sup> C |

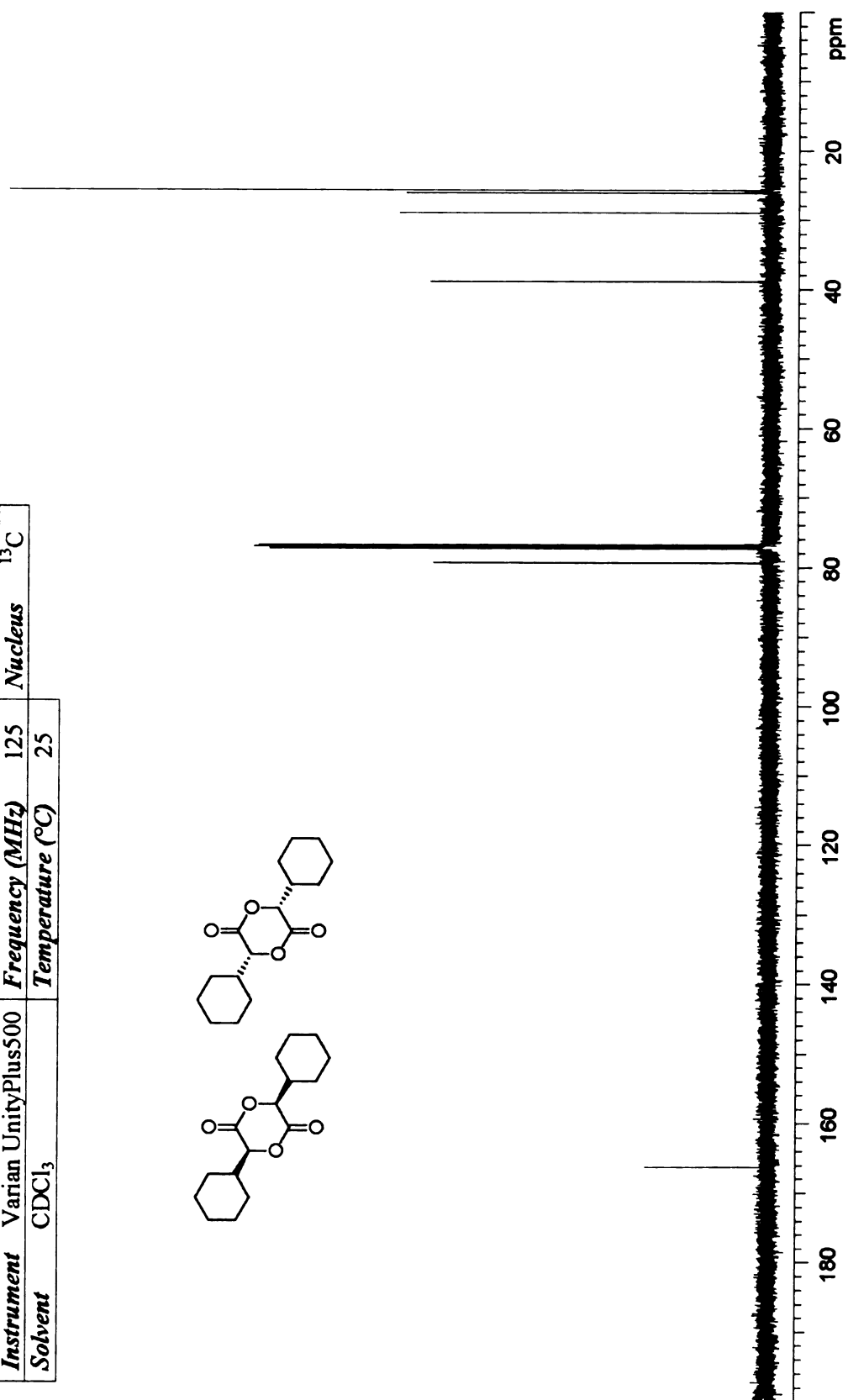
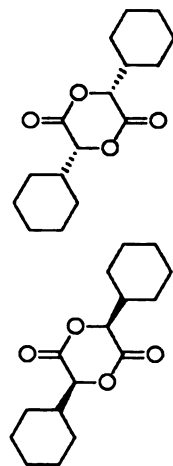


**Figure A- 8.** <sup>13</sup>C NMR spectrum of *rac*-dicyclohexylglycolide

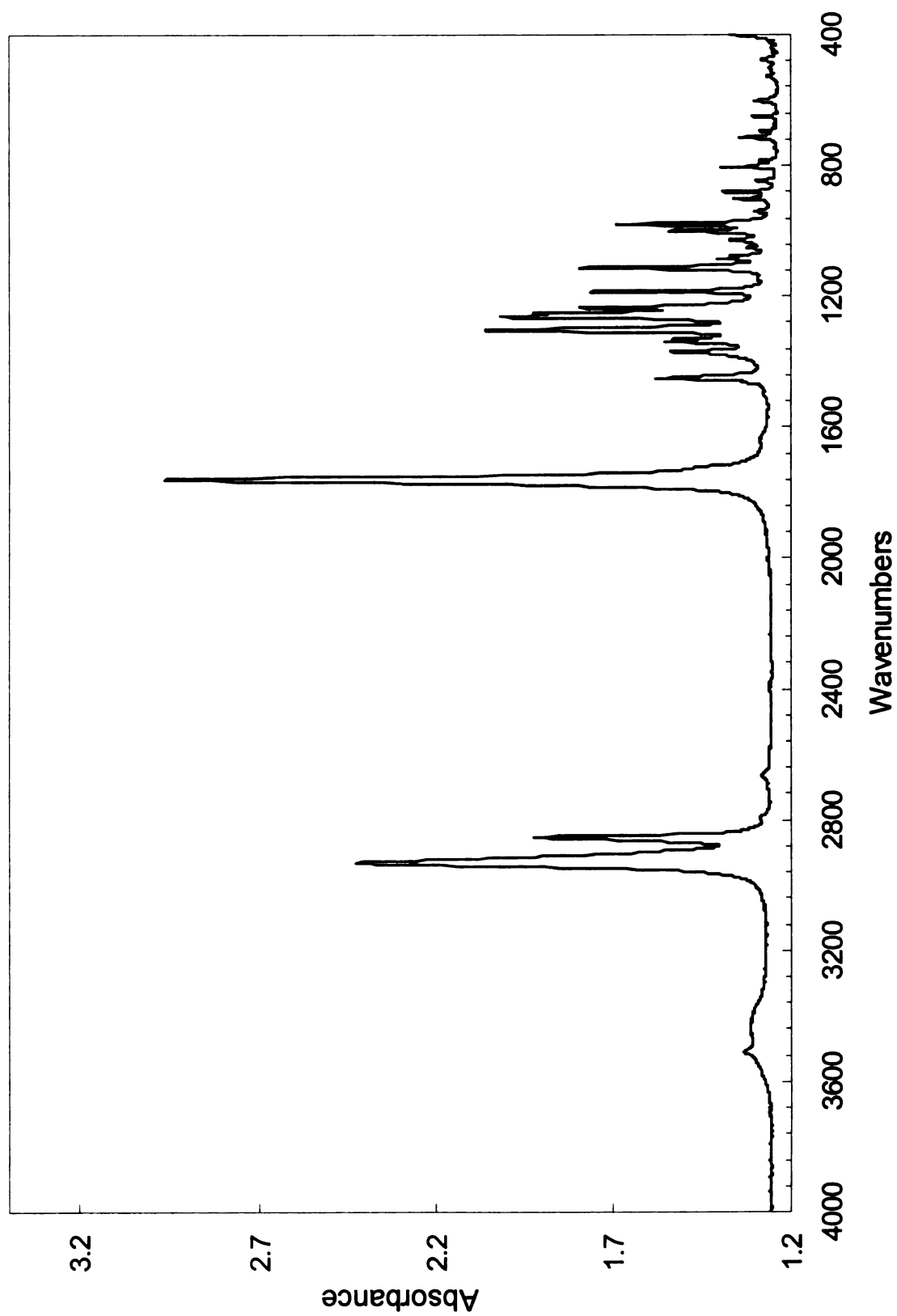


**Figure A-9.** FT-IR spectrum of *rac*-dicyclohexylglycolide

|                   |   |                         |     |                               |
|-------------------|---|-------------------------|-----|-------------------------------|
| <b>Sample</b>     | <i>meso</i> -3,6-dicyclohexyl-1,4-dioxane-2,5-dione |                         |     |                               |
| <b>Instrument</b> | Varian UnityPlus500                                 | <b>Frequency (MHz)</b>  | 500 | <b>Nucleus</b> <sup>1</sup> H |
| <b>Solvent</b>    | CDCl <sub>3</sub>                                   | <b>Temperature (°C)</b> | 25  |                               |

**Table of Integrals**

| No. | Chemical Shift (ppm) | Value |
|-----|----------------------|-------|
| 1   | 4.74 – 4.70          | 1     |
| 2   | 2.14 – 2.01          | 1.04  |
| 3   | 1.87 – 1.64          | 5.44  |
| 4   | 1.47 – 1.09          | 5.45  |

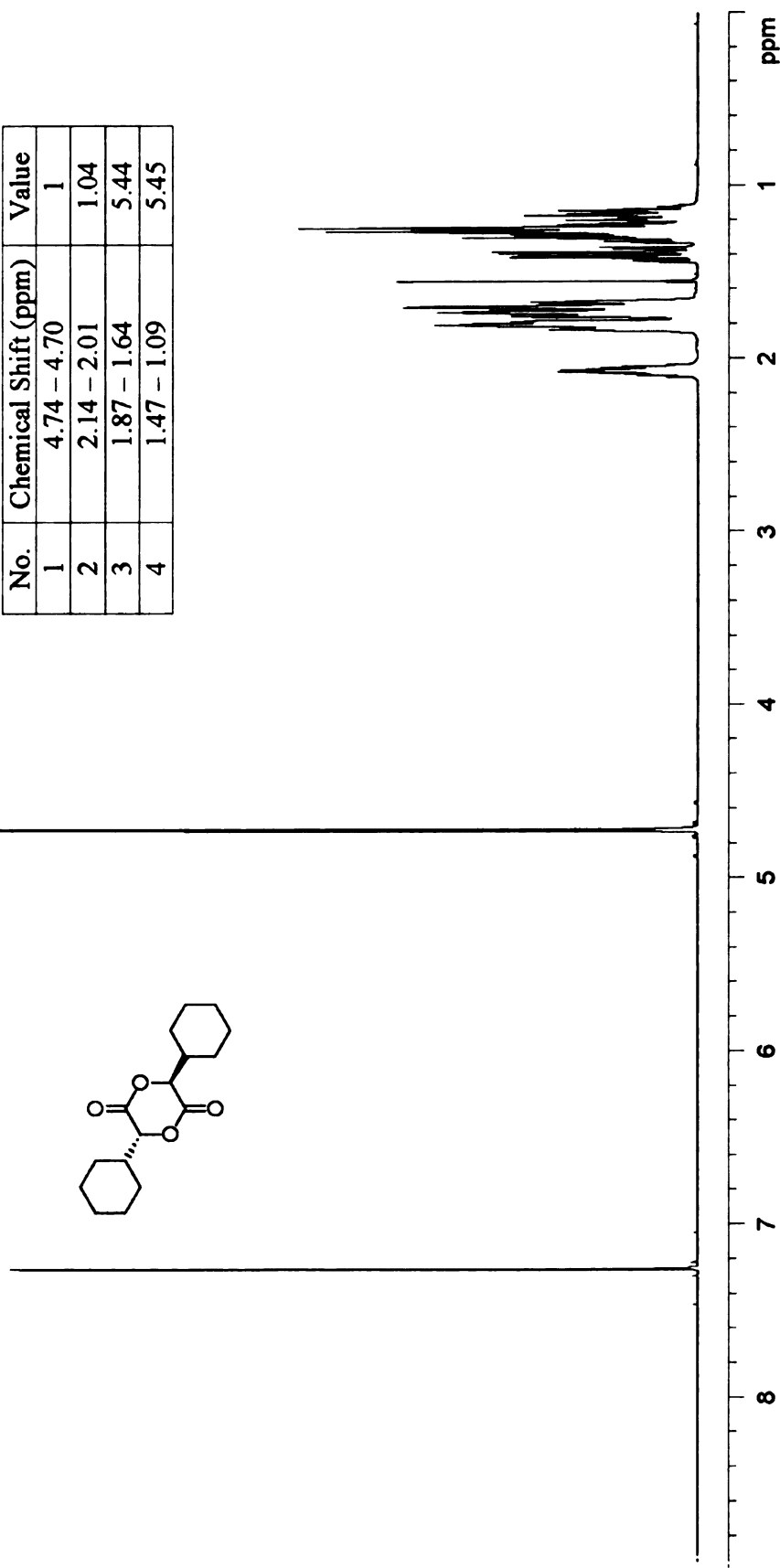


**Figure A-10.** <sup>1</sup>H NMR spectrum of *meso*-dicyclohexylglycolide

|                   |   |                         |                     |
|-------------------|---|-------------------------|---------------------|
| <b>Sample</b>     | <i>meso</i> -3,6-dicyclohexyl-1,4-dioxane-2,5-dione |                         |                     |
| <b>Instrument</b> | Varian UnityPlus500                                 | <b>Frequency (MHz)</b>  | 125 <sup>13</sup> C |
| <b>Solvent</b>    | CDCl <sub>3</sub>                                   | <b>Temperature (°C)</b> | 25                  |

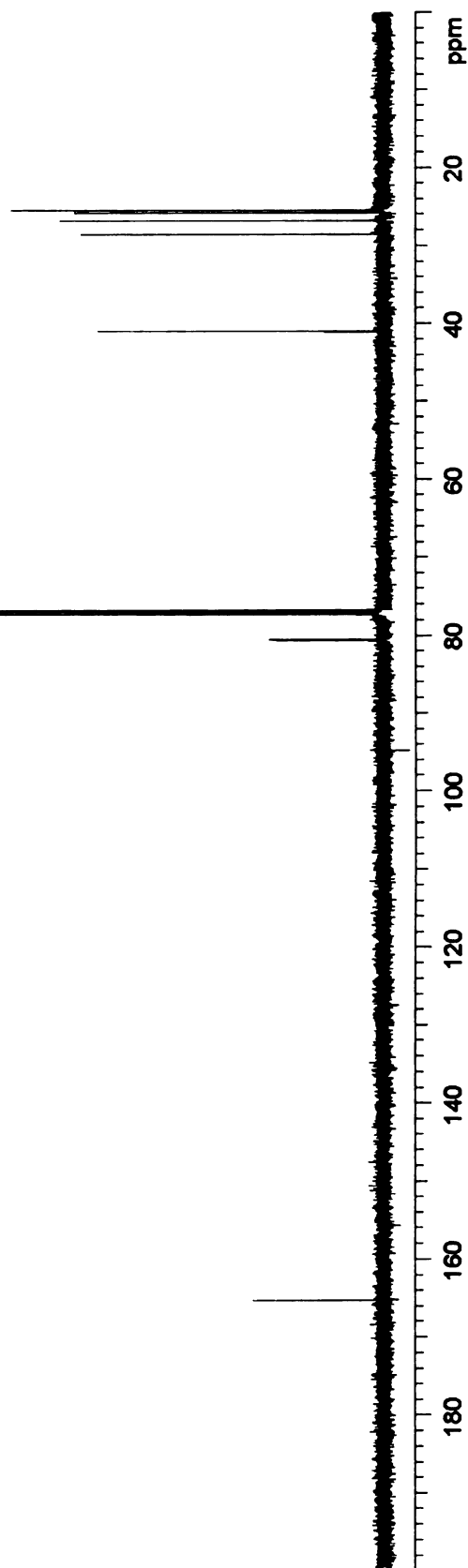
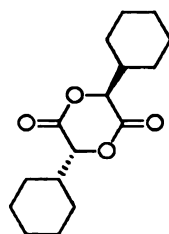


**Figure A- 11.** <sup>13</sup>C NMR spectrum of *meso*-dicyclohexylglycolide

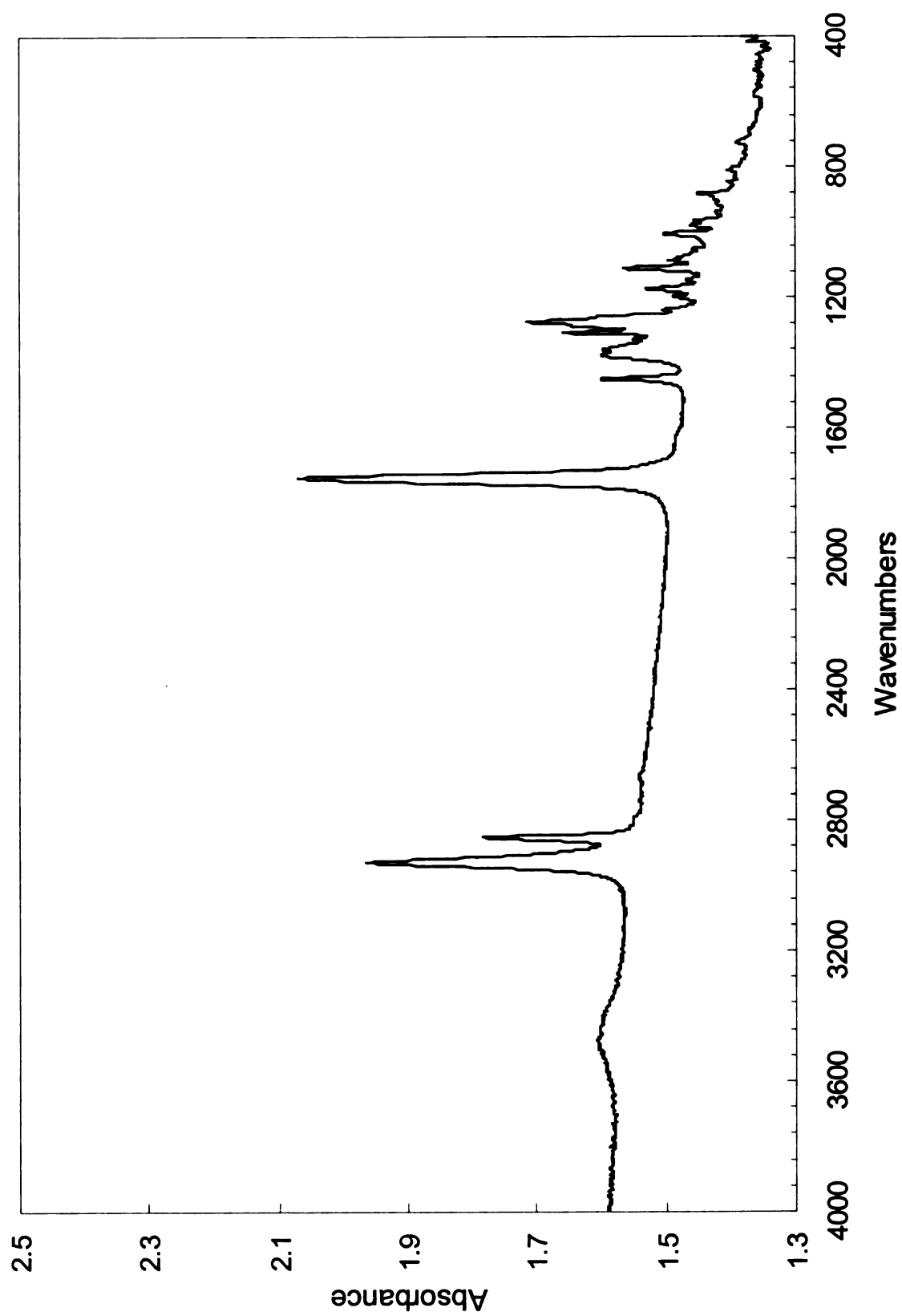


**Figure A- 12.** FT-IR spectrum of *meso*-dicyclohexylglycolide



|                   |  |                         |     |                               |
|-------------------|--|-------------------------|-----|-------------------------------|
| <b>Sample</b>     | (3 <i>R</i> ,6 <i>R</i> )-(+)-3,6-dicyclohexyl-1,4-dioxane-2,5-dione |                         |     |                               |
| <b>Instrument</b> | Varian UnityPlus500  | <b>Frequency (MHz)</b>  | 500 | <b>Nucleus</b> <sup>1</sup> H |
| <b>Solvent</b>    | CDCl <sub>3</sub>  | <b>Temperature (°C)</b> | 25  |                               |

**Table of Integrals**

| No. | Chemical Shift (ppm) | Value |
|-----|----------------------|-------|
| 1   | 4.70 – 4.64          | 1     |
| 2   | 2.21 – 2.09          | 1.00  |
| 3   | 1.88 – 1.63          | 5.37  |
| 4   | 1.54 – 1.41          | 1.07  |
| 5   | 1.39 – 1.09          | 4.29  |

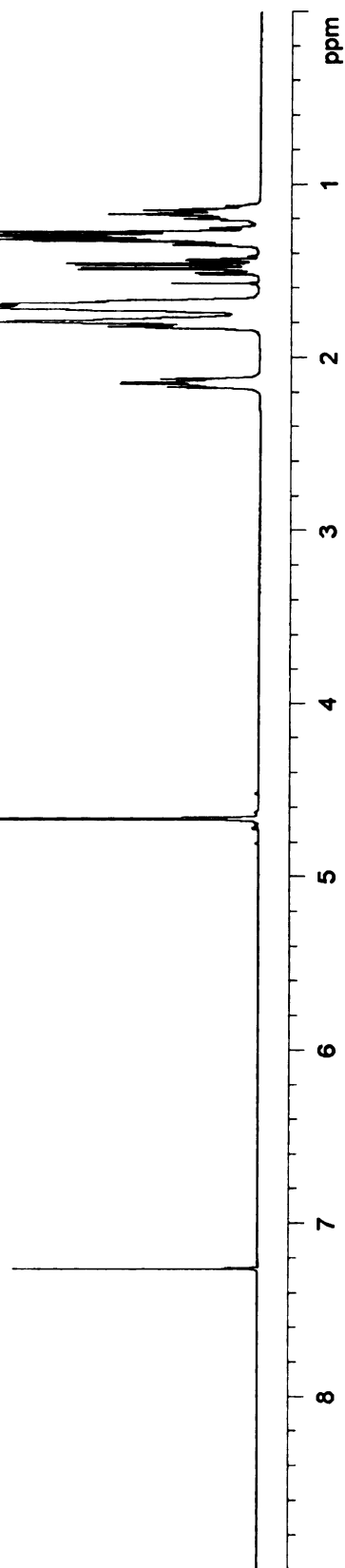
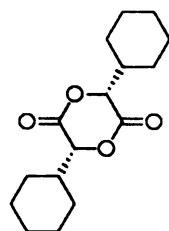


**Figure A-13.** <sup>1</sup>H NMR spectrum of *R,R*-dicyclohexylglycolide

|                   |  |                         |     |                                |
|-------------------|--|-------------------------|-----|--------------------------------|
| <b>Sample</b>     | (3 <i>R</i> ,6 <i>R</i> )-(+)-3,6-dicyclohexyl-1,4-dioxane-2,5-dione |                         |     |                                |
| <b>Instrument</b> | Varian UnityPlus500  | <b>Frequency (MHz)</b>  | 125 | <b>Nucleus</b> <sup>13</sup> C |
| <b>Solvent</b>    | CDCl <sub>3</sub>  | <b>Temperature (°C)</b> | 25  |                                |

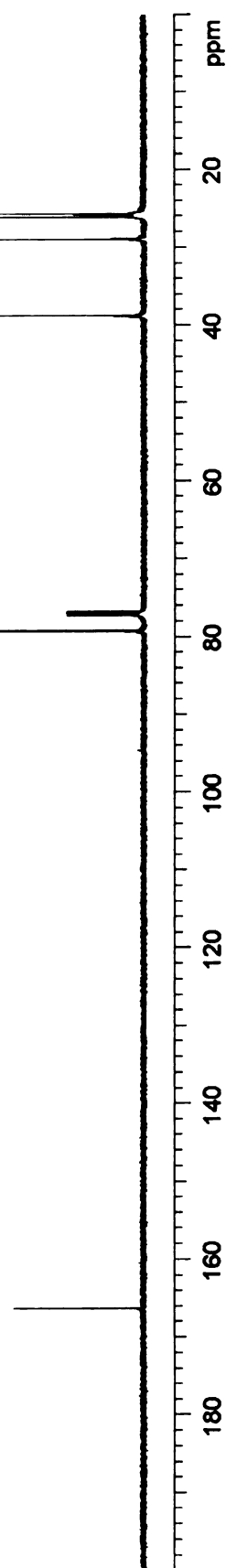
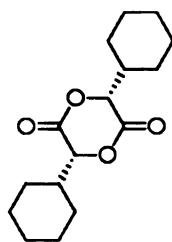


**Figure A- 14.** <sup>13</sup>C NMR spectrum of *R,R*-dicyclohexylglycolide

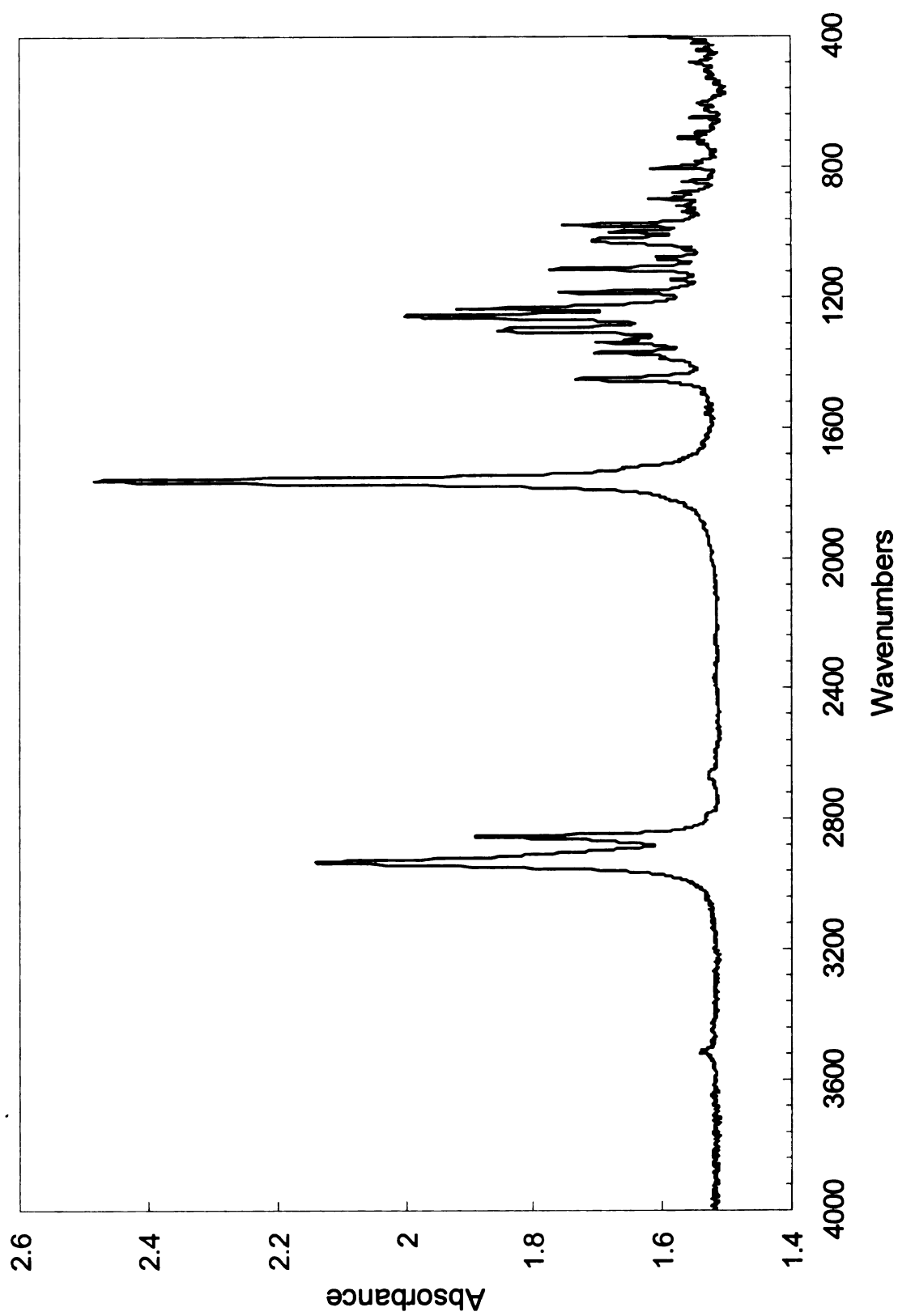


**Figure A- 15.** FT-IR spectrum of *R,R*-dicyclohexylglycolide

|                   |   |                         |     |                               |
|-------------------|---|-------------------------|-----|-------------------------------|
| <b>Sample</b>     | <i>rac</i> -3,6-diisopropyl-1,4-dioxane-2,5-dione |                         |     |                               |
| <b>Instrument</b> | Varian UnityPlus500                               | <b>Frequency (MHz)</b>  | 500 | <b>Nucleus</b> <sup>1</sup> H |
| <b>Solvent</b>    | CDCl <sub>3</sub>                                 | <b>Temperature (°C)</b> | 25  |                               |

**Table of Integrals**

| No. | Chemical Shift (ppm) | Value |
|-----|----------------------|-------|
| 1   | 4.72 – 4.69          | 1     |
| 2   | 2.55 – 2.47          | 1.06  |
| 3   | 1.19 – 1.14          | 3.55  |
| 4   | 1.09 – 1.04          | 3.51  |

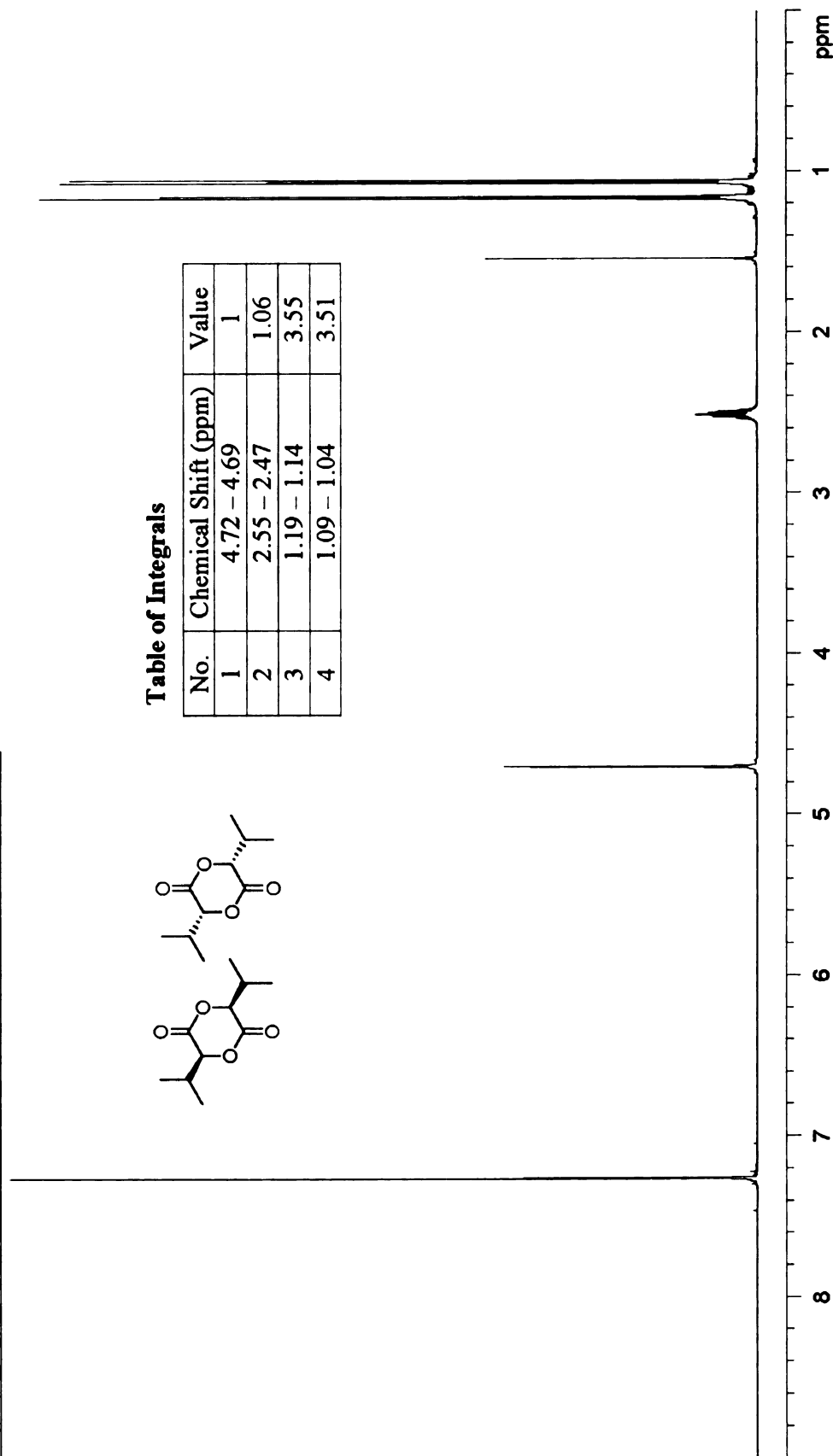
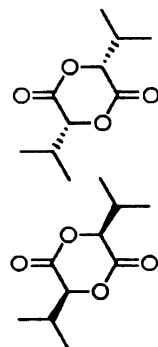


**Figure A- 16.** <sup>1</sup>H NMR spectrum of *rac*-diisopropylglycolide

|                   |   |                         |                 |
|-------------------|---|-------------------------|-----------------|
| <b>Sample</b>     | <i>rac</i> -3,6-diisopropyl-1,4-dioxane-2,5-dione |                         |                 |
| <b>Instrument</b> | Varian UnityPlus500                               | <b>Frequency (MHz)</b>  | 125             |
| <b>Solvent</b>    | CDCl <sub>3</sub>                                 | <b>Temperature (°C)</b> | 25              |
|                   |   | <b>Nucleus</b>          | <sup>13</sup> C |

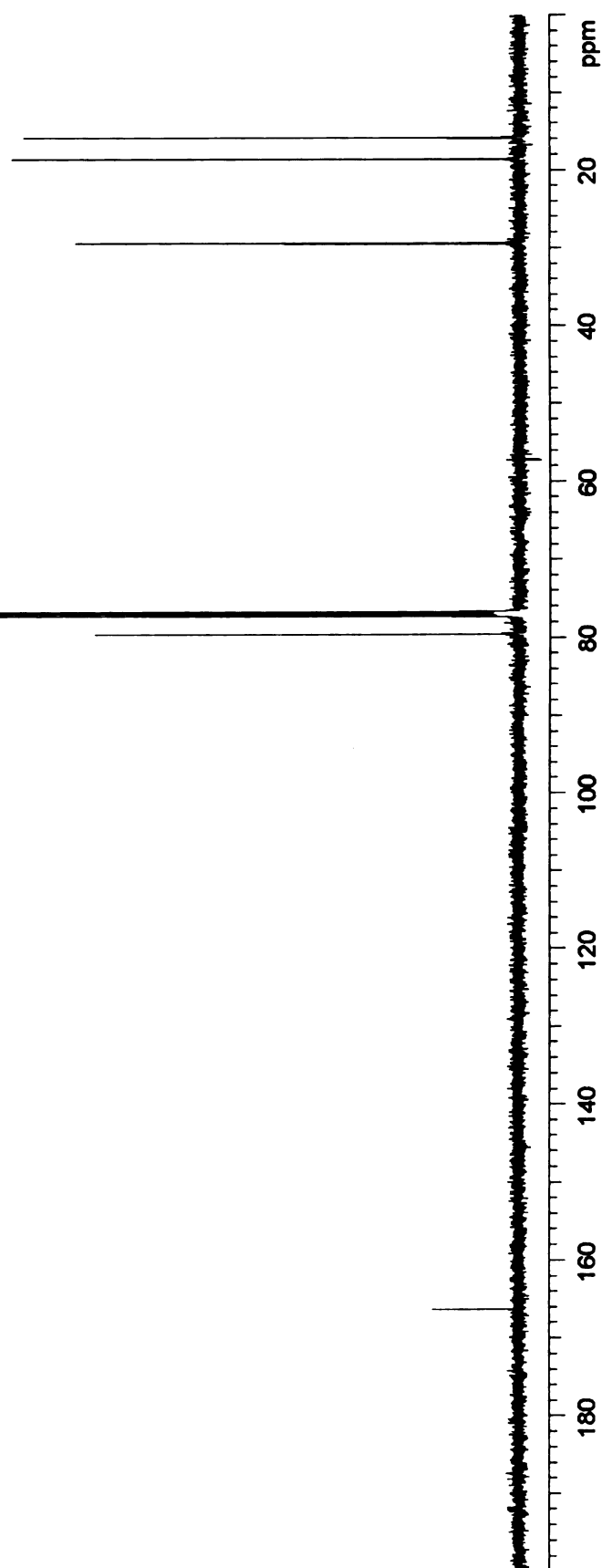
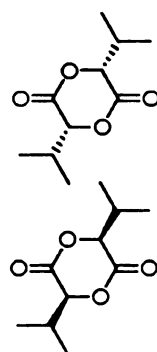


**Figure A- 17.** <sup>13</sup>C NMR spectrum of *rac*-diisopropylglycolide

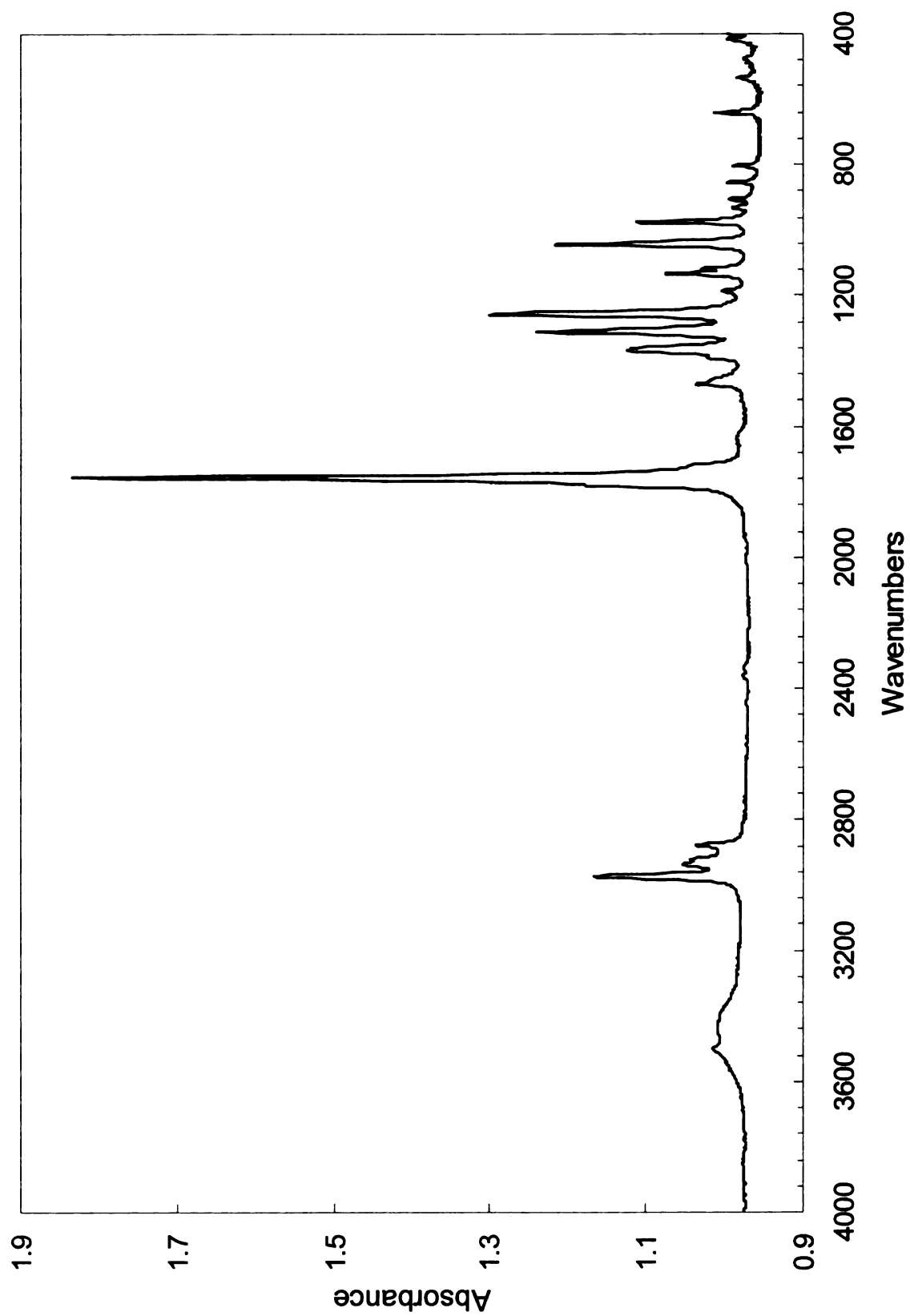


**Figure A- 18.** FT-IR spectrum of *rac*-diisopropylglycolide

|                   |   |                         |     |                               |
|-------------------|---|-------------------------|-----|-------------------------------|
| <b>Sample</b>     | <i>rac</i> -3-cyclohexyl-6-methyl-1,4-dioxane-2,5-dione |                         |     |                               |
| <b>Instrument</b> | Varian UnityPlus500                                     | <b>Frequency (MHz)</b>  | 500 | <b>Nucleus</b> <sup>1</sup> H |
| <b>Solvent</b>    | CDCl <sub>3</sub>                                       | <b>Temperature (°C)</b> | 25  |                               |

**Table of Integrals**

| No. | Chemical Shift (ppm) | Value |
|-----|----------------------|-------|
| 1   | 5.00 – 4.94          | 1     |
| 2   | 4.73 – 4.70          | 1.09  |
| 3   | 2.21 – 2.11          | 1.14  |
| 4   | 1.87 – 1.63          | 10.9  |
| 5   | 1.54 – 1.42          | 1.38  |
| 6   | 1.39 – 1.24          | 4.09  |
| 7   | 1.23 – 1.11          | 1.36  |

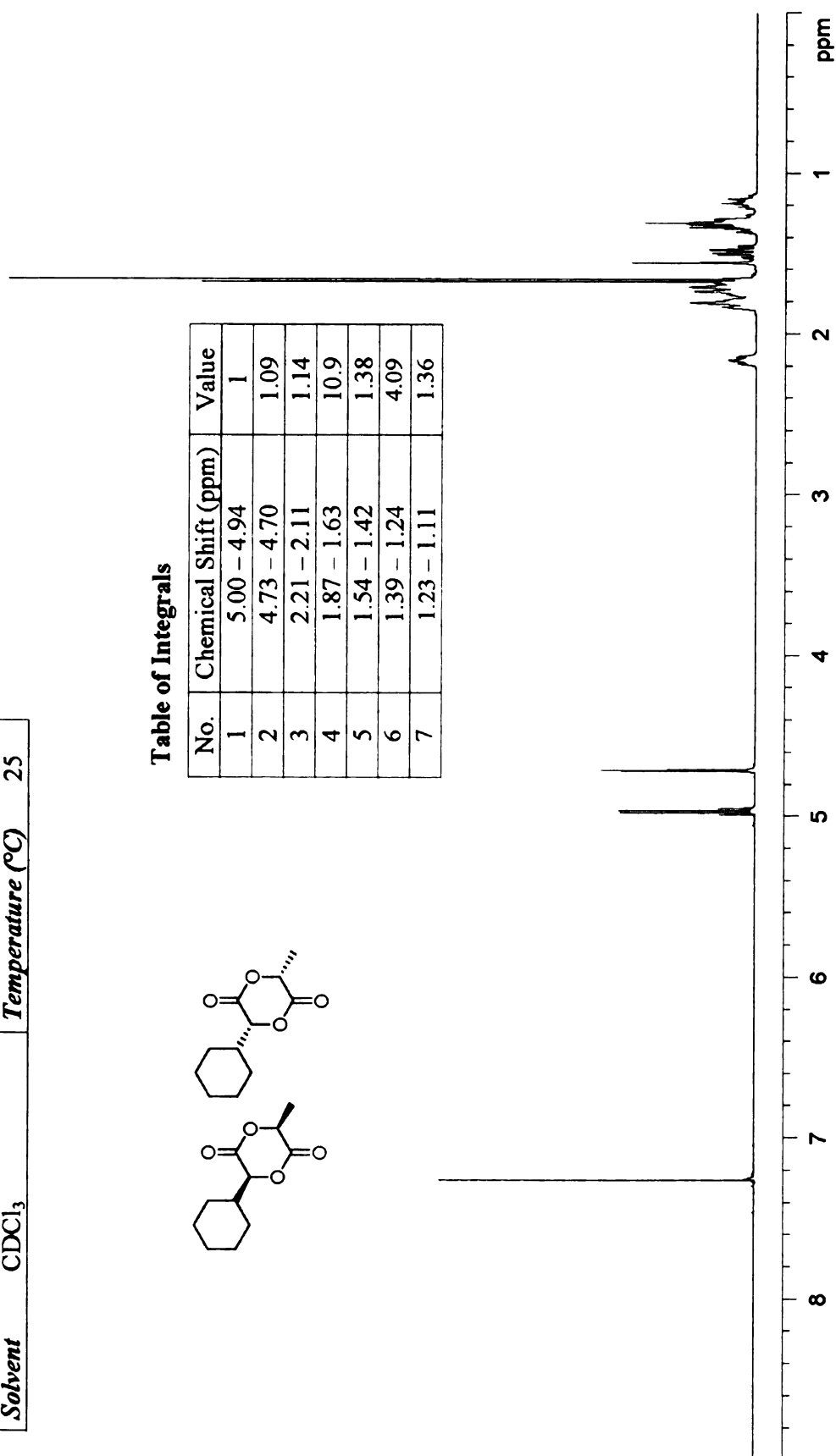
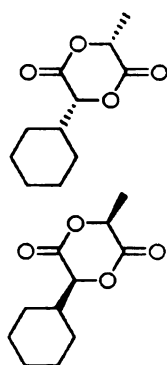


**Figure A- 19.** <sup>1</sup>H NMR spectrum of *rac*-methylcyclohexylglycolide

|                   |   |                         |     |                |                      |
|-------------------|---|-------------------------|-----|----------------|----------------------|
| <b>Sample</b>     | <i>rac</i> -3-cyclohexyl-6-methyl-1,4-dioxane-2,5-dione |                         |     |                |                      |
| <b>Instrument</b> | Varian UnityPlus500                                     | <b>Frequency (MHz)</b>  | 500 | <b>Nucleus</b> | <sup>1</sup> H (NOE) |
| <b>Solvent</b>    | CDCl <sub>3</sub>                                       | <b>Temperature (°C)</b> | 25  |                |                      |

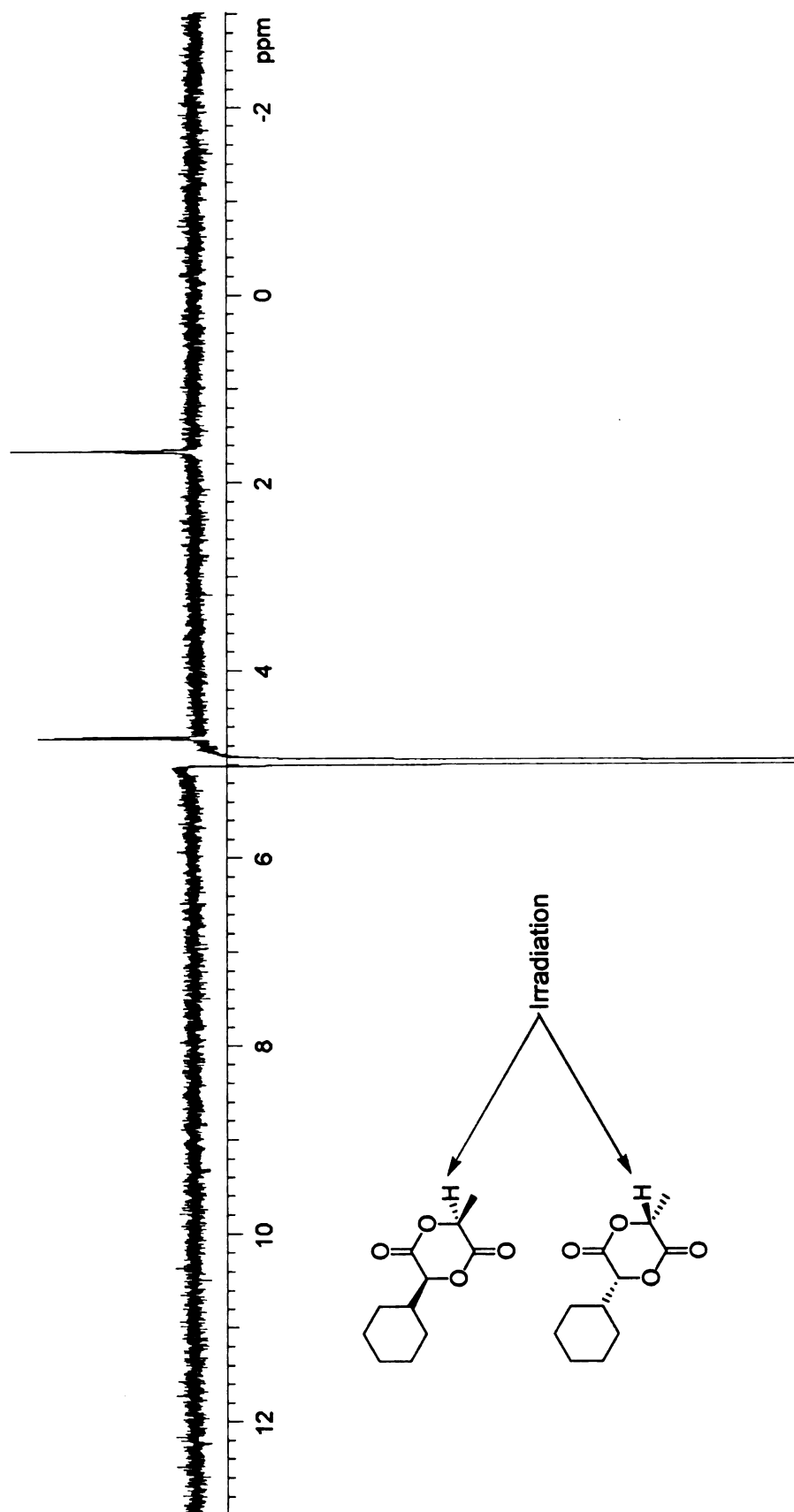


**Figure A-20.** NOE NMR spectrum of *rac*-methylcyclohexylglycolide



|                   |   |  |     |                                |
|-------------------|---|--|-----|--------------------------------|
| <b>Sample</b>     | <i>rac</i> -3-cyclohexyl-6-methyl-1,4-dioxane-2,5-dione |  |     |                                |
| <b>Instrument</b> | Varian UnityPlus500                                     | <b>Frequency (MHz)</b>                             | 125 | <b>Nucleus</b> $^{13}\text{C}$ |
| <b>Solvent</b>    | $\text{CDCl}_3$   | <b>Temperature (<math>^{\circ}\text{C}</math>)</b> | 25  |                                |

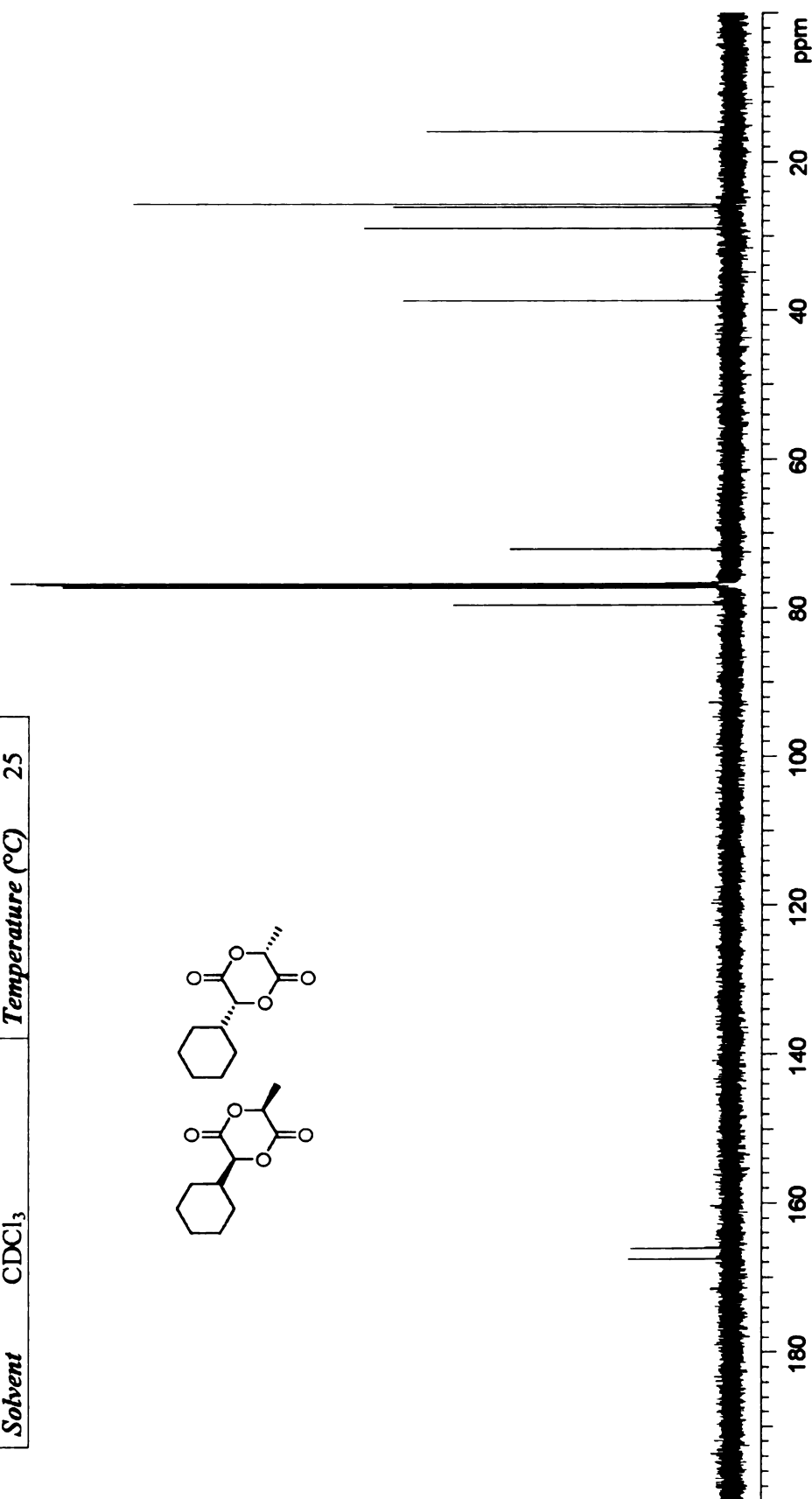
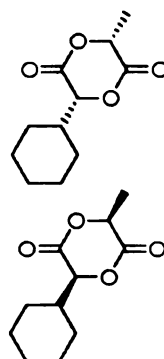


**Figure A-21.**  $^{13}\text{C}$  NMR spectrum of *rac*-methylcyclohexylglycolide

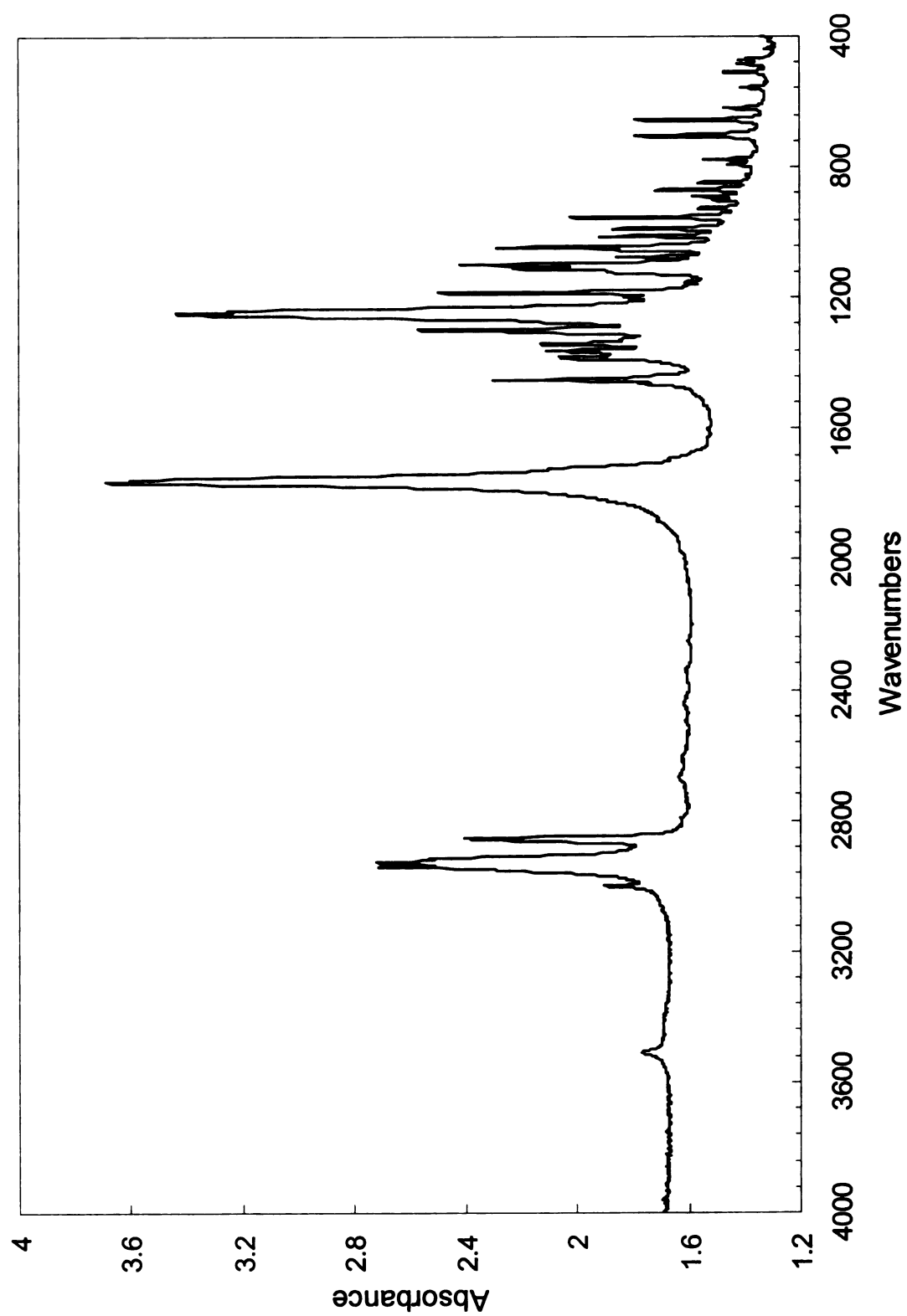


**Figure A- 22.** FT-IR spectrum of *rac*-methylcyclohexylglycolide

|                   |   |                         |                |
|-------------------|---|-------------------------|----------------|
| <b>Sample</b>     | <i>rac</i> -3-cyclohexyl-6- <i>n</i> -hexyl-1,4-dioxane-2,5-dione |                         |                |
| <b>Instrument</b> | Varian UnityPlus500   | <b>Frequency (MHz)</b>  | 500            |
| <b>Solvent</b>    | CDCl <sub>3</sub>   | <b>Temperature (°C)</b> | 25             |
|                   |   | <b>Nucleus</b>          | <sup>1</sup> H |

**Table of Integrals**

| No. | Chemical Shift (ppm) | Value |
|-----|----------------------|-------|
| 1   | 4.85 – 4.80          | 1     |
| 2   | 4.71 – 4.67          | 1.00  |
| 3   | 2.20 – 2.04          | 2.04  |
| 4   | 1.99 – 1.89          | 1.04  |
| 5   | 1.86 – 1.65          | 5.19  |
| 6   | 1.62 – 1.41          | 3.42  |
| 7   | 1.40 – 1.24          | 9.38  |
| 8   | 1.23 – 1.11          | 1.09  |
| 9   | 0.91 – 0.84          | 2.98  |

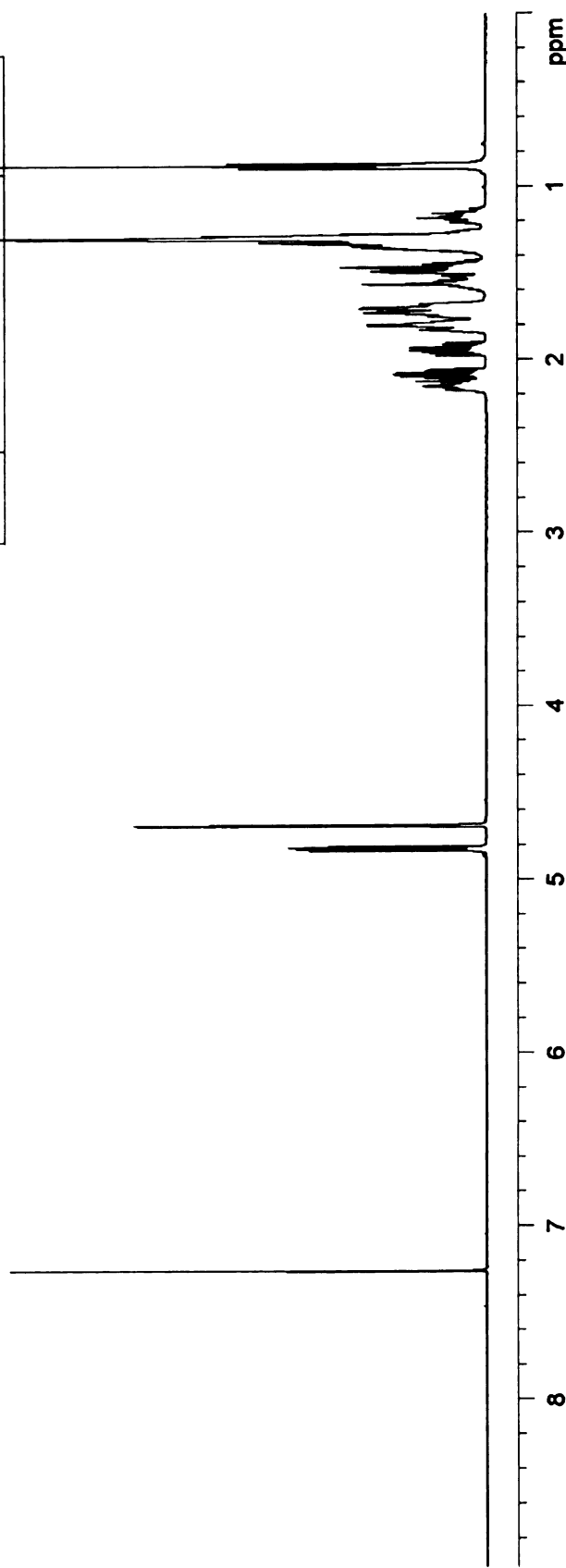
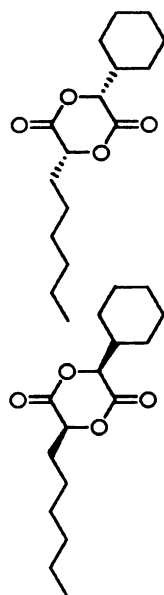


**Figure A-23.** <sup>1</sup>H NMR spectrum of *rac*-hexylcyclohexylglycolide

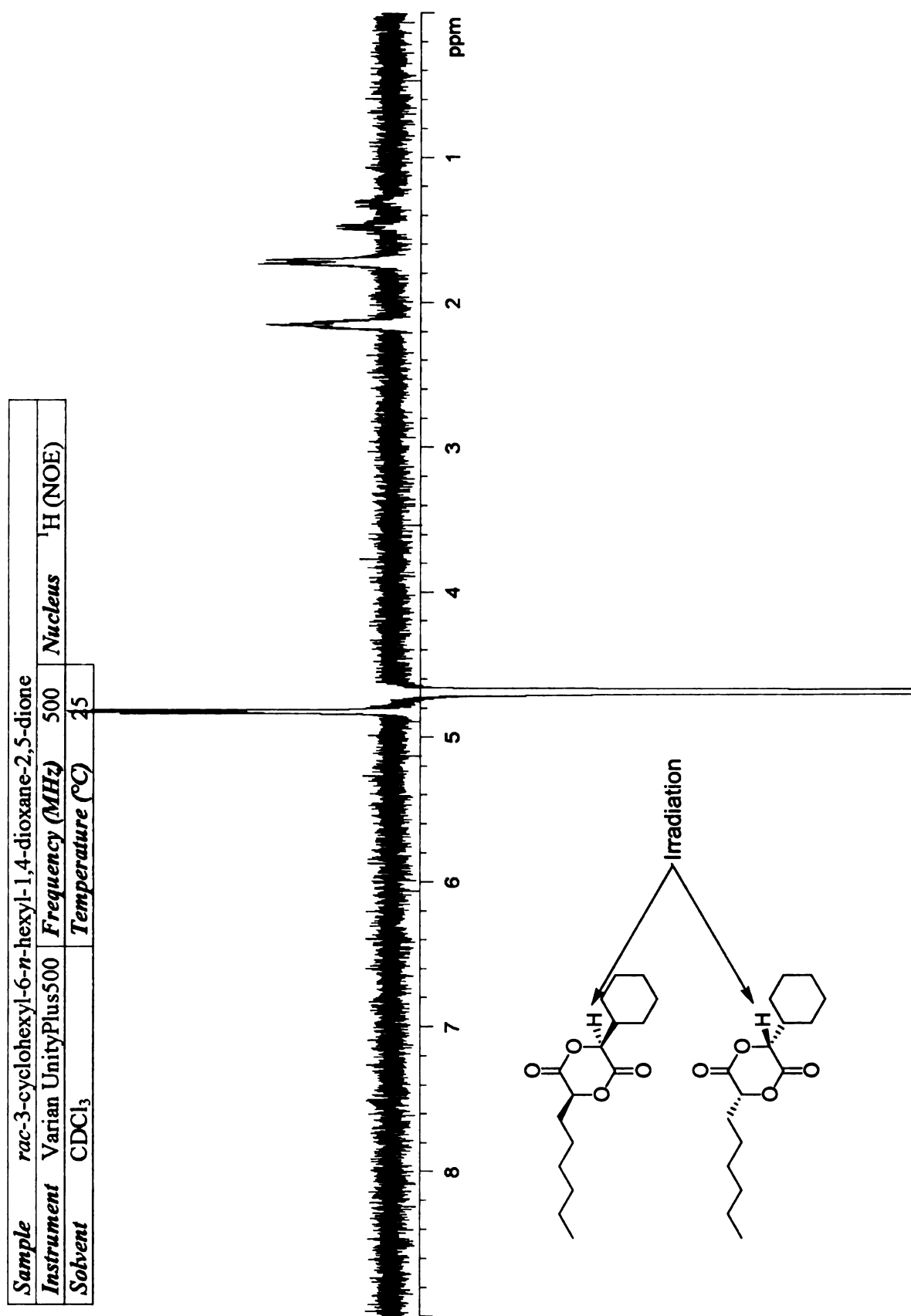


**Figure A-24.** NOE NMR spectrum of *rac*-hexylcyclohexylglycolide

|                   |   |                         |                 |
|-------------------|---|-------------------------|-----------------|
| <b>Sample</b>     | <i>rac</i> -3-cyclohexyl-6- <i>n</i> -hexyl-1,4-dioxane-2,5-dione |                         |                 |
| <b>Instrument</b> | Varian UnityPlus500   | <b>Frequency (MHz)</b>  | 125             |
| <b>Solvent</b>    | CDCl <sub>3</sub>   | <b>Temperature (°C)</b> | 25              |
|                   |   | <b>Nucleus</b>          | <sup>13</sup> C |

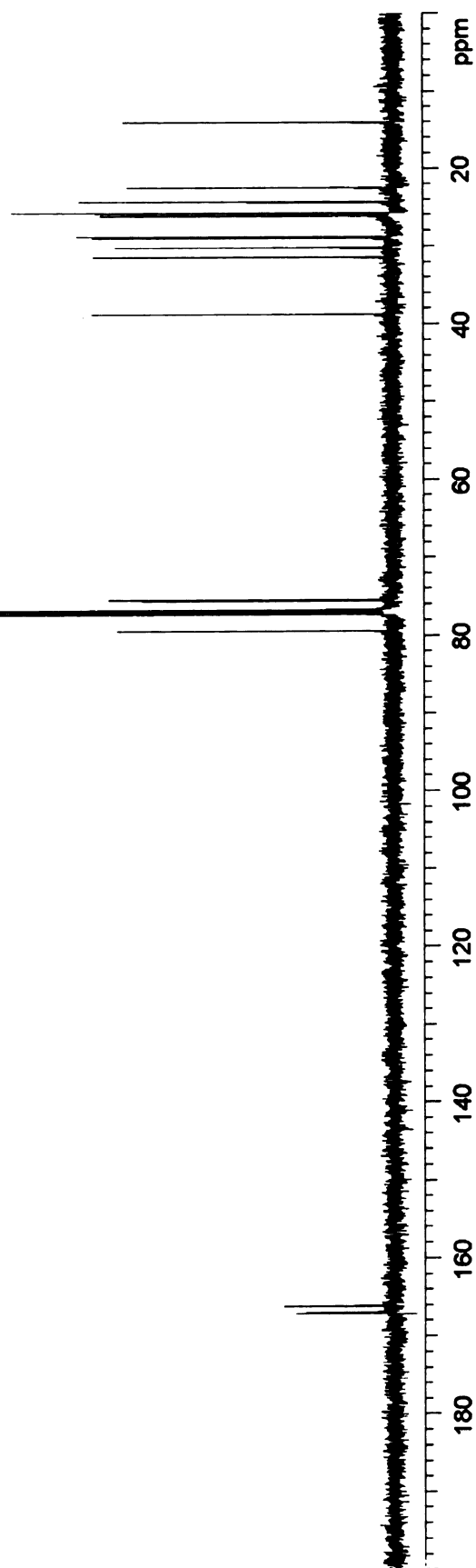
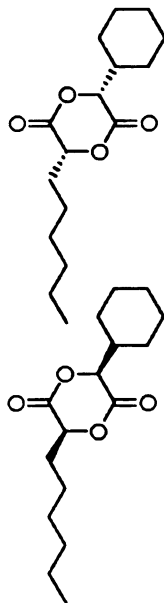


**Figure A-25.** <sup>13</sup>C NMR spectrum of *rac*-hexylcyclohexylglycolide

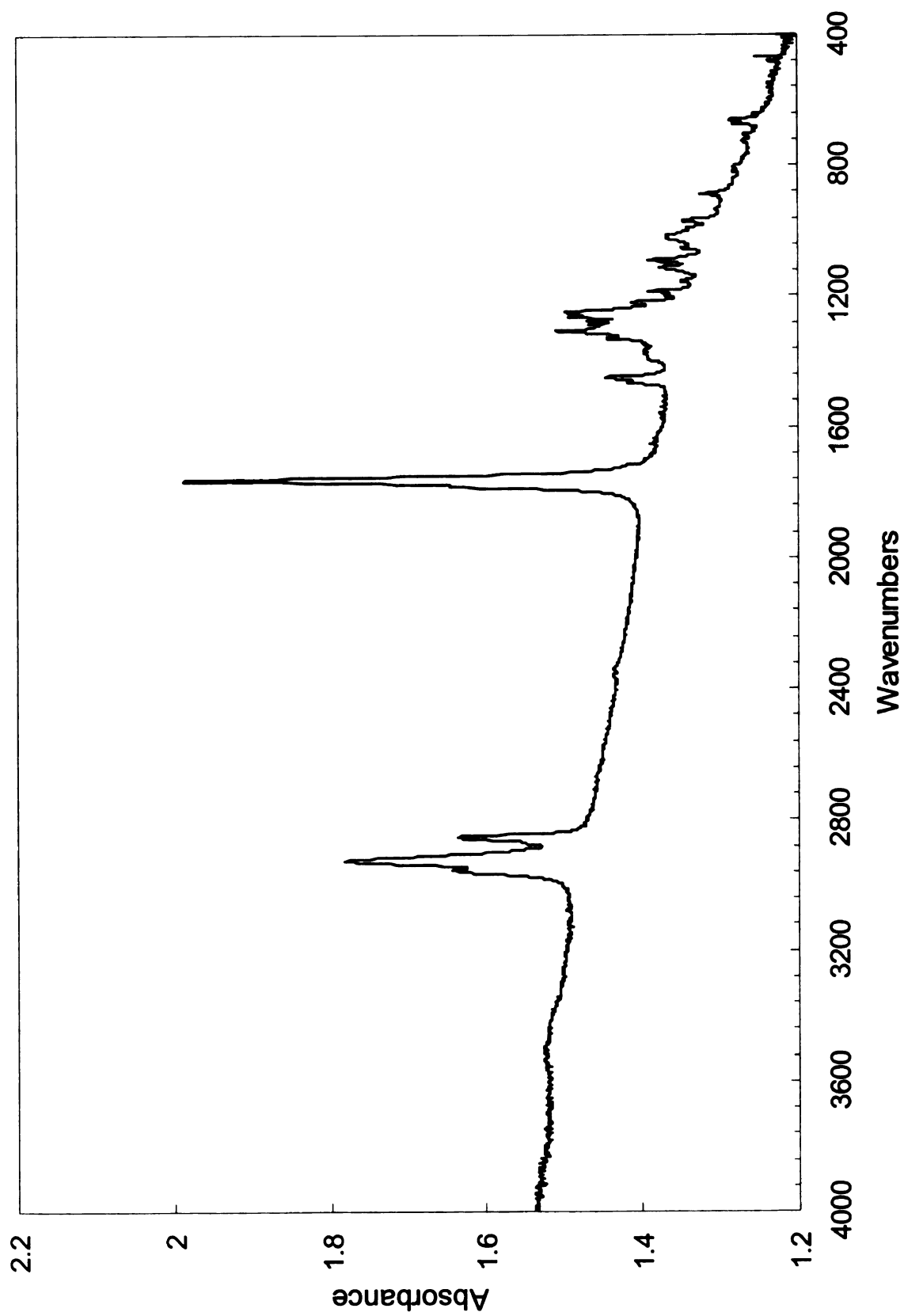


**Figure A- 26.** FT-IR spectrum of *rac*-hexylcyclohexylglycolide

|                   |                                      |                         |                |
|-------------------|--------------------------------------|-------------------------|----------------|
| <b>Sample</b>     | 1,4-benzodioxepin-3-methyl-2,5-dione |                         |                |
| <b>Instrument</b> | Varian UnityPlus500                  | <b>Frequency (MHz)</b>  | 500            |
| <b>Solvent</b>    | CDCl <sub>3</sub>                    | <b>Temperature (°C)</b> | 25             |
|                   |                                      | <b>Nucleus</b>          | <sup>1</sup> H |

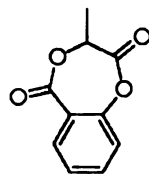


**Table of Integrals**

| No. | Chemical Shift (ppm) | Value |
|-----|----------------------|-------|
| 1   | 7.97 – 7.93          | 0.95  |
| 2   | 7.71 – 7.65          | 1.04  |
| 3   | 7.45 – 7.39          | 1.06  |
| 4   | 7.28 – 7.24          | 1.55  |
| 5   | 4.97 – 4.91          | 1     |
| 6   | 1.70 – 1.65          | 3.71  |

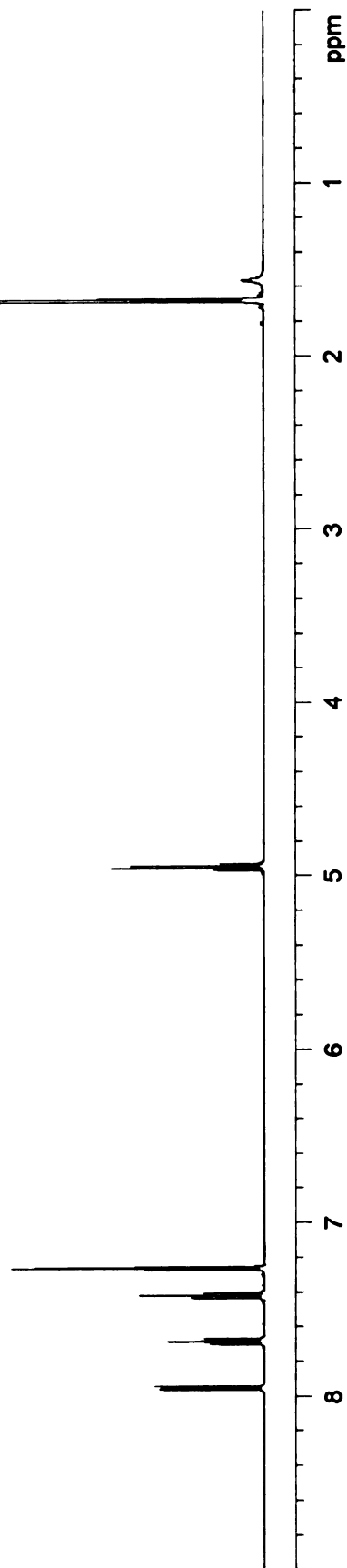


**Figure A-27.** <sup>1</sup>H NMR spectrum of 1,4-benzodioxepin-3-methyl-2,5-dione

|                   |                                      |                         |                 |
|-------------------|--------------------------------------|-------------------------|-----------------|
| <b>Sample</b>     | 1,4-benzodioxepin-3-methyl-2,5-dione |                         |                 |
| <b>Instrument</b> | Varian UnityPlus500                  | <b>Frequency (MHz)</b>  | 125             |
| <b>Solvent</b>    | CDCl <sub>3</sub>                    | <b>Temperature (°C)</b> | 25              |
|                   |                                      |                         | <b>Nucleus</b>  |
|                   |                                      |                         | <sup>13</sup> C |

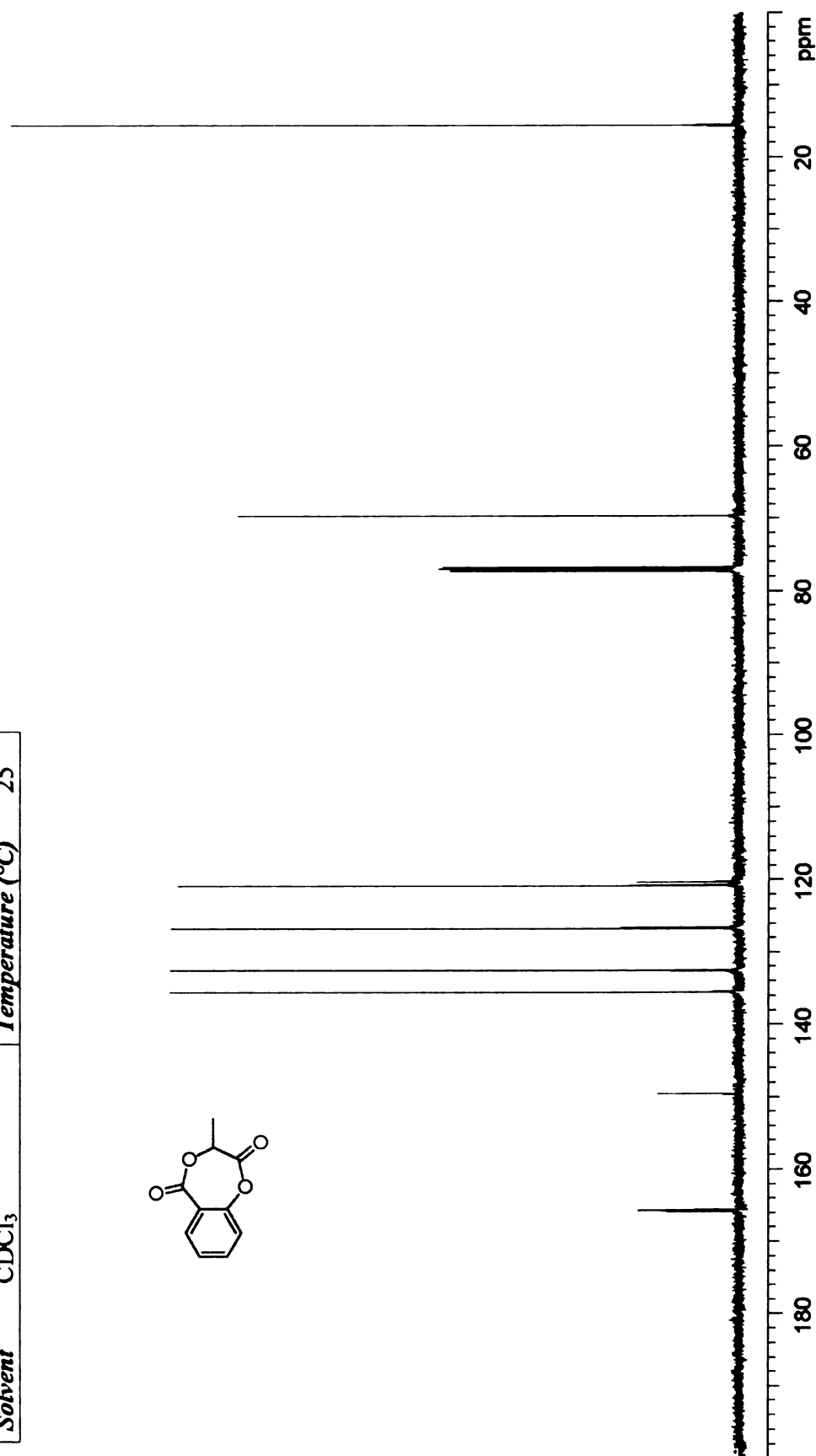
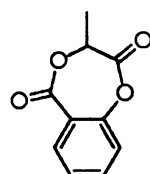


**Figure A-28.** <sup>13</sup>C NMR spectrum of 1,4-benzodioxepin-3-methyl-2,5-dione



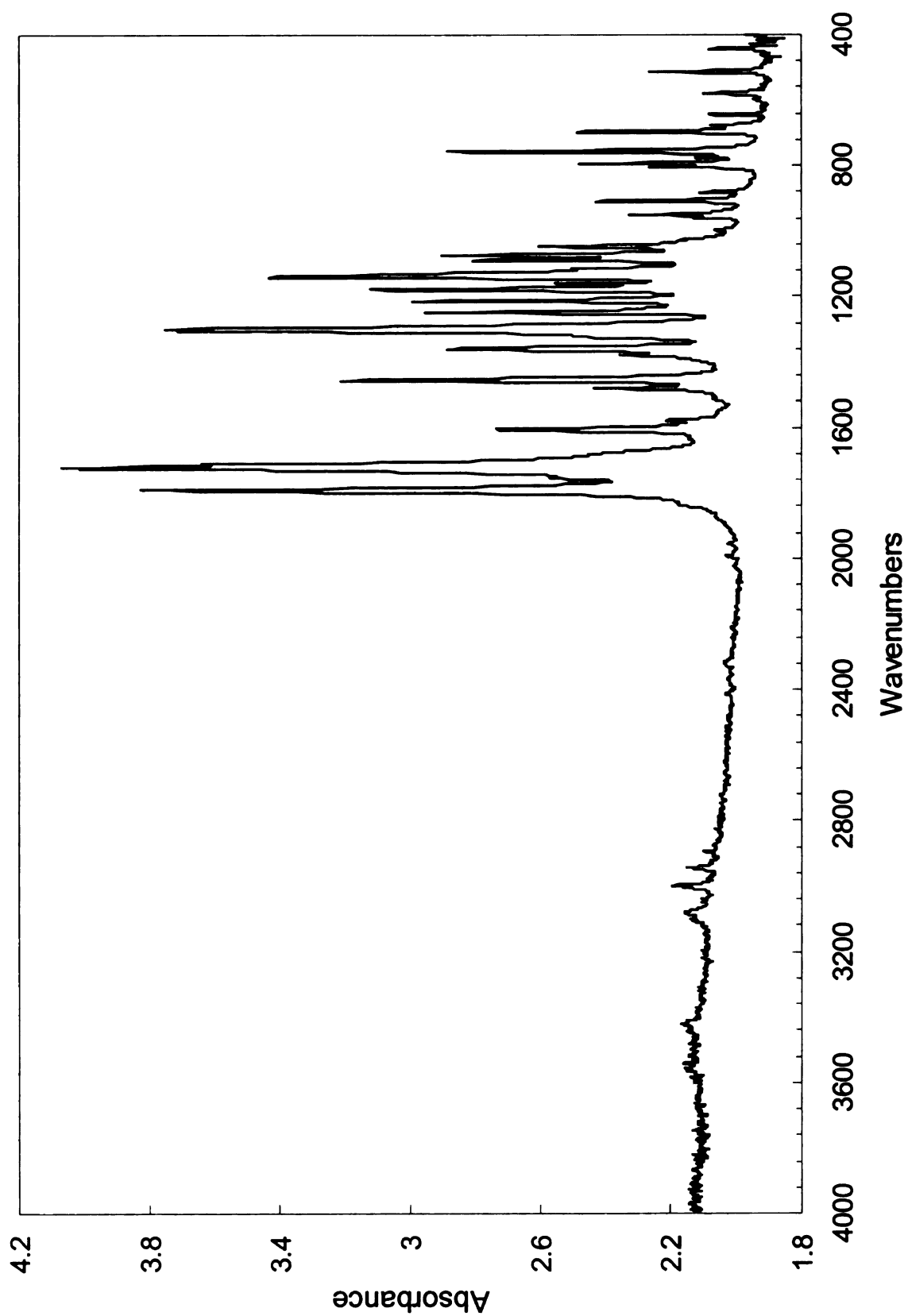


**Figure A- 29.** FT-IR spectrum of 1,4-benzodioxepin-3-methyl-2,5-dione

|                   |  |                         |     |                      |
|-------------------|--|-------------------------|-----|----------------------|
| <b>Sample</b>     | 1,4-benzodioxepin-3-cyclohexyl-2,5-dione |                         |     |                      |
| <b>Instrument</b> | Varian UnityPlus500                      | <b>Frequency (MHz)</b>  | 500 | <b><sup>1</sup>H</b> |
| <b>Solvent</b>    | CDCl <sub>3</sub>                        | <b>Temperature (°C)</b> | 25  |                      |

**Table of Integrals**

| No. | Chemical Shift (ppm) | Value |
|-----|----------------------|-------|
| 1   | 7.98 – 7.90          | 0.92  |
| 2   | 7.72 – 7.63          | 0.99  |
| 3   | 7.45 – 7.36          | 0.99  |
| 4   | 7.29 – 7.20          | 1.19  |
| 5   | 4.45 – 4.35          | 1     |
| 6   | 2.24 – 2.08          | 2.11  |
| 7   | 1.88 – 1.65          | 4.35  |
| 8   | 1.42 – 1.25          | 2.16  |
| 9   | 1.24 – 0.99          | 3.29  |

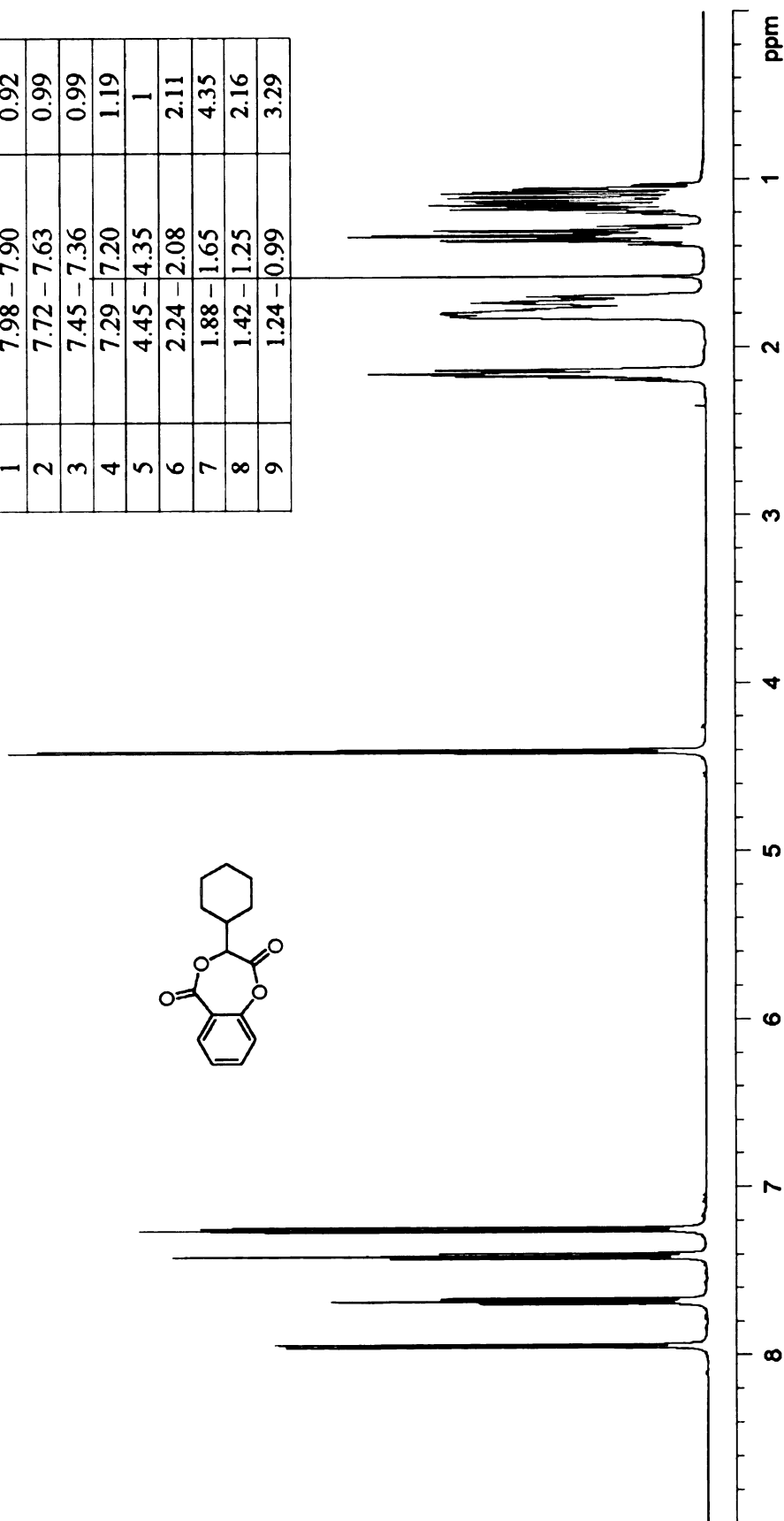


**Figure A-30.** <sup>1</sup>H NMR spectrum of 1,4-benzodioxepin-3-cyclohexyl-2,5-dione

|                   |  |  |     |                                |
|-------------------|--|--|-----|--------------------------------|
| <b>Sample</b>     | 1,4-benzodioxepin-3-cyclohexyl-2,5-dione |  |     |                                |
| <b>Instrument</b> | Varian UnityPlus500                      | <b>Frequency (MHz)</b>                             | 125 | <b>Nucleus</b> $^{13}\text{C}$ |
| <b>Solvent</b>    | $\text{CDCl}_3$                          | <b>Temperature (<math>^{\circ}\text{C}</math>)</b> | 25  |                                |

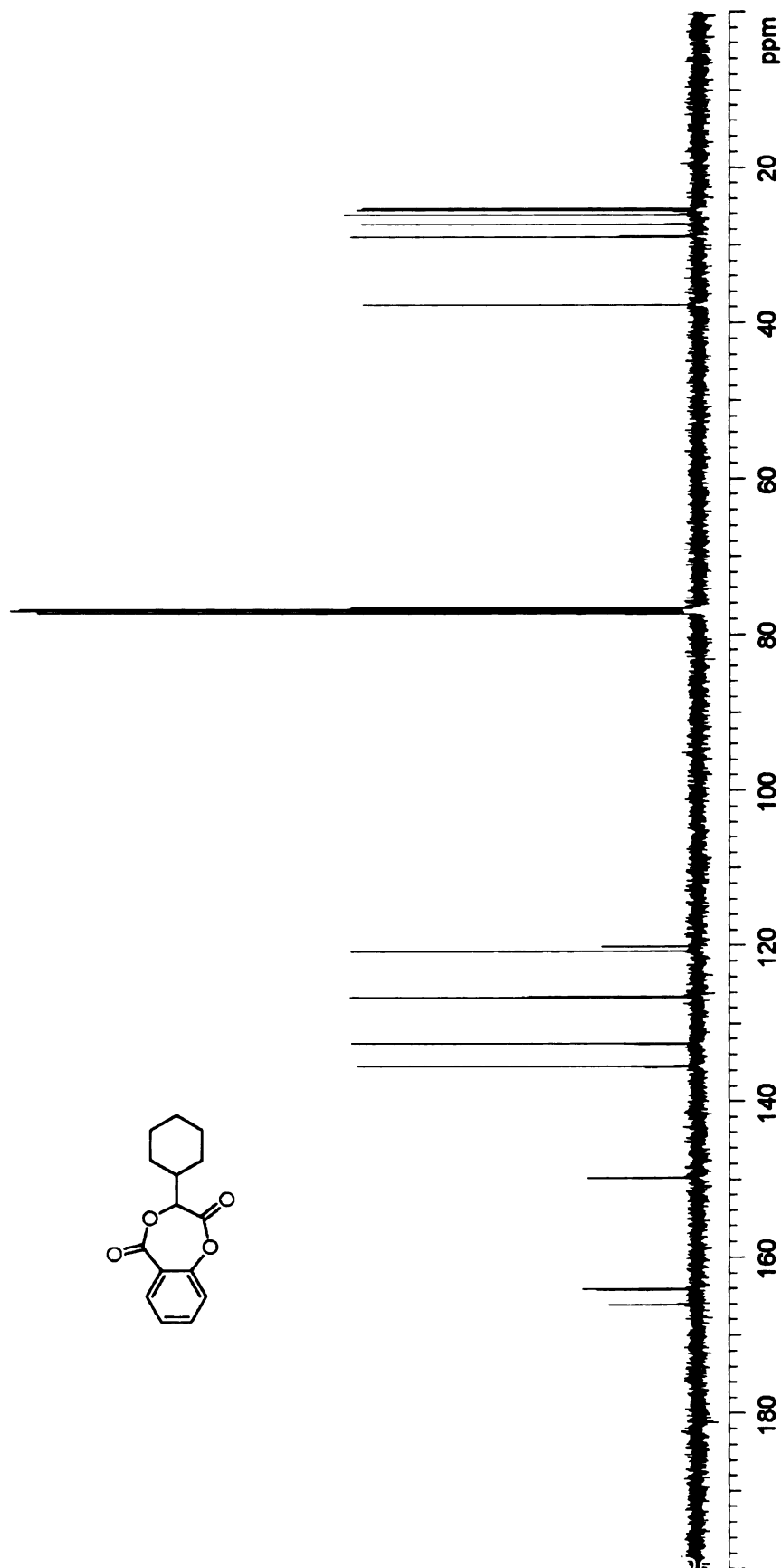
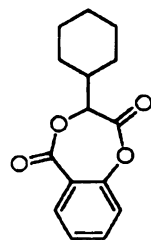


**Figure A-31.**  $^{13}\text{C}$  NMR spectrum of 1,4-benzodioxepin-3-cyclohexyl-2,5-dione

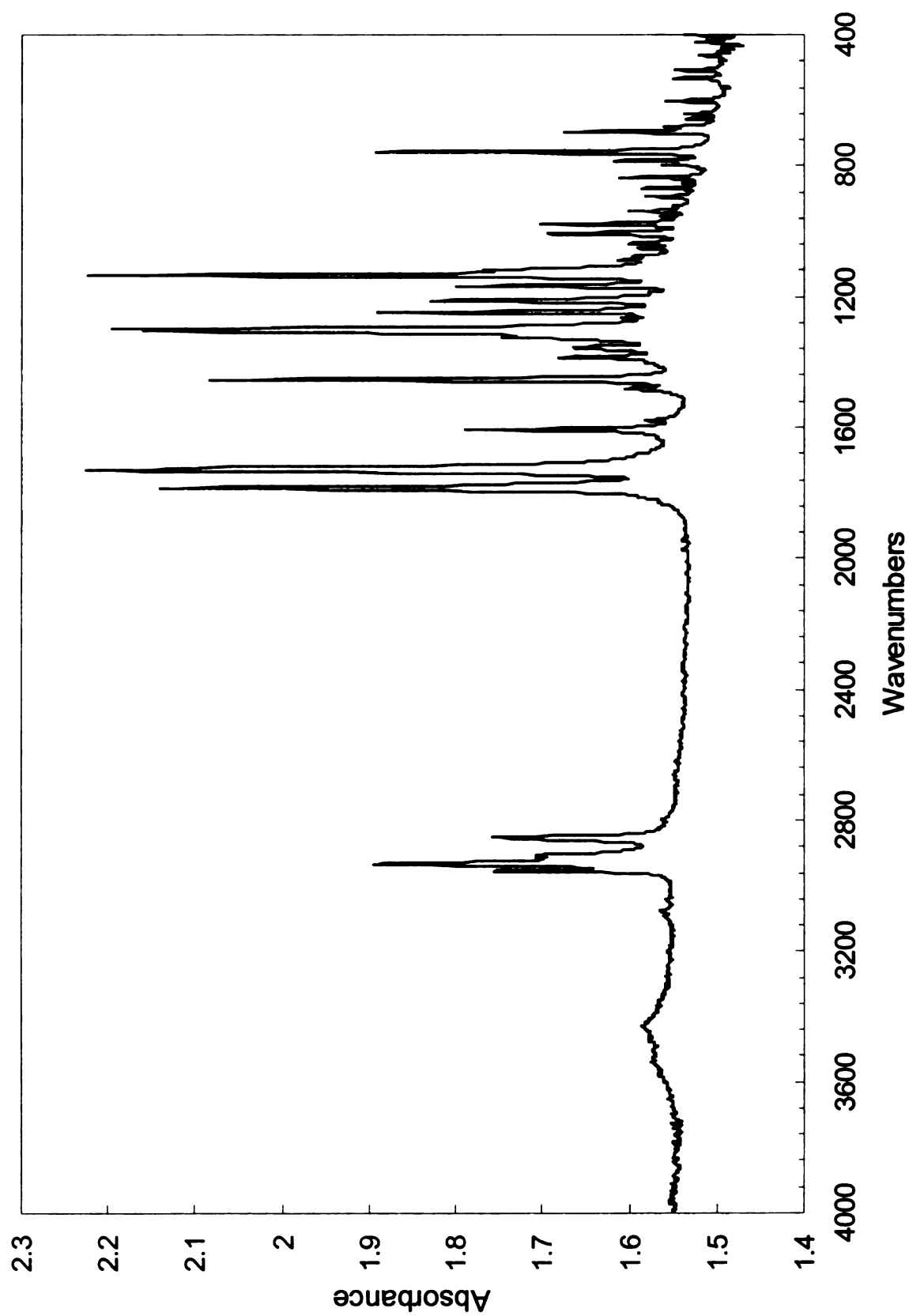


**Figure A- 32.** FT-IR spectrum of 1,4-benzodioxepin-3-cyclohexyl-2,5-dione

|                   |   |                         |                |
|-------------------|---|-------------------------|----------------|
| <b>Sample</b>     | poly( <i>rac</i> -3,6-dicyclohexyl-1,4-dioxane-2,5-dione) |                         |                |
| <b>Instrument</b> | Varian UnityPlus500                                       | <b>Frequency (MHz)</b>  | 500            |
| <b>Solvent</b>    | CDCl <sub>3</sub>   | <b>Temperature (°C)</b> | 25             |
|                   |   | <b>Nucleus</b>          | <sup>1</sup> H |

**Table of Integrals**

| No. | Chemical Shift (ppm) | Value |
|-----|----------------------|-------|
| 1   | 5.19 – 4.90          | 1     |
| 2   | 2.09 – 1.86          | 1.04  |
| 3   | 1.85 – 1.49          | 5.22  |
| 4   | 1.40 – 0.98          | 5.05  |

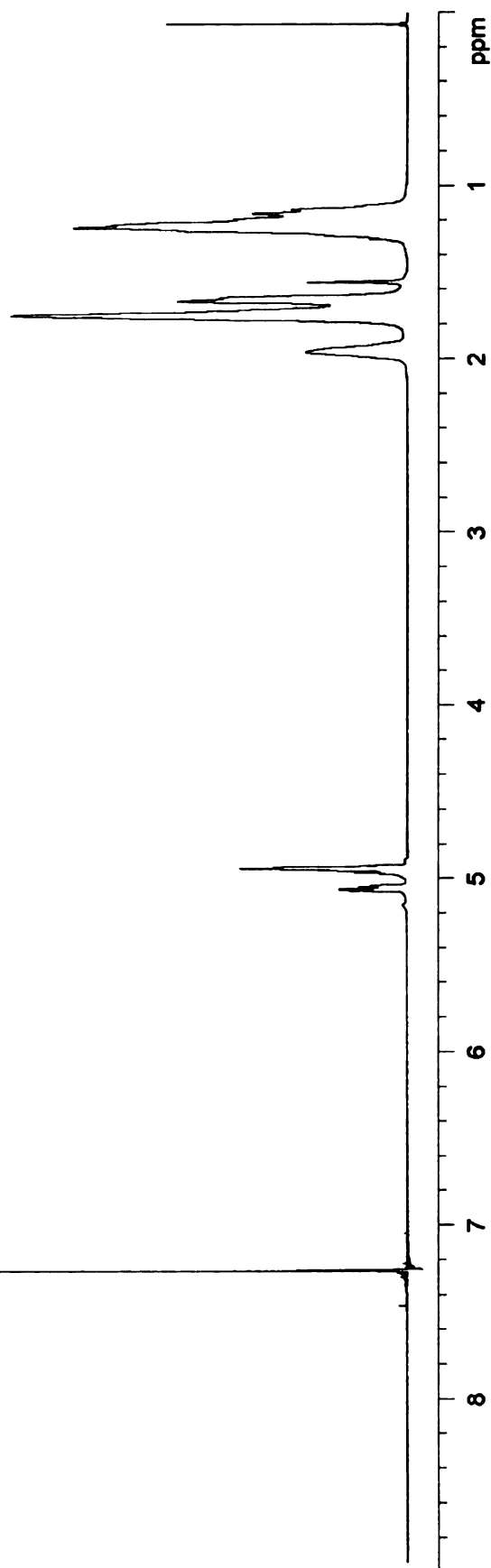
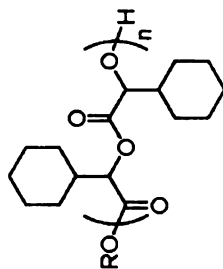


**Figure A- 33.** <sup>1</sup>H NMR spectrum of poly(*rac*-dicyclohexylglycolide)

|                   |   |                         |     |                 |
|-------------------|---|-------------------------|-----|-----------------|
| <b>Sample</b>     | poly( <i>rac</i> -3,6-dicyclohexyl-1,4-dioxane-2,5-dione) |                         |     | <sup>13</sup> C |
| <b>Instrument</b> | Varian UnityPlus500                                       | <b>Frequency (MHz)</b>  | 125 | <b>Nucleus</b>  |
| <b>Solvent</b>    | CDCl <sub>3</sub>   | <b>Temperature (°C)</b> | 25  |                 |

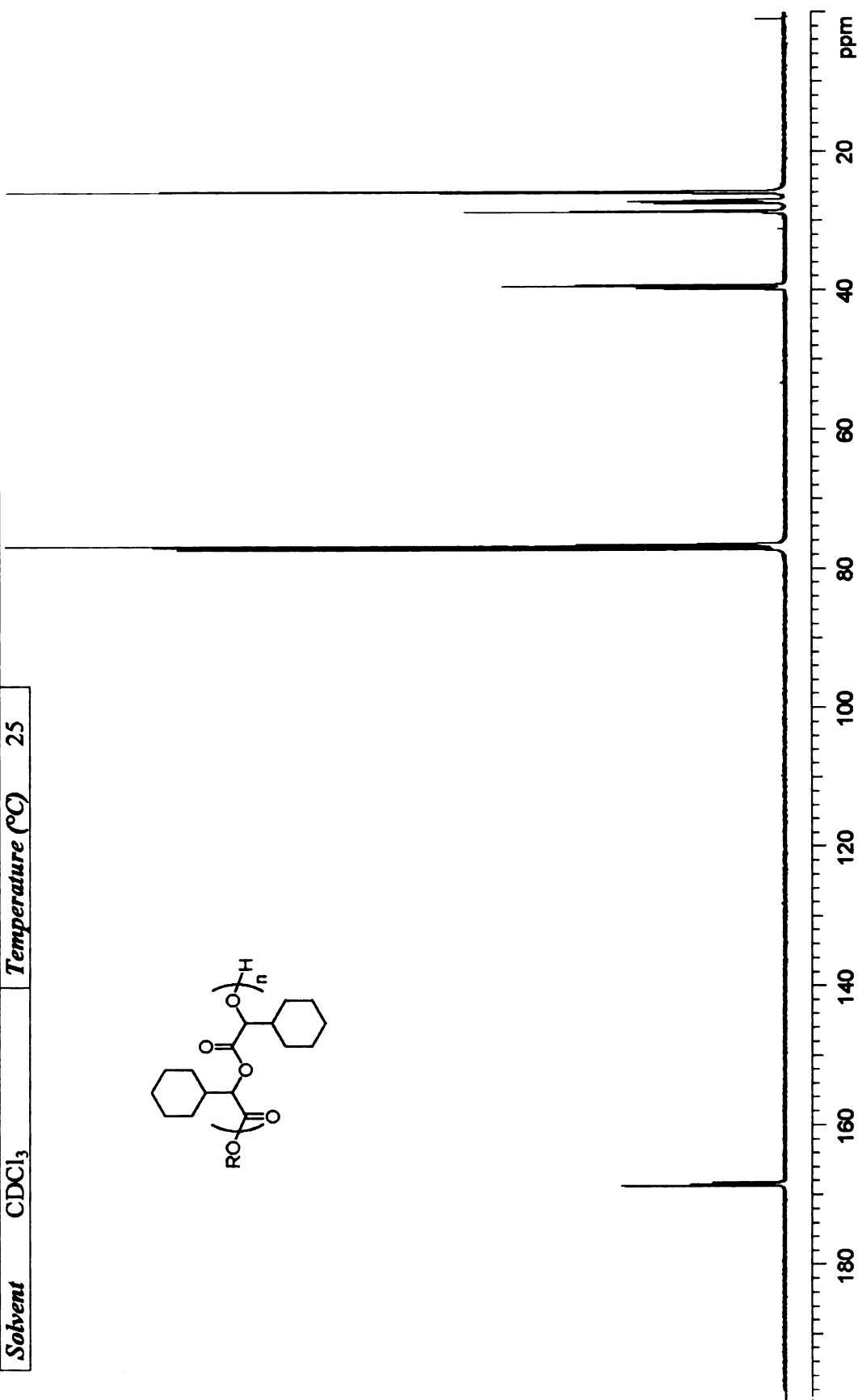
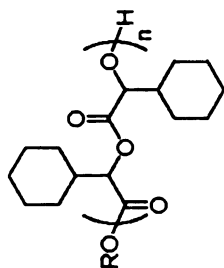


**Figure A- 34.** <sup>13</sup>C NMR spectrum of poly(*rac*-dicyclohexylglycolide)

|                   |  |                         |                |
|-------------------|--|-------------------------|----------------|
| <b>Sample</b>     | poly( <i>meso</i> -3,6-dicyclohexyl-1,4-dioxane-2,5-dione) |                         |                |
| <b>Instrument</b> | Varian UnityPlus500  | <b>Frequency (MHz)</b>  | 500            |
| <b>Solvent</b>    | CDCl <sub>3</sub>  | <b>Temperature (°C)</b> | 25             |
|                   |  | <b>Nucleus</b>          | <sup>1</sup> H |

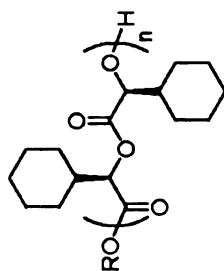


**Table of Integrals**

| No. | Chemical Shift (ppm) | Value |
|-----|----------------------|-------|
| 1   | 5.19 – 5.03          | 1     |
| 2   | 5.02 – 4.88          | 0.59  |
| 3   | 2.11 – 1.86          | 1.67  |
| 4   | 1.86 – 1.49          | 8.36  |
| 5   | 1.42 – 0.95          | 8.27  |

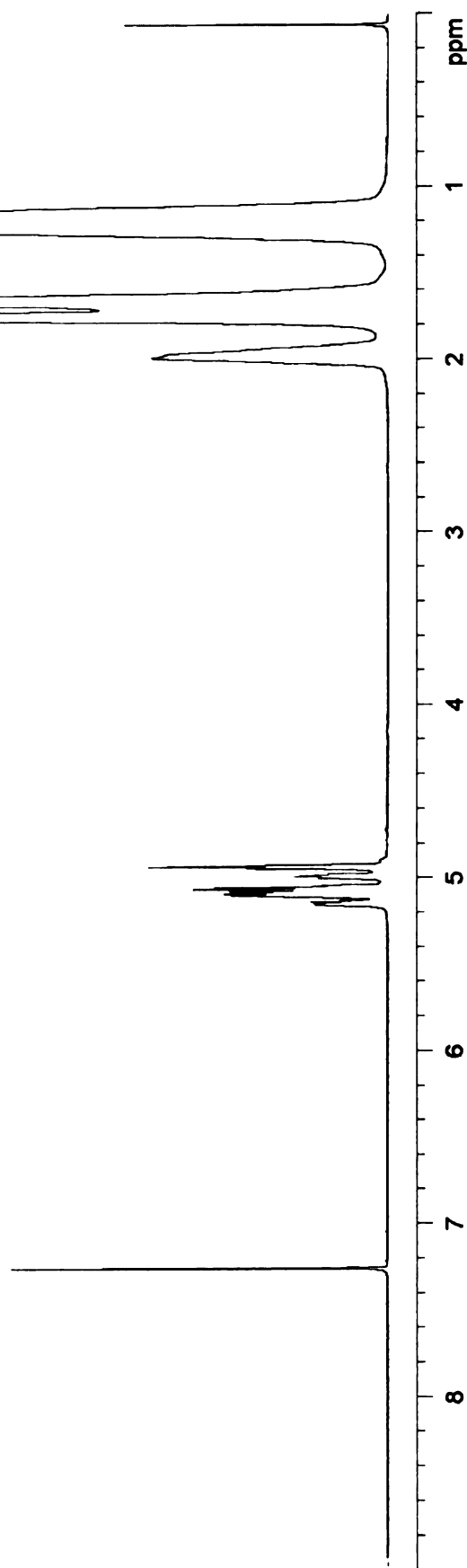


**Figure A- 35.** <sup>1</sup>H NMR spectrum of poly(*meso*-dicyclohexylglycolide)

|                   |  |                         |                 |
|-------------------|--|-------------------------|-----------------|
| <b>Sample</b>     | poly( <i>meso</i> -3,6-dicyclohexyl-1,4-dioxane-2,5-dione) |                         |                 |
| <b>Instrument</b> | Varian UnityPlus500  | <b>Frequency (MHz)</b>  | 125             |
| <b>Solvent</b>    | CDCl <sub>3</sub>  | <b>Temperature (°C)</b> | 25              |
|                   |  | <b>Nucleus</b>          | <sup>13</sup> C |

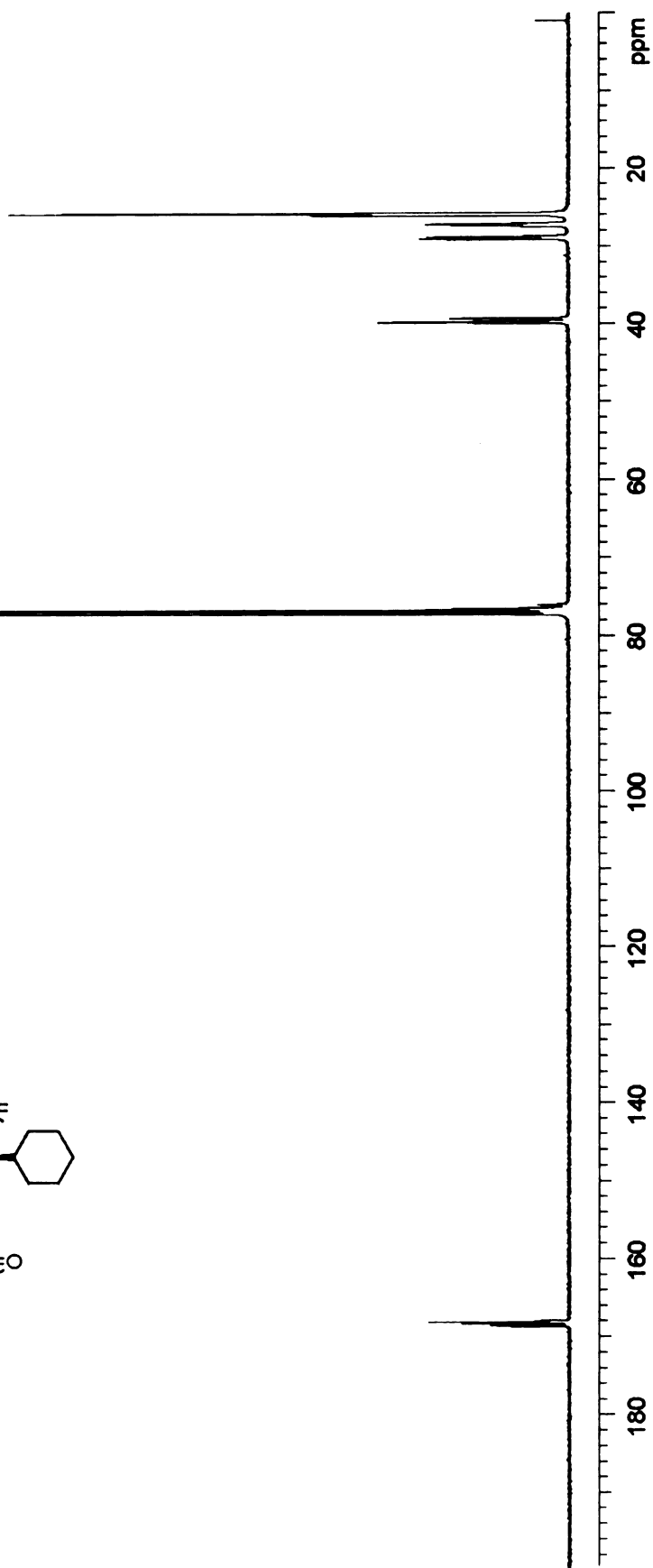
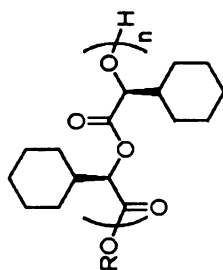


**Figure A- 36.** <sup>13</sup>C NMR spectrum of poly(*meso*-dicyclohexylglycolide)



|                   |   |                         |                    |
|-------------------|---|-------------------------|--------------------|
| <b>Sample</b>     | poly((3 <i>R</i> ,6 <i>R</i> )-(+)3,6-dicyclohexyl-1,4-dioxane-2,5-dione) |                         |                    |
| <b>Instrument</b> | Varian UnityPlus500   | <b>Frequency (MHz)</b>  | 500 <sup>1</sup> H |
| <b>Solvent</b>    | CDCl <sub>3</sub>   | <b>Temperature (°C)</b> | 25                 |

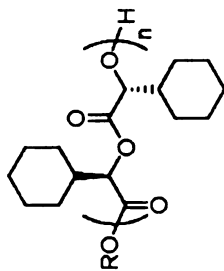


**Table of Integrals**

| No. | Chemical Shift (ppm) | Value |
|-----|----------------------|-------|
| 1   | 5.19 – 5.13          | 0.02  |
| 2   | 5.10 – 5.03          | 0.01  |
| 3   | 5.00 – 4.87          | 1     |
| 4   | 2.05 – 1.87          | 1.10  |
| 5   | 1.85 – 1.54          | 5.46  |
| 6   | 1.40 – 1.03          | 5.45  |

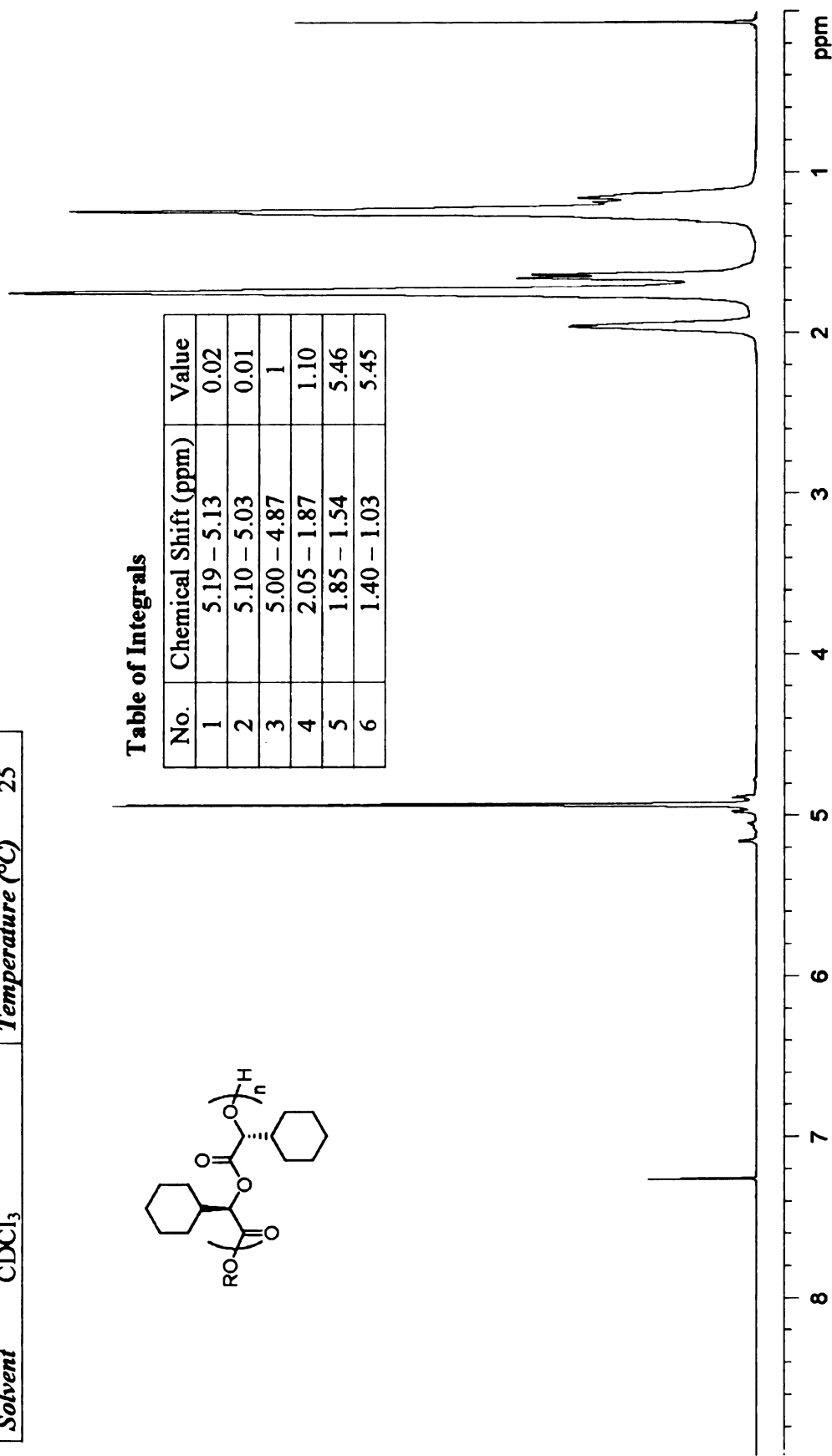


**Figure A- 37.** <sup>1</sup>H NMR spectrum of poly(*R,R*-dicyclohexylglycolide)

|                   |  |                         |     |                 |
|-------------------|--|-------------------------|-----|-----------------|
| <b>Sample</b>     | poly((3 <i>R</i> ,6 <i>R</i> )-(+)-3,6-dicyclohexyl-1,4-dioxane-2,5-dione) |                         |     | <sup>13</sup> C |
| <b>Instrument</b> | Varian UnityPlus500  | <b>Frequency (MHz)</b>  | 125 | <b>Nucleus</b>  |
| <b>Solvent</b>    | CDCl <sub>3</sub>  | <b>Temperature (°C)</b> | 25  |                 |

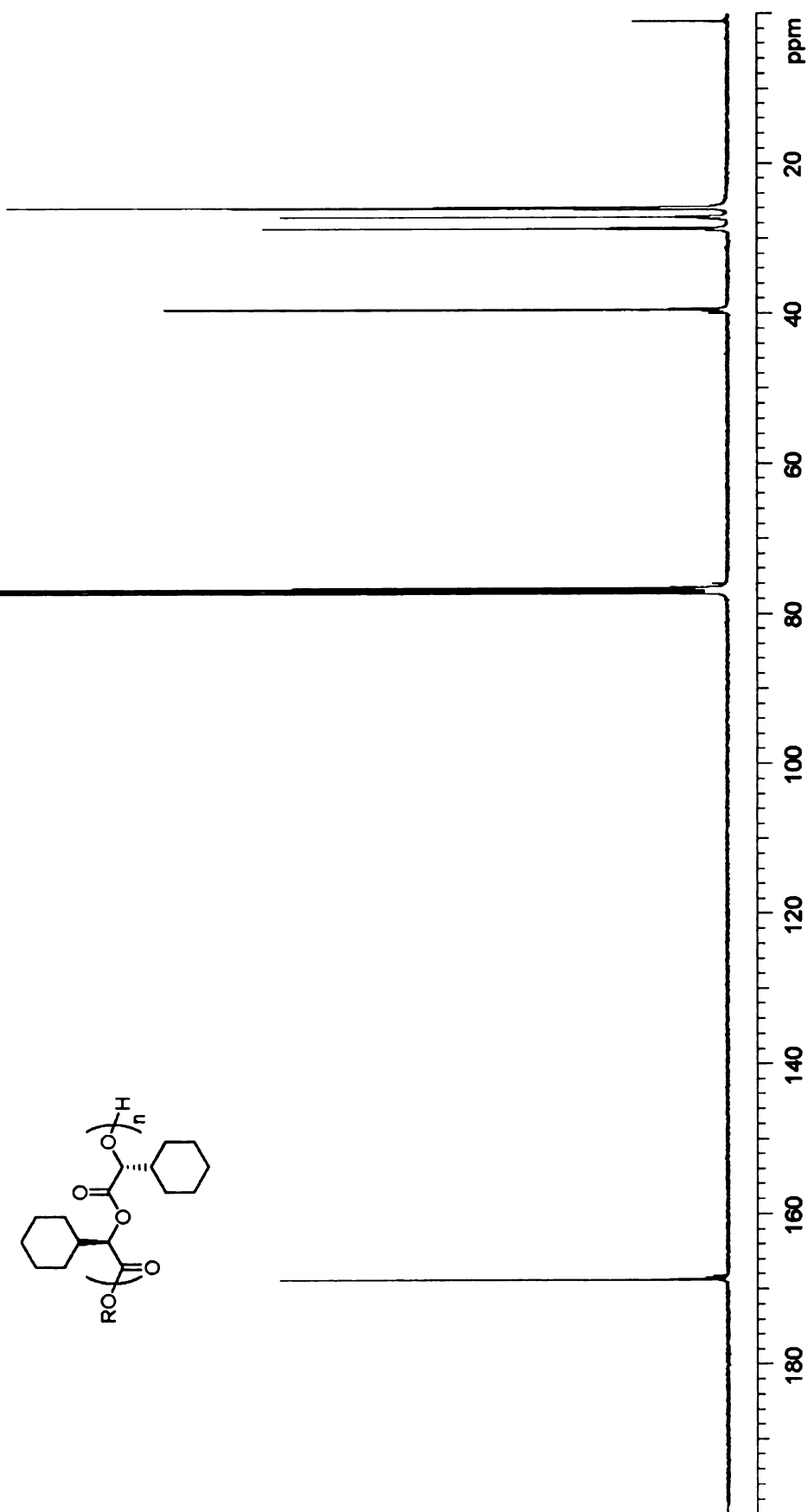


**Figure A-38.** <sup>13</sup>C NMR spectrum of poly(*R,R*-dicyclohexylglycolide)

|                   |  |                         |                |
|-------------------|--|-------------------------|----------------|
| <b>Sample</b>     | poly( <i>rac</i> -3,6-diisopropyl-1,4-dioxane-2,5-dione) |                         |                |
| <b>Instrument</b> | Varian UnityPlus500                                      | <b>Frequency (MHz)</b>  | 500            |
| <b>Solvent</b>    | CDCl <sub>3</sub>  | <b>Temperature (°C)</b> | 25             |
|                   |  | <b>Nucleus</b>          | <sup>1</sup> H |

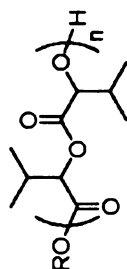


**Table of Integrals**

| No. | Chemical Shift (ppm) | Value |
|-----|----------------------|-------|
| 1   | 5.15 – 5.04          | 1     |
| 2   | 5.04 – 4.91          | 2.52  |
| 3   | 2.40 – 2.24          | 3.59  |
| 4   | 1.20 – 0.83          | 22.5  |

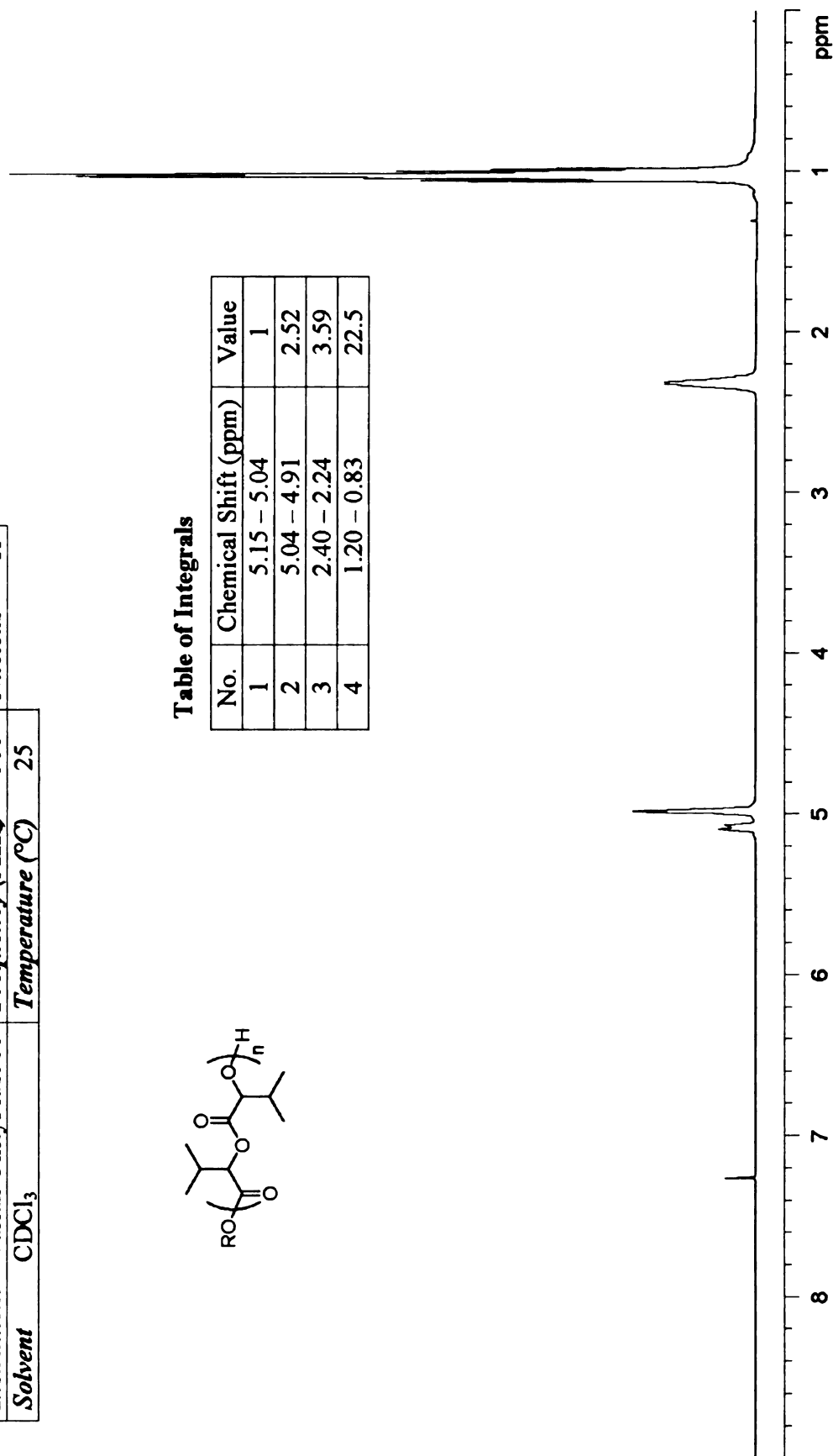


**Figure A- 39.** <sup>1</sup>H NMR spectrum of poly(*rac*-diisopropylglycolide)

|                   |  |                         |                 |
|-------------------|--|-------------------------|-----------------|
| <b>Sample</b>     | poly( <i>rac</i> -3,6-diisopropyl-1,4-dioxane-2,5-dione) |                         |                 |
| <b>Instrument</b> | Varian UnityPlus500                                      | <b>Frequency (MHz)</b>  | 125             |
| <b>Solvent</b>    | CDCl <sub>3</sub>  | <b>Temperature (°C)</b> | 25              |
|                   |  | <b>Nucleus</b>          | <sup>13</sup> C |

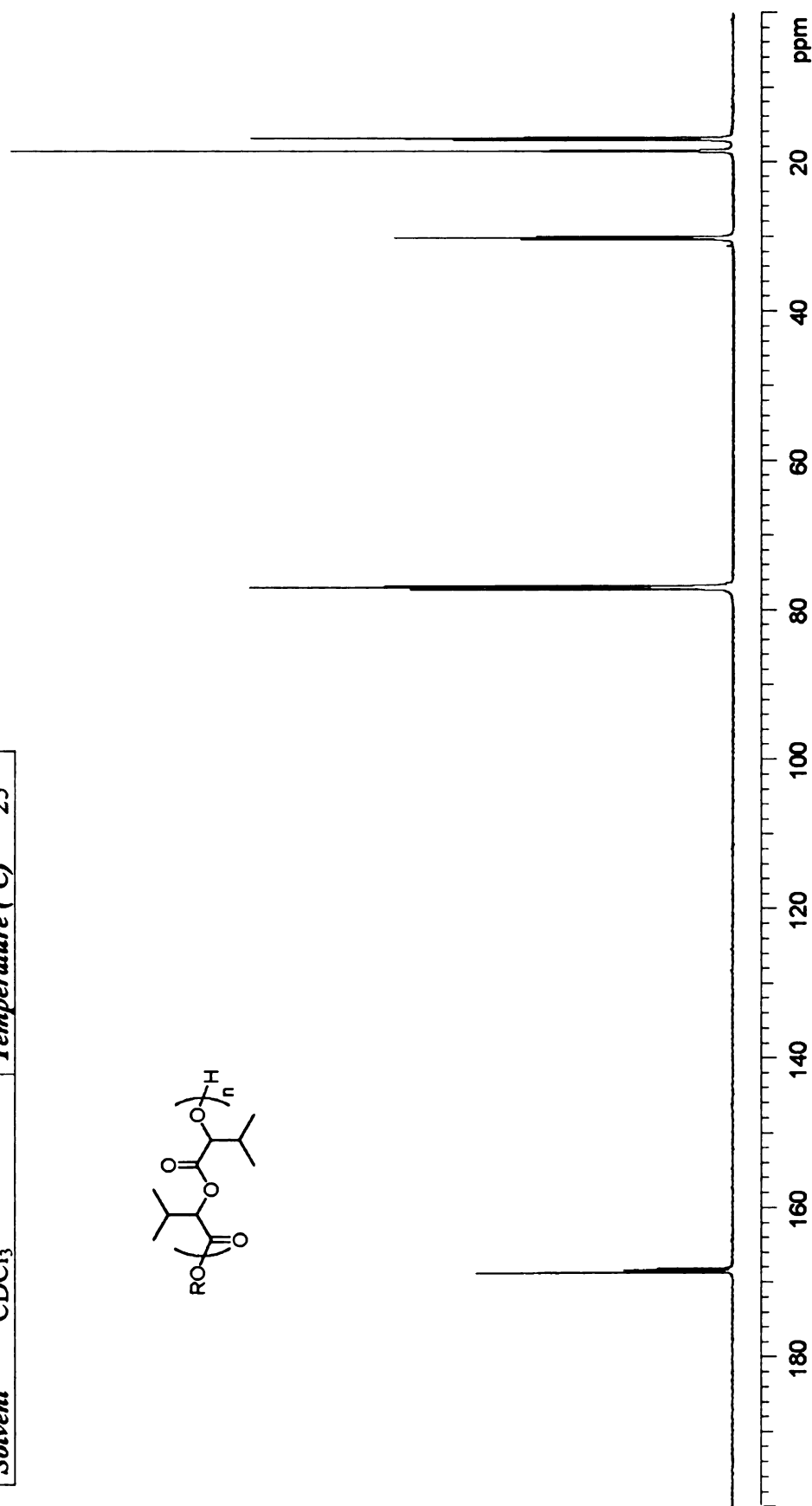
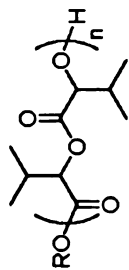


**Figure A-40.** <sup>13</sup>C NMR spectrum of poly(*rac*-diisopropylglycolide)

|                   |  |                         |     |                               |
|-------------------|--|-------------------------|-----|-------------------------------|
| <b>Sample</b>     | poly( <i>rac</i> -3-cyclohexyl-6-methyl-1,4-dioxane-2,5-dione) |                         |     |                               |
| <b>Instrument</b> | Varian UnityPlus500  | <b>Frequency (MHz)</b>  | 500 | <b>Nucleus</b> <sup>1</sup> H |
| <b>Solvent</b>    | CDCl <sub>3</sub>  | <b>Temperature (°C)</b> | 25  |                               |

**Table of Integrals**

| No. | Chemical Shift (ppm) | Value |
|-----|----------------------|-------|
| 1   | 5.34 – 5.10          | 1     |
| 2   | 5.07 – 4.87          | 1.03  |
| 3   | 2.08 – 1.90          | 1.06  |
| 4   | 1.85 – 1.47          | 8.95  |
| 5   | 1.37 – 1.03          | 5.44  |

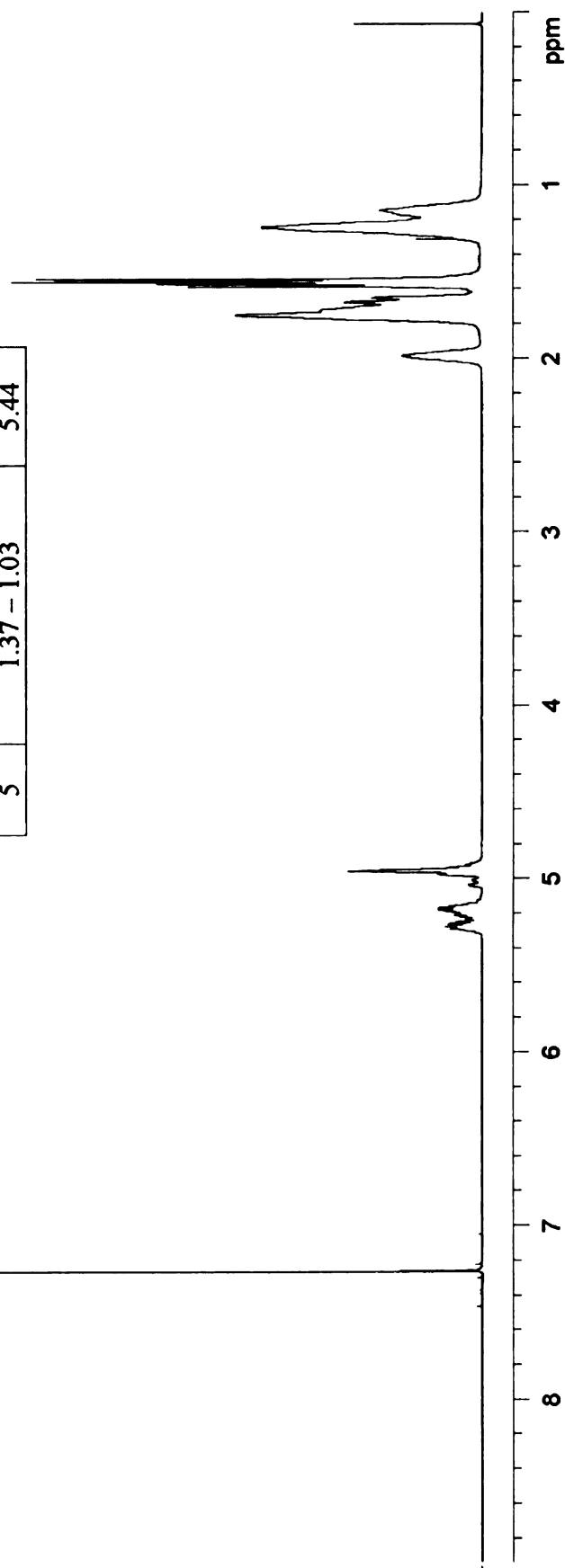
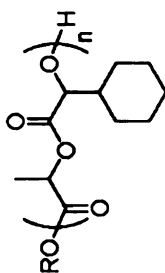


**Figure A- 41.** <sup>1</sup>H NMR spectrum of poly(*rac*-methylcyclohexylglycolide)

|                   |  |                         |     |                                |
|-------------------|--|-------------------------|-----|--------------------------------|
| <b>Sample</b>     | poly( <i>rac</i> -3-cyclohexyl-6-methyl-1,4-dioxane-2,5-dione) |                         |     |                                |
| <b>Instrument</b> | Varian UnityPlus500  | <b>Frequency (MHz)</b>  | 125 | <b>Nucleus</b> <sup>13</sup> C |
| <b>Solvent</b>    | CDCl <sub>3</sub>  | <b>Temperature (°C)</b> | 25  |                                |

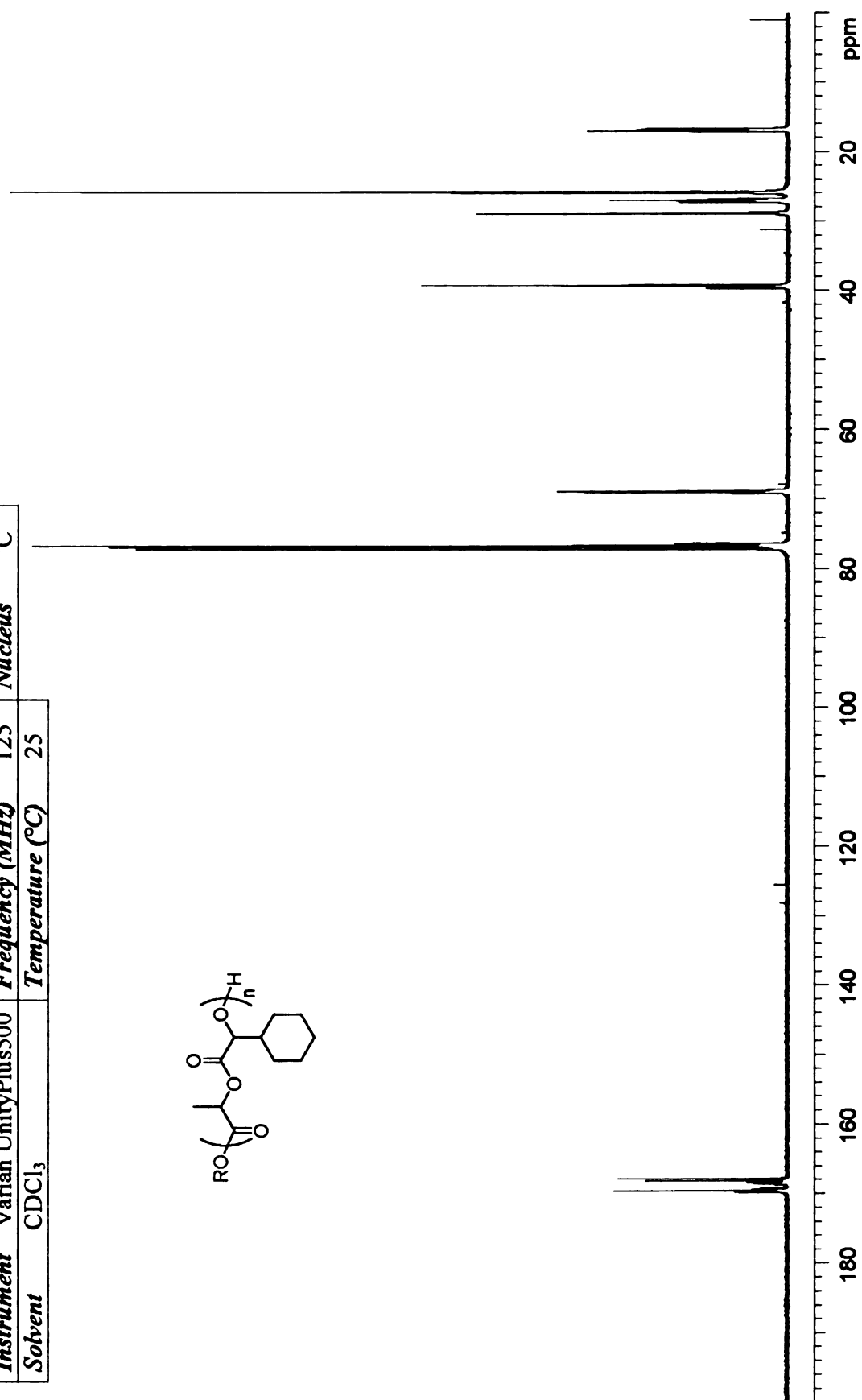
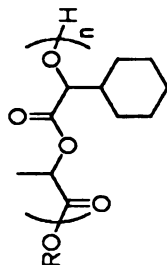


**Figure A-42.** <sup>13</sup>C NMR spectrum of poly(*rac*-methylcyclohexylglycolide)

|                   |  |                         |                               |
|-------------------|--|-------------------------|-------------------------------|
| <b>Sample</b>     | poly( <i>rac</i> -3-cyclohexyl-6- <i>n</i> -hexyl-1,4-dioxane-2,5-dione) |                         |                               |
| <b>Instrument</b> | Varian UnityPlus500  | <b>Frequency (MHz)</b>  | <b>Nucleus</b> <sup>1</sup> H |
| <b>Solvent</b>    | CDCl <sub>3</sub>  | <b>Temperature (°C)</b> | 25                            |

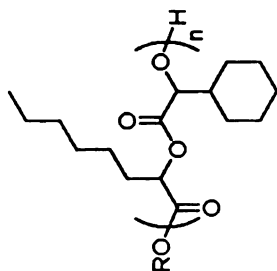


**Table of Integrals**

| No. | Chemical Shift (ppm) | Value |
|-----|----------------------|-------|
| 1   | 5.23 – 4.88          | 2     |
| 2   | 2.05 – 1.81          | 3.07  |
| 3   | 1.81 – 1.57          | 5.17  |
| 4   | 1.53 – 1.04          | 13.5  |
| 5   | 0.94 – 0.78          | 3.06  |

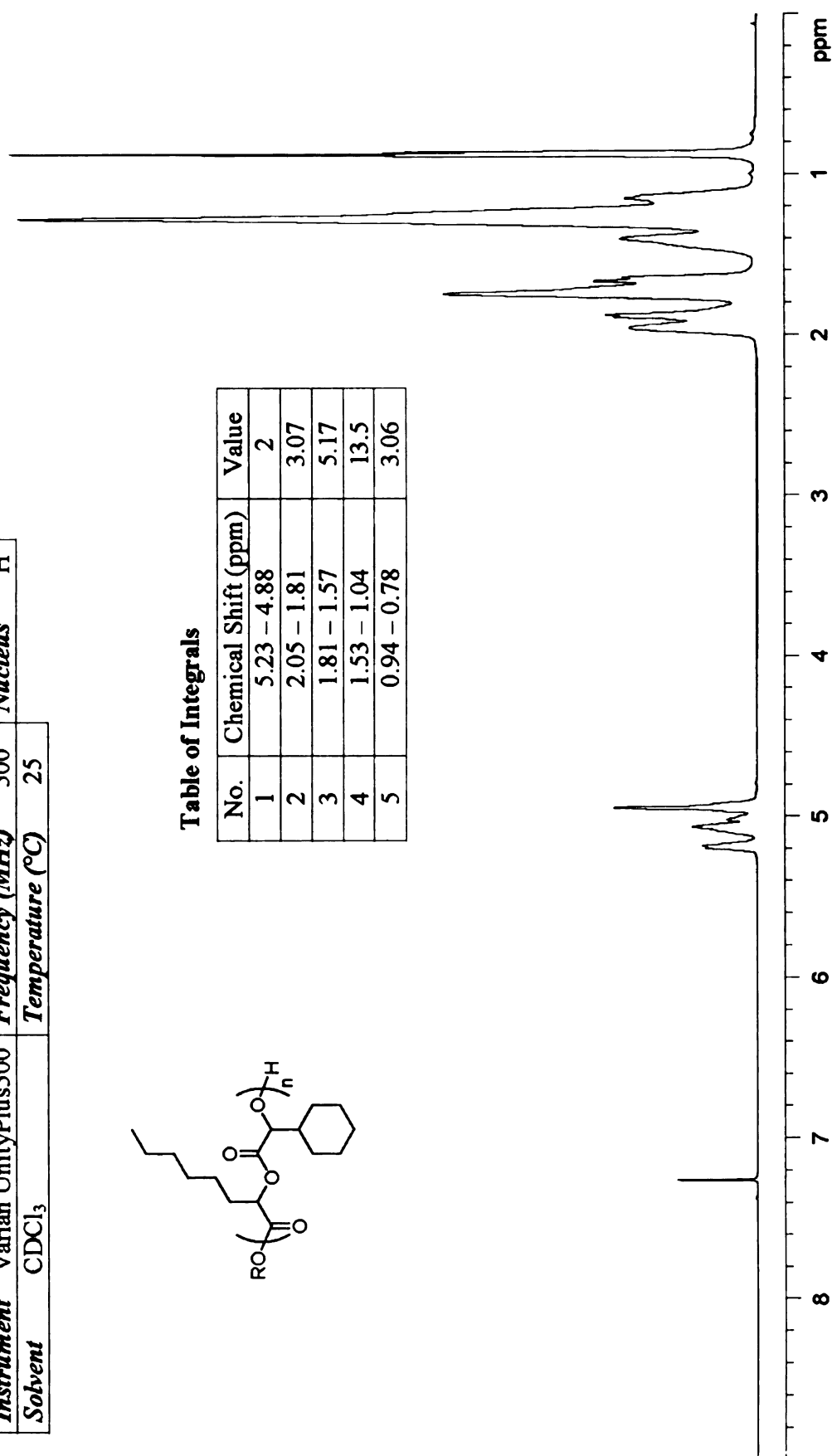


**Figure A-43.** <sup>1</sup>H NMR spectrum of poly(*rac*-hexylcyclohexylglycolide)

|                   |  |  |     |                                |
|-------------------|--|--|-----|--------------------------------|
| <b>Sample</b>     | poly( <i>rac</i> -3-cyclohexyl-6- <i>n</i> -hexyl-1,4-dioxane-2,5-dione) |  |     |                                |
| <b>Instrument</b> | Varian UnityPlus500  | <b>Frequency (MHz)</b>                             | 125 | <b>Nucleus</b> $^{13}\text{C}$ |
| <b>Solvent</b>    | $\text{CDCl}_3$  | <b>Temperature (<math>^{\circ}\text{C}</math>)</b> | 25  |                                |

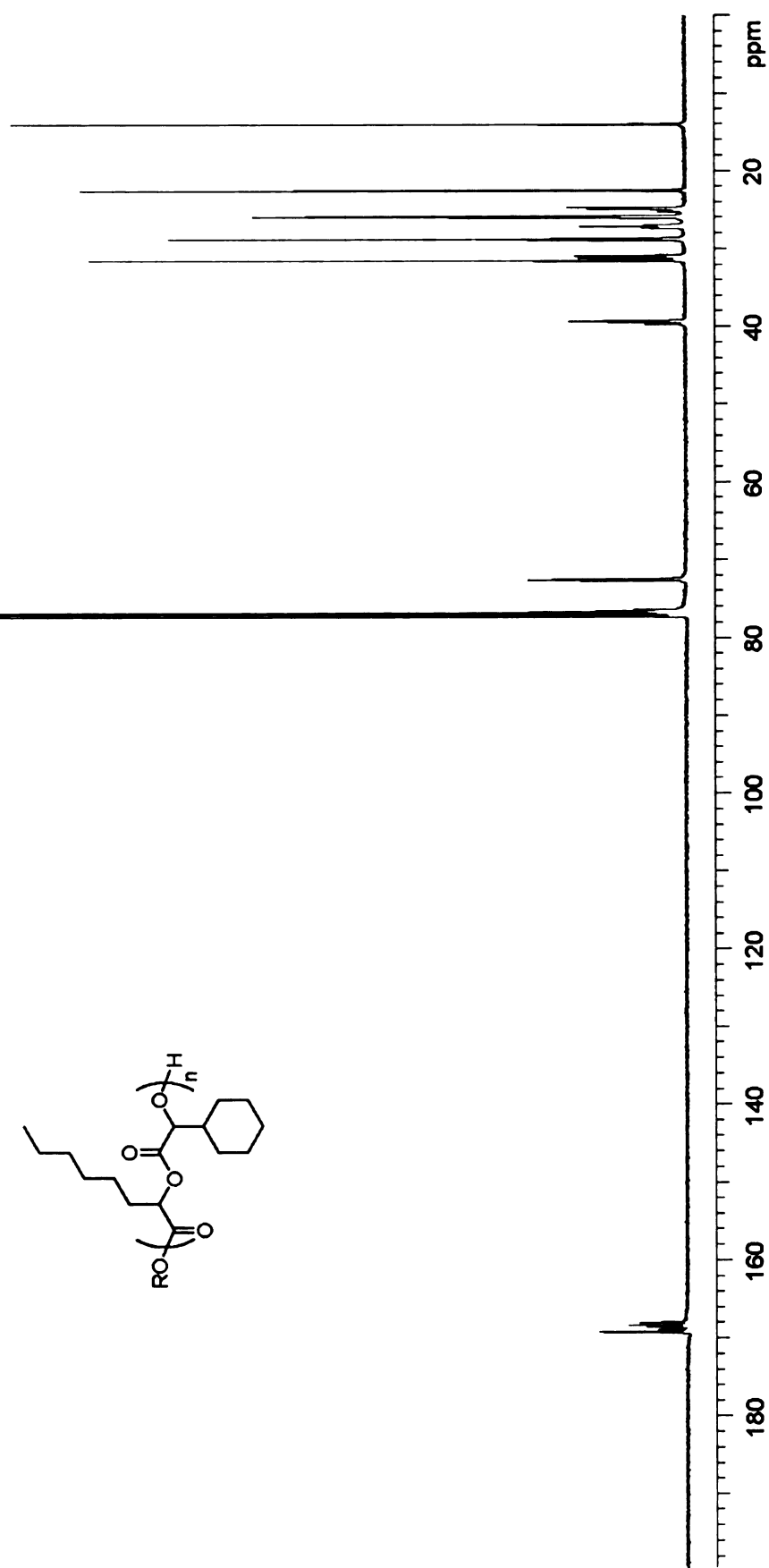


**Figure A-44.**  $^{13}\text{C}$  NMR spectrum of poly(*rac*-hexylcyclohexylglycolide)



|                   |  |                         |     |                             |
|-------------------|--|-------------------------|-----|-----------------------------|
| <b>Sample</b>     | poly(1,4-benzodioxepin-3-methyl-2,5-dione) |                         |     |                             |
| <b>Instrument</b> | Varian UnityPlus500                        | <b>Frequency (MHz)</b>  | 500 | <b>Nucleus</b> $^1\text{H}$ |
| <b>Solvent</b>    | $\text{CDCl}_3$                            | <b>Temperature (°C)</b> | 25  |                             |

**Table of Integrals**

| No. | Chemical Shift (ppm) | Value |
|-----|----------------------|-------|
| 1   | 8.13 – 8.05          | 1.00  |
| 2   | 7.57 – 7.45          | 1.04  |
| 3   | 7.34 – 7.22          | 1.15  |
| 4   | 7.17 – 7.11          | 1.01  |
| 5   | 5.62 – 5.54          | 1     |
| 6   | 1.85 – 1.78          | 3.01  |

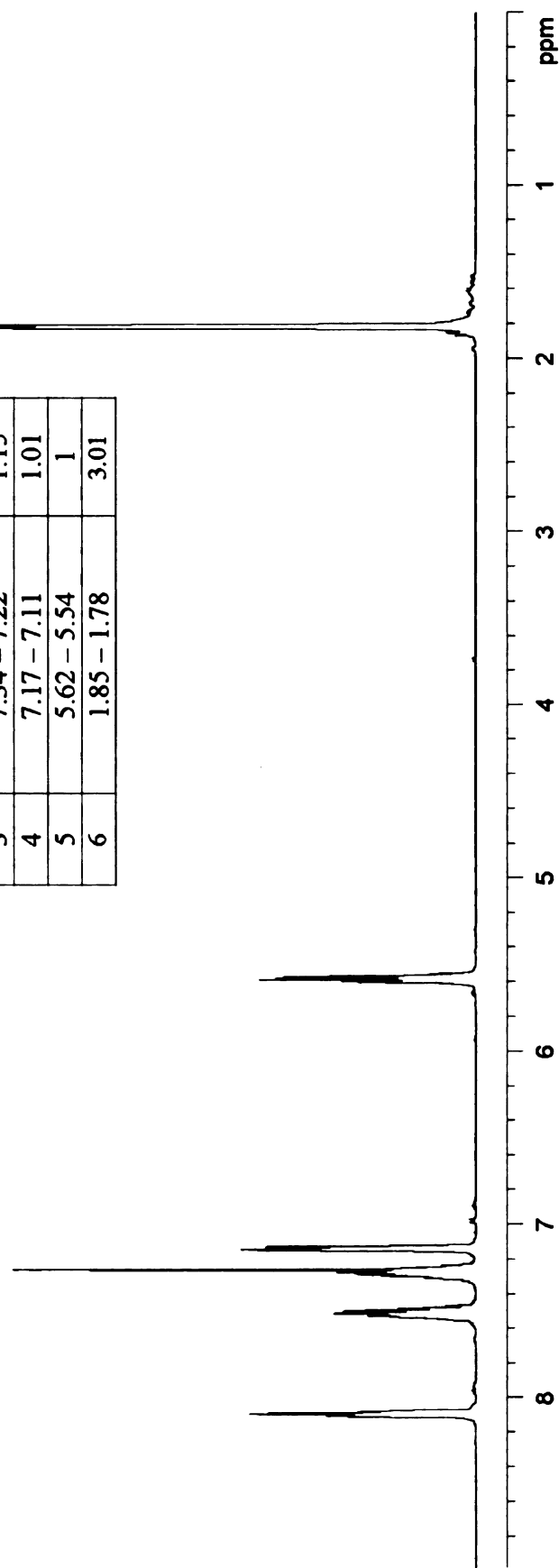
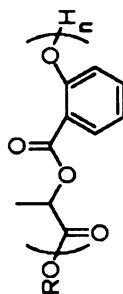


**Figure A- 45.**  $^1\text{H}$  NMR spectrum of poly(1,4-benzodioxepin-3-methyl-2,5-dione)

|                   |  |  |     |                                |
|-------------------|--|--|-----|--------------------------------|
| <b>Sample</b>     | poly(1,4-benzodioxepin-3-methyl-2,5-dione) |  |     |                                |
| <b>Instrument</b> | Varian UnityPlus500                        | <b>Frequency (MHz)</b>                             | 125 | <b>Nucleus</b> $^{13}\text{C}$ |
| <b>Solvent</b>    | $\text{CDCl}_3$                            | <b>Temperature (<math>^{\circ}\text{C}</math>)</b> | 25  |                                |

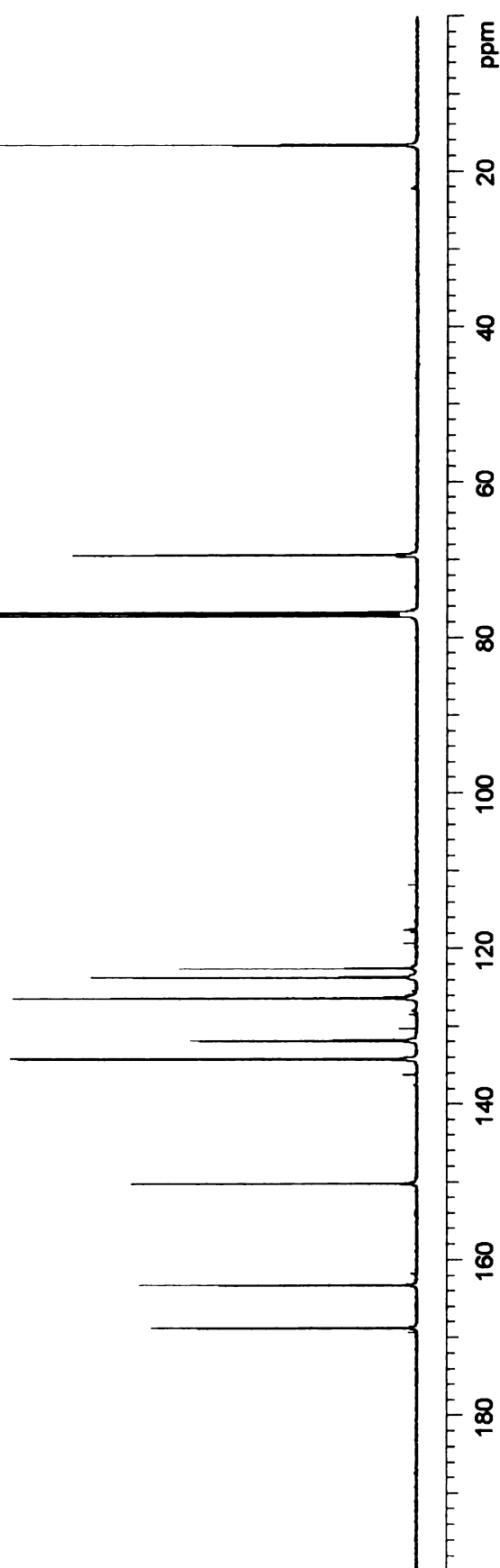
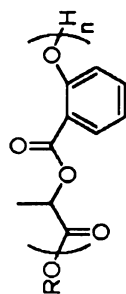


**Figure A- 46.**  $^{13}\text{C}$  NMR spectrum of poly(1,4-benzodioxepin-3-methyl-2,5-dione)

|                   |  |                         |                               |
|-------------------|--|-------------------------|-------------------------------|
| <b>Sample</b>     | poly(1,4-benzodioxepin-3-cyclohexyl-2,5-dione) |                         |                               |
| <b>Instrument</b> | Varian UnityPlus500                            | <b>Frequency (MHz)</b>  | 500                           |
| <b>Solvent</b>    | CDCl <sub>3</sub>                              | <b>Temperature (°C)</b> | 25                            |
|                   |  |                         | <b>Nucleus</b> <sup>1</sup> H |

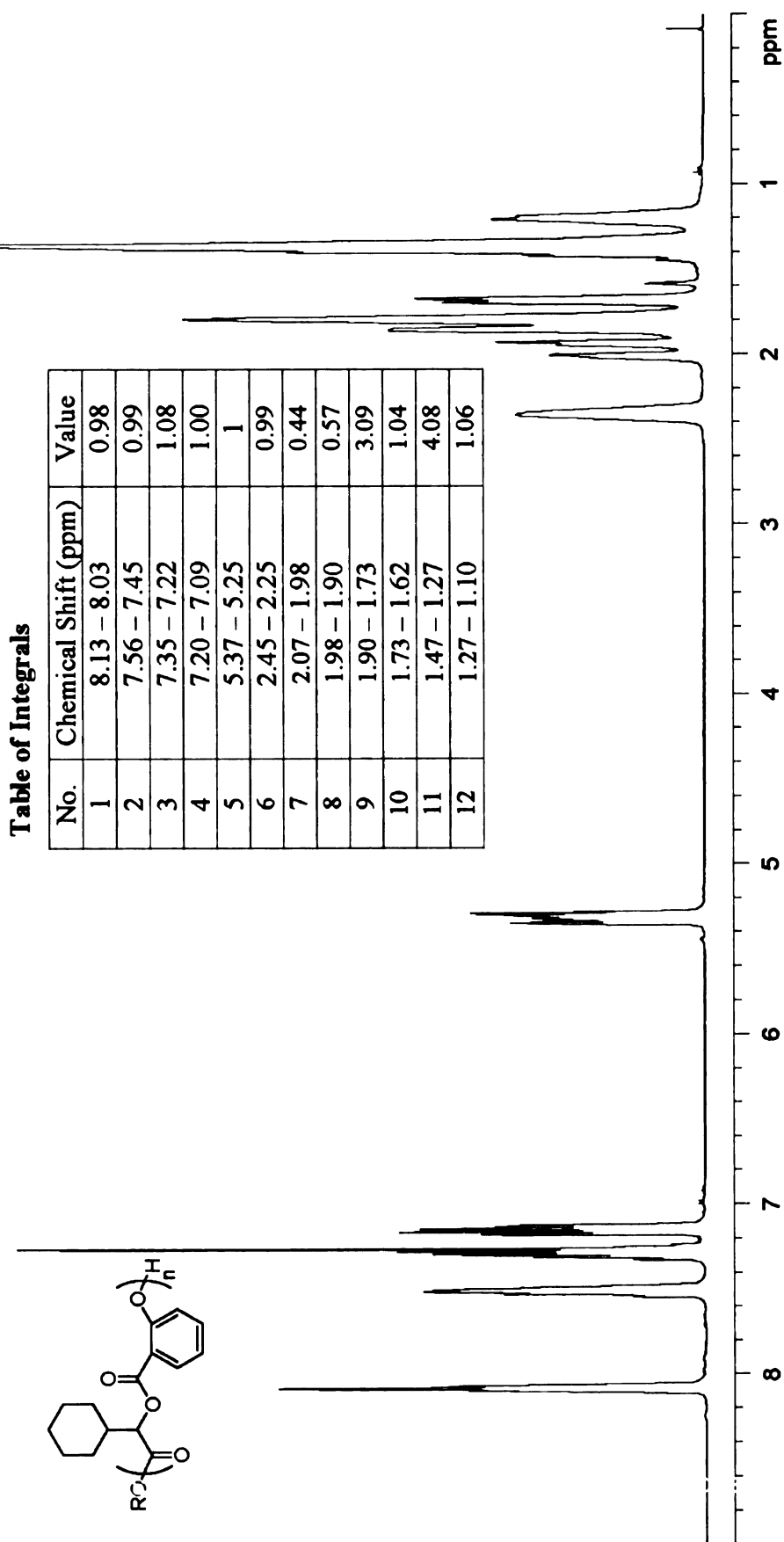


**Figure A- 47.** <sup>1</sup>H NMR spectrum of poly(1,4-benzodioxepin-3-cyclohexyl-2,5-dione)

|                   |  |                         |                     |
|-------------------|--|-------------------------|---------------------|
| <b>Sample</b>     | poly(1,4-benzodioxepin-3-cyclohexyl-2,5-dione) |                         |                     |
| <b>Instrument</b> | Varian UnityPlus500                            | <b>Frequency (MHz)</b>  | 125 <sup>13</sup> C |
| <b>Solvent</b>    | CDCl <sub>3</sub>                              | <b>Temperature (°C)</b> | 25                  |

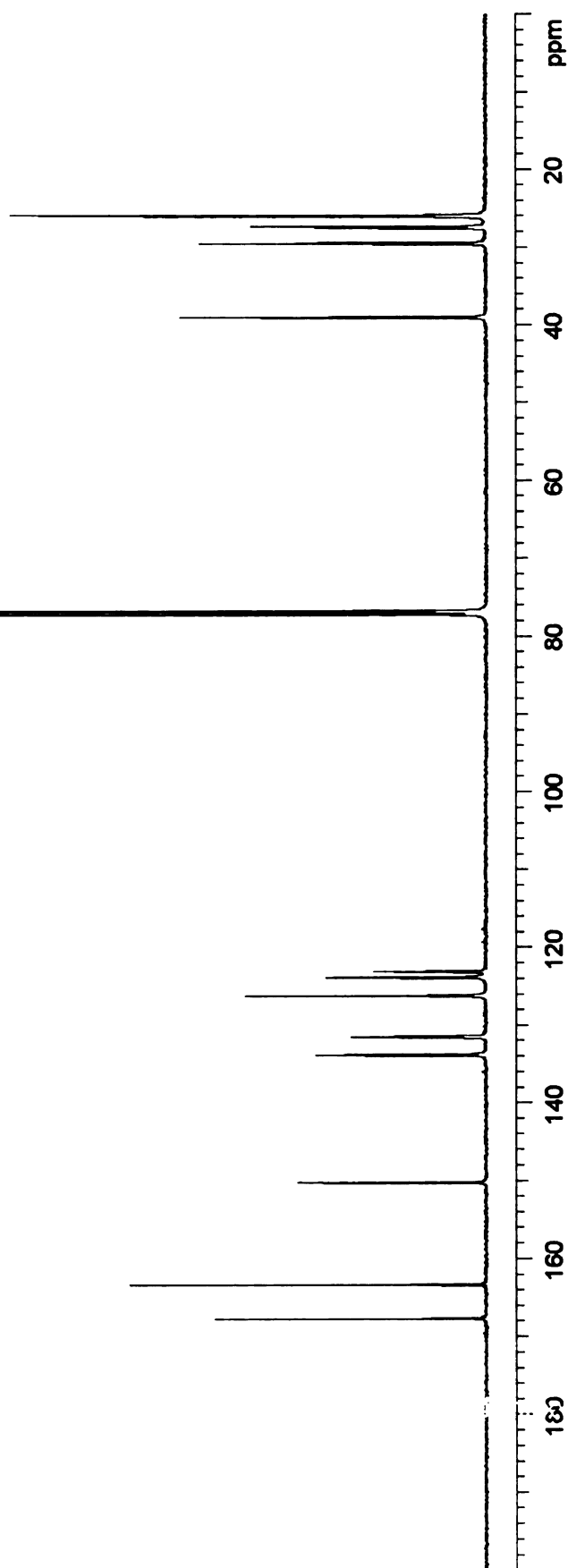
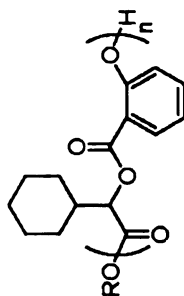


**Figure A- 48.** <sup>13</sup>C NMR spectrum of poly(1,4-benzodioxepin-3-cyclohexyl-2,5-dione)

## References

- 1 Schmitt, E. E.; Polistina, R. A. U.S. Pat. 3,297,033 (1967)
- 2 Wasserman, D.; Versfelt, C. C. U.S. Pat. 3,839,297 (1974)
- 3 Drumright, R. E.; Gruber, P. R.; Henton, D. E. *Adv. Mater.* **2000**, *12*, 1841-1846.
- 4 Vink, E. T. H.; Rabago, K. R.; Glassner, D. A.; Springs, B.; O'Connor, R. P.; Kolstad, J.; Gruber, P. R. *Macromol. Biosci.* **2004**, *4*, 551-564.
- 5 Vert, M. *Biomacromolecules* **2005**, *6*, 538-546.
- 6 Reeve, M. S.; McCarthy, S. P.; Downey, M. J.; Gross, R. A. *Macromolecules* **1994**, *27*, 825-831.
- 7 MacDonald, R. T.; McCarthy, S. P.; Gross, R. A. *Macromolecules* **1996**, *29*, 7356-7361.
- 8 Li, S. M.; McCarthy, S. *Macromolecules* **1999**, *32*, 4454-4456.
- 9 Tsuji, H.; Miyauchi, S. *Biomacromolecules* **2001**, *2*, 597-604.
- 10 Yamashita, K.; Kikkawa, Y.; Kurokawa, K.; Doi, Y. *Biomacromolecules* **2005**, *6*, 850-857.
- 11 Tokiwa, Y.; Jarerat, A. *Biotechnology Letters* **2004**, *26*, 771-777.
- 12 Masato, M.; Shinya, K. Eur. Pat. Appl. EP 1281766 (2003)
- 13 Iwakura, Y.; Iwata, K.; Matsuo, S.; Tohara, A. *Makromol. Chem.* **1971**, *146*, 21-32.
- 14 Yin, M. Dissertation, Michigan State University, 2000.
- 15 Yin, M.; Baker, G. L. *Macromolecules* **1999**, *32*, 7711-7718.
- 16 Trimaille, T.; Moller, M.; Gurny, R. *J. Polym. Sci., Part A: Polym. Chem.* **2004**, *42*, 4379-4391.
- 17 Augurt, T. A.; Rosensafft, M. N.; Perciaccante, V. A. U.S. Pat. 4,033,938 (1977)
- 18 Shen, Z. R.; Zhu, J. H.; Ma, Z. *Makromol. Chem.-Rapid* **1993**, *14*, 457-460.

- 19 Dong, C. M.; Qiu, K. Y.; Gu, Z. W.; Feng, X. D. *J. Polym. Sci., Part A: Polym. Chem.* **2001**, 39, 357-367.
- 20 Baker, G. L.; Smith, M. R. U. S. Pat. 6,469,133 (2002)
- 21 Chisholm, M. H.; Delbridge, E. E. *New J. Chem.* **2003**, 27, 1177-1183.
- 22 Saiyasombat, W.; Molloy, R.; Nicholson, T. M.; Johnson, A. F.; Ward, I. M.; Poshyachinda, S. *Polymer* **1998**, 39, 5581-5585.
- 23 Hall, H. K.; Schneider, A. K. *J. Am. Chem. Soc.* **1958**, 80, 6409.
- 24 Deibig, H.; Geiger, J.; Sander, M. *Makromol. Chem.* **1971**, 145, 123-131.
- 25 Drumright, R. E.; Hartmann, M.; Wolf, R. PCT Int. Appl. WO 2002100921 (2002)
- 26 Andronova, N.; Srivastava, R. K.; Albertsson, A. C. *Polymer* **2005**, 46, 6746-6755.
- 27 Amsden, B.; Wang, S.; Wyss, U. *Biomacromolecules* **2004**, 5, 1399-1404.
- 28 Younes, H. M.; Bravo-Grimaldo, E.; Amsden, B. G. *Biomaterials* **2004**, 25, 5261-5269.
- 29 Palmgren, R.; Karlsson, S.; Albertsson, A. C. *J. Polym. Sci., Part A: Polym. Chem.* **1997**, 35, 1635-1649.
- 30 Sterzel, H.; Laun, M. Eur. Pat. Appl. EP 632081 (1995)
- 31 Radano, C. P. Dissertation, Michigan State University, 2004.
- 32 Vogeley, N. J.; Baker, W.; Smith, M. R. *Polym. Prepr.* **2005**, 46, 336.
- 33 Scheibelhoffer, A. S.; Blose, W. A.; Harwood, H. J. *Polym. Prepr.* **1969**, 10, 1375-80.
- 34 Brodsky, B. H.; Du Bois, J. *Org. Lett.* **2004**, 6, 2619-2621.
- 35 Christoffers, J.; Oertling, H.; Fischer, P.; Frey, W. *Tetrahedron* **2003**, 59, 3769-3778.
- 36 Flintoft, R. J.; Buzby, J. C.; Tucker, J. A. *Tetrahedron Lett.* **1999**, 40, 4485-4488.
- 37 Molander, G. A.; Harris, C. R. *J. Am. Chem. Soc.* **1995**, 117, 3705-3716.
- 38 Jackson, J. A.; Hammond, G. B.; Wiemer, D. F. *J. Org. Chem.* **1989**, 54, 4750-4754.

- 39 Snell, K. D.; Draths, K. M.; Frost, J. W. *J. Am. Chem. Soc.* **1996**, *118*, 5605-5614.
- 40 Simmons, T. L.; Baker, G. L. *Biomacromolecules* **2001**, *2*, 658-663.
- 41 Simmons, T. L. Dissertation, Michigan State University, 2000.
- 42 Liu, T. Dissertation, Michigan State University, 2002.
- 43 Kajiyama, T.; Kobayashi, H.; Taguchi, T.; Kataoka, K.; Tanaka, J. *Biomacromolecules* **2004**, *5*, 169-174.
- 44 Ouchi, T.; Fujino, A. *Makromol. Chem.* **1989**, *190*, 1523-1530.
- 45 Kimura, Y.; Shirotani, K.; Yamane, H.; Kitao, T. *Macromolecules* **1988**, *21*, 3338-3340.
- 46 Ohya, Y.; Hirai, K.; Ouchi, T. *Makromol. Chem.* **1992**, *193*, 1881-1887.
- 47 Yang, J. Y.; Yu, J.; Pan, H. Z.; Gu, Z. W.; Cao, W. X.; Feng, X. D. *Chin. J. Polym. Sci.* **2001**, *19*, 509-516.
- 48 Yang, J. Y.; Yu, J.; Li, M.; Pan, H. Z.; Gu, Z. W.; Cao, W. X.; Feng, X. D. *Acta Chim. Sinica* **2001**, *59*, 1809-1812.
- 49 Yang, J. Y.; Yu, J.; Li, M.; Gu, Z. W.; Feng, X. D. *Chin. J. Polym. Sci.* **2002**, *20*, 413-417.
- 50 Benabdillah, K. M.; Coudane, J.; Boustta, M.; Engel, R.; Vert, M. *Macromolecules* **1999**, *32*, 8774-8780.
- 51 Marcincinova-Benabdillah, K.; Boustta, M.; Coudane, J.; Vert, M. *Biomacromolecules* **2001**, *2*, 1279-1284.
- 52 Abayasinghe, N. K.; Smith, D. W. *Abstr. Pap. Am. Chem. Soc.* **2001**, *222*, U272-U272.
- 53 Yang, K. K.; Wang, X. L.; Wang, Y. Z. *J. Macromol. Sci., Polym. Rev.* **2002**, *C42*, 373-398.
- 54 Lin, H. L.; Chu, C. C.; Grubb, D. J. *Biomed. Mater. Res.* **1993**, *27*, 153-166.
- 55 Raquez, J. M.; Degee, P.; Narayan, R.; Dubois, P. *Macromolecules* **2001**, *34*, 8419-8425.
- 56 Doddi, N.; Versfelt, C. C.; Wasserman, D. U.S. Pat. 4,032,988 (1977)
- 57 Esteves, L. M.; Marquez, L.; Muller, A. J. *J. Appl. Polym. Sci.* **2005**, *97*, 659-665.

- 58 Weipert, E. A. U. S. Pat. 3,020,289 (1962)
- 59 Schultz, H. S. U. S. Pat 3,063,967 (1962)
- 60 Schultz, H. S. U. S. Pat. 3,063,968 (1962)
- 61 Forschner, T. C. U. S. Pat. 5,310,945 (1994)
- 62 Merbouh, N.; Bobbitt, J. M.; Bruckner, C. *J. Org. Chem.* **2004**, *69*, 5116-5119.
- 63 Nishimura, T.; Onoue, T.; Ohe, K.; Uemura, S. *J. Org. Chem.* **1999**, *64*, 6750-6755.
- 64 Kakiuchi, N.; Nishimura, T.; Inoue, M.; Uemura, S. *Bull. Chem. Soc. Jpn.* **2001**, *74*, 165-172.
- 65 Nishida, H.; Yamashita, M.; Endo, T.; Tokiwa, Y. *Macromolecules* **2000**, *33*, 6982-6986.
- 66 Yoon, K. R.; Kim, Y.; Choi, I. S. *J. Polym. Res.* **2004**, *11*, 265-268.
- 67 Libiszowski, J.; Kowalski, A.; Szymanski, R.; Duda, A.; Raquez, J. M.; Degee, P.; Dubois, P. *Macromolecules* **2004**, *37*, 52-59.
- 68 Kricheldorf, H. R.; Damrau, D. O. *Macromol. Chem. Phys.* **1998**, *199*, 1089-1097.
- 69 Nishida, H.; Yamashita, M.; Nagashima, M.; Endo, T.; Tokiwa, Y. *J. Polym. Sci., Part A: Polym. Chem.* **2000**, *38*, 1560-1567.
- 70 Duda, A.; Kowalski, A.; Libiszowski, J.; Penczek, S. *Macromol. Symp.* **2005**, *224*, 71-83.
- 71 Shinno, K.; Miyamoto, M.; Kimura, Y.; Hirai, Y.; Yoshitome, H. *Macromolecules* **1997**, *30*, 6438-6444.
- 72 Bechtold, K.; Hillmyer, M. A.; Tolman, W. B. *Macromolecules* **2001**, *34*, 8641-8648.
- 73 Zhang, D. H.; Xu, J. Y.; Alcazar-Roman, L.; Greenman, L.; Cramer, C. J.; Hillmyer, M. A.; Tolman, W. B. *Macromolecules* **2004**, *37*, 5274-5281.
- 74 Partanen, A.; Ayras, P. *Finn. Chem. Lett.* **1977**, *7*, 208.
- 75 Carrillo, R.; Martin, V. S.; Lopez, M.; Martin, T. *Tetrahedron* **2005**, *61*, 8177-8191.
- 76 Yu, X. H.; Feng, J.; Zhuo, R. X. *Macromolecules* **2005**, *38*, 6244-6247.



- 77 Trollsas, M.; Lowenhielm, P.; Lee, V. Y.; Moller, M.; Miller, R. D.; Hedrick, J. L. *Macromolecules* **1999**, 32, 9062-9066.
- 78 Kimura, Y. Eur. Pat. Appl. EP 0522422 A2 (1993)
- 79 Hiki, S.; Taniguchi, I.; Miyamoto, M.; Kimura, Y. *Macromolecules* **2002**, 35, 2423-2425.
- 80 Kagan, F.; Birkenmeyer, R. D. *J. Am. Chem. Soc.* **1959**, 81, 1986-1991.
- 81 Shalaby, S. W.; Koelmel, D. F.; Arnold, S. U.S. Pat. 5,082,925 (1992)
- 82 Feng, Y. K.; Klee, D.; Keul, H.; Hocker, H. *Macromol. Chem. Phys.* **2000**, 201, 2670-2675.
- 83 Helder, J.; Kohn, F. E.; Sato, S.; Vandenberg, J. W.; Feijen, J. *Makromol. Chem.-Rapid* **1985**, 6, 9-14.
- 84 Helder, J.; Feijen, J.; Lee, S. J.; Kim, S. W. *Makromol. Chem.-Rapid* **1986**, 7, 193-198.
- 85 Tveld, P. J. A.; Dijkstra, P. J.; Vanlochem, J. H.; Feijen, J. *Makromol. Chem.* **1990**, 191, 1813-1825.
- 86 Barrera, D. A.; Zylstra, E.; Lansbury, P. T.; Langer, R. *J. Am. Chem. Soc.* **1993**, 115, 11010-11011.
- 87 Jorres, V.; Keul, H.; Hocker, H. *Macromol. Chem. Phys.* **1998**, 199, 825-833.
- 88 Intveld, P. J. A.; Shen, Z. R.; Takens, G. A. J.; Dijkstra, P. J.; Feijen, J. *J. Polym. Sci., Part A: Polym. Chem.* **1994**, 32, 1063-1069.
- 89 Jorres, V.; Keul, H.; Hocker, H. *Macromol. Chem. Phys.* **1998**, 199, 835-843.
- 90 Feng, Y. K.; Klee, D.; Hocker, H. *Macromol. Chem. Phys.* **1999**, 200, 2276-2283.
- 91 Shirahama, H.; Tanaka, A.; Yasuda, H. *J. Polym. Sci., Part A: Polym. Chem.* **2002**, 40, 302-316.
- 92 Kricheldorf, H. R.; Hauser, K. *Macromol. Chem. Phys.* **2001**, 202, 1219-1226.
- 93 Feng, Y. K.; Knufermann, J.; Klee, D.; Hocker, H. *Macromol. Chem. Phys.* **1999**, 200, 1506-1514.

- 94 Feng, Y. K.; Knufermann, J.; Klee, D.; Hocker, H. *Macromol. Rapid Commun.* **1999**, *20*, 88-90.
- 95 Feng, Y. K.; Klee, D.; Hocker, H. *Macromol. Biosci.* **2001**, *1*, 66-74.
- 96 Feng, Y.; Klee, D.; Hocker, H. *Macromol. Biosci.* **2004**, *4*, 587-590.
- 97 Feng, Y. K.; Klee, D.; Hocker, H. *J. Polym. Sci., Part A: Polym. Chem.* **2005**, *43*, 3030-3039.
- 98 Zhang, G. D.; Wang, D.; Feng, X. D. *Macromolecules* **1998**, *31*, 6390-6392.
- 99 Barrera, D. A.; Zylstra, E.; Lansbury, P. T.; Langer, R. *Macromolecules* **1995**, *28*, 425-432.
- 100 Veld, P. J. A. I.; Dijkstra, P. J.; Feijen, J. *Makromol. Chem.* **1992**, *193*, 2713-2730.
- 101 Ouchi, T.; Nozaki, T.; Okamoto, Y.; Shiratani, M.; Ohya, Y. *Macromol. Chem. Phys.* **1996**, *197*, 1823-1833.
- 102 Ouchi, T.; Nozaki, T.; Ishikawa, A.; Fujimoto, I.; Ohya, Y. *J. Polym. Sci., Part A: Polym. Chem.* **1997**, *35*, 377-383.
- 103 Ouchi, T.; Miyazaki, H.; Arimura, H.; Tasaka, F.; Hamada, A.; Ohya, Y. *J. Polym. Sci., Part A: Polym. Chem.* **2002**, *40*, 1218-1225.
- 104 John, G.; Tsuda, S.; Morita, M. *J. Polym. Sci., Part A: Polym. Chem.* **1997**, *35*, 1901-1907.
- 105 Jin, S.; Gonsalves, K. E. *Polymer* **1998**, *39*, 5155-5162.
- 106 John, G.; Morita, M. *Macromol. Rapid Commun.* **1999**, *20*, 265-268.
- 107 John, G.; Morita, M. *Macromolecules* **1999**, *32*, 1853-1858.
- 108 Tasaka, F.; Ohya, Y.; Ouchi, T. *Macromolecules* **2001**, *34*, 5494-5500.
- 109 Ouchi, T.; Shiratani, M.; Jinno, M.; Hirao, M.; Ohya, Y. *Makromol. Chem.-Rapid* **1993**, *14*, 825-831.
- 110 Wang, D.; Feng, X. D. *Macromolecules* **1997**, *30*, 5688-5692.
- 111 Wang, D.; Feng, X. D. *Macromolecules* **1998**, *31*, 3824-3831.
- 112 Deng, X. M.; Yao, J. R.; Yuan, M. L.; Li, X. H.; Xiong, C. D. *Macromol. Chem. Phys.* **2000**, *201*, 2371-2376.

- 113 Feng, Y.; Klee, D.; Hocker, H. *Macromol. Chem. Phys.* **2002**, *203*, 819-824.
- 114 Guan, H. L.; Xie, Z. G.; Zhang, P. B.; Deng, C.; Chen, X. S.; Jing, X. B. *Biomacromolecules* **2005**, *6*, 1954-1960.
- 115 Mori, K.; Takaishi, H. *Tetrahedron* **1989**, *45*, 1639-1646.
- 116 Stocker, J. H. *J. Org. Chem.* **1962**, *27*, 2288-2289.
- 117 Riley, D. P.; Shumate, R. E. *J. Org. Chem.* **1980**, *45*, 5187-5193.
- 118 Witzke, D. R.; Narayan, R.; Kolstad, J. J. *Macromolecules* **1997**, *30*, 7075-7085.
- 119 Kowalski, A.; Duda, A.; Penczek, S. *Macromolecules* **2000**, *33*, 7359-7370.
- 120 Abe, H.; Takahashi, N.; Kim, K. J.; Mochizuki, M.; Doi, Y. *Biomacromolecules* **2004**, *5*, 1606-1614.
- 121 Fan, Y. J.; Nishida, H.; Shirai, Y.; Endo, T. *Polym. Degrad. Stab.* **2004**, *84*, 143-149.
- 122 Wachsen, O.; Reichert, K. H.; Kruger, R. P.; Much, H.; Schulz, G. *Polym. Degrad. Stab.* **1997**, *55*, 225-231.
- 123 Kopinke, F. D.; Remmler, M.; Mackenzie, K.; Moder, M.; Wachsen, O. *Polym. Degrad. Stab.* **1996**, *53*, 329-342.
- 124 Nishida, H.; Mori, T.; Hoshihara, S.; Fan, Y. J.; Shirai, Y.; Endo, T. *Polym. Degrad. Stab.* **2003**, *81*, 515-523.
- 125 Zhang, J. M.; Sato, H.; Tsuji, H.; Noda, I.; Ozaki, Y. *Macromolecules* **2005**, *38*, 1822-1828.
- 126 Cao, C. Z.; Lin, Y. B. *J. Chem. Inf. Comp. Sci.* **2003**, *43*, 643-650.
- 127 Zhao, J.; Hahn, S. F.; Hucul, D. A.; Meunier, D. M. *Macromolecules* **2001**, *34*, 1737-1741.
- 128 Zell, M. T.; Padden, B. E.; Paterick, A. J.; Thakur, K. A. M.; Kean, R. T.; Hillmyer, M. A.; Munson, E. J. *Macromolecules* **2002**, *35*, 7700-7707.
- 129 Chisholm, M. H.; Iyer, S. S.; McCollum, D. G.; Pagel, M.; Werner-Zwanziger, U. *Macromolecules* **1999**, *32*, 963-973.
- 130 Kasperczyk, J. E. *Polymer* **1999**, *40*, 5455-5458.

- 131 Thakur, K. A. M.; Kean, R. T.; Hall, E. S.; Kolstad, J. J.; Munson, E. J. *Macromolecules* **1998**, *31*, 1487-1494.
- 132 Thakur, K. A. M.; Kean, R. T.; Hall, E. S.; Kolstad, J. J.; Lindgren, T. A.; Doscotch, M. A.; Siepmann, J. I.; Munson, E. J. *Macromolecules* **1997**, *30*, 2422-2428.
- 133 Hay, J. N. *J. Polym. Sci. Part A: General Papers* **1965**, *3*, 433-47.
- 134 Doi, Y.; Kanesawa, Y.; Kunioka, M.; Saito, T. *Macromolecules* **1990**, *23*, 26-31.
- 135 Gilding, D. K.; Reed, A. M. *Polymer* **1979**, *20*, 1459-1464.
- 136 Perego, G.; Vercellio, T.; Balbontin, G. *Makromol. Chem.* **1993**, *194*, 2463-2469.
- 137 Nakayama, A.; Kawasaki, N.; Arvanitoyannis, I.; Iyoda, J.; Yamamoto, N. *Polymer* **1995**, *36*, 1295-1301.
- 138 Schmidt, P.; Keul, H.; Hocker, H. *Macromolecules* **1996**, *29*, 3674-3680.
- 139 Feng, X. D.; Song, C. X.; Chen, W. Y.; Voong, S. T. *J. Polym. Sci., Part C: Polym. Lett.* **1983**, *21*, 593-600.
- 140 Kurcok, P.; Penczek, J.; Franek, J.; Jedlinski, Z. *Macromolecules* **1992**, *25*, 2285-2289.
- 141 Kricheldorf, H. R.; Meierhaack, J. *Makromolekulare Chemie-Macromolecular Chemistry and Physics* **1993**, *194*, 715-725.
- 142 Sipos, L.; Zsuga, M.; Deak, G. *Macromol. Rapid Commun.* **1995**, *16*, 935-940.
- 143 Ohya, Y.; Maruhashi, S.; Ouchi, T. *Macromolecules* **1998**, *31*, 4662-4665.
- 144 Chen, L.; Qiu, X. Y.; Deng, M. X.; Hong, Z. K.; Luo, R.; Chen, X. S.; Jing, X. B. *Polymer* **2005**, *46*, 5723-5729.
- 145 Ouchi, T.; Kontani, T.; Saito, T.; Ohya, Y. *J. Biomater. Sci., Polym. Ed.* **2005**, *16*, 1035-1045.
- 146 Wu, Y.; Zheng, Y. L.; Yang, W. L.; Wang, C. C.; Hu, J. H.; Fu, S. K. *Carbohydr. Polym.* **2005**, *59*, 165-171.
- 147 Arvanitoyannis, I.; Nakayama, A.; Kawasaki, N.; Yamamoto, N. *Polymer* **1995**, *36*, 2947-2956.
- 148 Choi, Y. R.; Bae, Y. H.; Kim, S. W. *Macromolecules* **1998**, *31*, 8766-8774.

- 149 Zhao, Y. L.; Qing, C.; Jing, J.; Shuai, X. T.; Bei, J. Z.; Chen, C. F.; Fu, X. *Polymer* **2002**, *43*, 5819-5825.
- 150 Trollsas, M.; Kelly, M. A.; Claesson, H.; Siemens, R.; Hedrick, J. L. *Macromolecules* **1999**, *32*, 4917-4924.
- 151 Satoh, T.; Tamaki, M.; Kitajyo, Y.; Maeda, T.; Ishihara, H.; Imai, T.; Kaga, H.; Kakuchi, T. *J. Polym. Sci., Part A: Polym. Chem.* **2006**, *44*, 406-413.
- 152 Gottschalk, C.; Frey, H. *Macromolecules* **2006**, *39*, 1719-1723.
- 153 Trollsas, M.; Atthoff, B.; Claesson, H.; Hedrick, J. L. *J. Polym. Sci., Part A: Polym. Chem.* **2004**, *42*, 1174-1188.
- 154 Zhao, Y. L.; Shuai, X.; Chen, C. F.; Xi, F. *Chem. Commun.* **2004**, 1608-1609.
- 155 Cai, Q.; Zhao, Y. L.; Bei, J. Z.; Xi, F.; Wang, S. G. *Biomacromolecules* **2003**, *4*, 828-834.
- 156 Cai, Q.; Bei, J. Z.; Wang, S. G. *Acta Polym. Sin.* **2004**, 719-725.
- 157 Tasaka, F.; Miyazaki, H.; Ohya, Y.; Ouchi, T. *Macromolecules* **1999**, *32*, 6386-6389.
- 158 Breitenbach, A.; Kissel, T. *Polymer* **1998**, *39*, 3261-3271.
- 159 Engwicht, A.; Girreser, U.; Muller, B. W. *Biomaterials* **2000**, *21*, 1587-1593.
- 160 Brostrom, J.; Boss, A.; Chronakis, L. S. *Biomacromolecules* **2004**, *5*, 1124-1134.
- 161 Simic, V.; Pensec, S.; Spassky, N. *Macromol. Symp.* **2000**, *153*, 109-121.
- 162 Zalusky, A. S.; Olayo-Valles, R.; Wolf, J. H.; Hillmyer, M. A. *J. Am. Chem. Soc.* **2002**, *124*, 12761-12773.
- 163 Frick, E. M.; Hillmyer, M. A. *Macromol. Rapid Commun.* **2000**, *21*, 1317-1322.
- 164 Li, J.; Ni, X. P.; Li, X.; Tan, N. K.; Lim, C. T.; Ramakrishna, S.; Leong, K. W. *Langmuir* **2005**, *21*, 8681-8685.
- 165 Sperling, L. H. *Introduction to Physical Polymer Science*; Third ed.; John Wiley & Sons, Inc., 2001.
- 166 Grijpma, D. W.; Pennings, A. J. *Macromol. Chem. Phys.* **1994**, *195*, 1649-1663.

- 167 Ryu, C. Y.; Ruokolainen, J.; Fredrickson, G. H.; Kramer, E. J.; Hahn, S. F. *Macromolecules* **2002**, *35*, 2157-2166.
- 168 Joziasse, C. A. P.; Veenstra, H.; Topp, M. D. C.; Grijpma, D. W.; Pennings, A. J. *Polymer* **1998**, *39*, 467-474.
- 169 Yuan, Y. M.; Ruckenstein, E. *Polym. Bull.* **1998**, *40*, 485-490.
- 170 Anderson, K. S.; Lim, S. H.; Hillmyer, M. A. *J. Appl. Polym. Sci.* **2003**, *89*, 3757-3768.
- 171 Anderson, K. S.; Hillmyer, M. A. *Polymer* **2004**, *45*, 8809-8823.
- 172 Knoll, K.; Niessner, N. *Macromol. Symp.* **1998**, *132*, 231-243.
- 173 Du, Y. J.; Lemstra, P. J.; Nijenhuis, A. J.; Vanaert, H. A. M.; Bastiaansen, C. *Macromolecules* **1995**, *28*, 2124-2132.
- 174 Rashkov, I.; Manolova, N.; Li, S. M.; Espartero, J. L.; Vert, M. *Macromolecules* **1996**, *29*, 50-56.
- 175 Li, S. M.; Rashkov, I.; Espartero, J. L.; Manolova, N.; Vert, M. *Macromolecules* **1996**, *29*, 57-62.
- 176 Li, S. M.; Vert, M. *Macromolecules* **2003**, *36*, 8008-8014.
- 177 Cohn, D.; Hotohely-Salomon, A. *Polymer* **2005**, *46*, 2068-2075.
- 178 Shin, D.; Shin, K.; Aamer, K. A.; Tew, G. N.; Russell, T. P.; Lee, J. H.; Jho, J. Y. *Macromolecules* **2005**, *38*, 104-109.
- 179 Knoll, A.; Magerle, R.; Krausch, G. *Macromolecules* **2001**, *34*, 4159-4165.
- 180 Dechy-Cabaret, O.; Martin-Vaca, B.; Bourissou, D. *Chem. Rev.* **2004**, *104*, 6147-6176.
- 181 Lenz, R. W.; Marchessault, R. H. *Biomacromolecules* **2005**, *6*, 1-8.
- 182 Mecking, S. *Angewandte Chemie-International Edition* **2004**, *43*, 1078-1085.
- 183 McInTyre, J. E. In *Modern Polyesters: Chemistry and Technology of Polyesters and Copolyesters*; Scheirs, J., Long, T. E., Eds.; John Wiley & Sons Ltd.: 2003, p 750.
- 184 Municipal Solid Waste Generation, Recycling, and Disposal in the United States: Facts and Figures for 2003 by EPA, 2005

- 185 Muller, R.-J. In *Handbook of biodegradable polymers*; Bastioli, C., Ed.; Rapra Technology Limited: 2005, p 303-337.
- 186 Kint, D. P. R.; Munoz-Guerra, S. *Polym. Int.* **2003**, *52*, 321-336.
- 187 Nagahata, R.; Sugiyama, J.; Goyal, M.; Asai, M.; Ueda, M.; Takeuchi, K. *J. Polym. Sci., Part A: Polym. Chem.* **2000**, *38*, 3360-3368.
- 188 Nagahata, R.; Sugiyama, J. J.; Goyal, M.; Goto, M.; Honda, K.; Asai, M.; Ueda, M.; Takeuchi, K. *Polymer* **2001**, *42*, 1275-1279.
- 189 Youk, J. H.; Boulares, A.; Kambour, R. P.; MacKnight, W. J. *Macromolecules* **2000**, *33*, 3600-3605.
- 190 Schmeltzer, R. C.; Schmalenberg, K. E.; Uhrich, K. E. *Biomacromolecules* **2005**, *6*, 359-367.
- 191 Prudencio, A.; Schmeltzer, R. C.; Uhrich, K. E. *Macromolecules* **2005**, *38*, 6895-6901.
- 192 Schmeltzer, R. C.; Anastasiou, T. J.; Uhrich, K. E. *Polym. Bull.* **2003**, *49*, 441-448.
- 193 Anastasiou, T. J.; Uhrich, K. E. *J. Polym. Sci., Part A: Polym. Chem.* **2003**, *41*, 3667-3679.
- 194 Bedell, C.; Deng, M.; Anastasiou, T. J.; Uhrich, K. E. *J. Appl. Polym. Sci.* **2001**, *80*, 32-38.
- 195 Auras, R.; Harte, B.; Selke, S. *Macromol. Biosci.* **2004**, *4*, 835-864.
- 196 Nederberg, F.; Connor, E. F.; Glausser, T.; Hedrick, J. L. *Chem. Commun.* **2001**, 2066-2067.
- 197 Nederberg, F.; Connor, E. F.; Moller, M.; Glauser, T.; Hedrick, J. L. *Angew. Chem., Int. Ed.* **2001**, *40*, 2712-2715.
- 198 Howe, R.; Rao, B. S.; Heyneker, H. *J. Chem. Soc. C* **1967**, 2510-2514.
- 199 Aggarwal, V. K.; Thomas, A.; Schade, S. *Tetrahedron* **1997**, *53*, 16213-16228.
- 200 Masamune, S.; Choy, W.; Kerdesky, F. A. J.; Imperiali, B. *J. Am. Chem. Soc.* **1981**, *103*, 1566-1568.

MICHIGAN STATE UNIVERSITY LIBRARIES



3 1293 02845 4423